# IMPROVING BONE HEALTH AND EGGSHELL QUALITY THROUGH MAINTAINING A DESIRED CALCIUM HOMEOSTASIS IN LAYING HENS

By

Qianru Hui

A Thesis Submitted to the Faculty of Graduate Studies of

The University of Manitoba

In partial fulfillment of the requirements

For the degree of

DOCTOR OF PHILOSOPHY

Department of Animal Science

University of Manitoba

Winnipeg, Manitoba

Canada. R3T 2N2

## ABSTRACT

Laying hens have an extra demand on calcium (Ca) homeostasis due to egg-laying. The calcium-sensing receptor (CaSR) plays a central role in Ca homeostasis. The thesis aimed to develop effective methods for maintaining desired Ca homeostasis in laying hens. The first study demonstrated that chicken CaSR (cCaSR) and chicken vitamin D receptor (cVDR) are widely distributed in the kidney, gastrointestinal tract, shell gland, and tibia in laying hens at different laying stages. The second study characterized cCaSR ligands in cCaSR-stably expressing HEK293 cells and investigated the binding modes between cCaSR and its ligands. Results showed that L-tryptophan (L-Trp) and inorganic $PO_4^{3-}$ are cCaSR modulators, acting as positive and negative allosteric modulators, respectively. The third study isolated chicken mesenchymal stem cells (MSCs) from broilers and layers and demonstrated that cCaSR and cVDR were expressed in broiler and layer MSCs. The osteogenic differentiation process in layer MSCs was faster than that in the broiler MSCs. L-Trp and 1,25-dihydroxycholecalciferol ($1,25OHD_3$) were found to regulate proliferation and osteogenic differentiation in broiler and layer MSCs, depending on the modulator's doses and treatment time. The fourth study was to investigate the interactive effects of Ca and L-Trp, and of Ca and 25-hydroxycholecalciferol (25HyD) substitution for vitamin $D_3$ on egg production, eggshell quality, bone health, and calcium homeostasis in Dekalb layers from 26 to 29 weeks of age. Results showed that increased dietary Trp levels increased serum Ca level, eggshell quality, and tibia traits. An interactive effect was found that Ca continued to increase the relative eggshell weight and eggshell thickness as Trp level increased. However, 25HyD did not improve egg production, eggshell quality, and bone health. Taken together, the cCaSR and cVDR are widely expressed in laying hens. $Ca^{2+}$ and L-Trp promoted osteogenic differentiation in chicken MSCs and they improved Ca utilization, eggshell quality, and bone health in laying hens.

1,25OHD$_3$ can facilitate chicken MSC proliferation, but 25HyD did not promote egg quality and bone health in laying hens. The results provide evidence for the potential application of cCaSR modulators and different vitamin D$_3$ sources to improve eggshell quality and bone health in laying hens.

## ACKNOWLEDGMENTS

I would like to express my sincere gratitude and appreciation to my esteemed advisor, Dr. Chengbo Yang, for his guidance, support, and assistance throughout my Ph.D. program. His constructive feedback and innovative ideas have constantly inspired me and propelled me forward in my research. Additionally, Dr. Yang provided me with numerous opportunities to present my findings in public, which helped to build my confidence and enthusiasm for my work. I would also like to extend my thanks to the other members of my advisory committee, Dr. Karmin O, Dr. Martin Nyachoti, and Dr. Francis Lin, for their valuable comments and suggestions on my thesis project.

I acknowledge and am deeply grateful for funding support provided by the Natural Sciences and Engineering Research Council of Canada (NSERC), Manitoba Egg Farmers (MEF), the University of Manitoba, and Wallenstein Feed & Supply Inc. for my research project. Additionally, I would like to express my appreciation for the various scholarships, fellowships, and awards I received, including IGES, IGSS, UMGF, FGS Travel Awards, the Sydney L. Morantz Scholarship, CSAS Travel Fellowship, Hyline International Genetics & Genomics Award, and the Chinese Government Award for Outstanding Self-Financed Students Abroad. These awards provided invaluable financial assistance throughout my Ph.D. program, and I am grateful for the support they provided.

I am deeply grateful for the professional and patient assistance and coordination support I received from Gemmar Maramot, Adekunle Onakomaiya, Don Chaput, and Jason Bourcier during my animal study. Additionally, I would like to thank Dr. Yulian Niu for spending time to voluntarily teach me immunohistochemical techniques. I would also like to express my gratitude

to Dr. Song Liu for providing access to the Instron tensile testing system, and to his student, Quintin Litke, for providing training on the Instron machine and for kindly answering my questions.

I would like to express my deepest appreciation to all members of the lab who supported me throughout my project, including Faith Omonijo, Zhigang Tan, Janghan Choi, Chongwu Yang, Xiaoya Zhao, Bingqi Dong, Yanhong Chen, Marion Mogire, Shunshun Jin, Haoxiang Xu, Changning Yu, Yujia Wu, Yuanyuan Zhou, Tao Wang, Orie Hochman, Arantxa Asun Pinar, and Laura Beens. I am also grateful to our technician, Fernando Esposito, research associates Dr. Shangxi Liu and Dr. Paula Azevedo, and postdoctoral fellow Dr. Peng Lu for their assistance with various difficulties with my project. In particular, I would like to express my special gratitude to Xiaoya Zhao for her selfless contribution to my animal study. As my good friend, she supported me through tough times and worked with me many days and nights to overcome difficult questions and experiments. I would also like to express appreciation for the kind help from the groups of Dr. Nyachoti, Dr. Rogiewicz, and Dr. House and all the administrative and technical staff of the Department of Animal Science.

I am truly indebted to my parents and my parents-in-law for their love and support, as well as to my friends for their help and company. In addition, my husband, Ran Chen, is also my best friend and mentor. I am so grateful that he always helps me with research challenges and encourages me to keep moving forward.

## DEDICATION

This thesis is dedicated to my beloved parents, Min Hui and Aijing Kang, and my beloved husband, Ran Chen, for their endless love and support.

## FOREWORD

This thesis was prepared in a manuscript format according to the guidelines of *Poultry Science* and is composed of four manuscripts. Some of the content of this thesis has been presented at academic conferences. Manuscript I was presented as a poster at the 2020 Animal Nutrition Conference of Canada (online), May-June; Manuscript II was presented orally at the Virtual 2021 Poultry Science Association Annual Meeting (online), July 19-22; Manuscript III was presented orally at the 2022 2nd Annual Canadian Poultry Research Forum (online), June 14-16. My published manuscripts and manuscripts under preparation and review are listed as follows:

**Manuscript I**: **Hui, Q.**, Zhao, X., Lu, P., Liu, S., Nyachoti, M., O, K., Yang, C. (2021). Molecular distribution and localization of extracellular calcium-sensing receptor (CaSR) and vitamin D receptor (VDR) at three different laying stages in laying hens (*Gallus gallus domesticus*). *Poult. Sci.*, 100(5): 101060. doi:10.1016/j.psj.2021.101060

**Manuscript II**: **Hui, Q.**, Dong, H., Zhao, X., Liu, S., Nyachoti, M., O, K., Yang, C. (2021). Tryptophan and phosphate sensing by the chicken extracellular calcium-sensing receptor via potential docking sites to initiate downstream G protein-coupled signaling cascades. *Anim. Feed Sci. Technol.*, under review.

**Manuscript III**: **Hui, Q.**, Zhao, X., O, K., and Yang, C. (2022). Effects of L-tryptophan and 1,25-dihydroxycholecalciferol on osteogenic differentiation of mesenchymal stem cells isolated from the compact bones of broilers and layers. *J. Agri. Food Chem.*, 70(34): 10476–10489. doi:10.1021/acs.jafc.2c03451

**Manuscript IV**: **Hui, Q.**, Zhao, X., Li, S., O, K., Nyachoti, M., and Yang, C. (2022). Interactive effects of calcium and L-tryptophan, and of calcium and 25-hydroxycholecalciferol

substitution for vitamin $D_3$ on egg production, eggshell quality, bone health, and calcium homeostasis in Dekalb laying hens from 26 to 29 weeks of age. under preparation.

## CONTRIBUTIONS OF AUTHORS

This thesis was l prepared by Qianru Hui and reviewed, revised, and approved by internal examiners including Dr. Chengbo Yang (advisor), Dr. Karmin O (committee member), Dr. Martin Nyachoti (committee member), and Dr. Francis Lin (committee member).

All manuscripts (chapter four to chapter seven) have been revised and approved by the co-authors, and the specific contributions of all listed authors are described below.

Chapter Four: Manuscript I. Chengbo Yang and Qianru Hui conceived of and designed this study. Qianru Hui, Xiaoya Zhao, Peng Lu, and Shangxi Liu performed experiments. Qianru Hui analyzed data and prepared figures; Qianru Hui drafted the manuscript. Qianru Hui, Xiaoya Zhao, Peng Lu, Shangxi Liu, Martin Nyachoti, Karmin O, and Chengbo Yang reviewed, edited, and revised the manuscript.

Chapter Five: Manuscript II. Chengbo Yang and Qianru Hui conceived of and designed this study. Qianru Hui, Huanhuan Dong, and Xiaoya Zhao performed experiments. Qianru Hui and Huanhuan Dong analyzed data and prepared figures; Qianru Hui drafted the manuscript. Qianru Hui, Huanhuan Dong, Xiaoya Zhao, Paula Azevedo, Shangxi Liu, Martin Nyachoti, Karmin O, Chengbo Yang reviewed, edited, and revised the manuscript.

Chapter Six: Manuscript III. Chengbo Yang and Qianru Hui conceived and designed this study. Qianru Hui and Xiaoya Zhao performed experiments. Qianru Hui analyzed data and prepared figures; Qianru Hui drafted the manuscript. Qianru Hui, Xiaoya Zhao, Karmin O, and Chengbo Yang reviewed, edited, and revised the manuscript.

Chapter Seven: Manuscript IV. Chengbo Yang and Qianru Hui conceived of and designed this study. Qianru Hui and Xiaoya Zhao performed experiments. Qianru Hui and Shengnan Li analyzed data and prepared tables; Qianru Hui drafted the manuscript. Qianru Hui, Xiaoya Zhao,

Shengnan Li, Karmin O, Martin Nyachoti, and Chengbo Yang reviewed, edited, and revised the manuscript.

## TABLE OF CONTENTS

**ABSTRACT** ..... **i**

**ACKNOWLEDGMENTS** ..... **iii**

**DEDICATION** ..... **v**

**FOREWORD** ..... **vi**

**CONTRIBUTIONS OF AUTHORS** ..... **viii**

**TABLE OF CONTENTS** ..... **x**

**LIST OF TABLES** ..... **xvi**

**LIST OF FIGURES** ..... **xviii**

**LIST OF ABBREVIATIONS** ..... **xxv**

**CHAPTER ONE: GENERAL INTRODUCTION** ..... **1**

**CHAPTER TWO: LITERATURE REVIEW** ..... **5**

2.1 Introduction ..... 6

2.2 Calcium in laying hens ..... 7

2.2.1 Function of calcium ..... 7

2.2.2 Calcium metabolism and homeostasis ..... 8

2.2.3 Calcium requirement ..... 11

2.2.4 Factors affecting calcium intake and utilization ..... 12

2.3 Modulators of calcium metabolism and homeostasis ..... 14

2.3.1 Hormones ..... 14

2.3.2 Vitamin D receptor (VDR) ..... 17

2.3.3 Calcium-sensing receptor (CaSR) ..... 18

2.3.4 Calcium transport-related proteins ..... 19

2.4 Structure-function relationships of calcium-sensing receptor ..... 24
2.4.1 Extracellular domain (ECD) ..... 27
2.4.2 Transmembrane domain (TMD) ..... 28
2.4.3 Intracellular domain (ICD) ..... 29
2.5 Intracellular signaling via coupling with heterotrimeric G proteins ..... 29
2.5.1 Heterotrimeric G Proteins ..... 29
2.5.2 Intracellular $Ca^{2+}$ mobilization ..... 30
2.5.3 Intracellular cAMP changes ..... 31
2.5.4 PKC activation ..... 32
2.5.5 MAPK activation ..... 33
2.5.6 Rho activation ..... 33
2.6 Calcium-sensing receptor modulators ..... 34
2.6.1 Orthosteric agonists ..... 34
2.6.2 Allosteric modulators ..... 36
2.7 Important tissues involved in maintaining calcium homeostasis ..... 38
2.7.1 Parathyroid ..... 38
2.7.2 Gastrointestinal tract (GIT) ..... 39
2.7.3 Kidney ..... 42
2.7.4 Bone ..... 43
2.7.5 Shell gland ..... 46
**CHAPTER THREE: HYPOTHESES AND OBJECTIVES ..... 47**
3.1 Hypotheses ..... 48
3.2 Objectives ..... 48

**CHAPTER FOUR: MANUSCRIPT I ..... 50**

4.1 Abstract ..... 51

4.2 Introduction ..... 52

4.3 Materials and methods ..... 54

4.3.1 Locus and structure of chicken (*Gallus gallus*) CaSR ..... 54

4.3.2 Animals and management ..... 55

4.3.3 Tissue collection and preparation ..... 55

4.3.4 Real-time quantitative polymerase chain reaction (Real-time RT-qPCR) ..... 55

4.3.5 Western blot analysis ..... 57

4.3.6 Immunohistochemistry ..... 58

4.3.7 Statistical analysis ..... 59

4.4 Results ..... 59

4.4.1 Structure and hydrophobicity analysis of cCaSR ..... 59

4.4.2 Relative mRNA abundance of cCaSR and cVDR ..... 63

4.4.3 Relative protein expression of cCaSR and cVDR ..... 65

4.4.4 Localization of cCaSR ..... 68

4.5 Discussion ..... 74

**BRIDGE TO CHAPTER FIVE ..... 80**

**CHAPTER FIVE: MANUSCRIPT II ..... 81**

5.1 Abstract ..... 82

5.2 Introduction ..... 83

5.3 Materials and methods ..... 86

5.3.1 Materials ..... 86

5.3.2 Expression vector ..... 87
5.3.4 Verification of the stable expression of cCaSR ..... 88
5.3.5 Cell viability ..... 89
5.3.6 Luciferase reporter assay ..... 90
5.3.7 Dose-response curve of $Ca^{2+}$ upon cCaSR activation ..... 90
5.3.8 Dose-response curve of $Ca^{2+}$ in the presence of L-Trp upon cCaSR activation ..... 90
5.3.9 Dose-response curve of $Ca^{2+}$ in the presence of NPS-R568 upon cCaSR activation ..... 91
5.3.10 Phosphate-induced inhibition of cCaSR ..... 91
5.3.11 The cAMP production assay ..... 91
5.3.12 Molecular docking and dynamics simulation ..... 92
5.3.13 Statistical analysis ..... 94
5.4 Results ..... 94
5.4.1 Identification of Flp-In™-293 cells stably expressing cCaSR ..... 94
5.4.2 Dose-effect of calcium on the viability of cCaSR-overexpressing Flp-In 293 cells ..... 94
5.4.3 The cCaSR signaling in response to L-Trp ..... 97
5.4.4 The cCaSR signaling in response to inorganic $PO_4^{3-}$ ..... 105
5.4.5 Molecular docking ..... 113
5.4.6 Molecular dynamics simulation ..... 118
5.5 Discussion ..... 122
**BRIDGE TO CHAPTER SIX ..... 130**
**CHAPTER SIX: MANUSCRIPT III ..... 131**
6.1 Abstract ..... 132
6.2 Introduction ..... 133

6.3 Materials and methods ..... 136
6.3.1 Isolation and culture of chicken compact bone MSCs ..... 136
6.3.2 MSC morphology ..... 137
6.3.3 MSC proliferation assay ..... 137
6.3.4 Real-time quantitative polymerase chain reaction (Real-time qPCR) ..... 137
6.3.5 Western blot analysis ..... 141
6.3.6 Alizarin red S (ARS) staining ..... 141
6.3.7 Alkaline phosphatase (ALP) activity assay ..... 142
6.3.8 Statistical analysis ..... 142
6.4 Results ..... 142
6.4.1 Identification of isolated broiler and layer MSCs ..... 142
6.4.2 Time- and dose-effect of L-Trp on chicken MSC proliferation ..... 145
6.4.3 Time- and dose-effect of L-Trp on chicken MSC osteogenic differentiation ..... 146
6.4.4 Effect of CaSR modulators and 1 nM $1,25(OH)_2D_3$ on chicken MSC proliferation . 154
6.4.5 Effect of CaSR modulators and 1 nM $1,25(OH)_2D_3$ on chicken MSC osteogenic differentiation ..... 155
6.5 Discussion ..... 165
**BRIDGE TO CHAPTER SEVEN ..... 171**
**CHAPTER SEVEN: MANUSCRIPT IV ..... 172**
7.1 Abstract ..... 173
7.2 Introduction ..... 174
7.3 Materials and methods ..... 177
7.3.1 Animals and housing ..... 177

7.3.2 Experimental design ..... 177
7.3.3 Data collection ..... 180
7.3.4 Egg and eggshell quality ..... 180
7.3.5 Tibia quality ..... 181
7.3.6 Ca homeostasis ..... 181
7.3.7 Statistical analysis ..... 182
7.4 Results ..... 182
7.4.1 Feed consumption, body weight, and egg production performance ..... 182
7.4.2 Egg and eggshell quality ..... 186
7.4.3 Tibia quality ..... 190
7.4.4 Ca homeostasis ..... 193
7.5 Discussion ..... 196
**CHAPTER EIGHT: GENERAL DISCUSSION ..... 201**
**CHAPTER NINE: SUMMARY AND FUTURE STUDIES ..... 207**
9.1 Summary ..... 207
9.2 Future studies ..... 208
**CHAPTER TEN: LITERATURE CITED ..... 209**

## LIST OF TABLES

**Table 4.1** Primers used in this study. ..... 56

**Table 5.1** Primers used in this study. ..... 88

**Table 5.2** Molecular docking analysis. ..... 113

**Table 6.1** Primers used in this study. ..... 138

**Table 7.1** Composition of Ca and Trp-deficient basal diet, *as fed basis* ..... 179

**Table 7.2** Feed consumption, body weight, and egg production performance in laying hens fed diets with three different levels of Ca and L-Trp from week 26 to week 29 of age ..... 184

**Table 7.3** Feed consumption, body weight, and egg production performance in laying hens fed diets with three different levels of Ca with or without a complete replacement of dietary vitamin $D_3$ (3000 IU/kg) with 25-hydroxycholecalciferol (25HyD, 75 μg/kg) from week 26 to week 29 of age ..... 185

**Table 7.4** Egg quality and egg composition in laying hens fed diets with three different levels of Ca and L-Trp from week 26 to week 29 of age ..... 187

**Table 7.5** Interaction means of relative eggshell weight and eggshell thickness in laying hens fed diets with three different levels of Ca and L-Trp from week 26 to week 29 of age ..... 188

**Table 7.6** Egg quality and egg composition in laying hens fed diets with three different levels of Ca with or without a complete replacement of dietary vitamin $D_3$ (3000 IU/kg) with 25-hydroxycholecalciferol (25HyD, 75 μg/kg) from week 26 to week 29 of age ..... 189

**Table 7.7** Tibia bone quality in laying hens fed diets with three different levels of Ca and L-Trp from week 26 to week 29 of age ..... 191

**Table 7.8** Tibia bone quality in laying hens fed diets with three different levels of Ca with or without a complete replacement of dietary vitamin $D_3$ (3000 IU/kg) with 25-hydroxycholecalciferol (25HyD, 75 μg/kg) from week 26 to week 29 of age ..... 192

**Table 7.9** Calcium homeostasis measurements in laying hens fed diets with three different levels of Ca and L-Trp from week 26 to week 29 of age ..... 194

**Table 7.10** Calcium homeostasis measurements in laying hens fed diets with three different levels of Ca with or without a complete replacement of dietary vitamin $D_3$ (3000 IU/kg) with 25-hydroxycholecalciferol (25HyD, 75 μg/kg) from week 26 to week 29 of age ..... 195

## LIST OF FIGURES

**Figure 2.1** Potential mode of calcium homeostasis in laying hens. ..... 10

**Figure 2.2** Transcellular absorption of calcium in the intestinal epithelial cell of laying hens. .. 22

**Figure 2.3** Schematic diagram of the 2D structure of chicken CaSR. ..... 26

**Figure 4.1** Schematic diagram of the chicken CaSR (cCaSR) gene exon/intron organization and protein domains..... 60

**Figure 4.2** Schematic diagram of the structure of chicken calcium-sensing receptor exported by PROTTER tool based on the protein sequence obtained from NCBI (Accession No: XP_416491.5). ..... 61

**Figure 4.3** Prediction three-dimensional model of a chicken calcium-sensing receptor disulfide-linked homodimeric extracellular domain structure based on a human calcium sensing receptor template using the SWISS-MODEL. ..... 62

**Figure 4.4** The relative mRNA abundance of chicken *calcium-sensing receptor* (*CaSR,* A) and chicken *vitamin D receptor* (*VDR,* B) in different tissues at three laying stages, and the relative mRNA abundance of *CaSR* (C) and *VDR* (D) in tibia at three different laying stages. ..... 64

**Figure 4.5** Representative western blot images (A) of chicken calcium-sensing receptor (cCaSR) and chicken vitamin D receptor (cVDR); the quantitative relative expression of cCaSR (B) and cVDR (C) in different tissues at the 40 weeks of age. ..... 66

**Figure 4.6** The relative mRNA abundance of chicken *calcium-sensing receptor* in kidney (A), proventriculus (C), duodenum (E), jejunum (G), ileum (I), colon (K), cecum (M), shell gland (O) and tibia (Q) and chicken *vitamin D receptor* in kidney (B), proventriculus (D), duodenum (F), jejunum (H), ileum (J), colon (L), cecum (N), shell gland (P) and tibia (R) at three different laying stages. ..... 67

**Figure 4.7** Haemotoxylin and Eosin (H&E) staining (1) and chicken calcium-sensing receptor (cCaSR) immunohistochemistry (2 and 3) in the kidney (A), proventriculus (B), duodenum (C), jejunum (D), ileum (E), colon (F), cecum (G), shell gland (H), and tibia (I) at the 19 weeks (a), 40 weeks (b) and 55 weeks (c) of age. ..... 73

**Figure 5.1** Identification of Flp-In™-293 cells stably expressing chicken CaSR by Western blot analysis. CAT means pcDNA™5/FRT/CAT vector was stably transfected in Flp-In™ 293 cells (transfection control). ..... 95

**Figure 5.2** Dose-effect of calcium on the viability of chicken CaSR-overexpressing Flp-In 293 cells. Cells were treated with calcium at different concentrations for 6 h. ..... 96

**Figure 5.3** Dose-effect of L-tryptophan on the viability of chicken CaSR-overexpressing Flp-In 293 cells. Cells were treated with L-tryptophan at different concentrations for 6 h. (A) Cells were incubated in the presence of 2.5 mM calcium. (B) Cells were incubated in the presence of 4.5 mM calcium. ..... 97

**Figure 5.4** Chicken CaSR response to L-tryptophan. Flp-In 293 cells stably expressed chicken CaSR were transiently transfected with vectors SRE-*luc2P*, NFAT-RE-*luc2P*, or SRF-RE-*luc2P* for 48 h. Firefly luciferase activity was measured after 6 hours induction with the addition of calcium and L-tryptophan using the dual-Glo assay system in a 96-well format. (A) $G_{\beta\gamma}$ potency ranking of different concentrations of L-tryptophan in the presence of 2.5 mM calcium, n = 4. (B) $G_{\beta\gamma}/G\alpha_i$ -mediated dose-response curve for calcium in the presence of L-tryptophan or not. n = 3. (C) $G\alpha_q$ potency ranking of different concentrations of L-tryptophan in the presence of 4.5 mM calcium, n = 4. (D) $G\alpha_q$ -mediated dose-response curve for calcium in the presence of L-tryptophan or not. n = 3. (E) $G\alpha_{12}$ potency ranking of different concentrations of L-tryptophan in the presence

of 2 mM calcium, n = 4. (F) $G\alpha_{12}$ -mediated dose-response curve for calcium in the presence of L-tryptophan or not. n = 3. ..... 99

**Figure 5.5** Effect of L-tryptophan on chicken CaSR activation. Flp-In 293 cells stably expressed chicken CaSR were transiently transfected with vectors SRE-*luc2P*, NFAT-RE-*luc2P*, or SRF-RE-*luc2P* for 48 h. Firefly luciferase activity was measured after 6 hours induction with the addition of calcium and L-tryptophan using the dual-Glo assay system in a 96-well format. (A) chicken CaSR response to different calcium concentrations in the presence of 1 mM L-tryptophan via the $G_{\beta\gamma}/G\alpha_i$ signaling pathway. (B) chicken CaSR response to different calcium concentrations in the presence of 1 mM L-tryptophan via the $G\alpha_q$ signaling pathway. (C) chicken CaSR response to different calcium concentrations in the presence of 1 mM L-tryptophan via the $G\alpha_{12}$ signaling pathway. The data were presented as mean ± SEM, n = 3..... 101

**Figure 5.6** $G\alpha_i$ -mediated dose-response curve for calcium in response to chicken CaSR activation in the presence of L-tryptophan or not reflected by forskolin-induced cAMP production. ..... 103

**Figure 5.7** Chicken CaSR response to different calcium concentrations in the presence of 1 mM L-tryptophan via the $G\alpha_i$ signaling pathway reflected by forskolin-induced cAMP production. The data were presented as mean ± SEM, n = 3. ..... 104

**Figure 5.8** Dose-effect of inorganic phosphate on the viability of chicken CaSR-overexpressing Flp-In 293 cells in the presence of calcium and 1 μM R568. Cells were treated with phosphate at the indicated concentrations for 6 h. (A) Cells were incubated in the presence of 1 mM calcium and 1 μM R568. (B) Cells were incubated in the presence of 2 mM calcium and 1 μM R568.. 105

**Figure 5.9** Dose-response curve for calcium in the presence of NPS R-568. Flp-In 293 cells stably expressed chicken CaSR were transiently transfected with vectors SRE-*luc2P*, NFAT-RE-*luc2P*, or SRF-RE-*luc2P* for 48 h. Firefly luciferase activity was measured after 6 hours incubation using

the dual-Glo assay system in a 96-well format. (A) $G_{\beta\gamma}/G\alpha_i$ -mediated dose-response curve for calcium in the presence of R568 or not. (B) $G\alpha_q$ -mediated dose-response curve for calcium in the presence of R568 or not. (C) $G\alpha_{12}$ -mediated dose-response curve for calcium in the presence of R568 or not. ..... 108

**Figure 5.10** Chicken CaSR response to inorganic phosphate. Flp-In 293 cells stably expressed chicken CaSR were transiently transfected with vectors SRE-*luc2P*, NFAT-RE-*luc2P*, or SRF-RE-*luc2P* for 48 h. Firefly luciferase activity was measured after 6 hours incubation using the dual-Glo assay system in a 96-well format. (A) Phosphate-induced $G_{\beta\gamma}/G\alpha_i$ inhibition of chicken CaSR. (B) Phosphate-induced $G\alpha_q$ inhibition of chicken CaSR. (C) Phosphate-induced $G\alpha_{12}$ inhibition of chicken CaSR. ..... 109

**Figure 5.11** $G\alpha_i$-mediated dose-response curve for calcium in response to chicken CaSR activation in the presence of NPS R-568 or not reflected by forskolin-induced cyclic adenosine monophosphate (cAMP) production. ..... 111

**Figure 5.12** The effect of chicken CaSR inhibition in response to inorganic phosphate on forskolin-induced cyclic adenosine monophosphate (cAMP) production via the $G\alpha_i$ signaling pathway. ..... 112

**Figure 5.13** The binding mode of ligands with chicken CaSR. (A) Overview of different ligands binding sites in the chicken CaSR homodimer. All binding sites are counted within one protomer. (B, C and D) Specific interactions of $Ca^{2+}$ with chicken CaSR in three different calcium binding sites. $Ca^{2+}$ ions are drawn as green spheres. (E and F) Specific interactions of phosphate with chicken CaSR in two different phosphate binding sites. Phosphate is drawn as orange sticks. (G) Binding pocket of L-tryptophan (L-Trp). (H) Surrounding residues around NPS R-568 (yellow) are shown in stick models. ..... 116

**Figure 5.14** Binding of L-tryptophan with chicken CaSR active site residues in the dynamic simulation process. 119

**Figure 5.15** Binding of NPS R-568 with chicken CaSR active site residues in the dynamic simulation process. 120

**Figure 5.16** Binding of phosphate with chicken CaSR active site residues in the dynamic simulation process. (A) Phosphate binding site 1. (B) Phosphate binding site 2. 121

**Figure 5.17** Schematic diagram of chicken CaSR signaling pathways 123

**Figure 6.1** Surface specific marker analysis of broiler and layer MSCs by real-time quantitative polymerase chain reaction in passage 1. 143

**Figure 6.2** Cell morphology at different stages and passages of broiler MSCs and layer MSCs isolated from leg compact bones. Broiler MSCs (A) passage 0 when forming obvious colonies; (B) passage 2-6 during growth; (C) passage 2-6 when reaching confluency; Layer MSCs (D) passage 0 when forming obvious colonies; (E) passage 2-6 during growth; (F) passage 2-6 when reaching confluency 144

**Figure 6.3** The proliferation rate of (A) broiler MSCs and (B) layer MSCs. Cells were treated with basal standard medium (SM, 1.8 mM $Ca^{2+}$), SM supplemented with high calcium (2.5 mM) and different concentrations of L-tryptophan (0, 0.5, 1, 2, 5, 10, 15 mM) for 1, 3, 5, and 7 days. 145

**Figure 6.4** The mRNA abundance of (A) *calcium-sensing receptor (CaSR)*, (B) *vitamin D receptor (VDR)*, and osteogenic genes including (C) *alkaline phosphatase (ALP)*, (D) *osteopontin (OPN)*, (E) *osteocalcin (OCN)*, (F) *bone morphogenetic protein 2 (BMP2)*, and (G) *runt-related transcription factor 2 (RUNX2)* during osteogenic differentiation in broiler MSCs 149

**Figure 6.5** The mRNA abundance of (A) *calcium-sensing receptor (CaSR)*, (B) *vitamin D receptor (VDR)*, and osteogenic genes including (C) *alkaline phosphatase (ALP)*, (D) *osteopontin (OPN)*,

(E) *osteocalcin (OCN)*, (F) *bone morphogenetic protein 2 (BMP2)*, and (G) *runt-related transcription factor 2 (RUNX2)* during osteogenic differentiation in layer MSCs ..... 151

**Figure 6.6** Protein expression of CaSR and VDR. (A and D) Representative western blot images of calcium-sensing receptor (CaSR) and vitamin D receptor (VDR). (B and E) The quantitative relative expression of CaSR and (C and F) VDR in broiler and layer MSCs differentiated for 7 days ..... 152

**Figure 6.7** The proliferation rate of (A) broiler MSCs and (B) layer MSCs ..... 154

**Figure 6.8** Calcium deposition and alkaline phosphatase (ALP) activity in broiler MSCs. (A) Alizarin red S (ARS) staining in broiler MSCs differentiated for 7 days. (B) Spectrophotometric quantification data of ARS staining. (C) ALP staining in broiler MSCs differentiated for 7 days. (D) Microscopic pictures of ALP staining. Scale bar represents 200 μm; (E) Microscopic pictures were quantified with mean grey value ..... 156

**Figure 6.9** Calcium deposition and alkaline phosphatase (ALP) activity in layer MSCs. (A) Alizarin red S (ARS) staining in broiler MSCs differentiated for 7 days. (B) Spectrophotometric quantification data of ARS staining. (C) ALP staining in broiler MSCs differentiated for 7 days. (D) Microscopic pictures of ALP staining. Scale bar represents 200 μm; (E) Microscopic pictures were quantified with mean grey value ..... 158

**Figure 6.10** The mRNA abundance of (A) *calcium-sensing receptor (CaSR)*, (B) *vitamin D receptor (VDR)*, and osteogenic genes including (C) *alkaline phosphatase (ALP)*, (D) *osteopontin (OPN)*, (E) *osteocalcin (OCN)*, (F) *collagen type I alpha 2 (COL1A2)*, (G) *bone morphogenetic protein 2 (BMP2)*, and (H) *runt-related transcription factor 2 (RUNX2)*, (I) *nuclear factor of activated T-cells 1 (NFATc1)*, and (J) *β-catenin (CTNNB1)* during osteogenic differentiation in broiler MSCs ..... 161

**Figure 6.11** The mRNA abundance of (A) *calcium-sensing receptor (CaSR)*, (B) *vitamin D receptor (VDR)*, and osteogenic genes including (C) *alkaline phosphatase (ALP)*, (D) *osteopontin (OPN)*, (E) *osteocalcin (OCN)*, (F) *collagen type I alpha 2 (COL1A2)*, (G) *bone morphogenetic protein 2 (BMP2)*, and (H) *runt-related transcription factor 2 (RUNX2)*, (I) *nuclear factor of activated T-cells 1 (NFATc1)*, and (J) *β-catenin (CTNNB1)* during osteogenic differentiation in layer MSCs..... 163

## LIST OF ABBREVIATIONS

| | |
|---|---|
| $1,25(OH)_2D_3$ | 1,25-dihydroxycholecalciferol |
| 25HyD | 25-hydroxycholecalciferol |
| AC | Adenylyl cyclase |
| ADFI | Average daily feed intake |
| ADH | Autosomal dominant hypocalcemia |
| AGA | aminoglycoside antibiotic |
| BSA | Bovine serum albumin |
| BW | Body weight |
| CA | Carbonic anhydrase |
| CT | Calcitonin |
| cAMP | Cyclic adenosine monophosphate |
| Ca | Calcium |
| CaSR | Calcium-sensing receptor |
| cCaSR | Chicken calcium-sensing receptor |
| cDNA | Complementary DNA |
| CRD | Cysteine-rich domain |
| cVDR | Chicken vitamin D receptor |
| DAG | Diacylglycerol |
| DMEM | Dulbecco's modified eagle medium |
| DTT | Dithiothreitol |
| ECD | Extracellular domain |

| | |
|---|---|
| $EC_{50}$ | Half-maximal effective concentration |
| EDTA | Ethylenediaminetetraacetic acid |
| ELISA | Enzyme-linked immunosorbent assay |
| EGF | Epidermal growth factor |
| ER | Endoplasmic reticulum |
| ERK1/2 | Extracellular signal-regulated kinases 1 and 2 |
| EBS | Eggshell breaking strength |
| EST | Eggshell thickness |
| ESW | Eggshell weight |
| FCR | Feed conversion rate |
| FHH | Familial hypocalciuric hypercalcemia |
| GIT | Gastrointestinal tract |
| GPCRs | G protein-coupled receptors |
| GSH | Glutathione |
| GTPases | Guanosine 5′-triphosphatases |
| HDEP | Hen-day egg production |
| HEK293 cells | Human embryonic kidney 293 cells |
| ICD | Intracellular domain |
| $IC_{50}$ | Half-inhibitory concentration |
| IP1 | Inositol monophosphate |
| IP3 | Inositol trisphosphate |
| JNK | c-Jun N-terminal kinase |
| LSM | least squares means |

| | |
|---|---|
| L-Trp | L-tryptophan |
| MAPK | Mitogen-activated protein kinase |
| mGluR | Metabotropic glutamate receptor |
| MSCs | Mesenchymal stem cells |
| NAM | Negative allosteric modulator |
| NF-κB | Nuclear factor kappa B |
| NSHPT | Neonatal severe hyperparathyroidism |
| NXC | $Na^{+}/Ca^{2+}$ exchanger |
| OPN | Osteopontin |
| PAM | Positive allosteric modulator |
| PBS | Phosphate buffer solution |
| PCR | Polymerase chain reaction |
| PDB | Protein data bank |
| $PI_3K$ | phosphatidylinositol 3-kinase |
| $PIP_2$ | phosphatidylinositol bisphosphate |
| PI-PLC | phosphatidylinositol-specific phospholipase C |
| PKA | Protein kinase A |
| PKC | Protein kinase C |
| PLC | Phospholipase C |
| PLCβ | Phospholipase Cβ |
| PMCA | Plasma membrane $Ca^{2+}$-ATPase |
| PMSF | phenylmethylsulfonyl fluoride |
| PTH | Parathyroid hormone |

| | |
|---|---|
| PTHrP | Parathyroid hormone-related protein |
| Retinoid X receptor | RXR |
| RhoA | Ras homolog family member A |
| TAL | Thick ascending limb |
| TMD | Transmembrane domain |
| TRPV | Transient receptor potential vanilloid |
| VDR | Vitamin D receptor |
| VDRE | Vitamin D response element |
| VFT | Venus Flytrap |

# CHAPTER ONE: GENERAL INTRODUCTION

Laying hens have a dynamic bone turnover associated with a daily egg-laying cycle. Because of rapid bone turnover and calcium mobilization from bones for eggshell formation, osteoporosis that involves the progressive loss of structural bone is a big challenge in the laying hen industry (Whitehead and Fleming, 2000). Osteoporosis is one of the major causes of bone fractures in laying hens. Bone fractures are associated with pain and animal welfare issues. In addition, economic factors such as egg production and eggshell quality are closely linked to issues concerning bones (Kim et al., 2012). In addition, eggshell quality has an impact on the profitability of the egg industry and food safety. Poor eggshell quality occurs mainly in the last third of the laying cycle (Lichovnikova, 2007). Calcium is one of the key nutrients required for optimal eggshell and bone quality in laying hens (Kebreab et al., 2009). Extensive research has been done on the topic of calcium in laying hens. However, most studies have focused on the effects of dietary calcium sources, requirements, particle sizes, and calcium: phosphorus ratio on laying hen performance and health (Keshavarz, 2003; Cufadar et al., 2011; Ganjigohari et al., 2018). Osteoporosis cannot be easily resolved by simply increasing dietary calcium contents and it is still the main skeletal disorder in laying hens (Fleming, 2008). Therefore, there is a need for future research to systemically understand calcium metabolism in laying hens and then to develop a method to improve calcium mobilization and utilization based on a desired calcium homeostasis in laying hens.

Calcium homeostasis refers to the constant $Ca^{2+}$ concentration in the extracellular fluid and it is maintained through feedback mechanisms involving in three classic hormones, i.e., the parathyroid hormone (PTH), the active form of vitamin $D_3$, and calcitonin as well as sex hormones in avian species by intestinal absorption, bone storage and resorption, and renal reabsorption (de Matos, 2008; Proszkowiec-Weglarz and Angel, 2013). The CaSR plays a central role in calcium

homeostasis because it can sense subtle changes in extracellular $Ca^{2+}$ and regulate PTH secretion (Conigrave, 2016). Chicken CaSR has been cloned and characterized, and it has 79% and 84% homology with human CaSR on the nucleotide and amino acid level, respectively (Diaz et al., 1997), and the in situ hybridization revealed that chicken CaSR is present in the parathyroid, kidney, brain, and small intestine (Diaz et al., 1997). The results indicated the presence of the functional CaSR in chickens with similar characteristics as mammalian CaSR, but only a few studies related to chicken CaSR have been conducted. Furthermore, it is not clear whether CaSR is expressed in the bone and shell gland in addition to its expression pattern in different tissues in laying hens.

It has been well recognized that mammalian CaSR can be activated by $Ca^{2+}$ and some other divalent and trivalent cations such as $Mg^{2+}$, $Al^{3+}$, $Sr^{2+}$, amino acids, peptides, polyamines, and artificial pharmacological calcimimetics or antagonists (Saidak et al., 2009). After activation or blockade, CaSR can selectively induce downstream G protein-coupled signaling pathways to regulate PTH secretion and further mediate calcium homeostasis (Chakravarti et al., 2012). So far, no one has systemically revealed chicken CaSR ligands and their modulation mechanisms. A cost-efficient and accurate way to find potent ligands of chicken CaSR requires a screening system that is specific to the target of chicken CaSR. As chicken CaSR has been cloned and identified in chickens (Diaz et al., 1997), screening its potent ligands can be done with an *in vitro* reporter cell system that can stably express chicken CaSR. Also, a chicken CaSR expression *in vitro* system is conducive to understanding ligand-specific downstream signaling pathways upon CaSR activation or blockade.

Bone-depositing osteoblasts form an unmineralized organic matrix consisting of collagen and a series of non-collagenous proteins and lipids which subsequently mineralize (Kerschnitzki et al.,

2014). Previous studies have suggested that a $Ca^{2+}$ sensing mechanism is present in osteoblasts and is involved in their migration and proliferation. Yamaguchi et al. (1998) demonstrated that the CaSR agonists, gadolinium, and neomycin, as well as high $Ca^{2+}$, could induce chemotaxis of mouse osteoblastic clonal cells. Exposure of primary osteoblasts or a variety of osteoblast-like cells to high levels of $Ca^{2+}$ or the polycationic CaSR agonists, neomycin, and gadolinium stimulate osteoblast proliferation, differentiation, and a matrix-mineralization capacity via activation of mitogen-activated protein kinase (Yamaguchi et al., 1998; Yamaguchi et al., 2000; Chattopadhyay et al., 2004; Dvorak et al., 2004). CaSR is involved in rat bone marrow and mesenchymal stem cell (MSC) proliferation, which has the potential for application in regenerative medicine (Martino et al., 2014; Ye et al., 2016). MSCs are multipotent stem cells that can differentiate into a variety of bone cell types including osteoblasts. However, the mechanisms by which CaSR modulators regulate the osteogenic differentiation of mesenchymal stem cells are not yet understood.

Overall, the following research gaps still need to be investigated:

1. The molecular distribution and localization of chicken CaSR and VDR in the kidney, gastrointestinal tract, shell gland, and bone, are still unclear (Study 1).

2. The potent chicken CaSR modulators are unknown. As well, the signaling cascades after chicken CaSR activation/blockade by its ligands are still unclear (Study 2).

3. The mechanisms by which CaSR modulators and 1,25-dihydroxycholecalciferol mediate proliferation and osteogenic differentiation of chicken MSCs are not yet understood (Study 3).

4. The application of CaSR modulators and vitamin $D_3$ in laying hens needs to be further illustrated (Study 4).

# CHAPTER TWO: LITERATURE REVIEW

## 2.1 Introduction

Laying hens have a high demand for calcium which is needed to form eggshells during the active egg-laying period. Calcium is the most important mineral in bone and eggshell structures. Generally, an eggshell contains approximately 2.4 g of calcium. Only 60–75% of the eggshell calcium can be provided by the feed, and the remainder must be supplied by bone storage (Mueller et al., 1964; Fleming 2008; Świątkiewicz et al., 2015). At the onset of sexual maturity, the formation of structural bone ceases, and medullary bone as a woven bone is formed to provide a labile source of calcium for shell formation (Whitehead and Fleming, 2000). After formation, laying hens experience a rapid and constant medullary bone remodeling, and this process leads to a more diffuse arrangement of medullary bone spicules throughout the marrow cavity. The decrease in the proximity between medullary bone and the structural bone surfaces results in the structural bone tissues being exposed to the effects of osteoclasts (Whitehead and Fleming, 2000; Korver, 2020). As structural bone is not replaced during egg laying period, the progressive structural bone loss/osteoporosis occurs. Osteoporosis is one of the major causes of bone fractures in laying hens. Bone fractures are associated with pain and animal welfare issues. In addition, economic factors such as egg production and eggshell quality are closely linked to issues concerning bones (Kim et al., 2012). Maintaining good eggshell quality is crucial for egg industry, as egg breakage accounts for 8-10% of total egg production and results in substantial economic losses (Ketta and Tůmová, 2016), and it meets the demands of various stakeholders, such as egg producers, processing plants, egg traders, and consumers. Better methods that can be practiced by various sectors of the egg industry are needed to mitigate osteoporosis. One of these methods is to restore or maintain the desired calcium homeostasis in laying hens so that more calcium is available for eggshell and bone formation. In this review, the way by which calcium is metabolized

and factors involved in regulating calcium homeostasis in laying hens is systematically discussed to giveinsight into the potential solutions to osteoporosis in laying hens.

## 2.2 Calcium in laying hens

### 2.2.1 Function of calcium

As with mammalian animals, calcium is an essential element and the most abundant metal in poultry. Basically, it serves two primary functions. First, calcium is the main component in building bones or eggshells. As a second function, calcium acts as a regulatory or messenger ion located in extracellular fluid or cytosol involving in a number of physiological and biochemical processes such as enzyme activity, hormone secretion, nerve conduction, blood clotting, intracellular signaling transduction, etc. (Rosol and Capen, 1996). In birds, the majority of calcium is stored in the bone as hydroxyapatite with the remaining present in the plasma membrane, cellular organelles, cytosol, and extracellular fluid (de Matos, 2008; Proszkowiec-Weglarz and Angel, 2013). There are three forms of calcium in the extracellular fluid: (1) ionized calcium; (2) calcium-containing compounds such as calcium citrate, calcium bicarbonate, and calcium lactate; (3) protein-bound calcium, accounting for 45% of total calcium, mainly to albumin and vitellogenin in birds (de Matos, 2008). Female birds go through dynamic and rapid calcium tunrover for eggshell formation during laying period. About 10% total body calcium is deposited in eggshell daily (Elaroussi et al., 1994), and the plasma ionized calcium is compleletly turned over 4 times per minute times every minute (Diaz et al., 1997). The ionized calcium ranges from 20% to 60% of the extracellular calcium in laying hens, which is about 50% in mammals (de Matos, 2008). Despite this, the ionized extracellular calcium concentration is between 1.2 mM and 1.3 mM, which is highly conserved in both mammals and poultry (Diaz et al., 1997; Proszkowiec-Weglarz and Angel, 2013). Any large shift in serum-ionized calcium is likely to have therapeutic

implications. The cytoplasm ionized calcium concentration is 10,000 times lower than the plasma ionized calcium concentration. The high concentration gradient shows the possibility that $Ca^{2+}$ can function as a signaling molecule to mediate intracellular signaling transduction and activate biological processes (Rosol and Capen, 1996). The extracellular calcium-sensing receptor (CaSR) is a homodimeric complex located in the plasma membrane of various cells, which can sense subtle changes in extracellular calcium concentration and thus induce the intracellular calcium mobilization between organelles and endoplasm and activate downstream signaling cascades to maintain calcium homeostasis. It is of biological significance to maintain calcium homeostasis via CaSR both in mammals and in poultry.

### 2.2.2 Calcium metabolism and homeostasis

Generally, calcium homeostasis is regulated through feedback mechanisms involving three classic hormones: parathyroid hormone (PTH), the active form of vitamin $D_3$, and calcitonin; as well as sex hormones (in layers), which is achieved by intestinal absorption, bone storage and resorption, and renal reabsorption (Proszkowiec-Weglarz and Angel, 2013). In addition to these pathways, the shell gland is a distinctive tissue that withdraws calcium for eggshell formation, which requires a high amount of calcium during egg-laying stages and imposes a huge extra demand on calcium homeostasis and requires several times as much calcium in the extracellular pool for eggshell calcification (Bar, 2009) (Figure 2.1).

The small intestine is the main site of calcium absorption (Bronner, 2009). Unlike in mammals, most of the calcium is absorbed between the duodenum and upper ileum, and the most effective site of calcium absorption in the laying hen is the jejunum (Hurwitz and Bar, 1966). Calcium is (re)absorbed by a transcellular active transport or a paracellular passive transport mechanism in the kidney and intestine. The active transport is a calcium transporter-dependent process, involving

three steps: entry across the brush border of the epithelium; intracellular diffusion; and extrusion at the basolateral membrane. In birds, the second and third steps are vitamin D-dependent because the calbindin$D_{28}$, plasma membrane $Ca^{2+}$ pumps (ATP2B1 and 2) and $Ca^{2+}/Na^{+}$ exchangers (SLC8A1 and 3) are regulated by a vitamin D response element (VDRE) (Nys and Le Roy, 2018). Paracellular transport depends on tight junctions. The active form of vitamin $D_3$, 1,25-dihydroxycholcalciferol [$1,25(OH)_2D_3$] is produced in the kidney because this step needs 1α-hydroxylase which is expressed predominantly in the kidney. The calcium reservoir of the medullary bone is formed with the onset of sexual maturity until shortly before the onset of egg production, which is mediated by estrogen (Whitehead, 2004). Bone resorption takes place in the medullary bone to release more calcium for eggshell formation during laying period.

Overall, maintaining calcium homeostasis is a complicated process, especially in laying birds. When plasma calcium is at a relatively low level (hypocalcemia, e.g. layers are fed a calcium deficient diet or at the laying peak), more PTH is secreted. The PTH exerts direct effects on bone and kidney and indirect effects on the intestine through vitamin $D_3$. 1α-hydroxylase is activated to produce more 1,25-dihydroxycholcalciferol [$1,25(OH)_2D_3$] in the kidney, which leads to the increase in vitamin $D_3$-dependent calcium absorption and reabsorption; and PTH also facilitates bone resorption. On the other hand, increased plasma calcium concentration (hypercalcemia) causes increased secretion of calcitonin and decreased secretion of PTH. Synthesis of $1,25(OH)_2D_3$ is also reduced, in turn resulting in decreased calcium absorption, reabsorption and bone resorption in the intestine, kidney, and bone respectively (Mundy and Guise, 1999). Hypercalcemia in birds is most often physiologic and associated with increased estrogen secretion and production of calcium-binding proteins (de Matos, 2008).

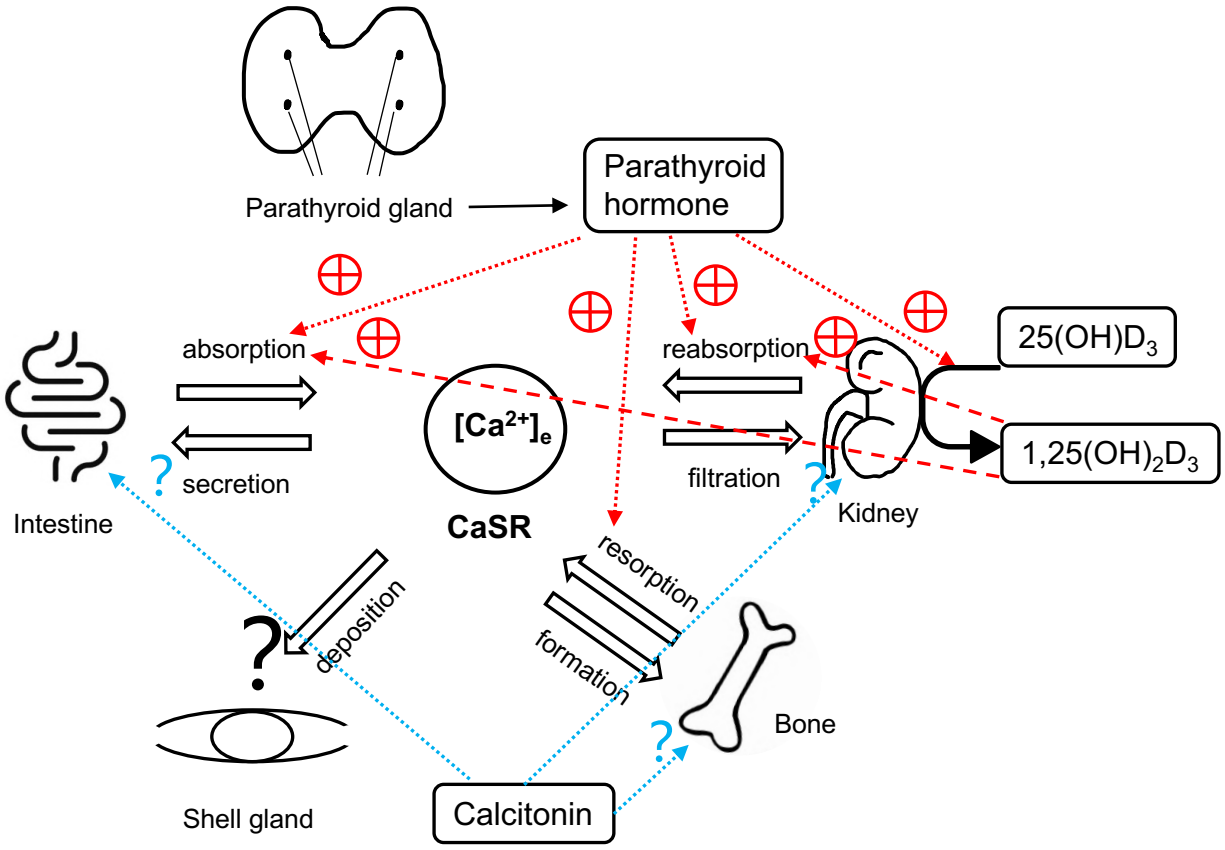


**Figure 2.1** Potential mode of calcium homeostasis in laying hens. Calcium homeostasis is regulated through feedback mechanisms involving three hormones: parathyroid hormone, active form of vitamin $D_3$ [$1,25(OH)_2D_3$], and calcitonin. Calcium homeostasis is achieved by intestinal absorption, bone storage and resorption, renal reabsorption, and shell gland withdrawal. Abbreviations: $[Ca^{2+}]_e$, $Ca^{2+}$ in extracellular fluid; CaSR, calcium-sensing receptor. "+" represents increase.

### 2.2.3 Calcium requirement

The recommended amounts of dietary calcium have been constantly adjusted over time to ensure that laying hens receive enough calcium to support eggshell formation during the laying period and to enable them to express their genetic potential. Common (1943) concluded that only about half of the ingested calcium was absorbed in laying hens according to previous studies. Peterson et al. (1960) reported that a level of dietary calcium of at least 3.4% was necessary for maximum eggshell quality. Using balance techniques, Hurwitz and Griminger (1962) estimated the calcium requirement to be between 2.4 and 3.6 g per hen per day in White Leghorn laying hens. The Subcommittee on Poultry Nutrition of the National Research Council (NRC) recommended a calcium requirement for laying hens of 2.25% and 2.75% of the diet in 1962 and 1966, respectively (NRC, 1962; NRC, 1966). Scott et al., (1971) demonstrated that the maximum production and eggshell quality were attained when the diet contains 3.5% calcium. The NRC (1984) estimated the calcium requirement to be at a constant level of 3.75 g per hen per day. Later. the NRC (1994) suggested the calcium requirement for Brown layers was 3.4% of dietary calcium for 110 g/d feed intake regardless of age. Bar et al. (2002) reported that a dietary calcium increases from 24-25 to 36-40 g/kg improved egg production, shell weight, shell thickness, and reduced mortality. Lichovnikova (2007) indicated that in the last third of production, the recommendation for calcium was 4.1 g/kg to ensure eggshell quality. Therefore, the calcium requirement recommended by the NRC (1994) seems inadequate for optimal eggshell qualities and egg production in the modern layer industry and the NRC requirement should be revised in the face of the new growth and production potential of laying hens. Nowadays, the management guide of Lohmann Tierzucht suggested that the calcium requirement for modern commercial Lohmann layers is 4-5 g per hen per day depending on the different laying stages (Lohmann Tierzucht, 2019). However, Bello and

Korver (2019) and Pongmanee et al. (2020) indicated that the current recommendations for calcium provided by the primary breeders are likely substantially higher than required by commercial laying hens. It is crucial to consider various factors such as the genetic potential, breeds, ages, laying stages, and interactions with other elements when determining the calcium requirements for laying hens.

### 2.2.4 Factors affecting calcium intake and utilization

The significance of calcium requirement in layer production can be determined by the amount of dietary calcium retained and excreted (Griminger and Lutz, 1964). Given the fact that the eggshell contains about 94% $CaCO_3$, which is equivalent to 2 grams of calcium (Ahmad et al., 2003), the eggshell quality, egg production, and size and weight of eggs are good indicators for evaluating calcium utilization. There are a number of factors that may influence the optimum level of calcium intake and utilization for laying hens: the strain of bird, laying stages, calcium sources, the particle size of calcium sources, the energy level of the diet, nutritional status, feed and feeding management, environmental conditions, and housing system.

Ahmad et al. (2003) reported that Bovanes hens (White Leghorn) required 5.57 g of calcium per hen per day for optimum performance and maximum egg production, which was higher than other commercial Leghorn hens. For Lohmann white/brown pullets before 18 weeks, the calcium requirement ranged from 0.9% to 2.5%. With the onset of laying period, the calcium requirement was increased with age from 3.8% to 4.5% (Lohmann Tierzucht, 2019). However, it is not always beneficial to further increase dietary Ca level when hens are fed adequate calcium because it may negatively affect the absorption and homeostasis of minerals (Pastore et al., 2012). Akbari Moghaddam Kakhki et al. (2019) has even reported that calcium intake beyond 4.2 g of Ca/bird/day did not lead to further improvement in eggshell thickness and decrease in eggshell

breaking strength. Previous study suggested that larger particles of $CaCO_3$ would be beneficial in most commercial egg strains (Roland, 1986). Lichovnikova (2007) reported that as a source of calcium in the last third of production, two-thirds of large particles should be included in the diet to ensure the eggshell quality. Brister Jr et al. (1981) demonstrated that replacing oyster shells with pulverized limestone improved eggshell quality no matter if the hens had an adequate calcium intake (>3.75 g/hen/day). Calcium sulfate is considered an inferior calcium source compared to calcium carbonate because excessive sulfate may cause negative effects on eggshell quality (Hurwitz and Rand, 1965). Calcium carbonate sources such as limestone, oyster shells, eggshells also show different *in vitro* solubilities as follows: fine limestone 85%, eggshells 14%, oyster shell 44%, and large limestone 49.5%, respectively (Lichovnikova 2007). Cheng and Coon (1990) reported that limestone solubility instead of particle size affected egg production and eggshell quality.

The nutritional role of calcium is closely related to the level of the dietary phosphorus and vitamin $D_3$. If the phosphorus and vitamin $D_3$ levels are inadequate, calcium utilization will be negatively affected. There is a complex relationship between calcium, phosphorus, vitamin $D_3$ and other hormones in calcium metabolism during laying (Pelicia et al., 2009). Phytic acid as an antinutritional factor is widely distributed in grains, cereals, lentils, etc., which affects dietary calcium and phosphorus availability. With phytase supplementation, the requirement of calcium and phosphorus might change. Lim et al. (2003) concluded that phytase supplementation improved egg production, but the effects of phytase were modified by dietary calcium levels. Härtel (1990) concluded that there were strong performance depressions and high mortality occurred when fed layers with the lowest phosphorus concentration and high calcium level.

Environmental factors such as temperature and lighting program influenced eggshell quality. Grizzle et al. (1992) found that increased temperatures (> 32°C) significantly reduced eggshell quality, and intermittent (midnight) lighting supplements in addition to natural daylight improved eggshell quality. Griminger and Lutz (1964) concluded that the housing system also affects the consumption of calcium supplements. Hens housed in individual cages had the highest calcium supplement consumption compared with hens housed in community cages and floor pens.

## 2.3 Modulators of calcium metabolism and homeostasis

### 2.3.1 Hormones

Calcium homeostasis is regulated via PTH, calcitonin, and the active form of vitamin $D_3$, and these three hormones have been characterized in birds (de Matos, 2008). In addition to the three classic calcium-regulating hormones, estrogen, androgens, and prostaglandins are very important for avian calcium metabolism (Bar, 2008).

PTH is an 88-amino acid peptide hormone produced by chief cells of the parathyroid gland in avian species in response to hypocalcemia (Dacke, 2000). Its structure is different from mammalian PTH which is an 84-amino acid peptide, but avian PTH exhibits a similar biological function to mammalian PTH and shares 56-65% homology in the active region (amino acid 1-34) with mammalian PTH (Dacke, 2000). The PTH exerts direct effects on bone and kidney and indirect effects on the intestine through vitamin $D_3$ (de Matos, 2008). When the plasma calcium concentration is low, PTH will be secreted and exert its function by mobilizing calcium from bone resorption; stimulating renal calcium reabsorption and $1,25(OH)_2D_3$ synthesis, intestinal calcium absorption facilitated by $1,25(OH)_2D_3$, and osteoclastic bone resorption. Its function is initiated by binding to the membrane PTH receptor (Rosenbaum et al., 2009), and the functional PTH receptor has been characterized in the chicken kidney and duodenum (Silve et al., 1982). PTH secretion is

inhibited by a feedback mechanism when plasma calcium concentration is high (Conigrave, 2016). The concentration of PTH in birds is lower compared with mammals, but it is increased during eggshell calcification. In addition, birds seem to be more sensitive to PTH than mammals, evidenced by blood calcium elevating in minutes compared with hours or days in mammals in respondse to intravenous injections of the hormone (de Matos, 2008). Parathyroid hormone-related protein (PTHrP) is a protein member of the PTH family secreted by mesenchymal stem cells. PTHrP was first discovered in human tumour tissues and recognized as a cause of malignancy-related hypercalcemia (Moseley et al., 1987; Stewart et al., 1987; Strewler et al., 1987). It has also been reported to be expressed during chicken embryologic development (Schermer et al., 1991). It shares a common receptor with PTH. The PTHrP isolated from chicken osteoclasts is associated with the inhibition of bone resorption (Moseley et al., 1987; Fenton et al., 1994). Moreover, the PTHrP level in the laying hen transiently increases when the egg moves through the oviduct, but it will gradually return to normal during the eggshell calcification period (de Matos, 2008). Avian PTHrP shares homology in the amino acid 1-34 with mammalian PTHrP (de Matos, 2008).

Vitamin D as a steroid hormone has two important forms: vitamin $D_2$ and vitamin $D_3$ (cholecalciferol). The bioactivity of vitamin $D_3$ is ten times higher than that of vitamin $D_2$ in avian species (DeLuca et al., 1988). Vitamin $D_3$ can either be ingested through the diet or synthesized in the skin from 7-dehydrocholesterol (a precursor of vitamin $D_3$) through exposure to ultraviolet light (Mundy and Guise, 1999). Then it will be converted to the active form in two steps to perform its function. First, cholecalciferol is hydroxylated at the 25 position which occurs in the liver to form 25-hydroxycholecalciferol (25HyD) by the 25-hydroxylase. This step is rapid, and it is not affected by plasma calcium concentration and other hormones (Norman, 1987). Second, 25HyD as the substrate is further hydroxylated at the C-1 position to form the active form of vitamin $D_3$,

$1,25(OH)_2D_3$, in the kidney by 1α-hydroxylase. During the second hydroxylation, $24,25(OH)_2D_3$ is the other product in the avian species, but the quantity of $24,25(OH)_2D_3$ is markedly lower than $1,25(OH)_2D_3$ (Norman, 1987). This step is regulated and affected by various factors in addition to itself via feedback inhibition. PTH, plasma calcium level, phosphorus, estrogens, prolactin, and growth hormone are all involved (de Matos, 2008). It has been reported that when hypocalcemia occurs, increased PTH secretion will cause an elevated production of $1,25(OH)_2D_3$ in the kidney and increased activity of the 1α-hydroxylase (de Matos, 2008). The predominant role of $1,25(OH)_2D_3$ in calcium homeostasis is facilitating calcium absorption via the active transcellular pathway in the duodenum and jejunum in avian species (Hurwitz and Bar, 1966; Proszkowiec-Weglarz and Angel, 2013). Previous studies reported that plasma calcium level was increased in chicks fed vitamin $D_3$-deficient diet compared to chicks fed control vitamin $D_3$ diet, and calcium mobilization in response to PTH injection was affected by vitamin $D_3$ (Gonnerman et al., 1975). Yarden et al. (2000) found an increase in plasma calcium by repletion of vitamin D-deficient chicks with a normal diet.

The chicken calcitonin (CT) gene has been isolated and sequenced. Its mRNA has two alternative splicings, coding either the precursor of calcitonin or the calcitonin gene-related protein (CGRP), and they are expressed in the ultimobranchial gland and brain, respectively (Minvielle et al., 1987). CT is secreted by the C-cells of the thyroid gland in response to hypercalcemia in mammals (Mundy and Guise, 1999). Chicken CT has been predicted to be a 32-amino acid peptide (Lasmoles et al., 1985). It is recognized that chicken CT plays a role in avian calcium homeostasis, but its precise function in different tissues has not been systemically demonstrated. Basically, CT is produced in response to high plasma calcium concentration or hypercalcemia by the inhibition of osteoclastic bone resorption (Norman and Hurwitz, 1993). The CT has been reported to circulate

at much higher levels in birds than in mammals (Dacke, 2000). Inadequate calcium included in chicken feed resulted in decreased plasma calcium concentration and CT concentration compared with chickens fed with adequate calcium (Eliam et al., 1988). In addition, Dempster et al. (1987) demonstrated that the osteoclast is not a target cell for calcitonin in the embryonic chick. Krzysik-Walker et al. (2007) confirmed the expression of CT in the chicken ovary and indicated ovarian CT was possibly involved in regulating follicular maturation.

### 2.3.2 Vitamin D receptor (VDR)

The $1,25(OH)_2D_3$-dependent gene can be transcribed when $1,25(OH)_2D_3$ binds to the intracellular VDR because it will trigger the formation of a heterodimer of the VDR with a partner protein retinoid X receptor (RXR). The heterodimer RXR-VDR-$1,25(OH)_2D_3$ complex then binds to the VDRE located in the promoter region of target genes, thereby activating the transcription (Bar, 2008). Several genes related to calcium transport and calcium metabolism have the VDRE sequence, including PTH, PTH-related proteins, calbindins, calcium ion channels, 24-hydroxylase, osteopontin, osteocalcin, CaSR, etc. (Bar, 2008; Proszkowiec-Weglarz and Angel, 2013). Human VDR complementary DNA (cDNA) was first isolated and cloned from the human intestine, and it has been demonstrated to belong to the steroid-receptor gene family (Baker et al., 1988). The cDNA of avian VDR was then cloned, and two vitamin D receptor mRNAs are 2.6 and 3.2 kb long, respectively (McDonnell et al., 1987). The mRNA of mammalian VDR is longer than that of avian species, but the encoded N-terminal of avian VDR is longer (Lu et al., 1997). Chicken VDR has been documented in various tissues such as the intestine (Lu et al., 1997), kidney (Lu et al., 1997), muscle (Zanello et al., 1997), shell gland (Yoshimura et al., 1997), bone (Pedrozo et al., 1999), and parathyroid gland (Garfia et al., 2002). In chicken, the expression of VDR is associated with sexual maturation and enterocyte differentiation (Wu et al., 1994). Moreover, chicken VDR is

distributed in the mucosal epithelium and tubular gland cells in the shell gland, and its expression is increased during sexual maturation and keeps even during molting (Yoshimura et al., 1997).

### 2.3.3 Calcium-sensing receptor (CaSR)

The CaSR is a homodimeric complex located in the cell membrane, and it belongs to the metabotropic glutamate receptor (mGluR) subclass of G-protein coupled receptors (GPCRs) superfamily (Jensen and Brauner-Osborne, 2007). The CaSR can sense subtle changes in extracellular calcium concentration and thus mediate PTH secretion to maintain calcium homeostasis via regulating intestinal absorption, bone storage and exchange, and renal reabsorption (Conigrave, 2016). In addition, the CaSR mediates a variety of physiological and pathophysiological processes such as ion channel activity, gene expression, inflammation, proliferation, differentiation, and apoptosis via inducing downstream signaling cascades. Since the extracellular CaSR was first cloned and characterized from the bovine parathyroid (Brown et al., 1993), it has drawn more attention because of its versatile roles in biological processes. It has been reported that the CaSR is widely expressed in multiple tissues including the parathyroid gland, kidney, bone, and gastrointestinal tract (GIT) in the human (Garrett et al., 1995), rat (Riccardi et al., 1995), rabbit (Butters JR et al., 1997), mouse (Oda et al., 2000), dog (Skelly and Franklin, 2007), and cat (Gal et al., 2010). The poultry CaSR was first cloned and identified from a chicken parathyroid gland (Diaz et al., 1997). The gene expression of the chicken CaSR in the kidney, parathyroid, small intestine, oviduct, and brain has also been verified (Deng et al., 2010). Notably, chicken CaSR was the first non-mammalian CaSR to be cloned and characterized. However, it still needs to be confirmed if the CaSR is present in shell gland and bone in laying hens.

### 2.3.4 Calcium transport-related proteins

#### 2.3.4.1 Proteins involved in the active transcellular pathway and passive paracellular pathway

Calcium transport in the female avian species is associated with calcium reabsorption, absorption, and withdrawal in the kidney, intestine, and shell gland, respectively. Like mammals, calcium is transported across the epithelium by an active transcellular pathway or a passive paracellular pathway in birds (Hurwitz, 1989), but the main calcium transport mechanisms in different tissues are distinct in birds (Bar 2009; Nys and Le Roy, 2018). In the kidney, calcium reabsorption is mainly achieved by passive paracellular transport, while the calcium withdrawal from plasma to shell gland fluid is mediated predominately by the active transcellular pathway (Nys and Le Roy, 2018). In the intestine, calcium absorption occurs mainly in the proximal intestine (Hurwitz and Bar, 1966), but the transport mechanism depends on the concentration of calcium in the gut lumen (Nys and Le Roy, 2018). Transcellular calcium transport involves three steps:

(1) Calcium enters the intestinal epithelium across the brush border membrane, which is facilitated by calcium channels transcription of transient receptor potential vanilloid 5 (TRPV5) or TRPV6 transporters. In mammals, TRPV5 and TRPV6 belong to the transient receptor potential (TRP) superfamily, vanilloid (V) subfamily, and they share 75% homology at the amino acid level (den Dekker et al., 2003). Both are expressed in the intestine and kidney, which are related to calcium transport and (re)absorption (Nijenhuis et al., 2005). Several studies have illustrated that the relative mRNA abundance of TRPV5 and TRPV6 varies in different tissues, and it is also different among species (Hoenderop et al., 2001; Weber et al., 2001). Generally, TRPV5 seems to be expressed mainly in the kidney, but TRPV6 shows higher expression in the small intestine in

mammals (den Dekker et al., 2003). Differently, in laying hens, it has been demonstrated that TRPV6 is expressed in the kidney, all intestinal segments, and shell gland (Yang et al., 2011; Yang et al., 2013), whereas the distribution and localization of TRPV5 hasnot yet been studied. Step one is rate limiting because the transcription of TRVP5 and 6, are regulated by different dietary calcium levels, and meanwhile, the gene expression of TRPV5 and 6 is vitamin $D_3$-dependent in humans (Bronner, 2003), but the presence of VDRE in TRPV6 in laying hens is still unclear (Nys and Le Roy, 2018).

(2) Calcium is translocated in the cytoplasm through binding to calcium-binding protein (calbindin$D_{28k}$ and calbindin$D_{9k}$). Unlike mammalian intestinal and renal tissues, where two types of calcium-binding protein calbindin$D_{28k}$ and calbindin$D_{9k}$ are expressed, calbindin$D_{28k}$ is the extremely predominant calcium-binding proteins compared to calbindin$D_{9k}$ in the avian intestine (Bar, 2009). Calbindin$D_{28k}$ has been reported to be expressed in the intestine, kidney, and shell gland in poultry (Wasserman and Taylor, 1966; Taylor and Wasserman, 1972; Bar et al., 1992). Different laying stages and egg laying cycles affect the expression of Calbindin$D_{28k}$ in the intestine and shell gland (Bar et al., 1992), and the distribution of calbindin proteins is positively correlated to $Ca^{2+}$ transport (Bar, 2009). Also, in the intestine, kidney, and shell gland, calbindins are identical: three variants of mRNA encode a major and two minor transcripts, but each of them codes for the same calbindin $D_{28k}$ consisting of 261 amino acids (Bar, 2009). Calbindin $D_{28k}$ is vitamin $D_3$-dependent, and it is the most extensively studied one among calcium transport proteins (Bar, 2009; Nys and Le Roy, 2018). Both gene expression and synthesis of calbindin $D_{28k}$ are affected by $1,25(OH)_2D_3$ in the chicken intestinal epithelial cells (Bar et al., 1990). In addition, the expression of TRVP6 and calbindin $D_{28k}$ is regulated by estrogen, which is probably attributed to the high requirement of calcium in female birds during laying (Bar, 2009).

(3) Extrusion at the basolateral membrane is mediated by the plasma membrane $Ca^{2+}$-ATPase (PMCA) and $Na^{+}/Ca^{2+}$ exchangers (NCXs) (Nys and Le Roy, 2018). This process is against the electrochemical gradient and thus it is energy dependent. PMCAs have more than 30 isomers. Among those, PMCA1b is the most predominant isomer expressed in mammalian and the chicken intestine and kidney (Bar, 2009). PMCA has been cloned and characterized in different segments of the chicken intestine (Cai et al., 1993). It has been reported that the VDRE was found in the promoter region of the human PMCA1 gene, and its transcription was mediated by $1,25(OH)_2D_3$ (Glendenning et al., 2000). The gene expression of chicken PMCA is also regulated by $1,25(OH)_2D_3$, as shown by an upregulation in its expression in the vitamin $D_3$-treated group compared to the vitamin $D_3$-depleted group, as reported by Cai et al. (1993). A few studies have supported the idea that estrogen regulates the gene expression and activity of PMCAs in mice (Van Cromphaut et al., 2003). PMCA in the shell gland of laying hens has been found in the apical-microvillar membrane of tubular gland cells facing the shell gland lumen instead of in the basolateral membrane (Bar, 2008). However, PMCA in the shell gland was not, or was only slightly regulated by $1,25(OH)_2D_3$ (Nys and De Laage, 1984; Grunder et al., 1990). Thinning eggshell induced by chlorophenylethylene is associated with decreased PMCA activity in birds, which demonstrated that PMCA is important for maintaining eggshell integrity and quality (Lundholm, 1997). The NCXs consist of three members NCX1, NCX2, and NCX3 in mammals (Lytton, 2007). NCX1 is the most important and predominant subtype among them, which is widely expressed in various tissues and organs such as the brain, heart, kidney, and GIT, and facilitates calcium (re)absorption (Liao et al., 2019). Like mammals, NXC1 is also expressed in the chicken intestine, and the protein and gene expression are regulated by $1,25(OH)_2D_3$ in vitamin D-deficient chicks (Centeno et al., 2011). As for calcium reabsorption in the kidney, NXC1 is

involved mainly in basolateral calcium efflux (Lytton, 2007). The PMCA and NXCs are also vitamin $D_3$-dependent (Bar, 2009; Nys and Le Roy, 2018).

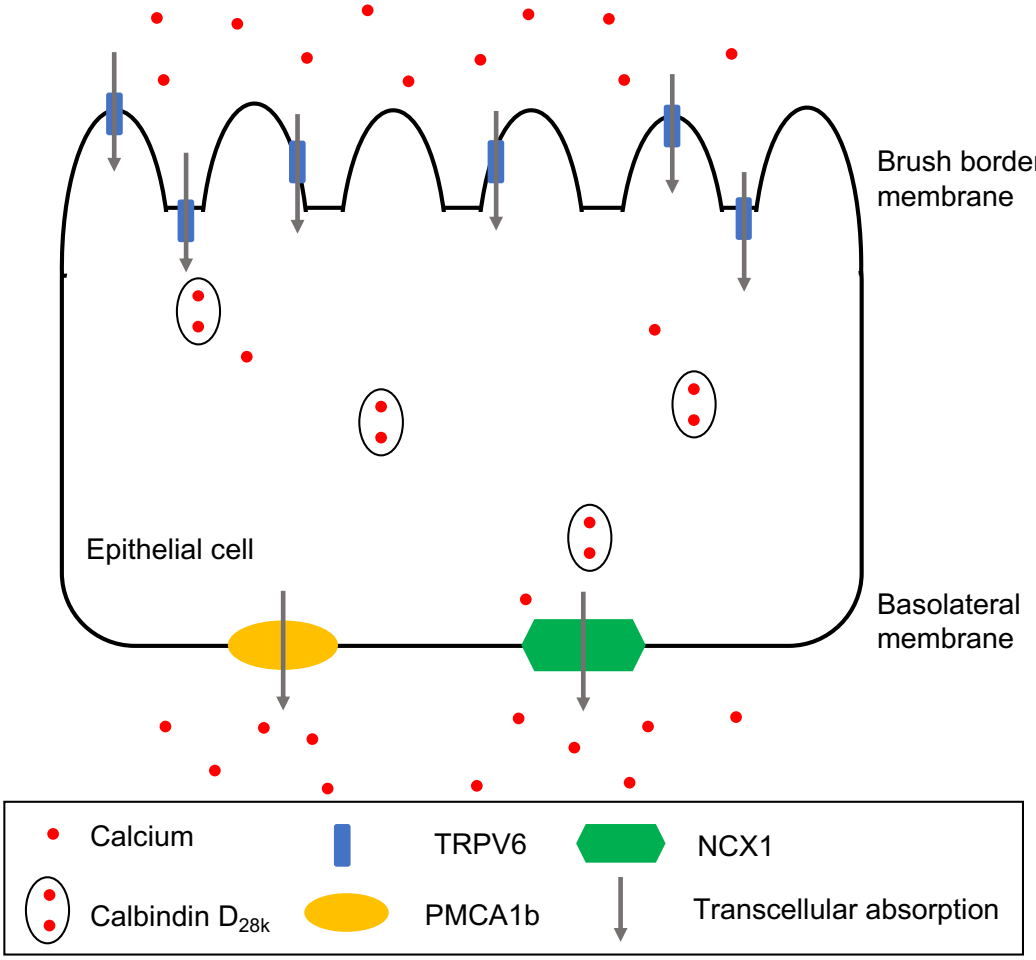


**Figure 2.2** Transcellular absorption of calcium in the intestinal epithelial cell of laying hens.

When calcium intake is high, or calcium concentration is saturated, paracellular calcium transport accounts for a substantial fraction throughout the length of the intestine (Bar, 2009). This process is driven by a luminal electrochemical gradient between blood plasma and the intestinal lumen (+ 5 to + 15 mV) and facilitated by tight junctions between adjacent epithelial cells. The integrity and tightness of the intestinal barrier are important for normal paracellular calcium transport. Some evidence has supported that $1,25(OH)_2D_3$ can promote paracellular calcium diffusion by increasing junction ion permeability and regulating the expression of tight junction proteins (Kutuzova and DeLuca, 2004; Fujita et al., 2008).

#### 2.3.4.2 Proteins associated with calcium transfer in the shell gland

Shell gland glandular cells transfer a large amount of calcium into the shell gland lumen against the concentration gradient with a 1.2-1.3 mM of $Ca^{2+}$ concentration in plasma and 6-10 mM in the lumen of the shell gland fluid depending on the stage of eggshell calcification (Nys and Le Roy, 2018). The electrochemical potential difference and the discontinuity of calcium secretion are harmful to passive transcellular calcium transport to the shell gland lumen. Instead, active transcellular calcium transport is predominant (Nys and Le Roy, 2018). Paracellular pathways for calcium transport in the shell gland have not yet been demonstrated.

The shell gland develops the ability to transfer large amounts of $Ca^{2+}$ and $HCO_3^-$ ions which serve as mineral precursors for the formation of eggshell $CaCO_3$ (Nys and Le Roy, 2018). In addition to the proteins mentioned in the calcium transport in the intestine, carbonic anhydrase (CA) and osteopontin (OPN) are two distinct groups of proteins involved in calcium transport in the shell gland. The CAs are a group of zinc-containing enzymes that catalyze the reversible hydration of carbon dioxide to bicarbonate. The transfer of calcium occurs mainly via the uterine glandular cells, and CAs are widely distributed in uterine glandular cells to support ion transport

under acidic conditions. At least four distinct gene families encode them, and at least 16 different α-CA isoforms have been identified in mammals (Supuran, 2008). CA2 isozymes have also been purified in avian tissues including the kidney, bone, intestine, and shell gland (Gay and Mueller, 1974; Holmes, 1977; Gabriella and Menghi, 1994). VDRE has been found in the promoter region of the CA2 gene (Quélo et al., 1994), and vitamin $D_3$ has been found to affect the CA activity in the shell gland of laying hens (Grunder et al., 1990). OPN is a glycosylated, highly phosphorylated protein, which is expressed in various tissues including the bone (Nakamura et al., 2003) and shell gland (Pines et al., 1995). It has been reported that OPN is involved in bone remodeling and affects the migration and maturation of osteoclast precursors and osteoclast activity (Bar, 2009). The expression of OPN is correlated with the shell calcification cycle, which means that the highest expression was found at the peak of eggshell formation in the shell gland (Pines et al., 1995). Also, its expression was regulated by growth factors and hormones like $1,25(OH)_2D_3$ (Han et al., 2003). However, the definitive function of OPN during eggshell formation has not been fully researched.

**2.4 Structure-function relationships of calcium-sensing receptor**

The cDNA of human CaSR is 3255 bp that encodes 1085 amino acids (Garrett et al., 1995), and its gene spans ~103 kb containing eight exons (Yun et al., 2007). The gene expression is closely related to transcription, and the transcription of human CaSR is driven by two promoters P1 and P2, with P2 being more active than P1. As VDRE is also located in the P1 and P2, the gene expression of human CaSR is regulated by $1,25(OH)_2D_3$, which has been verified (Canaff and Hendy, 2002). Chicken CaSR shares 79% and 84% homology with human CaSR on the nucleotide and amino acid levels, respectively (Diaz et al., 1997). The cDNA of chicken CaSR is 3177 bp which encodes 1059 amino acids (Diaz et al., 1997). Similar to human CaSR, as shown in Figure 2.2, chicken CaSR consists of three domains: a large hydrophilic N-terminal extracellular domain

(ECD) comprising 611 amino acids; a hydrophobic seven helical transmembrane domain (TMD) comprising 249 amino acids; and a hydrophobic C-terminal intracellular domain comprising 198 amino acids, which is slightly shorter than the human homologue (*vs*. 250 amino acids) (Diaz et al., 1997). Among that, the non-conserved segments are concentrated in an N-terminal 19-amino acid signal peptide and an intracellular domain (ICD) C-terminal tail which is involved in the G protein coupling signaling. The highly conserved region is between amino acids 24 and 308 in the ECD, especially between 91-250, presenting a completely uniform sequence, which is equivalent to the mGluR (Diaz et al., 1997). This highly conserved area might be related to maintaining CaSR function, which is evidenced by the fact that the mutation sites of mutations of the human CaSR associated with calcium homeostatic disorder hypercalcemia are located within this region (Aida et al., 1995). Similar to other mGluRs, human CaSR performs biological functions as a disulfide-linked homodimer. It contains 11 potential N-linked glycosylation sites: eight glycosylation sites are used and associated with the different forms of CaSR; the other three are not used so they do not affect CaSR signaling (Hendy et al., 2013). A western blot analysis using human CaSR-transfected HEK293 cells demonstrated four molecular forms of wild-type CaSR because of N-linked glycosylation: non-glycosylated monomer (~120 kDa), which is rarely detected in the absence of MG132 (an inhibitor of proteasome degradation); immaturely core-glycosylated, high-mannose monomer (~140 kDa), which is predominantly present in the ER; maturely glycosylated monomer (~160 kDa) present in the Golgi complex; and dimers (>280 kDa) (White et al., 2009).

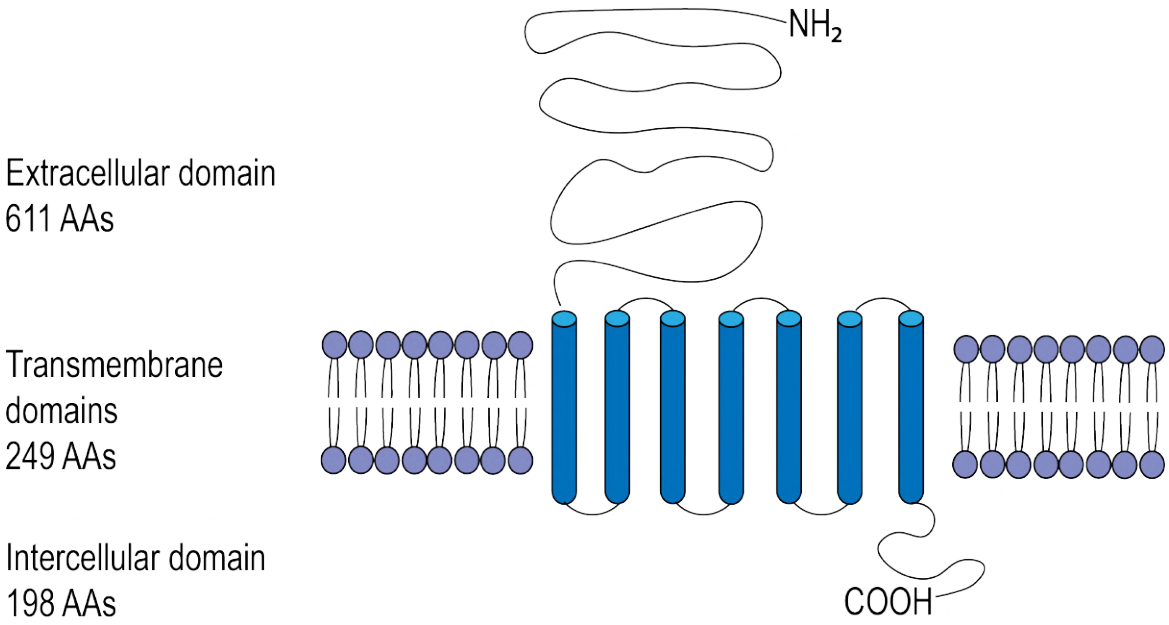


**Figure 2.3** Schematic diagram of the 2D structure of chicken CaSR.

### 2.4.1 Extracellular domain (ECD)

Ligand binding induces large conformational changes within the CaSR ECD homodimer. As reported in the human CaSR, the ECD of CaSR consists of a Venus Flytrap (VFT) module comprising two domains (Lobe1 and Lobe 2, 507 amino acids) and a cysteine-rich (CR) domain (57 amino acids) (Hu et al., 2001). The three-dimensional crystal structure of the entire ECD of the human CaSR in active and inactive states has been revealed (Geng et al., 2016). In both states, the two protomers interact side by side with facing opposite to each other. In fact, $Ca^{2+}$ binding alone cannot fully activate CaSR since CaSR remains in an inactive state regardless of the presence or absence of $Ca^{2+}$. Instead, CaSR is only transformed into the active state when an amino acid binds to the ECD (Geng et al., 2016). In the inactive-state structure, the two protomers present an open conformation with only one $Ca^{2+}$ binding to each protomer in Lobe 1. In the active structure, the two protomers exhibit a closed conformation by contacting both Lobe 1 and Lobe 2 with an L-amino acid binding to the cleft between Lobe 1 and Lobe 2, while $Ca^{2+}$ was bound to four sites of the VFT. The actions of $Ca^{2+}$ and amino acids on CaSR are interdependent, and they act as co-agonists to activate CaSR. Geng et al. (2016) first identified the four distinct $Ca^{2+}$ binding sites. Among the four sites (named 1 to 4) within one protomer, site 1 is located in a loop region at the top of the Lobe 1 domain, and $Ca^{2+}$ is supported by backbone carbonyl oxygen atoms of I81, S84, L87, and L88. Site 2 is positioned directly above the interdomain cleft in the Lobe1 domain, and it abuts the L-amino acid binding site in the cleft. The shared $Ca^{2+}$-binding mode at site 2 between the inactive and active structures suggests that the $Ca^{2+}$ bound at this site is an integral component of the CaSR structure. Site 3 is positioned at the edge of the interdomain cleft in Lobe 2 domain, and the $Ca^{2+}$ is coordinated by the hydroxyl groups of S302 and S303 either directly or indirectly through water molecules. Site 4 is part of the homodimer interface formed upon agonist binding,

bridging the Lobe 2 domain and CR domain, and the $Ca^{2+}$ ion is coordinated by three interfacial residues, including the carboxylate group of D234 and the carbonyl oxygen of E231 and G557 (Geng et al., 2016). The binding sites of anions ($PO_4^{3-}$ and $SO_3^{2-}$) were also found in the ECD of human CaSR (Geng et al., 2016). The active state is stabilized by $Ca^{2+}$, whereas the inactive conformation is reinforced by $PO_4^{3-}$ (Geng et al., 2016).

### 2.4.2 Transmembrane domain (TMD)

So far, the structures of full-length human (Ling et al., 2021) and chicken CaSR (Wen et al., 2021) have been revealed and demonstrated. Therefore, the confirmational changes in TMD upon ligand ($Ca^{2+}$ and L-Trp) binding to human and chicken CaSR are understood. It has been reported that the presence of $Ca^{2+}$ is necessary for the complete activation of human CaSR binding to L-Trp because $Ca^{2+}$ binding relays the conformational changes from ECD and further leading to the closure of two TMDs of dimeric CaSR (Ling et al., 2021). Wen et al. (2021) found out the binding modes of the positive modulator (evocalcet) and the negative allosteric modulator (NPS-2143) and chicken CaSR by cryo–electron microscopy. More structural mechanisms of activation of CaSR by different ligands are still to be revealed. It has been hypothesized that the conformational structure of helix 3 and 4 in the TMD might be altered after ligand activation (Wess, 1997). A843E mutation is the only mutation that has been identified to result in the activation of CaSR and it might alter the conformation of the TMD to promote G protein coupling (Zhao et al., 1999). The intracellular loop of TMD has been examined to be closely related to G protein-mediate signaling, especially L704 and F707 located in the second intracellular loop; L798, N802, and A804 located in the third intracellular loop (Chang et al., 2000). C677 and C765 in the first and second extracellular loops of the CaSR play an important role in maintaining the conformation of the CaSR (Ray et al., 2004).

### 2.4.3 Intracellular domain (ICD)

The ICD C-terminal tail is involved in the various functions of CaSR including cell surface expression, maintaining calcium homeostasis, and G protein-mediated cell signaling (Ray et al., 1997). It has been identified that the mutation at T876 caused hypercalcemic disorders, familial hypocalciuric hypercalcemia (FHH), and neonatal severe hyperparathyroidism (NSHPT) related to calcium homeostasis, and it also led to the decreased cell surface expression compared to the wild-type CaSR (Bai et al., 1997). Moreover, based on the relevant studies, researchers have confirmed and concluded that the proximate membrane region of ICD is critical for cell surface expression and G protein-mediated cell signaling (Gama and Breitwieser, 1998; Chang et al., 2001; Gal et al., 2010). A mutant truncated after S895 or R929 still exhibits a similar level of Gq signaling characteristic to that of wild-type CaSR, but two-point mutations at H880 and F882 lose 50-70% Gq signaling function (Chang et al., 2001). More recently, a novel naturally occurring deletion mutation related to autosomal dominant hypocalcemia (ADH) in the ICD has been found to inhibit signal transduction (Obermannova et al., 2016). In addition to the T888 mutant that inhibits the protein kinase C (PKC)-mediated phosphorylation of CaSR, the S875 mutant also shows the missing function of PKC phosphorylation, which suggests that T888 in tandem with S875 together control the function of CaSR and maintain calcium homeostasis (Binmahfouz et al., 2019).

## 2.5 Intracellular signaling via coupling with heterotrimeric G proteins

### 2.5.1 Heterotrimeric G Proteins

The intracellular CaSR signaling is known to be coupled with several heterotrimeric G proteins. According to the Gα subunit, they can be classified into four groups: $G_{q/11}$, $G_{i/o}$, $G_{12/13}$, and $G_s$ (Chakravarti et al., 2012). Gα protein subunit dissociates from βγ dimeric subunit, thereby

initiating a cascade of downstream signaling pathways and eventually inducing target gene transcription. It has been reported that CaSR activation by its agonist divalent cations induces intracellular calcium mobilization and inhibits cyclic adenosine monophosphate (Campbell and Smrcka) production via $G_{i/o}$ and $G_{q/11}$-mediated pathways in the bovine parathyroid cells (Chen et al., 1989). The $G_{12/13}$-mediated pathway induced by CaSR has also been confirmed to activate Rho and phospholipase D (PLD) and it works independently of $G_{i/o}$ and $G_{q/11}$ in Madin-Darby canine kidney cells. Overall, CaSR is capable of coupling with various G protein pathways: $G_{i/o}$ is involved in inhibiting the activity of adenylyl cyclase (AC) to suppress cyclic adenosine monophosphate cAMP generation and activate extracellular-signal-regulated kinase (ERK); $G_{q/11}$ stimulates phosphatidylinositol-specific phospholipase C (PI-PLC), and thus regulates inositol trisphosphate ($IP_3$) production, $Ca^{2+}$ mobilization, and activates protein kinase-C (PKC); $G_{12/13}$ stimulates PLD by activating the Rho family of small G proteins; and $G_{\beta\gamma}$ can also independently activate phosphatidylinositol 3-kinase ($PI_3K$) (Arthur et al., 1997; de Jesus Ferreira et al., 1998; Hart et al., 1998; Kifor et al., 2001).

### 2.5.2 Intracellular $Ca^{2+}$ mobilization

Intracellular $Ca^{2+}$ level increases after CaSR activation by its agonists such as $Ca^{2+}$ has been found in a variety of cell types via a $G_{q/11}$-mediated pathway (Brennan and Conigrave, 2009). In this signaling pathway, $G_{q/11}$ first activates PI-PLC, and then PI-PLC will hydrolyze its substrate, phosphatidylinositol bisphosphate ($PIP_2$) to produce $IP_3$ and diacylglycerol (DAG). $IP_3$ binding to high-affinity receptors induces the intracellular $Ca^{2+}$ release from cytoplasmic stores primarily in the ER and $Ca^{2+}$ oscillations. After the transient $Ca^{2+}$ release from the ER, the calcium transport channels like TRPC channels are activated to support the influx of extracellular calcium (Gees et al., 2010). Among these channels, TRPC1 has been documented to be involved in the CaSR-

activated calcium oscillations in human colonic epithelial cells (Rey et al., 2010). In the meantime, intracellular $Ca^{2+}$ concentration varies with oscillation frequency and extracellular $Ca^{2+}$ concentration (Conigrave and Ward, 2013). Oscillatory signaling is important in biology when downstream responses require a threshold amplitude or frequency or both (Conigrave and Ward, 2013). CaSR coupling to a $G_{q/11}$-mediated pathway has been recognized to inhibit PTH secretion. It has been confirmed that mice with both $G_q$ and $G_{11}$ double knock-out in parathyroid cells cannot suppress the PTH secretion by a feedback mechanism, and that they showed the same phenotypes as CaSR null mice, including hypercalcemia, hyperparathyroidism, relative hypocalciuria, skeletal abnormalities, retarded growth, and early postnatal death (Wettschureck et al., 2007; Rey et al., 2010). The chemotaxis and mitogenesis of MC3T3-E1 osteoblasts are PLC-dependent via a Gq-mediated pathway after CaSR activation (Godwin and Soltoff, 1997; Godwin and Soltoff, 2002).

### 2.5.3 Intracellular cAMP changes

The CaSR activation inhibits the activity of AC, thereby suppressing the production of cAMP via a $G_{i/o}$-mediated pathway or increasing the intracellular $Ca^{2+}$ via a $G_{q/11}$-mediated pathway to indirectly inhibit cAMP synthesis because elevated intracellular $Ca^{2+}$ concentration can inhibit the activity of AC isoforms (type 5, 6 and/or 9) or stimulate cAMP hydrolysis by activating phosphodiesterases (Chakravarti et al., 2012). Interestingly, elevated intracellular $Ca^{2+}$ concentration was also found to stimulate cAMP production and cyclooxygenase 2 expression in primary mouse osteoblasts via a PKA pathway, but the underlying mechanism is unknown (Choudhary et al., 2004). Suppression of cAMP levels accompanies high extracellular $Ca^{2+}$ concentration-induced suppression of PTH secretion in parathyroid cells (Brown et al., 1979a). This is an inhibitory mechanism that prevents hypercalcemia and PTH release via CaSR activation. However, the cAMP level can be also increased via $G_s$-mediated CaSR activation (through switch

bias from $G_i$ to $G_s$) in cancer cells such as breast cancer cells (Mamillapalli et al., 2008) and pituitary tumor cells (Mamillapalli and Wysolmerski, 2010). Mamillapalli et al. (2008) also reported that CaSR activation increased PTHrP production in immortalized murine mammary cells and human breast cells, indicating that the malignant transformation of breast epithelial cells can cause a reversal in the typical suppression of PTHrP by CaSR activation due to a change in G-protein coupling. It has not yet been clarified if the $G_s$-mediated pathway is related to the pathogenesis of all cancers. $G_{12/13}$ is also involved in CaSR-mediated stimulation of cAMP synthesis by the same mechanism that AC7 is activated (Jiang et al., 2008).

### 2.5.4 PKC activation

DAG, $PIP_2$ hydrolysate catalyzed by PI-PLC, in combination with $G_{q/11}$-mediated elevation of intracellular $Ca^{2+}$ concentration, activates PKC isoforms (PKCα, $\beta_I$, $\beta_{II}$, and γ), and DAG can also activate other PKC isoforms (PKCs δ, ε, η, and θ) independently (Chakravarti et al., 2012). It has been reported that the mutation of CaSR T888 (primary PKC phosphorylation site) to a non-phosphorylatable methionine causes autosomal dominant hypocalcemia in humans, suggesting that the PKC phosphorylation site of CaSR is important for regulating CaSR function and maintaining calcium homeostasis (Syndia et al., 2011). In addition to CaSR T888, which is recognized as a determinant PKC phosphorylation site, T646 and S794 in the first and third intracellular loops, and S895 and S915 in the ICD, are all PKC phosphorylation sites (Garrett et al., 1995; Bai et al., 1998). Furthermore, the NetPhos database predicts that CaSR has as many as 15 potential PKC phosphorylation sites including S875 (Binmahfouz et al., 2019). PKC is a feedback modulator of CaSR signaling, which can inhibit the PI-PLC pathway by phosphorylating the CaSR and uncoupling the CaSR from $G_q$ (Kawabata et al., 1996; Codazzi et al., 2001), or by phosphorylation of the PLCβ, which inhibits the $G_q$-mediated $IP_3$ production and $Ca^{2+}$ mobilization

(Kifor et al., 1990; Yue et al., 2000). In addition, PKC can also lower intracellular $Ca^{2+}$ concentration by accelerating $Ca^{2+}$ efflux (Usachev et al., 2002). PKC is important for activating downstream mitogen-activated protein kinases (MAPK) including extracellular signal-regulated kinases 1 and 2 (ERK1/2), c-Jun amino-terminal kinases (JNK), and p38 (Conigrave and Ward, 2013).

### 2.5.5 MAPK activation

MAPKs are involved in the intracellular signaling cascades in response to the extracellular stimulations via various receptors. Three subfamilies of MAPKs have been characterized in vertebrates: ERK, JNK, and p38 (Krens et al., 2006). ERK1/2 (Suh et al., 2009), p38 (Schmidpeter and Schmid, 2014), and JNK (Ishikawa et al., 1997) in chicken have been found. As mentioned above, ERK1/2 lies downstream of $G_{q/11}$-activated PKC, and MAPK can also be activated via the $G_{i/o}$-mediated pathway as well as the activation of β-arrestin in bovine parathyroid and CaSR-transfected HEK293 cells (Kifor et al., 2001). In addition, ERK phosphorylation by the CaSR is dependent on the tyrosine kinases-mediated pathway via tyrosine kinase-Ras-Raf-MEK-ERK (Koch et al., 1994). In this pathway, Ras activation was firstly mediated by $G_{\beta\gamma}$ followed by $G_{i/o}$-mediated ERK phosphorylation via subsequent signaling (Koch et al., 1994). One of the tyrosine kinases, SRC kinase, lies upstream of MAPK activation in response to CaSR stimulation in rat fibroblasts (McNeil et al., 1998). The other type of tyrosine kinases is transactivated receptor kinases such as epidermal growth factor (EGF), and ERK is phosphorylated by CaSR transactivating the EGF receptor (MacLeod et al., 2004).

### 2.5.6 Rho activation

The Rho family of small molecular weight guanosine-5'-triphosphatases (GTPases) mediate responses to $G_{q/11}$- and $G_{12/13}$-coupled GPCRs. $G_{12/13}$-mediated signaling activates PLD by the

CaSR stimulation, which produces phosphatidic acid by activating Rho (Huang et al., 2004). Biological actions of Rho, acting downstream of the CaSR, include regulation of cell-cell adhesion (Tu et al., 2008) and $G_q$-mediated intracellular $Ca^{2+}$ oscillations (Rey et al., 2005) and activation of choline kinase and phosphatidylinositol 4-kinase ($PI_4K$) (Huang et al., 2002), etc. Rho is also involved in actin stress-fiber assembly, which is important in constructing specific signaling scaffolds. The cytoskeletal actin-binding protein filamin acts as a scaffolding protein to bind CaSR for downstream signaling cascades (Awata et al., 2001) because filamin also interacts with Rho GEF Lbc, which mediates Rho activation (Pi et al., 2002). In addition, filamin has been demonstrated to participate in CaSR-mediated activation of MAPK ERK1/2 (Hjälm et al., 2001).

### 2.6 Calcium-sensing receptor modulators

There are two categories of CaSR ligands, namely orthosteric agonists and allosteric modulators (Saidak et al., 2009). Orthosteric agonists can directly bind to CaSR orthosteric sites where primary ligand $Ca^{2+}$ is bound to activate CaSR on their own; allosteric modulators, in contrast, bind to allosteric sites distinct from orthosteric sites on CaSR and require the presence of orthosteric agonists like $Ca^{2+}$ to activate CaSR concertedly (Saidak et al., 2009).

#### 2.6.1 Orthosteric agonists

In addition to $Ca^{2+}$, the other common orthosteric agonists are divalent and trivalent cations including $Mg^{2+}$, $Al^{3+}$, $Sr^{2+}$, $Mn^{2+}$, $Ni^{2+}$, $Ba^{2+}$ $Gd^{3+}$, and $La^{3+}$, polyamines such as spermine, and aminoglycoside antibiotics (Saidak et al., 2009; Chakravarti et al., 2012).

$Ca^{2+}$ binding sites in human CaSR have been clarified (Geng et al., 2016). As mentioned above, 1 out of 4 (in terms of one protomer) binding site is shared in both active form and inactive form of CaSR, which indicates that $Ca^{2+}$ is important for maintaining the structural function of CaSR, and it is directly linked to CaSR activation. The extracellular $Ca^{2+}$ concentration level is important

in CaSR activation and regulating PTH secretion, but the $Ca^{2+}$ level varies in different tissues. For example, the level of $Ca^{2+}$ beneath adherent to osteoclasts is remarkably higher than that in the blood (Silver et al., 1988). Other divalent and trivalent cations may act similarly to $Ca^{2+}$ on CaSR because it has been reported that there are four $Ca^{2+}$ binding sites on the ECD of activated CaSR, and the activation by these cations is highly cooperative (Conigrave et al., 2000a). They are all positively charged, and the higher positive charge density means the higher ligand potency (Brown et al., 1990). For example, $Gd^{3+}$ ($EC_{50}$ is ~ 20 μM) and $Pb^{2+}$ ($EC_{50}$ is ~100 μM) are more potent activators of the CaSR than $Ca^{2+}$ ($EC_{50}$ > 1 mM) and other divalent cations. $Al^{3+}$ is a weak agonist of the CaSR (Spurney et al., 1999). The potency of these cations has been ranked as $Gd^{3+} > Ba^{2+} > Ca^{2+} > Mg^{2+} > Al^{3+}$ (McGehee et al., 1997).

Polyamines including spermine, spermidine, and putrescine are well-known CaSR agonists (Quinn et al., 1997). They are produced by bacteria in the intestine, and the mucosa epithelial cells require polyamines to maintain their function including proliferation and development. CaSR is also found to be highly expressed along the entire GIT (Gama et al., 1997). Spermine, with four positive charges, is recognized as the most potent ligand of CaSR among these polyamines. The EC50 is ~500 μM in the presence of 0.5 mM $Ca^{2+}$, and PTH secretion is inhibited by 50% in the presence of 200 μM spermine (Quinn et al., 1997). The potency of polyamines to activate the CaSR has been ranked as spermine > spermidine > putrescine (Quinn et al., 1997). In addition, polyamines are important neurotransmitters, and they could be effective activators in the CaSR-mediated biological processes of the brain.

Principle antibiotic agonists of CaSR are bleomycin, gentamicin, and tobramycin, belonging to aminoglycoside antibiotics (AGAs). It has been reported that the $EC_{50}$ of gentamicin, tobramycin, and neomycin regarding the increases in intracellular $Ca^{2+}$ concentration is 258, 177,

and 43 μM in HEK293 cells transfected with the CaSR, respectively, ranking as neomycin > gentamicin ⩾ tobramycin > kanamycin (McLarnon et al., 2002). The activation potency of AGAs is positively correlated with the number of their attached amino groups and nephrotoxic potential (Saidak et al., 2009). AGAs can activate CaSR to induce intracellular $Ca^{2+}$ mobilization and PLC-dependent ERK activation, but the signaling also causes an adverse effect (nephrotoxicity) in the proximal tubular opossum kidney cells (Ward et al., 2002; Ward et al., 2005).

**2.6.2 Allosteric modulators**

Allosteric modulators are classified as positive allosteric modulators (PAMs), also called type II agonists and negative allosteric modulators (NAMs), and they require the presence of orthosteric agonists to exert their effects.

CaSR has been determined to be a broad-spectrum amino acid sensor (Conigrave et al., 2007). PAMs include naturally occurring compounds such as L-amino acids, glutathione (GSH) analogs, peptides, and synthetic compounds such as calcimimetics. NAMs are $H^+$, $Na^+$, $PO_4^{3-}$ and synthetic compounds such as calcilytics. Amino acids and CaSR are widely distributed along the GIT, and their interaction regulates various physiological and biochemical processes such as PTH secretion. Low protein diet treatment *in vivo* resulted in an elevation in serum PTH accompanied by an increase in cAMP level (Kerstetter et al., 1997). Furthermore, the aromatic L-amino acids including L-Phe, L-Trp, L-Tyr, and L-His, and some short aliphatic L-amino acids including L-Thr and L-Ala have been identified as PAMs of CaSR in the HEK293 cells transfected with the CaSR (Conigrave et al., 2000b; Conigrave et al., 2007). The active part of these aromatic amino acids is their aromatic side chains, and their potencies depend on extracellular $Ca^{2+}$ concentration. They cannot activate CaSR at a subthreshold $Ca^{2+}$ level (≤ 1.0 mM), but amino acids activate CaSR by mobilizing intracellular $Ca^{2+}$ and enhancing its sensitivity to $Ca^{2+}$ at $Ca^{2+}$ concentrations above

the threshold (> 1.0 mM). Especially at an extracellular $Ca^{2+}$ concentration of 2.5 mM, the aromatic amino acids are more effective than other amino acids in the HEK293 cells transfected with the CaSR, and the effectiveness of amino acids ligand to CaSR is ranked as aromatics > aliphatics, polar > acidic > basic, and branch-chain amino acids (Conigrave et al., 2000b). In addition, tripeptide GSH is a more potent PAM of CaSR than aromatic amino acids because it exhibits a larger side chain. In the structure, GSH has free α-amino and α-carboxyl groups, which facilitates GSH binding to CaSR (Kerstetter et al., 1997). The γ-glutamyl dipeptides, γ-Glutamyl cysteine, and γ-glutamyl valine, have been reported to be able to attenuate dextran sodium sulfate-induced colitis via CaSR activation in mice (Zhang et al., 2015a).

The synthetic allosteric modulators such as calcimimetics and calcilytics are for therapeutic and pharmaceutic use to regulate the disorder of calcium metabolism associated with CaSR. Calcimimetics (such as NPS R-467 and NPS R-568) acting as PAMs, share similar structure properties with aromatic L-amino acids, with an aromatic ring and positively charged amine groups (Nemeth et al., 1998). Calcimimetics have been used for the treatment of hyperparathyroidism because they can amplify the sensitivity of the CaSR to extracellular $Ca^{2+}$, leading to a decrease in PTH secretion, further decreasing blood $Ca^{2+}$ level (Block et al., 2004; Peacock et al., 2005). Calcilytics such as NPS 2143 and NPS 89636 are CaSR antagonists, but their structure is similar to that of calcimimetics. They are originally developed to treat osteoporosis by blocking CaSR and stimulating the endogenous PTH secretion (Nemeth et al., 2001; Nemeth, 2002). The $IC_{50}$ of NPS-2143 for blocking the CaSR is 43 nM by decreasing the cytoplasmic $Ca^{2+}$ concentration in the HEK293 cells expressing CaSR (Gowen et al., 2000), and 41 nM by stimulating PTH secretion from the bovine parathyroid cells (Nemeth et al., 2001), respectively.

The activity of the CaSR is modulated by pH (Quinn et al., 2004), ionic strength (Quinn et al., 1998), and anions such as $PO_4^{3-}$ (Brown et al., 1993), and they all negatively affect the activity of CaSR and the sensitivity of CaSR to its agonists. For example, with decreasing pH, CaSR is less sensitive to extracellular $Ca^{2+}$ and concentration and *vice versa*, but the sensitivity shows some recovery when the pH value is higher than 5.5 (Quinn et al., 2004). The extracellular NaCl concentration affects the activation of CaSR by $Ca^{2+}$ and spermine, and the higher the ionic strength, the lower the sensitivity of CaSR to its agonists (Quinn et al., 1998). Anion binding sites of CaSR are also located in its ECD, and there are two binding sites for $PO_4^{3-}$ in the active form of CaSR in each protomer (Geng et al., 2016). $PO_4^{3-}$ has also been reported to inhibit the production of intracellular $IP_3$ in the HEK293 cells expressing CaSR and to stimulate PTH secretion from freshly isolated human parathyroid cells (Geng et al., 2016; Centeno et al., 2019). The arginine residues at $PO_4^{3-}$ binding sites compete with polyamines which show more positive charges, thus decreasing the negative effect of $PO_4^{3-}$ on CaSR activation in the presence of polyamines (Geng et al., 2016). These findings suggest that $H^+$, $Na^+$, and $PO_4^{3-}$ are NAMs to CaSR. Different organs exhibit different ionic microenvironments, thereby affect the activation of CaSR and sensitivity of CaSR to its agonists, which facilitates maintaining calcium homeostasis.

## 2.7 Important tissues involved in maintaining calcium homeostasis

### 2.7.1 Parathyroid

Parathyroid cells have been reported to possess a $Ca^{2+}$ sensor function that can also recognize other di-, tri-, and polyvalent cations to induce intracellular signaling cascades by mediating $IP_3$ production and intracellular $Ca^{2+}$ mobilization. After that, CaSR was first cloned and characterized from bovine parathyroid (Brown et al., 1993). CaSR is also highly expressed in the chicken parathyroid glands (Diaz et al., 1997). Both in humans and rats, $1,25(OH)_2D_3$ treatment

upregulates *CaSR* transcription, as VDRE is located in the promoter of *CaSR* (Canaff and Hendy, 2002). It has been reported that CaSR is located in the caveolin-rich plasma membrane domains of both bovine parathyroid chief cells and endothelium of the parathyroid gland (Kifor et al., 1998). CaSR plays crucial roles in parathyroid function including regulating PTH secretion and proliferation of parathyroid cells (Brown, 2007). Generally, hypocalcemia triggers PTH secretion via CaSR, and then increased PTH recruits other tissues and organs including the kidney, GIT, and bone to function together to maintain plasma calcium homeostasis. PTH secretion from parathyroid cells is considered a parameter to evaluate disorders of calcium metabolism such as familial FHH, NSHPT, and ADH, and functions of CaSR mutants (Conigrave, 2016). As mentioned above, it has been documented that $G_{q/11}$ double knockout mice showed excessive PTH-related hypercalcemia, skeletal abnormalities, retarded growth, etc., which illustrated that $G_{q/11}$-mediated intracellular $Ca^{2+}$ mobilization regulates PTH secretion by activating CaSR (Wettschureck et al., 2007). In addition, CaSR activation stimulates $G_s$ and $G_i$-mediated changes in cAMP level, which regulates PTH secretion (Brown et al., 1977; Brown et al., 1979b; Fitzpatrick et al., 1986; Chen et al., 1989; Mamillapalli and Wysolmerski, 2010). Interestingly, Kos et al. (2003) found that CaSR is necessary for the fine regulation of serum calcium levels and renal calcium excretion independent of its effect on PTH secretion in $PTH^{-/-}CaSR^{-/-}$ mice.

### 2.7.2 Gastrointestinal tract (GIT)

GIT functions in nutrient digestion and absorption. The CaSR or CaSR transcripts have been found in GIT including the esophagus, stomach, small intestine, and large intestine in mammals (Chattopadhyay et al., 1998; Cheng et al., 1999), and in the duodenum and whole small intestine in avian species (Diaz et al., 1997; Deng et al., 2010). The CaSR is located on the basal layer of the normal human esophagus, and its activation induces intracellular signaling cascades including

ERK1/2 activation, intracellular calcium mobilization, and interleukin 8 (IL-8) secretion in the human esophageal epithelial cell line (Justinich et al., 2008). In the stomach, the CaSR has been reported to be expressed in the epithelial cells including G cells and parietal cells (Rutten et al., 1999; Buchan et al., 2001; Busque et al., 2005), which is involved in the gastric acid secretion and mucosal layer repair (Geibel and Hebert, 2009). The activation of CaSR in the isolated gastric epithelial cells induces the change of intracellular $Ca^{2+}$ concentration and a significant proliferative response (Rutten et al., 1999). The $H^+$ and $Cl^-$ extrusion was stimulated by hormonal or neuronal routes from parietal cells via the apical channel. The CaSR is located on the basolateral membrane of parietal cells. its activation by extracellular $Ca^{2+}/Mg^{2+}$ and L-amino acids stimulates PLC-mediated intracellular $Ca^{2+}$ release, leading to increased activity of $H^+$, $K^+$-ATPase (proton pump), and promoting the rate of acid secretion (Geibel et al., 2001). The CaSR also plays a role in regulating the secretion of gastrin in the G cells while reducing calcium influx after its activation via the PLC-mediated pathway (Buchan et al., 2001).

In addition to the stomach, the CaSR has been documented to be expressed in the different segments of the small and large intestine in mammals (Chattopadhyay et al., 1998; Zhao et al., 2019), but the expression pattern in the avian species is still unclear so far. The small intestine functions in digestion, absorption, and chemosensing. 90% of calcium is absorbed in the small intestine, with the remainder is absorbed in the stomach and large intestine (Bronner, 2009). Interestingly, the CaSR was detected in the intestinal epithelial cells including goblet cells, enteroendocrine cells, and Paneth cells except for absorptive enterocytes (Chattopadhyay et al., 1998; Hira et al., 2008). Zhao et al. (2022) has confirmed that CaSR is not expressed in the absorptive enterocytes of weaned piglets. Moreover, in different species, the principal site where calcium is absorbed in the intestine may differ. For example, over 60% of calcium uptake happens

in the ileum in mammals (Cramer and Copp, 1959; Partridge, 1978), whereas most of this uptake takes place in the jejunum in laying hens (Hurwitz and Bar, 1966). The CaSR is expressed mainly in the ileum among the small intestine in pigs (Zhao et al., 2019), but no more evidence supports other distribution patterns of CaSR in poultry. Therefore, the function of CaSR might not be closely associated with calcium absorption, but CaSR does play an important role in regulating the growth, proliferation, and differentiation of intestinal epithelium, and digestion and absorption of nutrients by chemosensing and hormone secretion (Geibel and Hebert, 2009; Tang et al., 2016). The CaSR is a multi-sensor, which can detect various nutritional ligands including mineral ions, polyamines, L-amino acids, and small peptides. The activation of CaSR induces a series of intracellular cascades associated with changes in second messengers like intracellular $Ca^{2+}$ and cAMP level, which regulates intestinal fluid secretion (Geibel et al., 2006) and cholecystokinin (Hira et al., 2008; Liou et al., 2011). Moreover, there are a number of endocrine cells located in the ileum, and they are able to secret hormones like glucagon-like peptide 1 and 2, peptide YY and oxyntomodulin to mediate satiety, intestinal motility, transit, gastric emptying, intestinal integrity, and permeability (Liou, 2013). The regulation pattern of CaSR in endocrine cells of the ileum needs to be explored further. In the human epithelial colorectal adenocarcinoma Caco-2 cells, the proliferative response was reported to be related to CaSR activation (Kállay et al., 1997). Moreover, the CaSR activation stimulates E-cadherin production and β-catenin suppression which is related to colorectal carcinogenesis (Chakrabarty et al., 2003). Colon functions in fluid absorption and secretion, thereby regulating water and electrolyte homeostasis. It has been reported that the CaSR is also involved in the colonic fluid transport in both surface and crypt cells (Sheinin et al., 2000).

### 2.7.3 Kidney

Calcium absorbed from the gut enters the blood and is filtered by the kidney. The kidney plays an important role in calcium homeostasis because the majority of filtered calcium (98%) is reabsorbed in the kidney in humans (Moor and Bonny, 2016). In hens, 99% of filtered calcium is reabsorbed in the kidney (Wideman Jr et al., 1987). The expression of the renal CaSR was first confirmed in the rat kidney (Riccardi et al., 1995). The mammalian renal CaSR mRNA is distributed throughout the nephron including the proximal tubule, thick ascending limb (TAL), distal tubule, and collecting duct (Riccardi et al., 1995; Riccardi and Brown, 2010). However, the CaSR protein localization is segment-specific in the kidney, and the polarity of receptor expression varies with cell type (Riccardi and Brown, 2010). Specifically, the CaSR is expressed at the base of the apical brush-border membranes of cells in the proximal tubule; in the basolateral membranes of TAL cells of Henle's loop and distal convoluted tubule cells; and in some type A intercalated cells in cortical collecting ducts (Riccardi et al., 1998). The chicken CaSR mRNA and protein were confirmed to be expressed in the kidney, and CaSR is located in some tubular cellular structures (Diaz et al., 1997). No reports on the distribution and localization patterns of CaSR in chicken kidneys have been published since then. The expression of CaSR has been demonstrated to be regulated by $1,25(OH)_2D_3$, PTH, and dietary phosphates in the kidney in mammals (Caride et al., 1998; Riccardi et al., 2000; Abukawa et al., 2001). In mammals, the majority (60-70%) of filtered calcium is reabsorbed in the proximal tubule; an additional 20-25% of filtered calcium reabsorption takes place in the TAL of Henle's loop; and 8-10% of filtered calcium is reabsorbed in the distal convoluted tubule (Ba and Friedman, 2004). Renal calcium reabsorption in the proximal tubule and TAL is transporter and hormone-independent via a paracellular pathway between the epithelial cells (Moor and Bonny, 2016). The PTH stimulates transcellular $Ca^{2+}$

absorption in renal distal convoluted tubules (Gesek and Friedman, 1992), where the active regulation of calcium reabsorption takes place. Activation of CaSR stimulates intracellular signaling cascades that can regulate renal function, which is involved in: (1) divalent mineral reabsorption and urine excretion; (2) water resorption; (3) calcium and inorganic phosphate homeostasis; (4) urinary acidification; and (5) renin release (Hebert et al., 1997; Riccardi and Brown, 2010). The CaSR activated by relatively high extracellular calcium concentration via the p38α MAPK pathway regulates the VDR expression in the proximal tubule human kidney (HK-2G) epithelial cells (Maiti et al., 2008). Evidence showed that $G_i$-coupled CaSR activation by extracellular $Ca^{2+}$ inhibited AC and cAMP level in the TAL but had no effects in the proximate tubules (Takaichi and Kurokawa, 1986; Takaichi and Kurokawa, 1988). Moreover, co-expression of $Ca^{2+}$-inhibitable type 6 AC and CaSR in the rat cortical TAL cells causes the suppression of cAMP levels after activating CaSR by extracellular $Ca^{2+}$, which illustrates the participation of PI-PLC-mediated intracellular calcium mobilization (de Jesus Ferreira et al., 1998).

### 2.7.4 Bone

The bone structure in avian species is distinct from that in mammals (Kim et al., 2012). Before sexual maturity, there are two types of bone providing structural integrity in egg-type birds: cortical bone and cancellous bone (Whitehead, 2004). The cortical bone is a compact structural bone, which is tightly packed and highly organized. The cancellous (trabecular) bone is a three-dimensional lattice-shaped honeycomb architecture located at the end of bones (Kim et al., 2012). The medullary bone is only formed when the female bird reaches sexual maturity, and it lines the surface of the structural bone (Whitehead, 2004). It is characterized by collagen fibers randomly arranged in its matrix and is mechanically weaker than structural bones. After formation, the medullary bone undergoes rapid remodeling which serves as a liable reservoir of calcium to

support eggshell calcification, especially at night when the calcium supply from the digestive tract is limited. When the hen is not forming an eggshell and has more calcium and phosphorus in the diet than needed, the medullary bone tissue is replenished, but the structural bone tissue is not (Korver, 2020). Medullary bone spicules become more diffuse arranged throughout the marrow cavity over the laying period. In the end, medullary bone may occupy the entire cavity of pneumatized bones and loosely attach to structural bone surfaces, leading to more structural bone is exposed to the action of osteoclasts, and then the progressive structural bone loss/osteoporosis would be the net effect (Korver, 2020).

The osteogenic cells isolated from hen medullary bone and chicken embryonic calvaria can form the bone-like matrix in both cortical bones and medullary bones (Hiyama et al., 1998). Moreover, alkaline phosphatase activity and its gene expression have been detected in osteogenic cells isolated from the medullary bone (Hiyama et al., 2005). Different from rat bone marrow cells in the late stages, the gene expression of two non-collagenous proteins related to the differentiation of osteoblasts is upregulated in the early stages in laying hens (Hiyama et al., 2005).

The CaSR has been documented to be involved in bone remodeling including bone formation and resorption and the proliferation, differentiation, migration, and other functions of bone cells (Marie, 2010). The CaSR is expressed in the rat and human osteosarcoma (osteoblastic-like) cell lines UMR-106 and SAOS-2 and CaSR agonists, gadolinium, and neomycin, as well as high $Ca^{2+}$, which could induce proliferation and chemotaxis of mouse osteoblastic clonal cells (Yamaguchi et al., 1998). Also, CaSR is involved in the osteoblastic differentiation of mouse MC3T3-E1 cells (Yamauchi et al., 2005). Immortalized or primary osteoblasts isolated from CaSR knockout mice are still able to respond to extracellular calcium, suggesting that other calcium-sensing receptors may control osteoblastic cells (Pi et al., 2000; Fromigué et al., 2009). Mesenchymal stem cells are

capable of going through osteogenic differentiation into osteoblasts which exhibit the classic response to PTH of elevated cAMP levels, and a bone-specific alkaline phosphatase activity (Caplan, 1991). The CaSR is involved in rat bone marrow and umbilical cord matrix mesenchymal stem cell proliferation, which has the potential for application in regenerative medicine (Martino et al., 2014; Ye et al., 2016). In addition, CaSR activation induced by calcimimetic R-568 has been reported to stimulate the osteogenic differentiation of mesenchymal stem cells isolated from human amniotic fluid and osteogenesis (Xu et al., 2012). The CaSR was also found to be expressed in osteoclast precursor cells, pre-osteoclasts, and osteoclasts (Kanatani et al., 1999). In osteoclasts, the detection of extracellular calcium concentration is necessary to elicit various intracellular signaling cascades that mediate gene expression and cell survival (Zaidi et al., 1999). Notably, activation of CaSR by high calcium levels was found to increase osteoclast apoptosis *in vitro* through activation of PLC and nuclear factor kappa B (NF-κB), indicating that the CaSR may play an important role in the control of osteoclastogenesis (Mentaverri et al., 2006).

Although the cellular signaling pathways related to CaSR activation by nutrients are still unclear, previous studies have reported that the exposure of primary osteoblasts or a variety of osteoblast-like cells to high levels of $Ca^{2+}$ or polycationic CaSR agonists, strontium, neomycin, and gadolinium stimulates osteoblast proliferation, differentiation, and a matrix-mineralization capacity via activation of mitogen-activated protein kinases such as extracellular signal-regulated protein kinases 1 and 2 or c-Jun N-terminal kinase (Yamaguchi et al., 1998; Dvorak et al., 2004; Chattopadhyay et al., 2007; Takaoka et al., 2010). However, the mechanisms by which CaSR modulators regulate the differentiation of osteoblast and mesenchymal stem cells are not yet understood.

### 2.7.5 Shell gland

The shell gland is recognized as a critical organ controlling eggshell quality and mass because it regulates eggshell calcification and calcium transport from plasma to the shell gland lumen (Eastin Jr and Spaziani, 1978; Jonchère et al., 2012). A variety of calcium and other ion transporters are located in the apical and basolateral membrane of glandular cells of the shell gland (Bar, 2009), but the expression of CaSR in the shell gland has not yet been reported. The $IP_3$ receptor 1, 2, and 3 have been documented to be involved in the calcium transfer in the shell gland because it induces endoplasmic calcium release, but its gene expression is unchanged in the presence or absence of eggshell calcification (Jonchère et al., 2012). This might be evidence to support that the CaSR is expressed in the shell gland because CaSR activation induces PLC-mediated intracellular $IP_3$ production and $Ca^{2+}$ mobilization via the $G_{q/11}$ pathway. More studies are needed to investigate whether CaSR is involved in other physiological and biochemical processes in the shell gland and whether it shows similar regulatory patterns compared to other tissues and organs.

# CHAPTER THREE: HYPOTHESES AND OBJECTIVES

### 3.1 Hypotheses

We hypothesized that CaSR is expressed in both shell gland and bone in laying hens, and that it performs the similar function (calcium homeostasis) and exhibits the similar characteristics (ligand recognition and biased agonism and antagonism via downstream G protein-coupled signaling) as mammlian CaSR. We also hypothesized that there is cross-talk between the CaSR and vitamin D system. By using CaSR modulators and different vitamin $D_3$ forms, we can potentially improve bone health and eggshell quality in laying hens. Specifically, 1) chicken CaSR and VDR are expressed in different tissues including the shell gland and tibia with varied expression patterns at different laying stages; 2) similar to human CaSR, L-Trp and inorganic $PO_4^{3-}$ are the allosteric modulator of chicken CaSR, which can activate or block chicken CaSR with biased downstream signaling, and each of these two modulators exhibit distinctive binding mechanism; 3) CaSR modulators ($Ca^{2+}$ and L-Trp) and 1,25-dihydroxycholecalciferol can mediate the proliferation and osteogenic differentiation of chicken MSCs; 4) the combined action of calcium and L-Trp as well as calcium and 25-hydroxycholecalciferol can boost calcium utilization and eventually improve production performance, egg quality, and bone health in laying hens.

### 3.2 Objectives

The overall objective of the thesis was to investigate the effect of CaSR modulators and different types of vitamin $D_3$ on bone health and eggshell quality through restoring or maintaining calcium homeostasis in laying hens, and to identify the underlying molecular and cellular mechanisms. The specific objectives were to 1) investigate the molecular distribution and localization of poultry CaSR in the gastrointestinal tract, shell gland and bone in laying hens; 2) characterize potential poultry CaSR ligands in an in vitro stable expression cell line using a luciferase reporter system; 3) investigate the effects of CaSR modulators and 1,25-

dihydroxycholecalciferol on the proliferation and differentiation of MSCs isolated from compact bones of chickens; and 4) investigate the effects of CaSR modulators and 25-hydroxycholecalciferol on egg production performance, eggshell quality, bone health, and calcium homeostasis in laying hens.

## CHAPTER FOUR: MANUSCRIPT I

**Molecular distribution and localization of extracellular calcium-sensing receptor (CaSR) and vitamin D receptor (VDR) at three different laying stages in laying hens (*Gallus gallus domesticus*)**[1]

[1] **Hui, Q.**, X. Zhao, P. Lu, S. Liu, M. Nyachoti, O. Karmin, and C. Yang. 2021. Molecular distribution and localization of extracellular calcium-sensing receptor (CaSR) and vitamin D receptor (VDR) at three different laying stages in laying hens (*Gallus gallus domesticus*). Poultry Science 100(5):101060.

## 4.1 Abstract

The extracellular calcium-sensing receptor (CaSR) and vitamin D receptor (VDR) play important roles in regulating calcium mobilization, calcium absorption and calcium homeostasis, and they could be potential therapeutic targets for osteoporosis in laying hens. The present study investigated the molecular distribution of CaSR and VDR and the localization of CaSR in the kidney, proventriculus (true stomach), duodenum, jejunum, ileum, colon, cecum, shell gland and tibia of laying hens at three different laying stages (19, 40 and 55 weeks). The results showed that the relative mRNA abundance of CaSR in the kidney, ileum, proventriculus, duodenum, and colon was higher ($P < 0.05$) than the other tissues at 40 and 55 weeks. The relative mRNA abundance of CaSR in the tibia was higher ($P < 0.05$) at 55 weeks than at 40 weeks. However, there were no significant differences in the relative protein abundance of CaSR among all tested tissues at peak production (40 weeks), or in each tissue at the three different laying stages ($P > 0.05$). The relative mRNA abundance of VDR was higher ($P < 0.05$) in the small intestine (duodenum, jejunum, and ileum) when compared with other tissues at the three different laying stages. The relative protein abundance of VDR in the duodenum was higher ($P < 0.05$) than that in the proventriculus, colon, and cecum. There were no significant differences in the VDR expression among the tested tissues at the three different laying stages ($P > 0.05$). The immunohistochemical results showed that the positive staining was found widely in each tissue. Moreover, different laying stages did not affect the localization of CaSR except for the tibia tissue. In conclusion, similar to VDR, CaSR was widely expressed not only in the gut but also in the tibia and shell gland in laying hens. The expression level of CaSR and VDR in all tested tissues was unchanged at the different laying stages.

**Key words:** Calcium-sensing receptor, vitamin D receptor, localization, distribution, laying hen

## 4.2 Introduction

Laying hens have a dynamic bone turnover associated with the daily egg-laying cycle. Because of rapid bone turnover and calcium mobilization from bones for eggshell formation, osteoporosis is a big challenge in the laying hen industry that involves the progressive loss of structural bone (Whitehead and Fleming, 2000). Osteoporosis is one of the major leading causes of bone fractures in laying hens. Bone fractures are associated with pain and animal welfare issues. In addition, economic factors such as egg production and eggshell quality are closely linked to issues concerning bones (Kim et al., 2012). Calcium is the most important mineral in maintaining the structural integrity of bones and eggshells (Olgun and Aygun, 2016). Approximately 2.4 g of calcium is required in approximately 20 h for a laying hen to calcify a 60 g shelled egg (Fleming, 2008). Only 60% to 75% of the eggshell calcium can be provided by the feed and the remainder must be mobilized from bone stores (Fleming, 2008). Also, calcium absorption, femur ash, and eggshell quality decline with age (Al-Batshan et al., 1994). Therefore, it is critical to maximize skeletal mineralization through calcium supplementation in laying hen diets before sexual maturity, so they have sufficient calcium or bone density to support egg laying. However, most dietary interventions are ineffective during the laying period. Calcium deficiency affects eggshell quality and also stimulates the secretion of parathyroid hormone (PTH) and vitamin D synthesis, which in turn leads to the depletion of calcium in the bone (Rath et al., 2000). Hypocalcemia or inadequate calcium levels in the blood decreases bone strength (Rath et al., 2000). An excess of calcium decreases phosphorous availability and reduces feed intake, which negatively affects eggshell quality and bone strength. Taken together, restoring or maintaining the desired calcium homeostasis by nutritional solutions might be an effective strategy to improve bone health and eggshell quality in laying hens.

Extensive research has been done on the topic of calcium in laying hens. However, most studies have focused on the effects of dietary calcium sources, requirements, particle sizes, and calcium: phosphorus ratio on laying hen performance and health (Keshavarz, 2003; Cufadar et al., 2011; Ganjigohari et al., 2018). Osteoporosis cannot be easily solved by simply increasing dietary calcium contents and it is one of common diseases in laying hens globally. Calcium homeostasis is regulated through PTH, active form of vitamin $D_3$, calcitonin, vitamin D receptor (VDR), calcium transporters and calcium-sensing receptor (CaSR) (Proszkowiec-Weglarz and Angel, 2013). CaSR is a homodimeric complex located in the cell membrane and belongs to class C G-protein coupled receptor (GPCR) (Jensen and Brauner-Osborne, 2007). It can sense subtle changes in extracellular calcium concentration and thus mediating PTH secretion to maintain calcium homeostasis via regulating intestinal absorption, bone storage and exchange, and renal reabsorption (Conigrave, 2016). In addition, CaSR mediates a variety of physiological and pathophysiological processes such as ion channel activity, gene expression, inflammation, proliferation, differentiation, and apoptosis via inducing downstream signaling cascades. Chicken CaSR (cCaSR) has 79% and 84% homology with human CaSR on the nucleotide and amino acid level, respectively. The in situ hybridization has revealed that CaSR is present in the parathyroid, kidney, brain and small intestine (Diaz et al., 1997). Yarden et al. (2000) have shown that the gene expression of cCaSR in the parathyroid gland is inversely associated with changes in plasma calcium concentration caused by a vitamin D-deficient diet. All these results indicate that the functional CaSR in chickens may possess similar characteristics to mammalian CaSR and play an important role in avian calcium homeostasis.

It has been reported that CaSR is widely expressed in multiple tissues including the parathyroid gland, kidney, bone, and gastrointestinal tract (GIT) in humans, rat, and swine, etc.

(Abukawa et al., 2001; Kos et al., 2003; Quarles, 2003; Al-Dujaili et al., 2016; Zhao et al., 2019). CaSR also plays a central role in human calcium homeostasis by influencing bone modeling and remodeling, and recently becoming a potential therapeutic target for osteoporosis in postmenopausal women (Halse et al., 2014; Liang et al., 2016). However, it is not clear whether CaSR is expressed in the proventriculus, bone and shell gland in laying hens. It has been demonstrated that chicken VDR (cVDR) is expressed in the kidney (Lu et al., 1997), intestine (Lu et al., 1997), and shell gland (Yoshimura et al., 1997) of laying hens. We hypothesized that similar to cVDR, cCaSR is expressed in the proventriculus, shell glands and bones in laying hens. The objective of the present study was to investigate the molecular distribution and localization of poultry CaSR and VDR in the kidney, GIT, shell gland and bone in laying hens at three different laying stages.

## 4.3 Materials and methods

### 4.3.1 Locus and structure of chicken (*Gallus gallus*) CaSR

The nucleotide sequence and amino acid sequence information of cCaSR was collected from the National Center for Biotechnology Information (NCBI, Accession No: XM_416491.6 and XP_416491.5) and Ensembl genome database (ENSGALG00000038405). The schematic diagram of the c*CaSR* gene exon/intron organization and protein domains was drawn using an online tool Exon-Intron Graphic Maker (http://www.wormweb.org/exonintron). The secondary structure diagram of the cCaSR was constructed using PROTTER (http://wlab.ethz.ch/protter/start/). The predicted three-dimensional model of a cCaSR disulfide-linked homodimeric extracellular domain (ECD) structure was based on a human CaSR template (Geng et al., 2016) using the SWISS-MODEL (https://swissmodel.expasy.org/interactive).

### 4.3.2 Animals and management

A total of 18 Lohmann LSL-Classic laying hens at 19 weeks (six birds), 40 weeks (six birds) and 55 weeks (six birds) of age were obtained from the Poultry Unit, Glenlea Research Station, University of Manitoba. Birds had *ad libitum* access to feed and water, and they were housed and maintained in accordance with the Canadian Council on Animal Care (CCAC) guidelines for the care and use of farm animals in research, teaching, and testing (CCAC, 2009). The experimental protocol (F18-043) was approved by the Fort Garry Campus Animal Care Committee at the University of Manitoba. Hens were fed a mash diet that was formulated to meet or exceed the nutritional requirements specified in the management guide (Lohmann Tierzucht, 2019).

### 4.3.3 Tissue collection and preparation

Six birds were euthanized using carbon dioxide asphyxiation at 19, 40 and 55 weeks of the laying period, respectively. Kidney, proventriculus, duodenum, jejunum, ileum, colon, cecum, shell gland and tibia were collected. Intestinal contents were flushed with ice-cold phosphate-buffered saline (PBS). Collected tissues were immediately frozen in liquid nitrogen and then stored at -80 °C. Frozen samples were then individually ground to a fine powder using liquid nitrogen and a tissue pulverizer (59013N, Cole-Parmer, Vernon Hills, IL, USA) for RNA and protein extraction. Tissues were fixed in a 10% buffered formalin (Fisher Scientific, Waltham, MA, USA) for 24 h, and then formalin was replaced with 70% ethanol for longer storage for the paraffin block preparation.

### 4.3.4 Real-time quantitative polymerase chain reaction (Real-time RT-qPCR)

Total RNA extraction from each tissue was conducted using TRIzol$^{TM}$ reagent (Invitrogen Life Technologies, Waltham, MA, USA) as described in the manufacturer's instructions. The quantity and quality of RNA were analyzed by Nanodrop 2000 spectrophotometer (Thermo

Scientific, Waltham, MA, USA), and the integrity of RNA was checked by RNA electrophoresis in agarose gel. Next, the first-strand cDNA was synthesized using the iScript™ cDNA Synthesis kit (Bio-Rad, Hercules, CA, USA) according to the corresponding manufacturer's protocol. The relative mRNA abundances of CaSR and VDR were measured using SYBR Green Supermix (Bio-Rad) by a CFX Connect™ Real-Time PCR Detection System (Bio-Rad). PCR amplification was performed at a set of three min at 95 °C, then 40 cycles of 20 s at 95 °C, 30 s at 60 °C and 30 s at 72 °C. At the end of each cycle, the fluorescence was monitored for 10 s. Each reaction was completed with a melting curve analysis to ensure the specificity of the reaction. Primers used in this study are listed in Table 1. Relative gene expression was calculated using the $2^{-\Delta\Delta Ct}$ method (Livak and Schmittgen, 2001). Because of the big gap of threshold cycle (Ct) value for the reference gene when comparing tibia with other tissues, the target gene expression of tibia was shown separately.

**Table 4.1** Primers used in this study.

| Genes | Accession No. | Primer sequences (5'→ 3') |
|---|---|---|
| *Gallus CaSR* | XM_416491.6 | Forward: CAAACCAACGGGCACAGAAG |
| | | Reverse: ATGCACTCCACTGATTCGGG |
| *Gallus VDR* | AF011356.1 | Forward: CCGGATTCAGGGATCTGACG |
| | | Reverse: AAGTCATTGCTTCCGCAGGT |
| *Gallus GAPDH* | NM_204305 | Forward: ACTGTCAAGGCTGAGAACGG |
| (Reference) | | Reverse: CACCTGCATCTGCCCATTTG |

### 4.3.5 Western blot analysis

The relative protein expression of CaSR and VDR was determined by Western blot analysis. Ground tissue samples were homogenized and lysed by a homogenizer (Powergen 125, Fisher Scientific) using pre-cooled RIPA buffer containing Halt™ protease and phosphatase inhibitor cocktail (Thermo Scientific) on ice. Sample lysates were centrifuged at 12,500 × g for 15 min to remove the insoluble debris. Total protein concentration was determined using the Pierce™ BCA protein assay kit (Waltham, MA, USA) as described in the manufacturer's instructions. Protein was then denatured using 4 x Laemmli sample buffer (Bio-Rad) with 0.1 M dithiothreitol (DTT) at 95 °C for 9 min, the denatured protein samples (70 μg) were loaded and separated by 4–15% Mini-PROTEAN® TGX Stain-Free™ Protein Gels (Bio-Rad), and transferred onto a polyvinylidene difluoride (PVDF, Bio-Rad) membrane. Each membrane was blocked using 5% skim milk powder dissolved in tris-buffered saline with 0.1% Tween 20 (TBST) for 1 h at room temperature, and then incubated with the rabbit polyclonal anti-CaSR antibody (1:1000, ab137408, Abcam, Cambridge, MA, USA) and VDR Monoclonal Antibody (9A7) (1:2000, MA1-710, Thermo Scientific) at 4 °C overnight. Secondary antibody incubation used horseradish peroxidase-conjugated goat anti-rabbit IgG (65-6120, 1:1000, Thermo Scientific) and horseradish peroxidase-conjugated anti-rat IgG (112-035-003, 1:5000, Jackson Immuno Research Laboratories, West Grove, PA, USA). Images were detected by ChemiDoc™ Imaging Systems (Bio-Rad) after incubation with Clarity Max™ Western ECL Substrate (Bio-Rad). The densitometry of the target protein bands was quantified by Image Lab Software (Bio-Rad) and normalized to the total protein. The quantitative results were presented as relative to the kidney (in different tissues) at the 40 weeks of age or relative to the 19 weeks of age (at different ages) in each tissue.

### 4.3.6 Immunohistochemistry

Fixed tissues were processed and embedded in paraffin according to our previously published method (Zhao et al., 2019). Paraffin blocks were sectioned at 5 μm and put two sections on each Superfrost plus microscope slide (Fisher Scientific). Slides were then deparaffinized in xylene twice and then rehydrated in ethanol diluted serially in Mili-Q water (100%, 90%, 80% and 70%) and finally rinsed in Mili-Q water. Firstly, sections were stained with hematoxylin and eosin (H&E) to check the morphological state of the tissues. For immunohistochemical staining, antigen retrieval was conducted by incubating slides in 10 mM sodium citrate with 0.5% Tween™ 20 (pH at 6) in a water bath at 95 °C for 10 min. Sections were incubated with a mixture of 3% hydrogen peroxide and 10% methane for 10 min to block endogenous peroxidases, followed by the incubation with Avidin/Biotin Blocking system (Biolegend, San Diego, CA, USA) according to the manufacturer's instruction, and then sections were blocked with normal donkey serum (1:20, 017-000-001, Jackson Immuno Research Laboratories) for 1 h. Sections were incubated with a rabbit polyclonal anti-CaSR antibody (1:50, ab137408, Abcam) diluted in 2% bovine serum albumin (BSA) overnight at 4 °C. Next, Biotin-SP-AffiniPure Donkey Anti-Rabbit IgG (H+L) (1:500, 711-065-152, Jackson ImmunoResearch Laboratories) was incubated for 1 h at room temperature, and followed by the peroxidase-conjugated streptavidin incubation (1:500, Jackson ImmunoResearch Laboratories) at room temperature for 30 min. The color was visualized using Pierce™ DAB Substrate Kit (PI34002, Thermos scientific), and counterstained with Mayer's Hematoxylin Solution (Sigma-Aldrich, St. Louis, MO, USA). Sections incubated without primary antibody were set as a negative control. Slides were finally scanned and photographed by using a Zeiss Axio Scope (Carl-Zeiss Ltd, Jena, Germany).

### 4.3.7 Statistical analysis

Statistical analyses were carried out using SAS 9.4 (the SAS Institute, Cary, NC) and all figures were made using GraphPad Prism 6 software (San Diego, CA, USA). Results were expressed as the mean ± SEM. Statistical significance was determined using one-way ANOVA followed by Tukey's multiple-comparison test. $P$ value < 0.05 was considered statistically significant.

## 4.4 Results

### 4.4.1 Structure and hydrophobicity analysis of cCaSR

Based on the information obtained from NCBI and Ensembl genome database, a schematic diagram of the cCaSR gene exon/intron and protein domains is shown in Figure 4.1. The cCaSR gene which maps the chicken chromosome 1q has 7 exons, spanning ~ 42 kb. The T-cell antigen *CD86* gene lies upstream and cysteine protease inhibitor *CSTB* gene lies downstream of the cCaSR gene. Exons 1-7 encode 1059 amino acids (AAs) of cCaSR protein; ECD is encoded by 1833 nucleotides of exon 1 to exon 6 including signal peptides encoded by 57 nucleotides of exon 1; transmembrane domain (TMD) is encoded by 747 nucleotides of exon 6; and intracellular domain (ICD) is encoded by 594 nucleotides of exon 7. The schematic diagram of the secondary structure of cCaSR protein is shown in Figure 4.2. The cCaSR consists of 1,059 AAs and divides into three domains: 1) a large N-terminal ECD that is comprised of the first 611 AAs containing a 19 AA N-terminal signal peptide; 2) a seven helical TMD that is comprised of 250 AAs; and 3) a C-terminal ICD that is comprised of 198 AAs. The three-dimensional model of a cCaSR ECD structure was predicted based on a human CaSR template using SWISS-MODEL (Figure 4.3). The cCaSR functions in the form of disulfide-linked homodimers. The ECD is the main site where ligands bind, consisting of a large extracellular Venus Flytrap (VFT) module (Lobe1 and Lobe 2) and a cysteine-rich (CR) domain which connects the VFT module to the TMD.

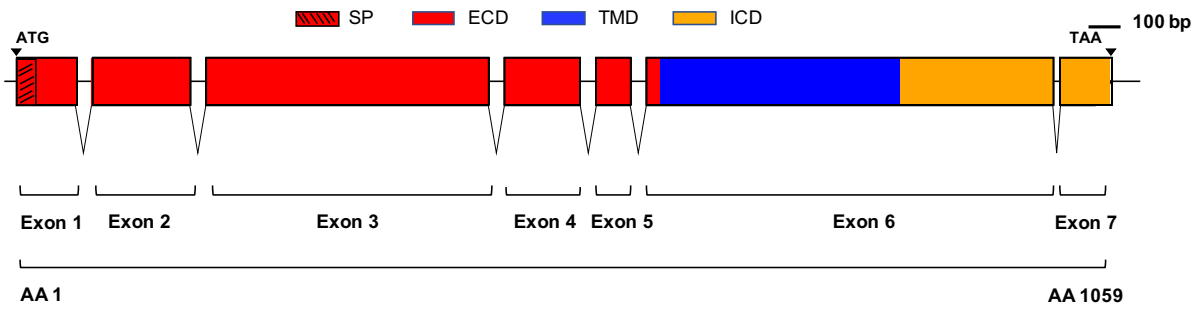


**Figure 4.1** Schematic diagram of the chicken CaSR (cCaSR) gene exon/intron organization and protein domains. Exons were drawn to the scale, but introns were not. There are seven exons and six introns in the cCaSR gene. Filled bars represent mRNA coding regions including exon 1-7. ATG, initiation codon; TAA, stop codon. The cCaSR protein contains 1,059 amino acid residues. SP, signal peptide; ECD, extracellular domain; TMD, transmembrane domain; ICD, intracellular domain.

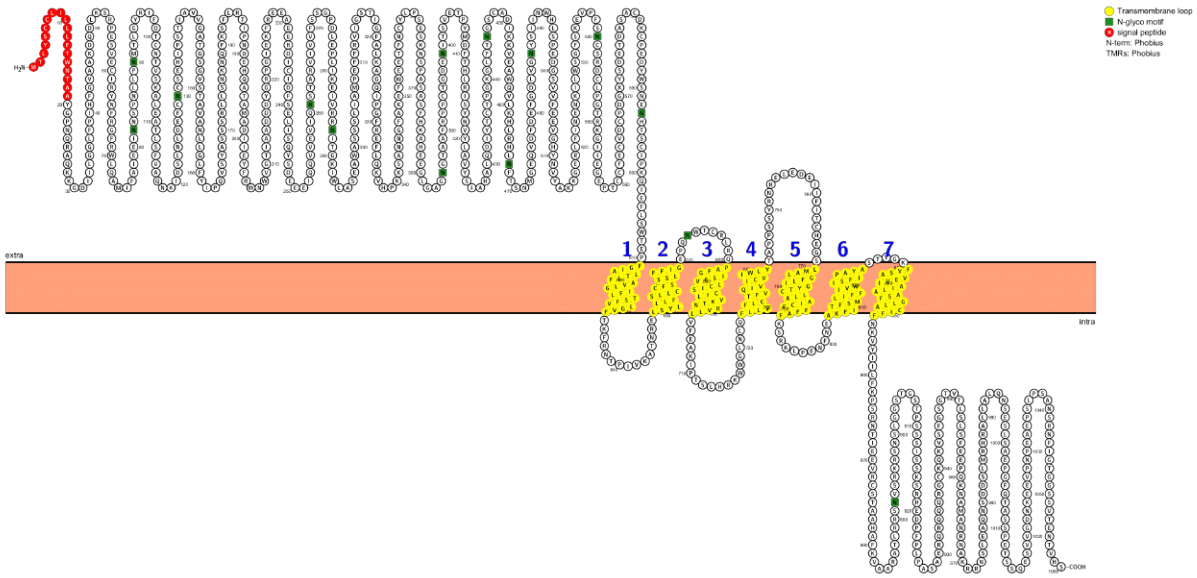


**Figure 4.2** Schematic diagram of the structure of chicken calcium-sensing receptor exported by PROTTER tool based on the protein sequence obtained from NCBI (Accession No: XP_416491.5).

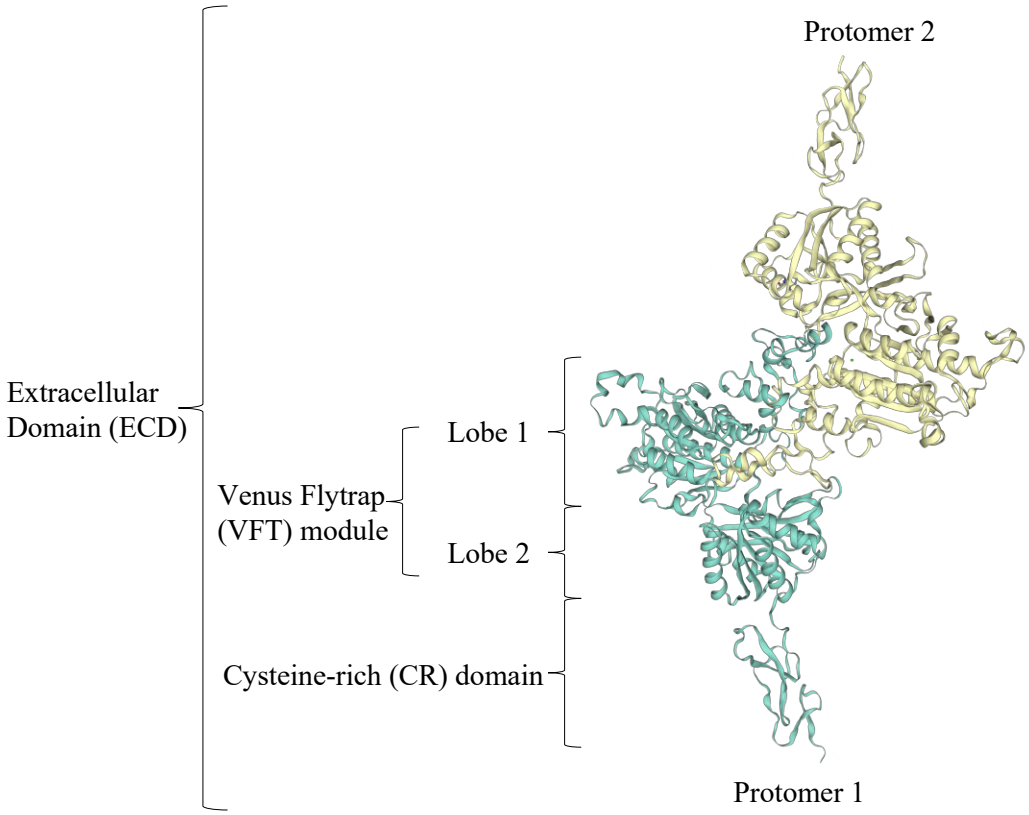


**Figure 4.3** Prediction three-dimensional model of a chicken calcium-sensing receptor disulfide-linked homodimeric extracellular domain structure based on a human calcium-sensing receptor template using the SWISS-MODEL.

### 4.4.2 Relative mRNA abundance of cCaSR and cVDR

The relative mRNA abundance of cCaSR and cVDR in the kidney, proventriculus, duodenum, jejunum, ileum, colon, cecum, shell gland, and tibia are shown in Figure 4.4. The results showed that the mRNA of cCaSR and cVDR was widely expressed in the kidney, proventriculus, gut, bone and shell gland of laying hens. The relative mRNA abundance of cCaSR in the cecum was significantly higher at 19 than at 40 and 55 weeks ($P < 0.05$). The relative mRNA abundance of cCaSR in the kidney, ileum, proventriculus, duodenum, and colon was significantly higher than that in other tissues at 40 weeks ($P < 0.05$). In the tibia, the relative mRNA abundance of cCaSR was significantly higher at 55 than that at 40 weeks ($P < 0.05$). The relative mRNA abundance of cVDR was at a relatively high level in the small intestine (duodenum, jejunum, and ileum) when compared with other tissues at the three different laying stages, but these differences were not significant. Moreover, the relative expression of cVDR in the shell gland was significantly higher at 40 than at 19 and 55 weeks ($P < 0.05$).

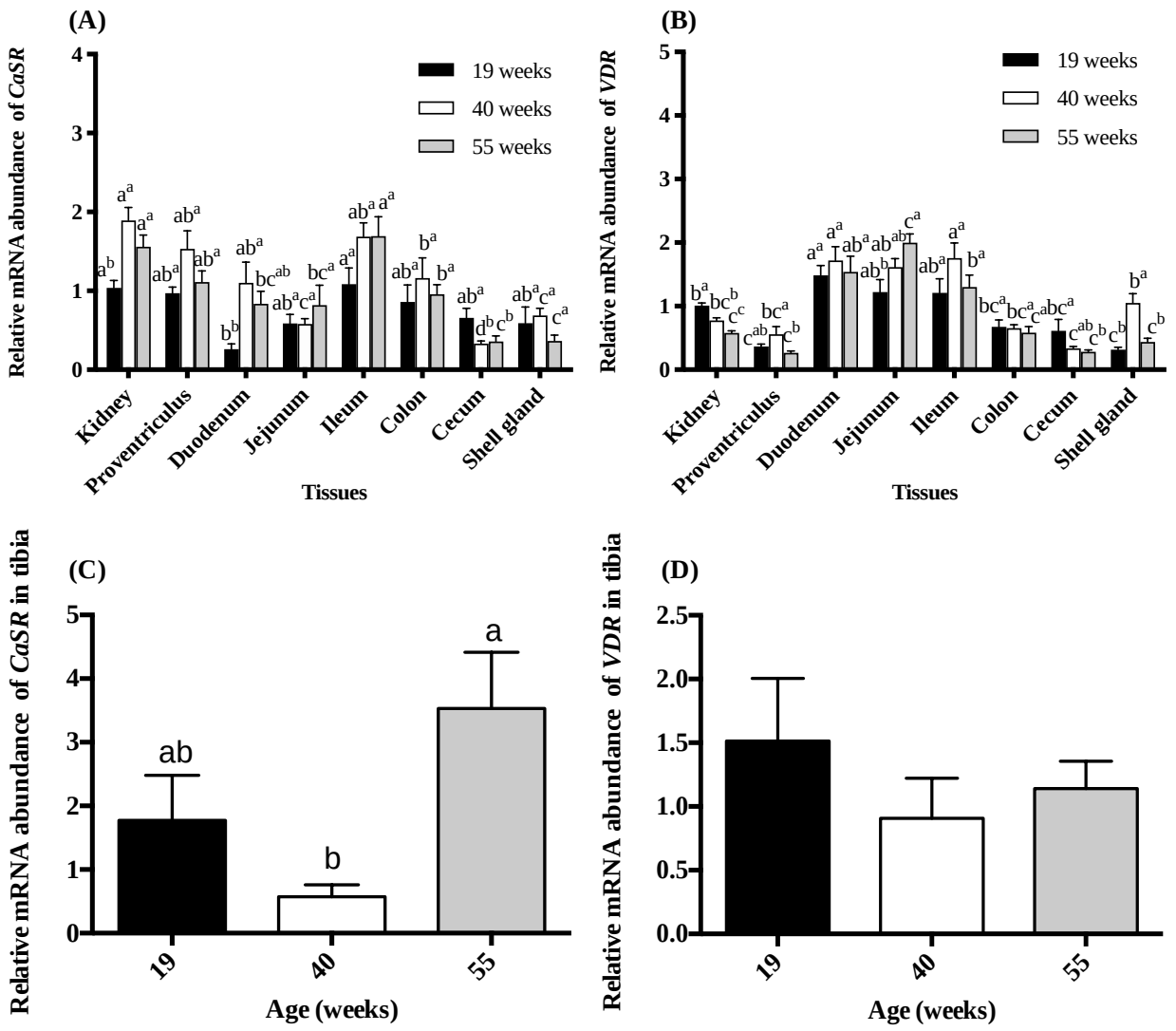


**Figure 4.4** The relative mRNA abundance of chicken *calcium-sensing receptor* (*CaSR,* A) and chicken *vitamin D receptor* (*VDR,* B) in different tissues at three laying stages, and the relative mRNA abundance of *CaSR* (C) and *VDR* (D) in tibia at three different laying stages. Data were presented as mean ± SEM, n = 6. Different letters represent a significant difference among different tissues, and different letter superscripts represent a significant difference at different laying stages ($P < 0.05$).

### 4.4.3 Relative protein expression of cCaSR and cVDR

As shown in Figure 4.5, the protein of cCaSR and cVDR was widely expressed in the kidney, proventriculus, gut, tibia and shell gland of laying hens at 40 weeks. Western blot images show that cCaSR are expressed in four bands with varied molecular weights (Figure 5A), and the bands for quantitating are indicated in "*": 1) more than 250 kDa; 2) between 150 and 250 kDa; 3) and 4) below 150 kDa. The band of chicken VDR was exhibited between 50 and 75 kDa (around 60 kDa) in each tissue (Figure 4.5A). Figure 4.5B shows the quantified number of the four bands of cCaSR. The relative cCaSR protein abundance was not different among the different organs ($P > 0.05$) in the different organs at 40 weeks. Figure 4.5C shows quantitative relative expression of cVDR. The relative cVDR protein abundance was significantly higher in the duodenum than in the proventriculus, colon, and cecum ($P < 0.05$) at 40 weeks. However, no significant difference was observed among the kidney, proventriculus, jejunum, ileum, colon, cecum, and shell gland at 40 weeks ($P > 0.05$). As shown in Figure 4.6A to 4.6R, the protein of cCaSR and cVDR was expressed at the different ages of laying hens. No significant differences in the relative protein abundance of cCaSR and cVDR were observed among tissues at the three different laying stages ($P > 0.05$).

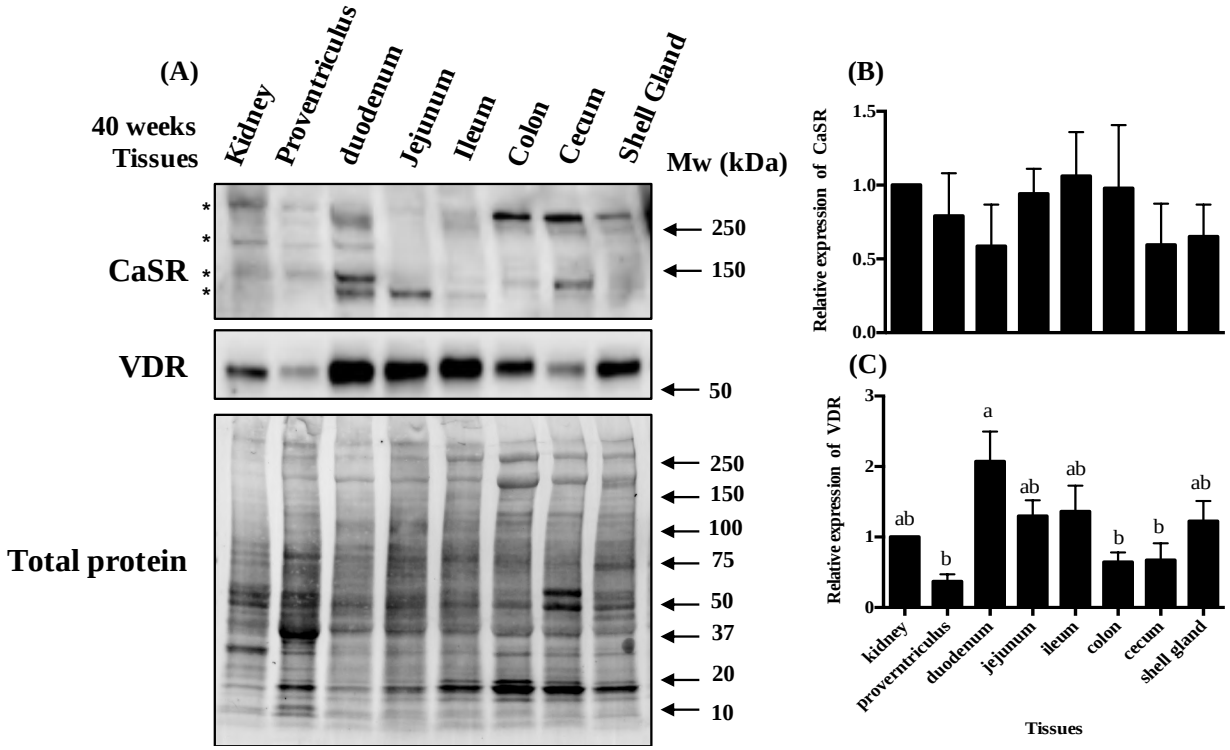


**Figure 4.5** Representative western blot images (A) of chicken calcium-sensing receptor (cCaSR) and chicken vitamin D receptor (cVDR); the quantitative relative expression of cCaSR (B) and cVDR (C) in different tissues at the 40 weeks of age. Data were presented as mean ± SEM, n = 6. Different letters represent a significant difference ($P < 0.05$). Bands for quantitating are indicated in "*".

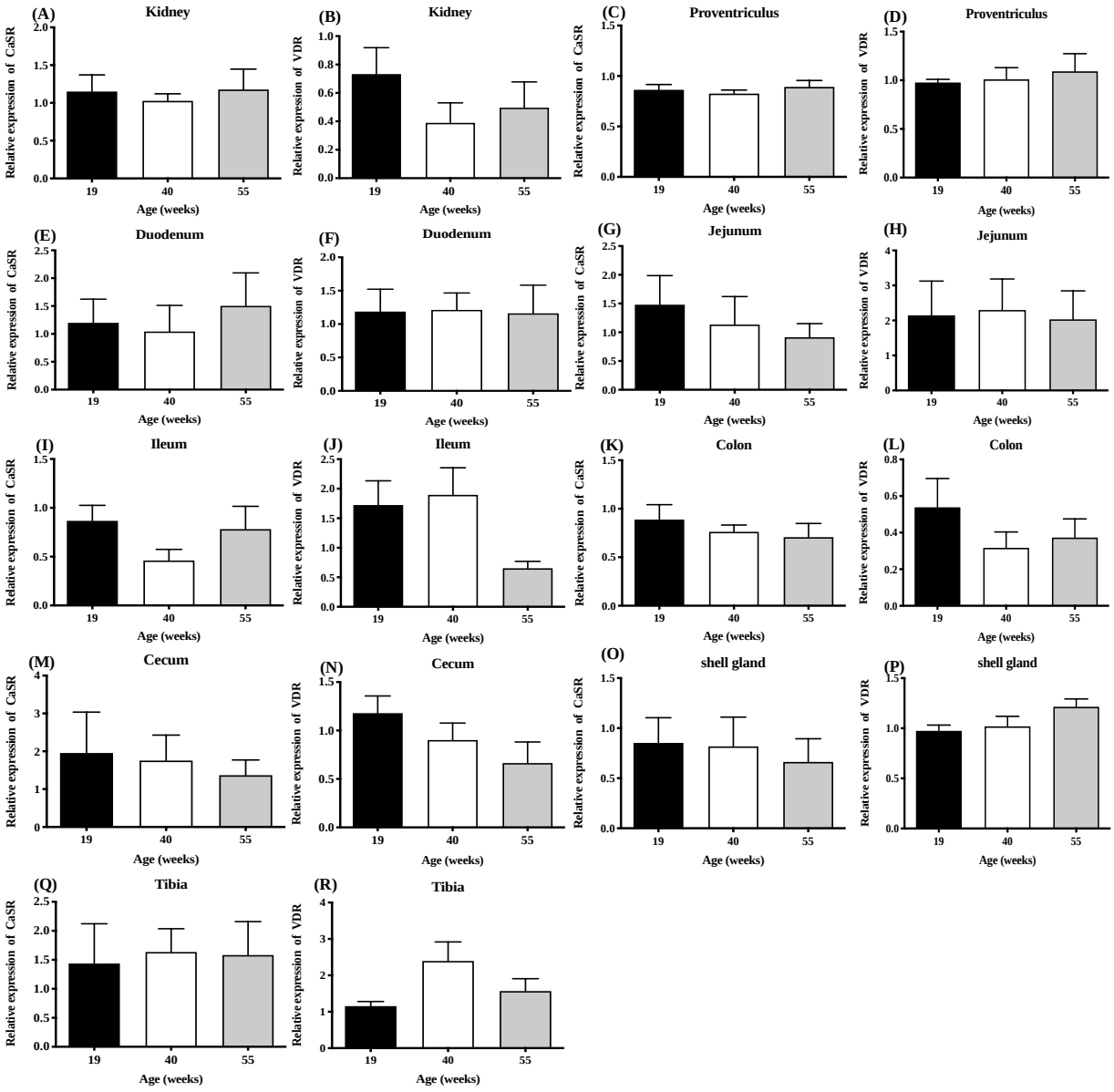


**Figure 4.6** The relative mRNA abundance of chicken *calcium-sensing receptor* in kidney (A), proventriculus (C), duodenum (E), jejunum (G), ileum (I), colon (K), cecum (M), shell gland (O) and tibia (Q) and chicken *vitamin D receptor* in kidney (B), proventriculus (D), duodenum (F), jejunum (H), ileum (J), colon (L), cecum (N), shell gland (P) and tibia (R) at three different laying stages. Data were presented as mean ± SEM, n = 6.

### 4.4.4 Localization of cCaSR

The localization of cCaSR in the kidney, proventriculus, gut, shell gland and tibia at different laying stages was detected by immunohistochemical staining. As shown in Figure 4.7, the positive brown staining was found widely in each tissue at different laying stages. In the kidney, the positive cCaSR staining was widely detected in the nephron, and mainly in the renal tubules. In the proventriculus, cCaSR was distributed on the surface of serrated secretory tubules. In the small intestine including duodenum, jejunum, and ileum, the positive staining was distributed widely along the simple columnar epithelium of the villus and crypts. In the large intestine including colon and cecum, the positive staining was mainly seen in the epithelium of crypts of Lieberkühn. In the shell gland, immunohistochemical positivity was primarily found in the stratified cuboidal epithelium. In the tibia, the clear immunohistochemical positivity was distributed within different laying stages. The positive staining was mainly detected in compact structural bone (cortical bone) at 19 weeks of age, and mainly in the medullary bone (as circled in red) at the 40 weeks of age. At 55 weeks of age, the immunohistochemical positivity was found in both medullary bone (as circled in red) and cortical bone.

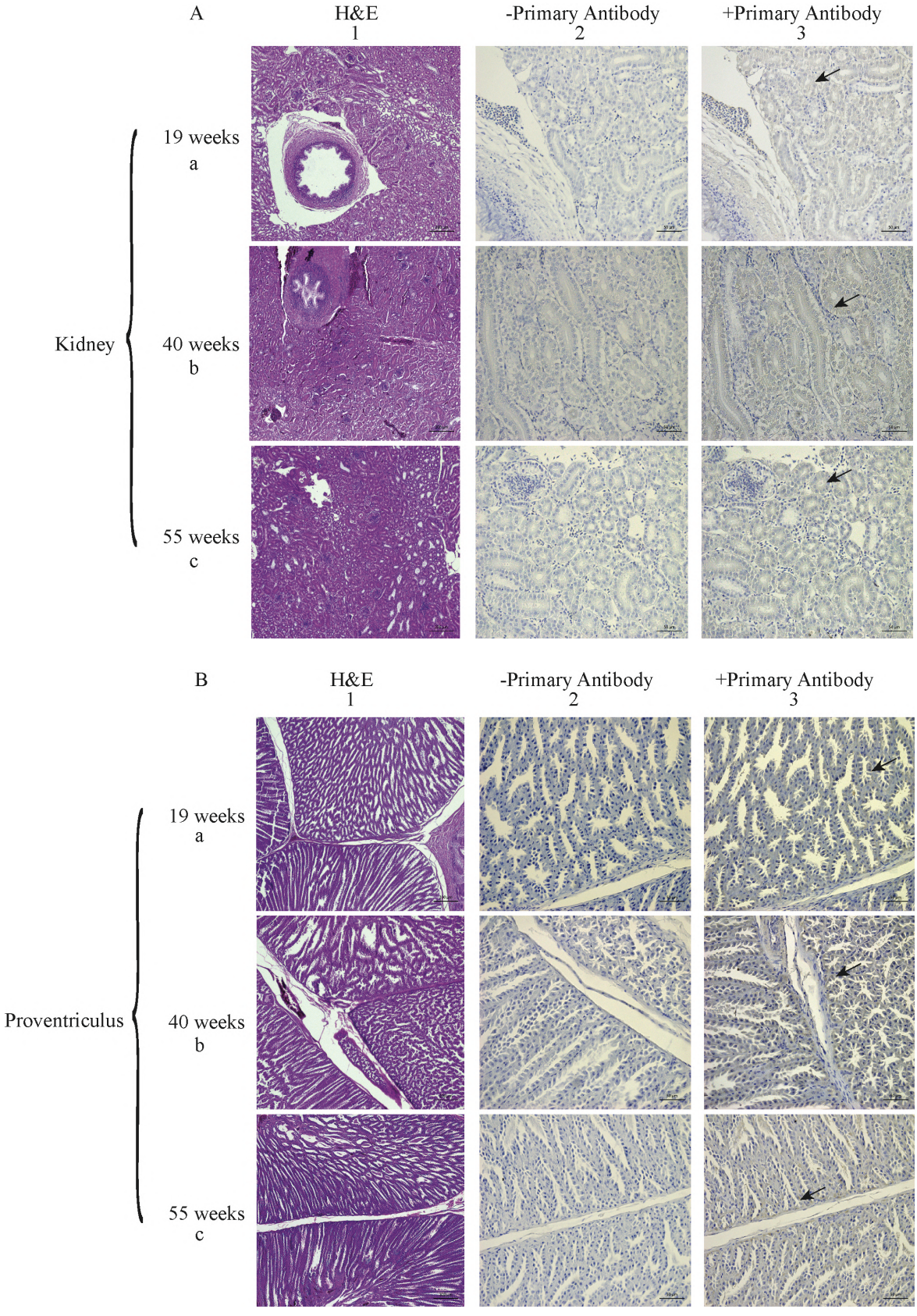
A
H&E
1
-Primary Antibody
2
+Primary Antibody
3
Kidney
19 weeks
a
40 weeks
b
55 weeks
c
B
H&E
1
-Primary Antibody
2
+Primary Antibody
3
Proventriculus
19 weeks
a
40 weeks
b
55 weeks
c

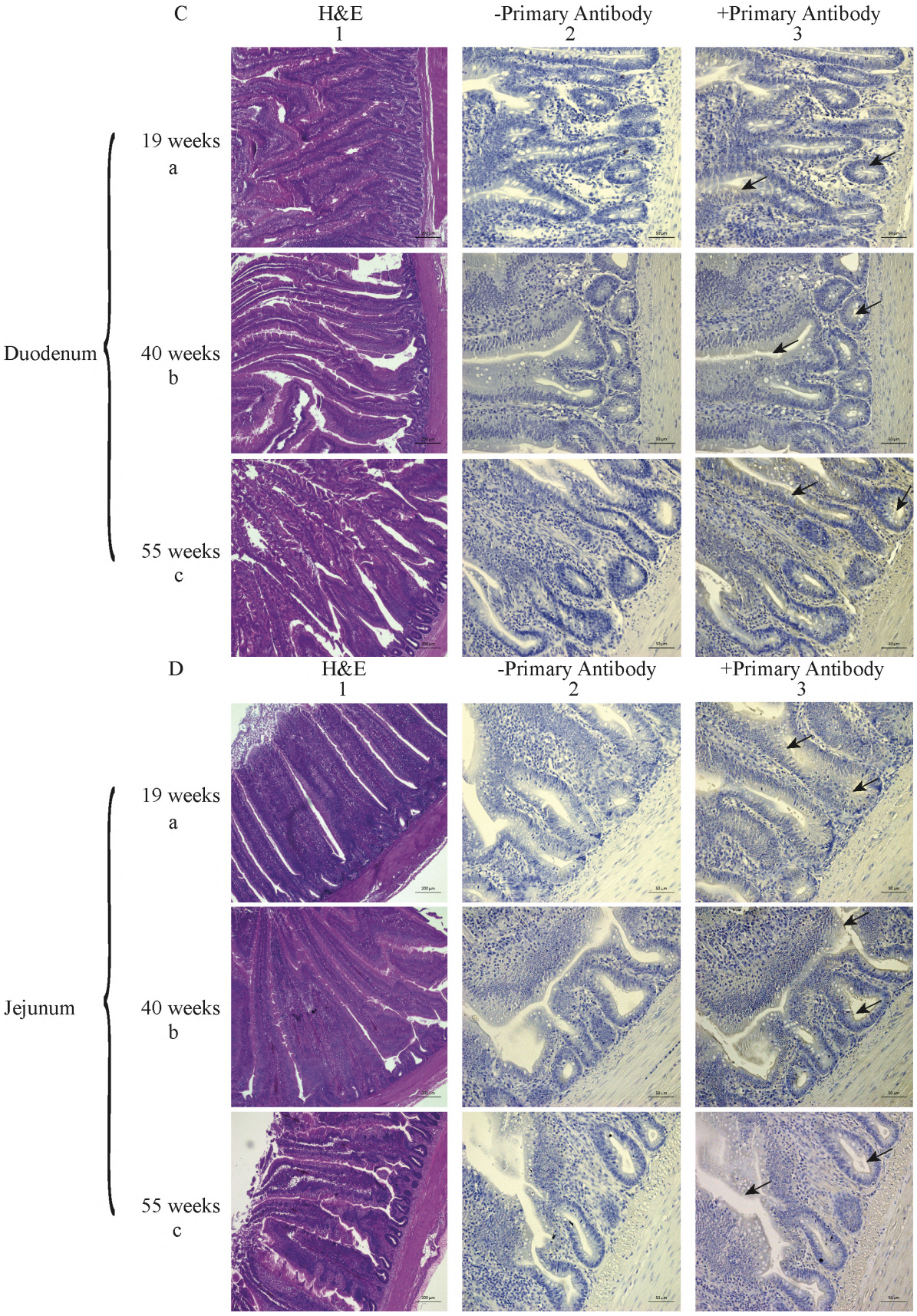
C
H&E
1
-Primary Antibody
2
+Primary Antibody
3
Duodenum
19 weeks
a
40 weeks
b
55 weeks
c
D
H&E
1
-Primary Antibody
2
+Primary Antibody
3
Jejunum
19 weeks
a
40 weeks
b
55 weeks
c

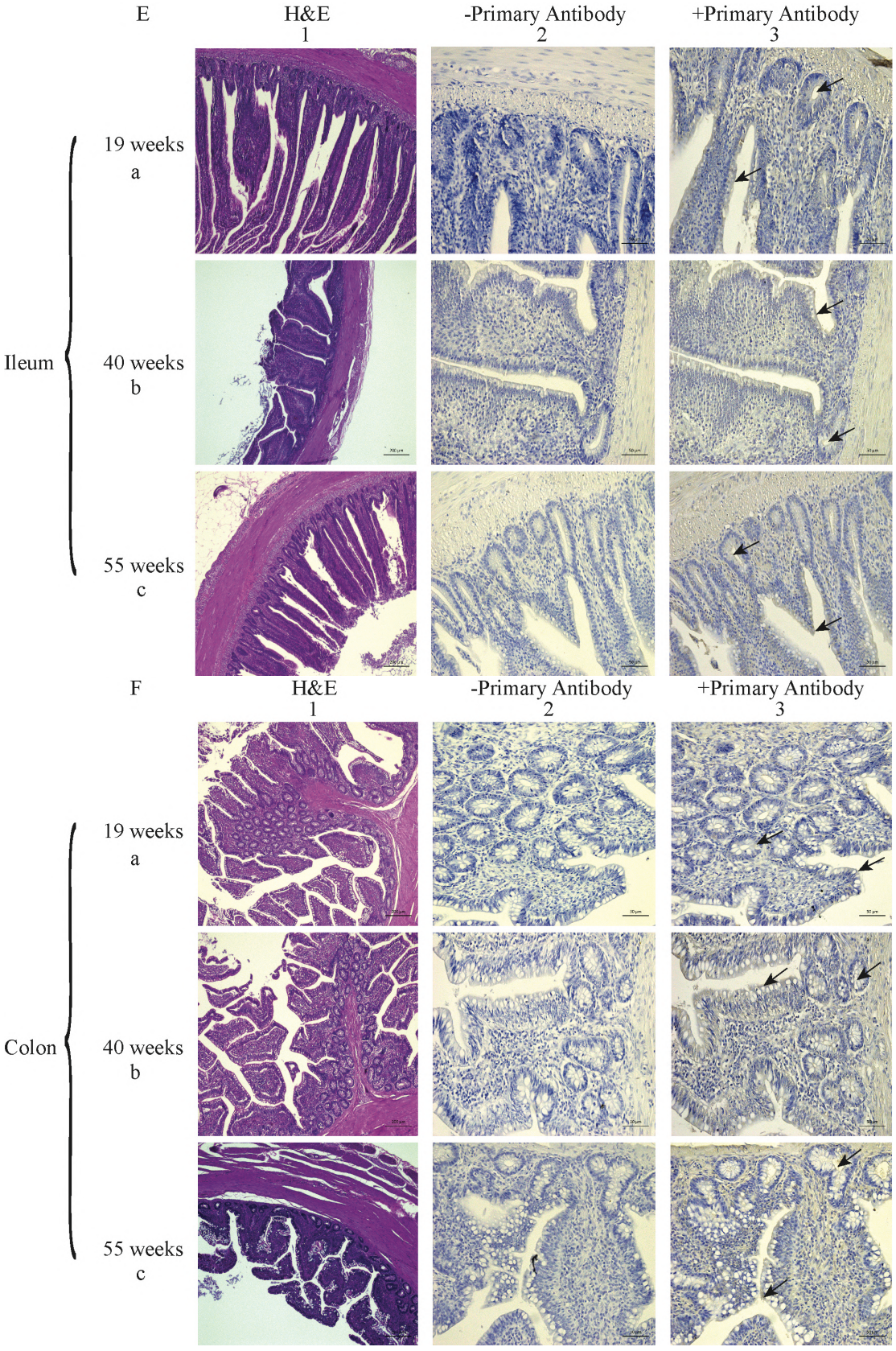
E
H&E
1
-Primary Antibody
2
+Primary Antibody
3
Ileum
19 weeks
a
40 weeks
b
55 weeks
c
F
H&E
1
-Primary Antibody
2
+Primary Antibody
3
Colon
19 weeks
a
40 weeks
b
55 weeks
c

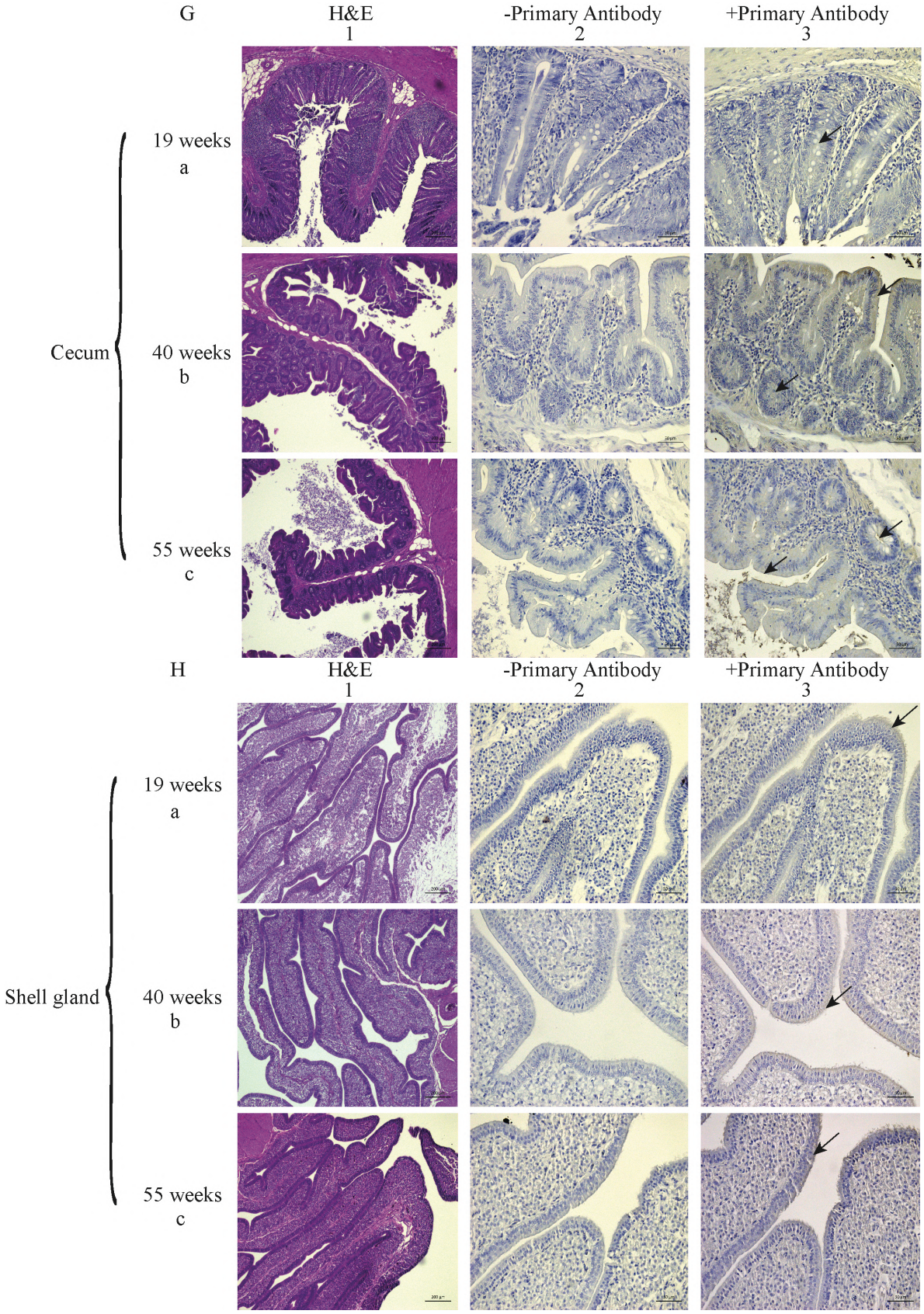
G
H&E
1
-Primary Antibody
2
+Primary Antibody
3
Cecum
19 weeks
a
40 weeks
b
55 weeks
c
H
H&E
1
-Primary Antibody
2
+Primary Antibody
3
Shell gland
19 weeks
a
40 weeks
b
55 weeks
c

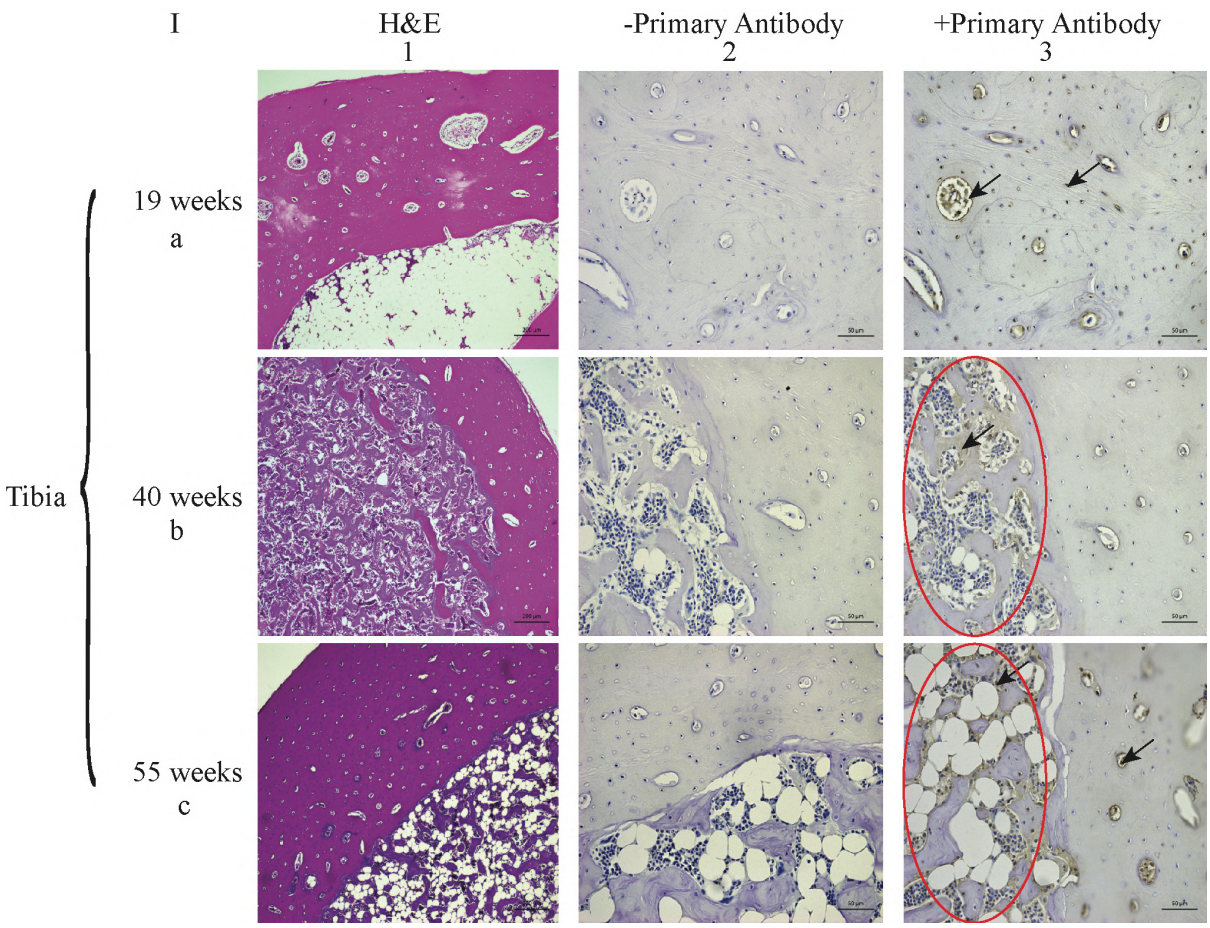


**Figure 4.7** Haemotoxylin and Eosin (H&E) staining (1) and chicken calcium-sensing receptor (cCaSR) immunohistochemistry (2 and 3) in the kidney (A), proventriculus (B), duodenum (C), jejunum (D), ileum (E), colon (F), cecum (G), shell gland (H), and tibia (I) at the 19 weeks (a), 40 weeks (b) and 55 weeks (c) of age. Chicken CaSR immunoreactions are indicated as brown staining (+Primary Antibody, black arrows) and they are in contrast to blue counterstaining of the nuclei (-Primary Antibody). Medullary bone in the tibia is indicated in red circles. Scale bar for H&E staining represents 200 µm, and for cCaSR immunohistochemistry is 50 µm. Black arrows indicate positive staining.

## 4.5 Discussion

Previous studies suggest that cCaSR has similar characteristics with mammalian CaSR and may also play very important roles in avian calcium homeostasis because of the close conservation of the amino acid sequence of the cCaSR with human CaSR (Diaz et al., 1997) and other mammalian CaSR (Brown et al., 1993; Riccardi et al., 1995; Zhao et al., 2019). Also, the expression of cCaSR in the parathyroid gland is regulated by the plasma calcium concentrations and vitamin D level in the diet (Yarden et al., 2000). In the present study, cCaSR was predicted to show a similar secondary and three-dimensional crystal structure with mammalian CaSR (Diaz et al., 1997), and the cCaSR was able to respond to exogenous $Ca^{2+}$, $Mg^{2+}$ and $Gd^{3+}$ (Diaz et al., 1997), which may support the hypothesis that cCaSR could play similar roles as mammalian CaSR. It has been well documented that in addition to calcium, a variety of nutritional ligands including di- and trivalent cations, AAs, pharmacological agents, polyamines, and polypeptides in mammals can activate CaSR (Magno et al., 2011; Zhao et al., 2019). Therefore, the cCaSR may share similar ligands with the mammal CaSR. The cCaSR has a large hydrophilic ECD, a seven helical hydrophobic TMD and a small hydrophilic ICD, and functions to detect ionized plasma calcium concentration, which shows a similar variation range to mammals, of between 1.2 mM and 1.3 mM to maintain calcium homeostasis (Diaz et al., 1997). Therefore, it would be critical to characterize the functions of cCaSR and its potential ligands including nutrients, non-nutritional compounds and tastants, which might help to develop novel approaches to reduce the incidence of osteoporosis in laying hens.

The distribution of cCaSR and cVDR is closely related to their function. In this study, the results demonstrated that cCaSR and cVDR were expressed in the kidney, proventriculus, duodenum, jejunum, ileum, colon, and cecum, which is consistent with the cCaSR expression

profile from previous studies in the kidney, duodenum and the whole small intestine (Diaz et al., 1997; Deng et al., 2010). Notably, the gene and protein expression, and the distribution pattern of cCaSR in the different segments of the GIT, shell gland, and tibia was reported for the first time in the current study. Moreover, our results demonstrated that similar to cVDR, cCaSR is also distributed in the shell glands and tibia of laying hens, similar to what has been reported by others (Berry et al., 1996; Yoshimura et al., 1997). Similar to mammalian CaSR, the expression of cCaSR in the bones may be related to the calcium homeostasis and bone turnover in laying hens. However, the role of cCaSR in the shell glands is not known but may be related to eggshell formation because the shell gland is involved in the synthesis and secretion of substances for the formation of distinct layers of the eggshell (Bar, 2009).

In the present study, the higher gene expression of *cCaSR* was found in the kidney, proventriculus (true stomach), and small intestine especially the ileum, which is consistent with that in mammals (Hebert, 1996; Brown and MacLeod, 2001; Fudge and Kovacs, 2004; Hebert et al., 2004; Zhao et al., 2019). However, the higher gene expression of *cVDR* was only found in the small intestine (duodenum, jejunum, and ileum), which is consistent with its function. The CaSR maintains calcium homeostasis by regulating parathyroid gland, kidney, GIT and the secretion of PTH, calcitonin and $1,25(OH)_2D_3$. The kidney is responsible for the reabsorption of calcium and other mineral ions such as magnesium, and to the amount of minerals being excreted. Moreover, renal calcium status is a part of calcium homeostasis that closely affects homeostatic regulation of calcium and the secretion of its regulators [PTH, calcitonin, and $1,25(OH)_2D_3$] because of feedback mechanisms (Riccardi and Brown, 2010). Therefore, detecting and monitoring renal calcium levels is critical to systematically regulate calcium homeostasis. Lots of evidence showed that CaSR is widely distributed along the epithelium of the GIT where digestion and absorption of nutrients

occur (Cheng et al., 1999; Hebert et al., 2004). Changes in $Ca^{2+}$ concentration are also associated with secretion of gastrin, gastric acid, and $HCO_3^-$ in the stomach, which is important for food digestion (Cheng et al., 1999). The proventriculus is the true stomach in poultry and performs the same function as the stomach in mammals, which can secret gastric acid and enzymes to initiate protein digestion. Proteins are broken down by proteases into smaller peptides and AAs during the digestion. L-AAs and other small peptides are known to be potent ligands for CaSR (Congrave et al., 2020; Zhang et al., 2015). This might be the reason why the expression level of cCaSR was much higher in the proventriculus. The small intestine undertakes the most absorption and chemosensing of nutrients. The gut chemosensing system is considered to be performed by the GPCRs that recognize nutrients, chemicals, and even microorganisms, and then initiates a downstream signaling cascade to maintain mineral homeostasis, and to regulate feed intake, gut function, and metabolism (Roura et al., 2019). Also, CaSR as a multimodal sensor can bind many nutrients especially $Ca^{2+}$ and L-AAs, that might mediate nutrient absorption. Within the small intestine, unlike in mammals, the majority of calcium absorption does not take place in the ileum in laying hens (Hurwitz and Bar, 1966), but the expression of cCaSR in the ileum was higher than that in the duodenum and jejunum, which was consistent with the results of CaSR distribution in pigs (Zhao et al., 2019). This might be attributed to more hormones secreted by ileal enteroendocrine cells, which depends on the signaling of cellular calcium mobilization (Liou, 2013). There are various hormones such as glucagon-like peptide 1 and 2, peptide YY and oxyntomodulin that are secreted by L cells in the ileum, regulating satiety, intestinal motility, transit, gastric emptying, intestinal integrity, and permeability, etc. (Liou, 2013). These results also illustrated that the predominant role of cCaSR might not be to directly regulate calcium absorption. Instead, the principal function of cCaSR is probably sensing the changes of calcium concentration

to communicate with other receptors and mediate various biological processes via hormones or downstream signaling pathways to maintain the homeostasis of calcium or other nutrients. Compared to CaSR, the function of VDR is more specific, which assists calcium absorption through calcium transporters. The most of calcium is absorbed in the small intestine explaining why cVDR is mainly expressed in the small intestine. When $1,25(OH)_2D_3$ diffuses into cells, it binds to either cytoplasmic or nuclear VDR, and then trigger the formation of a heterodimer of VDR with a partner protein that binds to vitamin D response element (VDRE) located in the promoter region of target genes. VDRE has been found in a number of genes in mammals including $25(OH)D_3$ 24-hydroxylase, PTH, calbindin $D_{9k}$ and $D_{28k}$, calcium ion channels, CaSR, and osteocalcin, which are related to calcium absorption and homeostasis (Lu et al., 2000; Hendy and Canaff, 2016). However, during the process of calcium absorption in the small intestine, VDR is not the only element to respond to $1,25(OH)_2D_3$. Alternatively, $1,25(OH)_2D_3$ only takes minutes to hours to exert effects via binding to the other protein without going through longer genomic pathways (Huhtakangas et al., 2004). Therefore, other possibilities should be considered regarding the regulation of calcium absorption and homeostasis in layers.

Nevertheless, the expression of cCaSR did not vary significantly in different tissues at peak production (40 weeks of age). Western blot images showed that CaSR had different forms in chickens. As the cCaSR exhibits a high homology and a similar molecular weight to mammal CaSR, the different forms of cCaSR might have similar modifications. Therefore, in this study, approximately 120 kDa band might be unglycosylated cCaSR protein; approximately 140 kDa band might be the core-glycosylated, high-mannose form of cCaSR (in the endoplasmic reticulum); approximately 160 kDa might be maturely glycosylated form of cCaSR (in the Golgi complex); more than 250 kDa band might be dimers and higher-order oligomers of cCaSR (White et al.,

2009). In different tissues, we also observed that different forms of CaSR are expressed in different quantities. Various modifications and rapid turnover of CaSR probably resulted in a stable total amount of cCaSR. Calcium is absorbed by both an active transcellular pathway, and by a passive paracellular pathway through tight junctions. Most calcium transport proteins involved in the active transcellular pathway depend on $1,25(OH)_2D_3$ and VDR. Among the small intestine, the duodenum has a highly active transport system (Christakos et al., 2011). That might be the reason why the expression of VDR in the duodenum is higher than that in other segments of the small intestine at peak production. Interestingly, different laying stages rarely affected the expression of both cCaSR and cVDR, which illustrated the importance of cCaSR and cVDR to regulate calcium homeostasis throughout the whole laying period.

The cCaSR was expressed in tubular structures of the nephron. This finding is consistent with previous research by Diaz et al. (1997), who confirmed the presence of cCaSR in certain tubular cellular structures. Calcium absorbed from the gut enters the blood and is filtered by the kidney. In hens, 99% of filtered calcium is reabsorbed in the kidney (Wideman Jr et al., 1987). In addition, the rat CaSR has been identified in various segments of the nephron, with the polarity of its expression varying according to the specific cell type within each segment (Riccardi et al., 1998). This unique distribution pattern implies that it can sense alterations taking place in both the urinary space and the interstitial plasma (Riccardi and Brown, 2010). The GIT is another major site where cCaSR is located. The positive staining was found along the epithelium of the small intestine, which was consistent with what has been reported in mammals (Chattopadhyay et al., 1998; Zhao et al., 2019). It has been reported that CaSR is present in goblet cells and enteroendocrine cells (Hira et al., 2008). Although enteroendocrine cells account for ~1% of epithelial cells, they play an important role in hormone secretion to communicate with other cells and relay signals to the

brain thus regulating gut function and metabolism (Liou, 2013). Therefore, it is of significance that a large number of GPCRs such as CaSR and taste receptors located in enteroendocrine cells contribute to nutrient sensing. Notably, the bone types in the female avian are distinctive from that in mammals, which includes cortical, cancellous, and medullary bones during egg laying (Kim et al., 2007). Medullary bone is a highly labile secondary bone, providing calcium for eggshell formation by its resorption (Kim et al., 2012). It has been reported that hormones (estrogen and androgen) regulate the formation of the medullary bone (Fisher and Schraer, 1982). Medullary bone resorption is a crucial biological process to release calcium, which is undertaken by osteoclasts. It has been reported that CaSR is expressed in osteoclasts. Activation of osteoclasts may result in the proliferation, differentiation, and apoptosis of osteoclasts (Dvorak et al., 2004; Mentaverri et al., 2006). This indicates that CaSR might be an important receptor to regulate bone resorption and maintain calcium homeostasis in laying hens.

In conclusion, this study demonstrated that cCaSR and cVDR are widely distributed in the kidney, proventriculus, duodenum, jejunum, ileum, colon, cecum, shell gland, and tibia of laying hens at different laying stages, especially cCaSR in the proventriculus, shell gland and tibia, and its distribution pattern in the GIT, which was reported for the first time. Relative expressions of cCaSR and cVDR varied in different tissues but did not change significantly among different laying stages. In addition, the localization in different tissues and the crystal structure of cCaSR was also highly similar to mammalian CaSR, which is evidence to support that cCaSR could be a potential therapeutic target for osteoporosis in laying hens.

## BRIDGE TO CHAPTER FIVE

In chapter four, the molecular distribution and localization of the chicken CaSR and VDR in different tissues at different laying stages in laying hens were investigated. We first confirmed that the CaSR is expressed in the shell gland and tibia. Our results illustrated the high similarity between human and chicken CaSR in terms of their structures and expression patterns. In chapter five, we will further explore the underlying mechanism by which chicken CaSR performs its function through constructing a chicken CaSR overexpression *in vitro* system to 1) characterize the roles of the chicken CaSR 2) identify potential nutritional chicken CaSR ligands; 3) reveal the chicken CaSR response mechanism to nutritional ligands and downstream biased signaling cascades; and 4) to simulate ligand binding sites and modes.

## CHAPTER FIVE: MANUSCRIPT II

**Modulation mechanism of L-tryptophan and phosphate to the chicken extracellular calcium-sensing receptor via downstream G protein-coupled signaling cascades and their binding modes**[2]

[2]**Qianru Hui**, Huanhuan Dong, Xiaoya Zhao, Paula Azevedo, Shangxi Liu, Martin Nyachoti, Karmin O, Chengbo Yang

Under review in *Animal Feed Science and Technology.*

## 5.1 Abstract

Laying hens have a dynamic bone turnover and a high demand for calcium from both feed and bone stores due to the daily egg-laying cycle. This study aims to reveal the modulation mechanism and binding sites of a nutritional agonist (L-Trp) and a nutritional antagonist (inorganic $PO_4^{3-}$) to the chicken extracellular calcium-sensing receptor (cCaSR), and to provide evidence for maintaining the desired calcium homeostasis and preventing or attenuating chicken osteoporosis through the cCaSR modulation. Based on the luciferase reporter system, the two modulators showed biased agonism or antagonism through the $G\alpha_q$, $G_{\beta\gamma}/G\alpha_i$, $G\alpha_{12}$, and $G\alpha_i$-mediated signaling pathways and induced the changes in the second messengers, including intracellular $Ca^{2+}$, extracellular signal-regulated kinase (ERK) 1/2, RhoA, and cyclic adenosine monophosphate (cAMP), respectively. L-Trp-induced cCaSR activation required the presence of $Ca^{2+}$, and the $Ca^{2+}$ concentration affected the activation potency. The half-maximal effective concentration ($EC_{50}$) value for $Ca^{2+}$ left-shifted by 12.88%, 5.18%, and 1.02% in the $G\alpha_q$, $G_{\beta\gamma}/G\alpha_i$, and $G\alpha_{12}$-mediated signaling pathways in the presence of 1 mM L-Trp, while the half-maximal inhibitory concentration ($IC_{50}$) of cAMP level for $Ca^{2+}$ right-shifted by 10.15% in the $G\alpha_i$-mediated signaling pathway in the presence of 1 mM L-Trp. The cCaSR response was significantly inhibited with increasing inorganic $PO_4^{3-}$ concentration by 92.97%, 31.50%, and 30.23% in the $G\alpha_q$, $G_{\beta\gamma}/G\alpha_i$, and $G\alpha_{12}$-mediated signaling pathways at 2 mM of $PO_4^{3-}$ compared with the control (0.9 mM $PO_4^{3-}$). The cAMP level was significantly increased by 51.20% ($P < 0.05$) at 5 mM of $PO_4^{3-}$ compared with the control in the $G\alpha_i$-mediated signaling pathway. Therefore, both L-Trp and $PO_4^{3-}$ were biased toward the $G\alpha_q$-mediated NFAT-RE signaling pathway. According to molecular docking and dynamics results, L-Trp shows one binding site in the extracellular domain (ECD) of cCaSR. In addition to hydrogen bonds, its aromatic side chain is conducive to binding with hydrophobic

interactions; $PO_4^{3-}$ shows two binding sites also in the ECD of cCaSR, with the hydrogen bonds being the main bond type. In conclusion, this study demonstrates that L-Trp and inorganic $PO_4^{3-}$ were cCaSR modulators, acting as positive and negative allosteric modulators, respectively, with biased agonism and antagonism, which provided evidence for cCaSR as a potential therapeutic target in chicken osteoporosis.

**Key words**: Chicken extracellular calcium-sensing receptor; L-tryptophan; Inorganic phosphate; G protein-coupled signaling; Molecular docking

## 5.2 Introduction

The extracellular calcium-sensing receptor (CaSR) is a homodimeric complex located in the cell membrane, and it belongs to the metabotropic glutamate receptor (mGluR) subclass of the G protein-coupled receptors (GPCRs) superfamily (Jensen and Brauner-Osborne, 2007). This receptor can sense subtle changes in extracellular $Ca^{2+}$ concentration and mediate PTH secretion to maintain calcium homeostasis via regulating intestinal absorption, bone storage and exchange, and renal reabsorption (Conigrave, 2016). In addition, CaSR mediates a variety of (patho)physiological processes, such as ion channel activity, gene expression, inflammation, proliferation, differentiation, and apoptosis by triggering downstream signaling cascades (Brown et al., 1979a; Kallay, 2018).

Laying hens have a rapid bone turnover and high calcium demand because of the daily egg-laying cycle. Insufficient dietary calcium for eggshell calcification is supplemented by medullary bone resorption. Over time, the modeling and remodeling of medullary bone contributes to a more diffuse arrangement of medullary bone spicules and the decrease in the proximity between medullary bone and the structural bone surfaces, resulting in the structural bone tissues being

exposed to the effects of osteoclasts (Korver, 2020). As the structural bone is not replaced, the net effect is structural bone loss and the progressive development of layer osteoporosis (Whitehead and Fleming, 2000). Osteoporosis is one of the major causes of bone fractures in laying hens. Bone fractures are associated with pain and animal welfare issues. In addition, economic factors such as egg production and eggshell quality are closely linked to issues concerning bones (Kim et al., 2012). Restoring or maintaining the desired calcium homeostasis using a nutritional approach might be an effective strategy for improving bone health and eggshell quality in laying hens. The CaSR is involved in detecting subtle changes in extracellular $Ca^{2+}$ and maintaining calcium homeostasis (Kallay, 2018), thus it might be a potential and promising therapeutic target in osteoporosis in laying hens.

It is well recognized that there are two categories of CaSR ligands: orthosteric agonists and allosteric modulators (Saidak et al., 2009). Orthosteric agonists can directly bind to CaSR orthosteric sites where the primary ligand $Ca^{2+}$ is bound to activate CaSR. Allosteric modulators including positive allosteric modulators (PAMs) and negative allosteric modulators (NAMs), bind to allosteric sites distinct from orthosteric sites on CaSR, and require the presence of $Ca^{2+}$ to activate CaSR concertedly (Saidak et al., 2009). The aromatic L-amino acids such as L-Trp and some short aliphatic L-amino acids including L-Thr and L-Ala were identified as PAMs of CaSR (Conigrave et al., 2000b; Conigrave et al., 2007). $PO_4^{3-}$ has also been reported to be a NAM (Centeno et al., 2019).

The application of these allosteric modulators enhances/reduces the sensitivity of CaSR to extracellular $Ca^{2+}$. The CaSR is a broad-spectrum L-amino acid sensor (Conigrave et al., 2007). Previous studies have reported that L-aromatic amino acids were more potent PAMs of CaSR than other amino acids (Conigrave et al., 2000b). In addition, Trp is an essential amino acid, and it is

involved in the synthesis of some functional metabolites, such as serotonin (Le Floc'h et al., 2011). Its dietary requirement is at a relatively low level and decreases with age (Li et al., 2010). Generally, Trp obtained from conventional layer diets can meet the requirement, but proper supplementation of Trp showed beneficial effects on eggshell quality and immune function, as well as reducing stress and enhancing appetite (Macelline et al., 2021). Calcilytics such as NPS 2143 and NPS 89636 are CaSR antagonists. They have shown great potential for human osteoporosis treatment by blocking CaSR and stimulating the endogenous PTH secretion (Nemeth et al., 2001; Nemeth, 2002). Inorganic $PO_4^{3-}$ as a NAM has been reported to block CaSR in the stably transfected human CaSR HEK293 cells via a non-competitive antagonism, reducing receptor efficacy but not potency (Centeno et al., 2019). A large amount of phosphorus is stored in the form of phytic acid in plant-based feed ingredients, but phytic acid is a common anti-nutritional factor that has negative effects on phosphorus utilization in feed ingredients and causes phosphorus pollution (Cowieson et al., 2006). Phytase supplementation in the feed is a good strategy for alleviating the negative effects caused by phytic acid in laying hens (Bello and Korver, 2019), and the free $PO_4^{3-}$ released from phytic acid might create a great potential for CaSR modulation. Moreover, Geng et al. (2016) have presented the first crystal structures of the extracellular domain of human CaSR in active and inactive states, and the binding sites of $Ca^{2+}$, L-Trp, and $PO_4^{3-}$ have been identified. Wen et al. (2021) demonstrated that L-Trp was also an agonist of chicken CaSR.

It has been recognized that GPCRs show "functional selectivity" or "biased signaling" after ligand binding (Seyedabadi et al., 2019). Generally, different ligands have different binding sites to the GPCR and induce the distinct conformational reorganization of the receptor and then preferentially select one or more downstream pathways to transduce signals. It is of significance to understand the mechanism of the biased signaling for cCaSR because it may provide the

theoretical evidence for chicken osteoporosis drug/nutritional modulator discovery to increase therapeutic benefits and minimize the side effects for biased ligands (Thomsen et al., 2012; Leach et al., 2015). However, no systematic study has been conducted to investigate how CaSR initiates downstream signaling cascades and biased agonism/antagonism of CaSR regarding the Gα and $G_{\beta\gamma}$ subunits. Moreover, the binding mechanism of L-Trp and $PO_4^{3-}$ to chicken CaSR is still unclear. In this study, we hypothesized that, as with human CaSR, L-Trp and inorganic $PO_4^{3-}$ are able to activate or block cCaSR with biased downstream signaling, and each modulator exhibits a distinctive binding mechanism. The objectives of this study were to investigate two potent nutritional ligands L-Trp (agonist) and inorganic $PO_4^{3-}$ (antagonist) to cCaSR and how the extracellular signals were transmitted via intracellular coupling with heterotrimeric G proteins after cCaSR was activated or blocked; and to predict the potential binding sites and modes for these two modulators by molecular docking and dynamics.

## 5.3 Materials and methods

### 5.3.1 Materials

Flp In™-293 cell line (Catalog No. R750-07) and pcDNA™ 5/FRT vector (Catalog No. V6010-20) were purchased from Life Technologies (Waltham, MA, USA). The cyclic adenosine monophosphate (cAMP) response element (CRE) Firefly Luciferase vector (pGL4.29 E8471), nuclear factor of activated T-Cells response element (NFAT-RE) Firefly Luciferase vector (pGL4.30, E8481), serum response element (SRE) Firefly Luciferase vector (pGL4.33, E1340), serum response factor response element (SRF-RE) Firefly Luciferase vector (pGL4.34, E1350), and Dual-Glo® Luciferase Assay System (E2940) were purchased from Promega (Madison, WI, USA). The cAMP-Gi assay kit (62AM9PEB) was purchased from Cisbio (Codolet, France). The pRL-TK *Renilla* Luciferase reporter vector was kindly provided by Dr. Abdelilah Soussi Gounni's

lab as a gift. All other reagents and chemicals were from Sigma Aldrich (St. Louis, MO, USA) unless otherwise stated.

### 5.3.2 Expression vector

Chicken (*Gallus gallus*) CaSR complementary DNA containing a C-terminal Flag-tag and two restriction enzyme sites (AflII and XholI) were synthesized and inserted into a pcDNA3.1(+) expression vector (GeneUniversal, Anhui, China). Next, chicken (*Gallus gallus*) CaSR complementary DNA containing a C-terminal Flag-tag after signal peptides were digested and inserted into a pcDNA$^{TM}$ 5/FRT vector for further experiment.

### 5.3.3 Cell culture and generation of stable transfected cCaSR Flp-In$^{TM}$ cell line

Flp In$^{TM}$ 293 cells were cultured in a Dulbecco's modified Eagle's medium (DMEM) high glucose containing 1.8 mM $CaCl_2$, 0.078 mM L-Trp, and 0.9 mM $NaH_2PO_4$ from Gibco/Life Technologies (Gibco/Life Technologies, Cat. No: 11965092) supplemented with 10% fetal bovine serum (FBS) and 50 U/mL penicillin/streptomycin (Gibco/Life Technologies) at 37°C with a 5% $CO_2$ atmosphere. DMEM (high glucose and no phosphates) containing 1.8 mM $CaCl_2$ and 0.078 mM L-Trp (Gibco/Life Technologies, Cat. No: 11971025, Gibco) and DMEM (high glucose, no glutamine, and no calcium) containing 0.078 mM L-Trp and 0.9 mM $NaH_2PO_4$ (Gibco/Life Technologies, Cat. No: 21068028) were also used for measuring the dose-response curve of $Ca^{2+}$ upon cCaSR activation. A Stable Flp-In$^{TM}$ 293 cell line expressing chicken CaSR (cCaSR-293) were generated by cotransfecting with pcDNA$^{TM}$5/FRT vectors containing chicken CaSR genes and pOG44 plasmids which expresses the Flp recombinase, and pcDNA$^{TM}$5/FRT/CAT vectors and pOG44 plasmids were cotransfected in Flp In$^{TM}$ 293 (CAT-293) cells as a transfection control using lipofectamine 2000 transfection reagent (Life Technologies) followed by hygromycin selections. Cells were selected from a single colony and cultured.

### 5.3.4 Verification of the stable expression of cCaSR

When cells reached 70-80% confluence in 6-well plates after three to four weeks, the quantitative real-time RT-PCR and Western blot were conducted to verify the expression of gene/protein of interest.

Total RNA extraction from cells was conducted using TRIzol™ reagent (Invitrogen Life Technologies, Waltham, MA, USA) as described in the manufacturer's instructions. The first-strand cDNA was synthesized using the iScript™ cDNA Synthesis kit (Bio-Rad, Hercules, CA, USA) according to the corresponding manufacturer's protocol. The relative mRNA abundance of CaSR was measured using SYBR Green Supermix (Bio-Rad) by a CFX Connect™ Real-Time PCR Detection System (Bio-Rad). PCR amplification was performed at a set of three min at 95°C, then 40 cycles of 20 s at 95°C, 30 s at 60°C, and 30 s at 72°C. At the end of each cycle, the fluorescence was monitored for 10 s. Each reaction was completed with a melting curve analysis to ensure the specificity of the reaction. Threshold cycle (Ct) values of the target and reference gene were detected (Table 5.1).

**Table 5.1** Primers used in this study.

| Genes | Accession No. | Primer sequences (5'→ 3') |
|---|---|---|
| *Gallus CaSR* | XM_416491.6 | Forward: CAAACCAACGGGCACAGAAG |
| | | Reverse: ATGCACTCCACTGATTCGGG |
| *Homo sapiens GAPDH* | NM_001115114.1 | Forward: CCGTCTTGAGAAACCTGCCA |
| (Reference) | | Reverse: GGATGAACGGCAATCCCCAT |

Note: cCaSR: chicken calcium-sensing receptor; hGAPDH: human GAPDH.

The relative protein expression of CaSR and Flag tag was determined by Western blot analysis. Cells were lysed using pre-cooled RIPA buffer containing Halt™ protease and phosphatase inhibitor cocktail (Thermo Scientific) on ice. Total protein concentration was determined using the Pierce™ BCA protein assay kit (Waltham, MA, USA) as described in the manufacturer's instructions. Protein was then denatured using a 4 × Laemmli sample buffer (Bio-Rad) with 0.1 M dithiothreitol (DTT) at 95 °C for 9 min. Then, the denatured protein samples (30 μg) were loaded and separated by 4–15% Mini-PROTEAN® TGX Stain-Free™ Protein Gels (Bio-Rad), and transferred onto a polyvinylidene difluoride (PVDF, Bio-Rad) membrane. Each membrane was blocked using 5% skim milk powder dissolved in tris-buffered saline with 0.1% Tween 20 (TBST) for 1 h at room temperature, and then incubated with the rabbit polyclonal anti-CaSR antibody (1:2000, ab137408, Abcam, Cambridge, MA, USA) and mouse anti-DDDDK-Tag mAb-Tag Monoclonal Antibody (AE005) (1:2000, MA1-710, Thermo Scientific) at 4 °C overnight. Secondary antibody incubation used horseradish peroxidase (HRP)-conjugated goat anti-rabbit IgG (65-6120, 1:5000, Thermo Scientific) and HRP-conjugated goat anti-mouse IgG (31430, 1:1000, Thermo Scientific). Images were detected by ChemiDoc™ Imaging Systems (Bio-Rad) after incubation with Clarity Max™ Western ECL Substrate (Bio-Rad). The densitometry of the target protein bands was quantified by Image Lab Software (Bio-Rad) and normalized to reference (*β-actin*).

**5.3.5 Cell viability**

Cell viability was measured using WST-1 cell proliferation reagent (Sigma-Aldrich, MO, USA) according to the manufacturer's protocol. Briefly, cells were seeded into a 96-well plate. The WST-1 reagent was diluted by 1:30 in a DMEM high glucose medium (calcium and glutamine free) before use. After the incubation at 37°C for 30 min, the absorbance was measured at 450 nm

using a Synergy™ H4 Hybrid Multi-Mode Microplate Reader (BioTek, Vermont, USA). Cell viability results are expressed as a percentage of the specified control or the maximum in the group.

### 5.3.6 Luciferase reporter assay

The stably transfected cCaSR-293 cells and transfection control CAT-293 cells were seeded into 96-well plates with the density of $5 \times 10^4$ cells/well and cultured until the cells reached 70-80% confluence. The pGL4.30 [luc2P/NFAT-RE/Hygro], pGL4.33 [luc2P/SRE/Hygro], pGL4.34 [luc2P/SRF-RE/Hygro] vectors were then transiently transfected into cCaSR-293 and CAT-293 cells with a ratio (Firefly vector: *Renilla* vector = 10:1) using lipofectamine 2000 transfection reagent (Life Technologies) for 4 h according to the manufacturer's protocol. The cells were then cultured in the DMEM containing 10% FBS. After 36 h, cells were serum-starved in the medium containing 1.25 mM $CaCl_2$ and 1% FBS overnight.

### 5.3.7 Dose-response curve of $Ca^{2+}$ upon cCaSR activation

The complete medium was then aspirated and replaced with different concentrations (0, 0.5, 1, 2, 4, 6, 8, 16 mM) of $CaCl_2$ (diluted in DMEM, high glucose, no glutamine, no calcium). After 6 h, Firefly and *renilla* luciferase activities were measured using the Dual-Luciferase® Reporter Assay System according to the protocol by a Synergy™ Hybrid Multi-Mode Microplate Reader (BioTek, Winooski, VT). The reading parameters were as follows: the chemiluminescence mode was auto gain, and the integration time was 1s, no delay. Data were expressed as relative luminescence units (RLU) by calculating with the following equation: RLU = (Firefly $RLU_{cCaSR}$/*renilla* $RLU_{cCaSR}$) - (Firefly $RLU_{CAT}$/*renilla* $RLU_{CAT}$).

### 5.3.8 Dose-response curve of $Ca^{2+}$ in the presence of L-Trp upon cCaSR activation

A stock solution of L-Trp was prepared at 40 mM and diluted to the working concentration (1 mM) in a DMEM high glucose medium (calcium and glutamine free) just before use. The

procedures of luciferase reporter assays were described in detail in section 5.3.6 of the Materials and methods.

### 5.3.9 Dose-response curve of $Ca^{2+}$ in the presence of NPS-R568 upon cCaSR activation

NPS R-568 is a calcimimetic and it is a PAM of human CaSR used clinically, hereafter R568. In consideration of the risk of calcium and phosphate association, R568 was included to induce a cCaSR response (Centeno et al., 2019). A stock solution of R568 was prepared at 5.6 mM in DMSO and diluted to the working concentration (1 μM) in a DMEM high glucose medium (calcium and glutamine free) just before use. The procedures of luciferase reporter assays were described in detail in section 5.3.6 of the Methods.

### 5.3.10 Phosphate-induced inhibition of cCaSR

Phosphate was prepared in the form of phosphate buffer (200 mM) with $Na_2HPO_4$ and $KH_2PO_4$ in a 4:1 ratio (pH = 7.4) and diluted to different working concentrations in a DMEM high glucose medium (calcium and glutamine free) just before use. The procedures of luciferase reporter were carried out as mentioned above.

### 5.3.11 The cAMP production assay

The cAMP level was measured using a cAMP Gi kit (Cisbio, Codolet, France). The assay procedures were conducted according to the manufacturer's protocol. Briefly, the stably transfected cCaSR-293 cells and transfection control CAT-293 cells were centrifuged and resuspended in a DMEM high glucose medium (calcium and glutamine free) at a concentration of 400,000 cells/mL. In a white low volume 384-well plate, 5 μL of cell suspension and 4 μL of test compounds containing IBMX (0.5 mM) and ligands were mixed. The plate was sealed and incubated at 37 ℃ for 30 min. then, 1 μL of forskolin (2.5 μM) was added followed by 30 min incubation at 37 ℃. At last, 5 μL of lysis & detection buffer containing cAMP Eu-cryptate reagent

was added to each well followed by the addition of 5 μL of lysis & detection buffer containing cAMP d2 antibody. The plate was incubated for 1 h at room temperature. The fluorescence emission was measured at 620 nm and 665 nm using a Synergy™ H4 Hybrid Multi-Mode Microplate Reader (BioTek, Vermont, USA).

### 5.3.12 Molecular docking and dynamics simulation

#### 5.3.12.1 Template protein and ligand preparation

The crystal structure of *Gallus gallus* CaSR target protein (PDB ID: 7DD6, resolution: 3.20 Å) was retrieved from the RCSB Protein Data Bank (https://www.rcsb.org/structure/). The protein was prepared and refined using the module of Protein Preparation Wizard in the Schrödinger Maestro software (Schrödinger, LLC, New York, USA). The crystal water was removed, the missing hydrogen atoms were added, and the missing bond information and the missing peptide segments were repaired. The protein was then energy-minimized and geometric structure-optimized (constraint minimization using the opls3e force field). The structures of L-Trp, NPS R-568, and $PO_4^{3-}$ were created using ChemDraw Ultra 12.0, and they were prepared through hydrogenation, structure optimization, and energy minimization according to the default settings of the LigPrep module in the Schrödinger Maestro software.

#### 5.3.12.2 Molecular docking study

The processing and optimization of virtual screening were completed using the Glide module in the Schrödinger Maestro software. When screening in Glide module, the target protein was introduced to specify the appropriate location in receptor grid generation. The active site of the protein was defined as the centroid of the 10 Å box. The visualization after docking was completed using PyMOL 2.1 software to analyze the interaction modes between ligands and the cCaSR, and the interactions with residues around the active site. Ligand binding free energy to the cCaSR was

estimated to validate the docking protocol and evaluate the accuracy of docking procedures using GlideScore, according to the scoring function below (Friesner et al., 2004):

$$\Delta Gbind = C_{lipo-lipo}\sum f(T|r) + C_{hbond-neuto-neut}\sum g(\Delta r)h(\Delta\alpha) + C_{hbond-charged-charged}\sum g(\Delta r)h(\Delta\alpha) + C_{max-metal-ion}\sum f(T|m) + C_{rotb}H_{rotb} + C_{polar-phob}V_{polar-phob} + C_{coul}E_{coul} + C_{vdW}E_{vdW} + solvationerms$$

**5.3.12.3 Molecular dynamics simulation**

The MD simulation of docked complexes was carried out using Desmond version 2020. OPLS3e force field was used to initiate the MD simulation, and the system was solvated using the TIP3 water model. The neutralization of the system was performed by adding counter ions. Energy minimization of the entire system was performed using OPLS3e. The geometry of water molecules, the bond lengths, and the bond angles of heavy atoms were restrained using the SHAKE algorithm. Simulation of the continuous system was executed by applying periodic boundary conditions and long-range electrostatics was maintained using the particle mesh Ewald method. The equilibration of the system was achieved using an NPT ensemble with the temperature at 300 k and pressure at 1.0 bar. The coupling of temperature-pressure parameters was done using the Berendsen coupling algorithm. On post-preparation of the system, the production run was performed for 20 ns with a time step of 1.2 fs, and trajectory recording was done for every 20 ps summing up to 1000 frames. RMSD (Root mean square deviation) was calculated for the backbone atoms and was analyzed graphically to understand the nature of protein-ligand interactions. RMSF for each residue was calculated to analyze the major conformational changes in the residues between the initial state and dynamic state.

### 5.3.13 Statistical analysis

All experiments were conducted with at least three replicates and the results were expressed as the mean ± SEM. Statistical analyses were carried out using GraphPad Prism 8 (San Diego, CA, USA). Statistical significance was determined using one-way ANOVA followed by Dunnett's or Tukey's multiple-comparison test. *P* value < 0.05 was considered statistically significant. Dose–response (stimulation/inhibition) curves were fitted by non-linear regression using the model for dose-response with variable slope (four parameters) in GraphPad Prism 8 (San Diego, CA, USA).

## 5.4 Results

### 5.4.1 Identification of Flp-In™-293 cells stably expressing cCaSR

As no Ct value of cCaSR gene was detected in the CAT-293 cells, the calculation method of the $2^{-\Delta\Delta Ct}$ was not applicable. The Ct value of the cCaSR gene was 19.34 ± 0.07 (mean±SEM), and the Ct value of the human GAPDH gene was 18.21 ± 0.11 (mean ± SEM) in the cCaSR-293 cells. The gene expression level of cCaSR was close to that of the reference gene, illustrating that the expression level of CaSR was very high in the cCaSR-293 cells. In addition, western blotting images show that both cCaSR and flag-tag were over-expressed in the Flp-In™-293 cells compared with the CAT transfection control (Figure 5.1).

### 5.4.2 Dose-effect of calcium on the viability of cCaSR-overexpressing Flp-In 293 cells

Figure 5.2 shows that a $Ca^{2+}$ concentration at 0.25 mM significantly inhibited cell viability while cells incubated with a $Ca^{2+}$ at concentrations between 0.5 and 16 mM kept a positive status for 6 h. Thus, a $Ca^{2+}$ concentration at 0.25 mM was harmful to cells and was not suitable for further experiments.

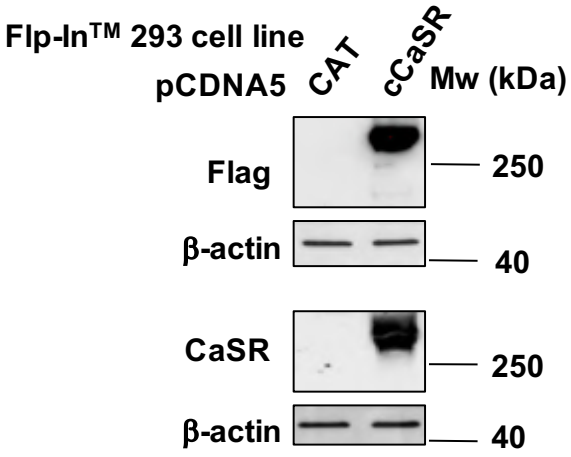


**Figure 5.1** Identification of Flp-In™-293 cells stably expressing chicken CaSR by Western blot analysis. CAT means pcDNA™5/FRT/CAT vector was stably transfected in Flp-In™ 293 cells (transfection control).

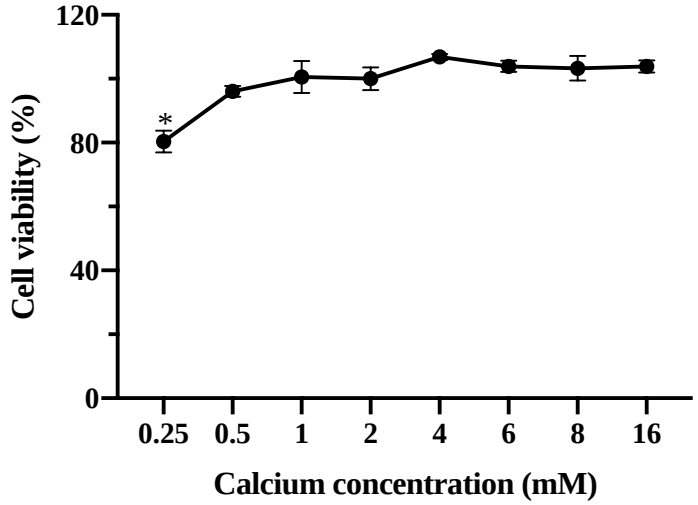


**Figure 5.2** Dose-effect of calcium on the viability of chicken CaSR-overexpressing Flp-In 293 cells. Cells were treated with calcium at different concentrations for 6 h. All data were presented as mean ± SEM, n = 5. Significant differences ($P < 0.05$) compared to 2 mM calcium are indicated on the graph with asterisks (*).

### 5.4.3 The cCaSR signaling in response to L-Trp

As shown in Figure 5.3, cell viability when incubated with L-Trp in the presence of $Ca^{2+}$ was measured ahead of activation assays. Preliminary experiments suggested that the half maximal effective concentration ($EC_{50}$) value for $Ca^{2+}$ via SRE and SRF-RE reporters-mediated signaling assays were around 2.5 mM and 2 mM, and the $EC_{50}$ value for $Ca^{2+}$ via NFAT-RE reporter-mediated signaling assay was around 4.5 mM (these results were also consistent with Figure 5.4B, D, and F). Figure 5.3A shows that L-Trp concentrations at 10 and 15 mM significantly reduced the cell viability in the presence of 2.5 mM $Ca^{2+}$ ($P < 0.05$), but Figure 5.3B shows that different L-Trp concentrations did not negatively affect cell viability in the presence of 4.5 mM $Ca^{2+}$ ($P > 0.05$).

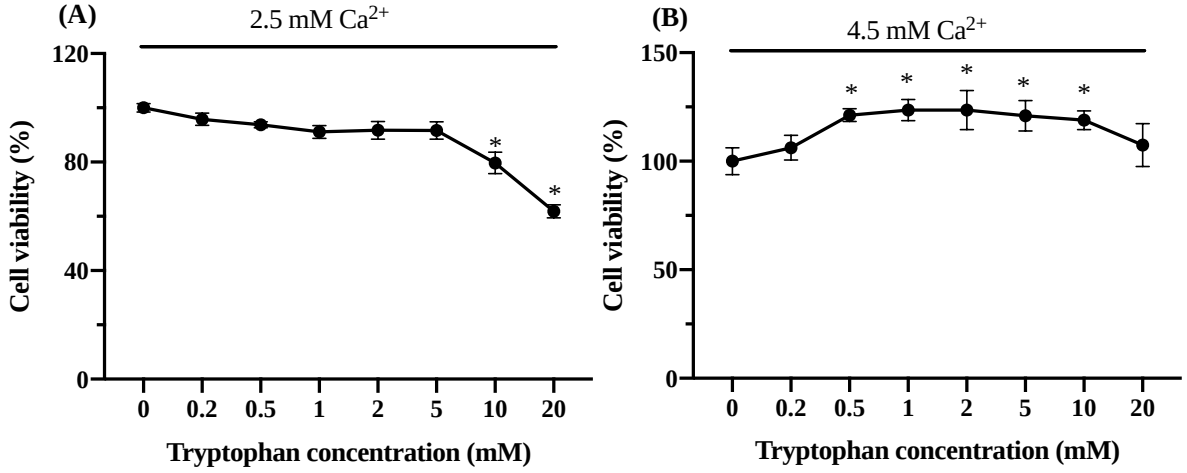


**Figure 5.3** Dose-effect of L-tryptophan on the viability of chicken CaSR-overexpressing Flp-In 293 cells. Cells were treated with L-tryptophan at different concentrations for 6 h. (A) Cells were incubated in the presence of 2.5 mM calcium. (B) Cells were incubated in the presence of 4.5 mM calcium. All data were presented as mean ± SEM, n = 5. Significant differences ($P < 0.05$) compared to 0 mM tryptophan in the presence of calcium are indicated on the graph with asterisks (*).

In the SRE reporter-mediated signaling assay, cCaSR response to $Ca^{2+}$ and L-Trp is shown in Figures 5.4A and 5.4B. Figure 5.4A shows that L-Trp concentration at 5 mM significantly suppressed the response intensity of the SRE reporter ($P < 0.05$), thus 1 mM L-Trp was selected as the working concentration for further assay. Figure 5.4B shows that the $EC_{50}$ value for $Ca^{2+}$ in the presence of 1 mM L-Trp left-shifted from 2.64 mM to 2.51 mM (decreased by 5.18%) compared with that in the absence of L-Trp. Figure 5.5A shows the effect of L-tryptophan on cCaSR activation via the $G_{\beta\gamma}/G\alpha_i$ signaling pathway. When $Ca^{2+}$ was at 1.5 mM, 1 mM L-Trp significantly increased $G_{\beta\gamma}/G\alpha_i$-coupled cCaSR activation ($P < 0.05$).

In the NFAT-RE reporter-mediated signaling assay, cCaSR response to different concentrations of $Ca^{2+}$ in the presence of L-Trp is shown in Figures 5.4C and 5.4D. Figure 5.4C shows that 0, 0.2, and 5 mM L-Trp significantly decreased the activation of cCaSR response in the presence of 4.5 mM $Ca^{2+}$ ($P < 0.05$). The activation at 1 mM L-Trp was at a relatively high level, thus 1 mM L-Trp was selected for further assay. Figure 5.4D shows that $EC_{50}$ value for $Ca^{2+}$ left-shifted from 4.58 mM to 3.99 mM (decreased by 12.88%) after 1 mM L-Trp incubation. Figure 5.5B shows the effect of L-Trp on cCaSR activation via the $G\alpha_q$ signaling pathway. When $Ca^{2+}$ was at 0.5, 2, 5, and 6 mM, 1 mM L-Trp significantly increased $G\alpha_q$-coupled cCaSR activation ($P < 0.05$).

In the SRF-RE reporter-mediated signaling assay, cCaSR response to different concentrations of $Ca^{2+}$ in the presence of L-Trp is shown in Figures 5.4E and 5.4F. Figure 5.4E shows that the SRF-RE reporter response to 1 mM L-Trp was at a relatively high level in the presence of 2 mM $Ca^{2+}$, and 1 mM L-Trp was selected for further assay. Figure 5.4F shows that the $EC_{50}$ value for $Ca^{2+}$ basically kept stable, from 1.98 mM to 1.96 mM (decreased by 1.02%), after 1 mM L-Trp

stimulation. Figure 5.5C shows that, when $Ca^{2+}$ concentrations were at 3.5 and 6 mM, 1 mM L-Trp significantly increased $G\alpha_{12}$-coupled cCaSR activation ($P < 0.05$).

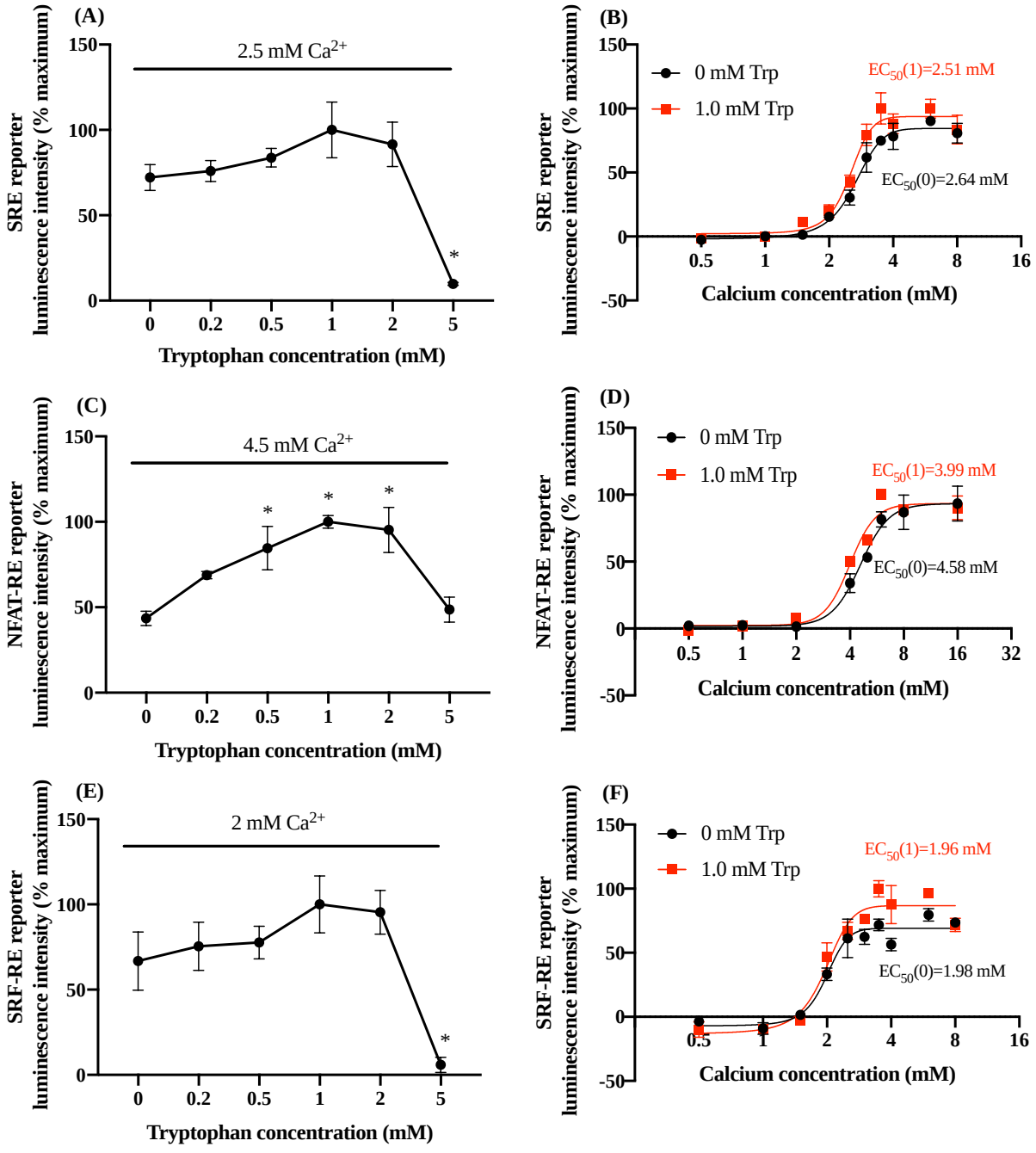


**Figure 5.4** Chicken CaSR response to L-tryptophan. Flp-In 293 cells stably expressed chicken CaSR were transiently transfected with vectors SRE-*luc2P*, NFAT-RE-*luc2P*, or SRF-RE-*luc2P*

for 48 h. Firefly luciferase activity was measured after 6 hours induction with the addition of calcium and L-tryptophan using the dual-Glo assay system in a 96-well format. (A) $G_{\beta\gamma}$ potency ranking of different concentrations of L-tryptophan in the presence of 2.5 mM calcium, n = 4. (B) $G_{\beta\gamma}/G\alpha_i$ -mediated dose-response curve for calcium in the presence of L-tryptophan or not. n = 3. (C) $G\alpha_q$ potency ranking of different concentrations of L-tryptophan in the presence of 4.5 mM calcium, n = 4. (D) $G\alpha_q$ -mediated dose-response curve for calcium in the presence of L-tryptophan or not. n = 3. (E) $G\alpha_{12}$ potency ranking of different concentrations of L-tryptophan in the presence of 2 mM calcium, n = 4. (F) $G\alpha_{12}$ -mediated dose-response curve for calcium in the presence of L-tryptophan or not. n = 3. The data were presented as mean ± SEM. Significant differences ($P < 0.05$) compared with 0 mM tryptophan in the presence of calcium are indicated on the graph with asterisks (*).

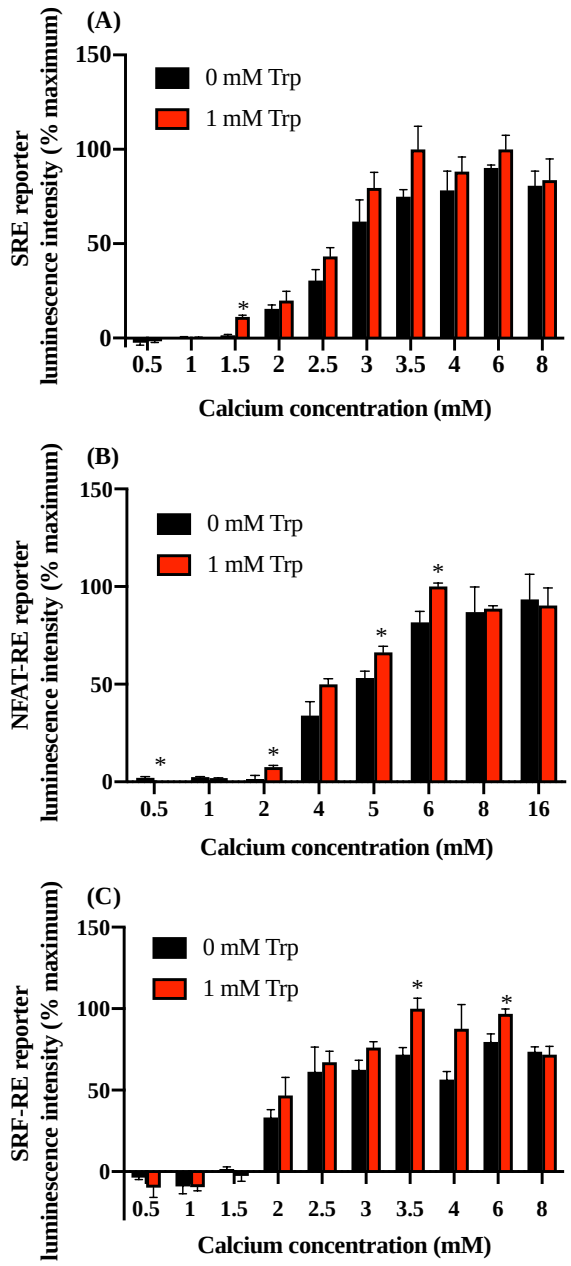


**Figure 5.5** Effect of L-tryptophan on chicken CaSR activation. Flp-In 293 cells stably expressed chicken CaSR were transiently transfected with vectors SRE-*luc2P*, NFAT-RE-*luc2P*, or SRF-RE-*luc2P* for 48 h. Firefly luciferase activity was measured after 6 hours induction with the addition of calcium and L-tryptophan using the dual-Glo assay system in a 96-well format. (A) chicken CaSR response to different calcium concentrations in the presence of 1 mM L-tryptophan via the $G_{\beta\gamma}/G\alpha_i$ signaling pathway. (B) chicken CaSR response to different calcium concentrations in the

presence of 1 mM L-tryptophan via the $G\alpha_q$ signaling pathway. (C) chicken CaSR response to different calcium concentrations in the presence of 1 mM L-tryptophan via the $G\alpha_{12}$ signaling pathway. The data were presented as mean ± SEM, n = 3. Significant differences ($P < 0.05$) between 0 and 1 mM L-tryptophan concentrations at a specific calcium concentration are indicated on the graph with asterisks (*).

Different from the luciferase reporter system, a direct cAMP assay can reflect the immediate changes in cAMP production in response to cCaSR activation, which was more suitable for detecting the decreased cAMP level if cCaSR was activated. Figure 5.6 shows the dose-response curve for calcium in the presence of L-Trp via the $G\alpha_i$ signaling pathway reflected by forskolin-induced cAMP production. The half maximal inhibitory concentration ($IC_{50}$) value for $Ca^{2+}$ right-shifted from 3.84 mM to 4.23 mM (increased by 10.15%) in the presence of 1 mM L-Trp. Figure 5.7 shows that 1mM L-Trp significantly lowered the cAMP level at $Ca^{2+}$ concentrations from 0.5 mM to 10 mM ($P < 0.05$).

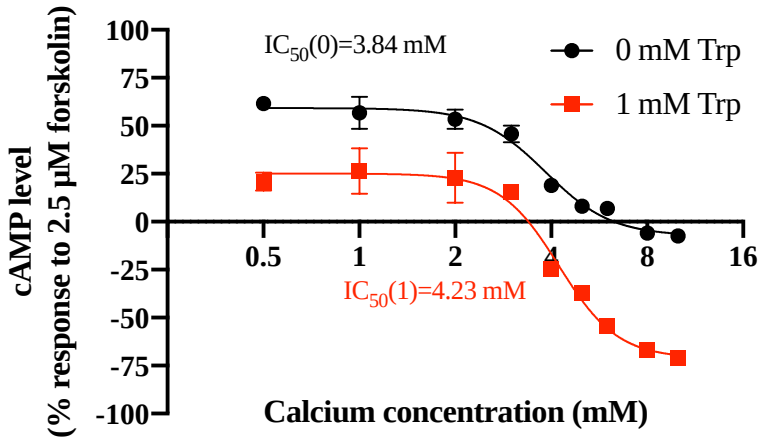


**Figure 5.6** $G\alpha_i$ -mediated dose-response curve for calcium in response to chicken CaSR activation in the presence of L-tryptophan or not reflected by forskolin-induced cAMP production. The data were presented as mean ± SEM. n = 3.

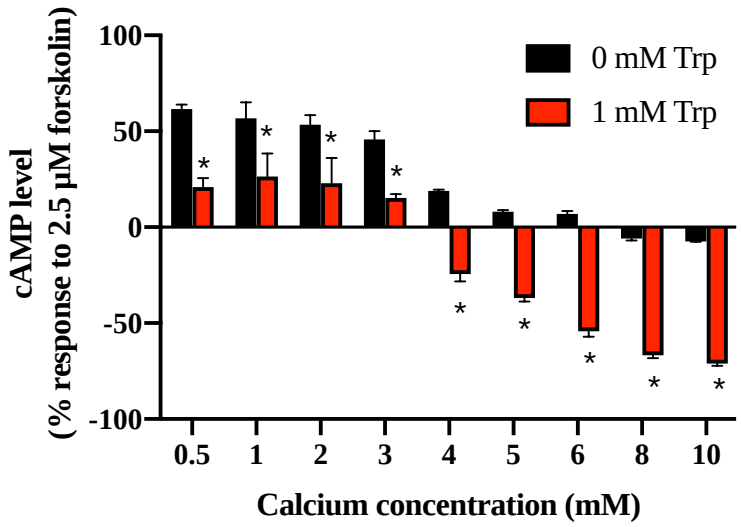


**Figure 5.7** Chicken CaSR response to different calcium concentrations in the presence of 1 mM L-tryptophan via the $G\alpha_i$ signaling pathway reflected by forskolin-induced cAMP production. The data were presented as mean ± SEM, n = 3. Significant differences ($P < 0.05$) between 0 and 1 mM L-tryptophan concentrations at a specific calcium concentration are indicated on the graph with asterisks (*).

### 5.4.4 The cCaSR signaling in response to inorganic $PO_4^{3-}$

Figure 5.8 shows that the dose-effect of $PO_4^{3-}$ on the viability of chicken CaSR-overexpressing Flp-In 293 cells when co-cultured with calcium and R568. Figure 5.8A shows that tested $PO_4^{3-}$ concentrations did not negatively affect the cell viability in the presence of 1 mM $Ca^{2+}$ + 1 μM R568. However, $PO_4^{3-}$ concentrations at 5 and 10 mM significantly reduced the cell viability ($P < 0.05$) in the presence of 2 mM $Ca^{2+}$ + 1 μM R568 (Figure 5.8B).

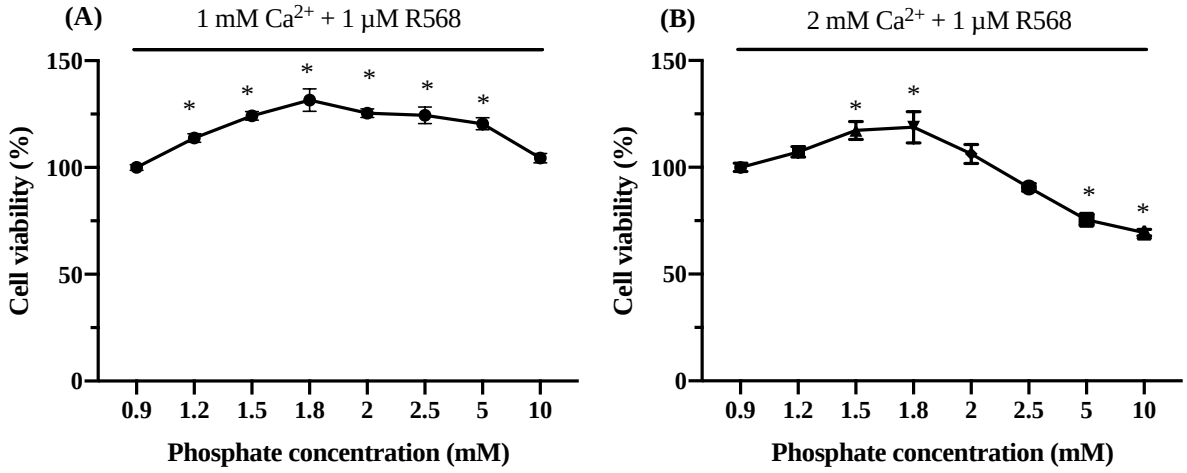


**Figure 5.8** Dose-effect of inorganic phosphate on the viability of chicken CaSR-overexpressing Flp-In 293 cells in the presence of calcium and 1 μM R568. Cells were treated with phosphate at the indicated concentrations for 6 h. (A) Cells were incubated in the presence of 1 mM calcium and 1 μM R568. (B) Cells were incubated in the presence of 2 mM calcium and 1 μM R568. The data were presented as mean ± SEM, n = 5. Significant differences ($P < 0.05$) compared to 0.9 mM inorganic phosphate are indicated on the graph with asterisks (*).

Figure 5.9A exhibits that 1 μM R568 left-shifted $EC_{50}$ value for $Ca^{2+}$ from 3.05 mM to 0.97 mM (decreased by 68.20%), indicating that calcimimetic, R568, also worked for cCaSR and it can partially replace $Ca^{2+}$ function on cCaSR activation. Thus, 1 mM $Ca^{2+}$ + 1 μM R568 was used for $PO_4^{3-}$-induced inhibition assay. In the SRE reporter-mediated signaling assay, cCaSR response to different concentrations of $PO_4^{3-}$ is shown in Figure 5.10A. $PO_4^{3-}$-induced inhibition of cCaSR exacerbated with $PO_4^{3-}$ concentration growth. When $PO_4^{3-}$ concentration was $\geqslant$ 2 mM, it decreased by 31.50% from 0.9 to 2 mM $PO_4^{3-}$.

Figure 5.9B shows that 1 μM R568 left-shifted the $EC_{50}$ value for $Ca^{2+}$ from 4.45 mM to 2.33 mM (decreased by 47.64%), thereby selecting 2 mM $Ca^{2+}$ + 1 μM R568 for further assay. In the NFAT-RE reporter-mediated signaling assay, the cCaSR response to different concentrations of $PO_4^{3-}$ is shown in Figure 5.10B. The cCaSR response by NFAT-RE decreased with increasing $PO_4^{3-}$ concentration. When the $PO_4^{3-}$ concentration was $\geqslant$ 1.8 mM, the cCaSR response was significantly reduced compared with 0.9 mM $PO_4^{3-}$ ($P < 0.05$), and it decreased by 74.68% and 92.97% from 0.9 to 1.8 mM $PO_4^{3-}$ and from 0.9 to 2 mM $PO_4^{3-}$, respectively.

Figure 5.9C shows that 1 μM R568 left-shifted the $EC_{50}$ value for $Ca^{2+}$ from 2.80 mM to 0.95 mM (decreased by 66.07%), and 1 mM $Ca^{2+}$ + 1 μM R568 was selected for further assay. In the SRF-RE reporter-mediated signaling assay, the cCaSR response to different $PO_4^{3-}$concentrations is shown in Figure 5.10C. The cCaSR response was inhibited with increasing $PO_4^{3-}$ concentration. When the $PO_4^{3-}$ concentration was $\geq$ 2 mM, cCaSR responses were significantly lower than that at 0.9 mM $PO_4^{3-}$ ($P < 0.05$), and it was decreased by 30.23% from 0.9 to 2 mM $PO_4^{3-}$.

Figure 5.11 shows that 1 μM R568 right-shifted the $EC_{50}$ value for $Ca^{2+}$ from 3.84 mM to 1.91 mM (decreased by 50.26%), and 1 mM $Ca^{2+}$ + 1 μM R568 was selected for further assay. However, as shown in Figure 5.12, the cAMP production via the $G\alpha_i$ signaling pathway was increased after

cCaSR was blocked with increasing $PO_4^{3-}$ concentration. The cAMP level was significantly increased by 51.20% ($P < 0.05$) when the $PO_4^{3-}$ concentration was 5 mM compared with the control of 0.9 mM $PO_4^{3-}$.

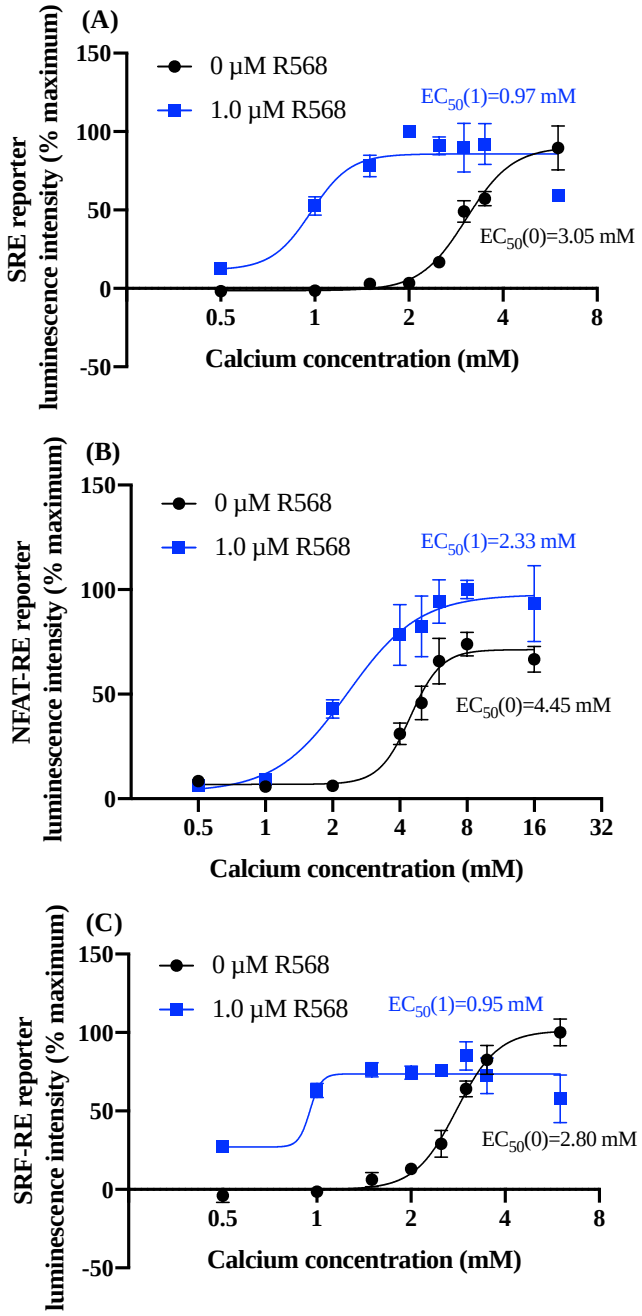

**Figure 5.9** Dose-response curve for calcium in the presence of NPS R-568. Flp-In 293 cells stably expressed chicken CaSR were transiently transfected with vectors SRE-*luc2P*, NFAT-RE-*luc2P*, or SRF-RE-*luc2P* for 48 h. Firefly luciferase activity was measured after 6 hours incubation using the dual-Glo assay system in a 96-well format. (A) $G_{\beta\gamma}/G\alpha_i$ -mediated dose-response curve for calcium in the presence of R568 or not. (B) $G\alpha_q$ -mediated dose-response curve for calcium in the presence of R568 or not. (C) $G\alpha_{12}$ -mediated dose-response curve for calcium in the presence of R568 or not. The data were presented as mean ± SEM, n = 3.

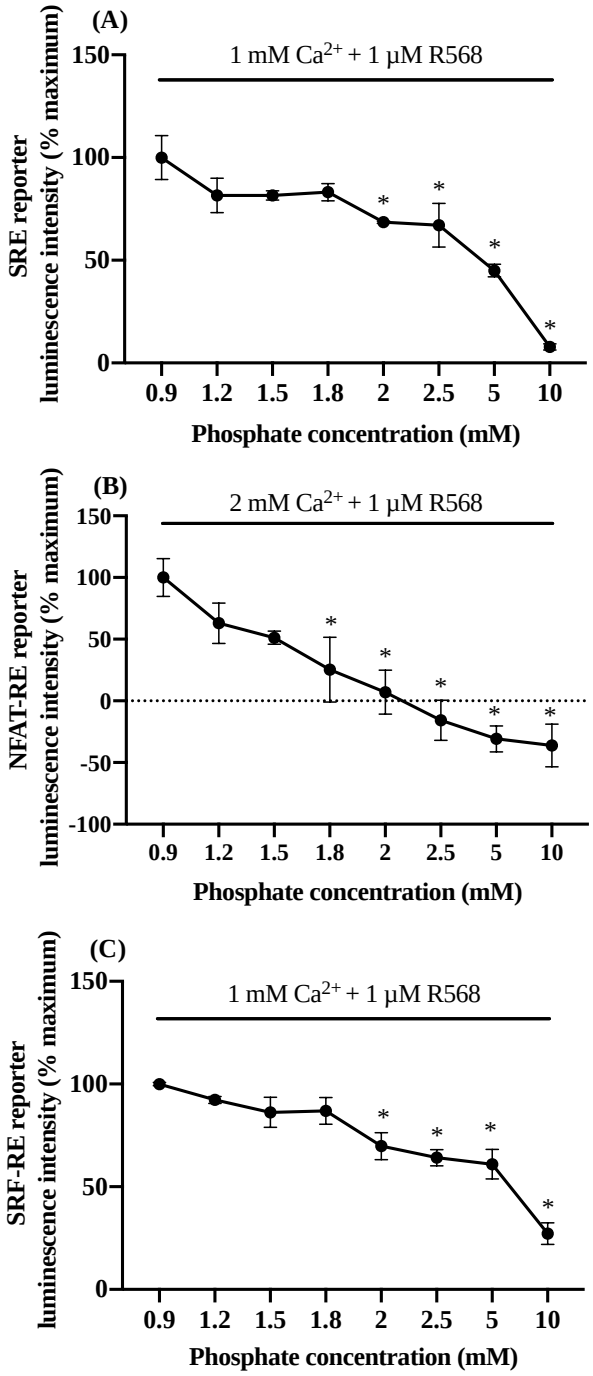


**Figure 5.10** Chicken CaSR response to inorganic phosphate. Flp-In 293 cells stably expressed chicken CaSR were transiently transfected with vectors SRE-*luc2P*, NFAT-RE-*luc2P*, or SRF-RE-*luc2P* for 48 h. Firefly luciferase activity was measured after 6 hours incubation using the dual-Glo assay system in a 96-well format. (A) Phosphate-induced $G_{\beta\gamma}/G\alpha_i$ inhibition of chicken CaSR.

(B) Phosphate-induced $G\alpha_q$ inhibition of chicken CaSR. (C) Phosphate-induced $G\alpha_{12}$ inhibition of chicken CaSR. The data were presented as mean ± SEM, n = 3. Significant differences ($P < 0.05$) compared to 0.9 mM inorganic phosphate are indicated on the graph with asterisks (*).

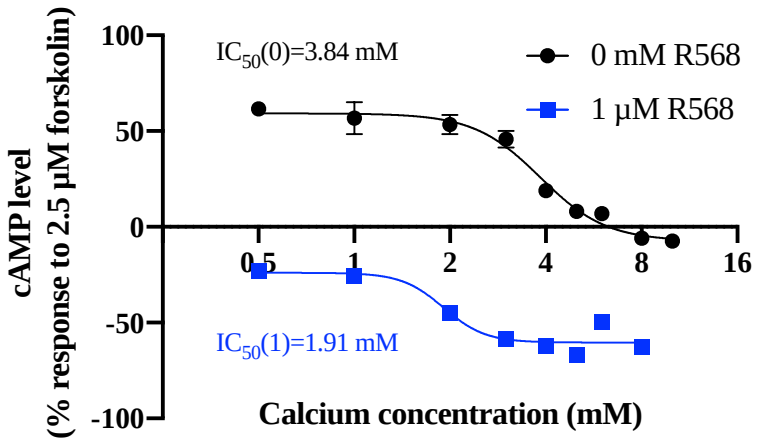


**Figure 5.11** $G\alpha_i$-mediated dose-response curve for calcium in response to chicken CaSR activation in the presence of NPS R-568 or not reflected by forskolin-induced cyclic adenosine monophosphate (cAMP) production. The data were presented as mean ± SEM. n = 3.

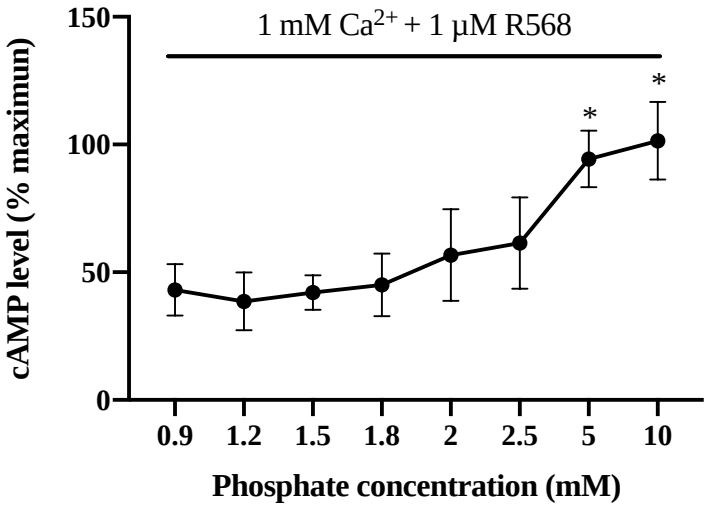


**Figure 5.12** The effect of chicken CaSR inhibition in response to inorganic phosphate on forskolin-induced cyclic adenosine monophosphate (cAMP) production via the $G\alpha_i$ signaling pathway. The data were presented as mean ± SEM, n = 3. Significant differences ($P < 0.05$) compared to 0.9 mM inorganic phosphate are indicated on the graph with asterisks (*).

### 5.4.5 Molecular docking

According to the results of the molecular docking simulation (Table 5.2), ligands (L-Trp, R-568, and $PO_4^{3-}$) exhibited interactions with the active site of cCaSR including hydrogen bonds, π-π interactions, and hydrophobic interactions. Among three ligands, R568 as a calcimimetic showed the lowest free binding energy (-7.81 kcal/mol), meaning the highest docking score, which was superior to nutritional ligands L-tryptophan ((-7.06 kcal/mol) and phosphate (-7.87 kcal/mol).

**Table 5.2** Molecular docking analysis.

| Ligand | Compound Structure | Interactions | Glide binding energy score (kcal/mol) |
|---|---|---|---|
| L-tryptophan | 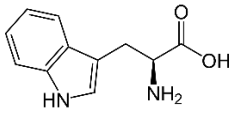 | Hydrogen bonds, Hydrophobic interactions, π-interactions | -7.06 |
| NPS R-568 | 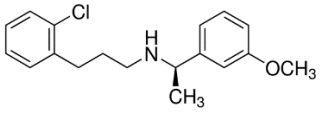 | Hydrogen bonds, Hydrophobic interactions, π-interactions | -7.81 |
| Phosphate ($PO_4^{3-}$) | 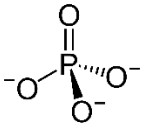 | Hydrogen bonds | -6.87 |

Binding sites and binding modes between cCaSR and ligands ($Ca^{2+}$, L-Trp, NPS R-568, and $PO_4^{3-}$) are shown in Figure 5.13. The active sites and binding pocket of nutritional ligands to cCaSR are located in ECD, and the binding site of calcimimetic, NPS R-568 is located in the transmembrane domain (TMD). $Ca^{2+}$ is an orthostatic modulator of CaSR, and $Ca^{2+}$ shows three binding sites in ECD in each protomer of cCaSR (Figure 5.13B, C, and D). Site 1 is located in the Lobe 1, and $Ca^{2+}$ is positioned by hydroxyl groups of Thr 100 and Ala 144 via hydrogen bonds. Site 2 is located at the interdomain cleft of the Venus Flytrap (VFT) module. It is coordinated by the hydroxyl group of Ser 302 and the backbone carbonyl oxygen atom of Arg 66 via hydrogen bonds. Site 3 is sandwiched between VFT and cysteine-rich domain (CRD) and is supported by the backbone carbonyl oxygen atom of Asp 234 and Gly 556 via hydrogen bonds. The L-Trp binding site is located at the interdomain cleft of the VFT module within ECD (Figure 5.13G), which is close to $Ca^{2+}$ binding site 1. Hydrogen bonds are the main type of binding mode. Residue Ser 147 and Ser 170 interacts with the backbone carbonyl oxygen of L-Trp through hydrogen bonds; Ala 168 and Ser 170 interacts with backbone amino nitrogen of L-Trp through hydrogen bonds; and side-chain indole nitrogen of L-Trp forms a hydrogen bond with Glu 297. As ligand L-Trp belonging to aromatic amino acids, π-interactions are found to coordinate the binding. A C-H-π interaction is found between L-Trp and Tyr 218, and a π-π T-shaped stacking is found between L-Trp and Trp 70, thus L-Trp is stabilized by residues Trp 70 and Tyr 218 through hydrophobic interactions. The binding site of R568 is located in the TMD of cCaSR (Figure 5.13H), and R568 is held in place by Phe 683, Phe 687, Leu 772, Ile 776, Phe 813, Phe 820, Tyr 824, and Ile 840 through hydrophobic interaction and stabilized by residues Gln 680 and Glu 836 via the side chain amino nitrogen of R568 through hydrogen bonds. R568 is coordinated with residues Phe 820 and Phe 813 involving π-π stacking. As shown in Figures 5.13E and F, there are two anion phosphate

binding sites located in each lobe of the VFT module. Phosphate forms multiple hydrogen bonds with surrounding residues. The first site shows that phosphate binds with side chains of residues Arg 66, Arg 69, Ser 302, and Trp 70 through hydrogen bonds; the second binding site of phosphate is coordinated with residue His 192, Thr 195, Lys 225, Lys 516, and Arg 519 through hydrogen bonds.

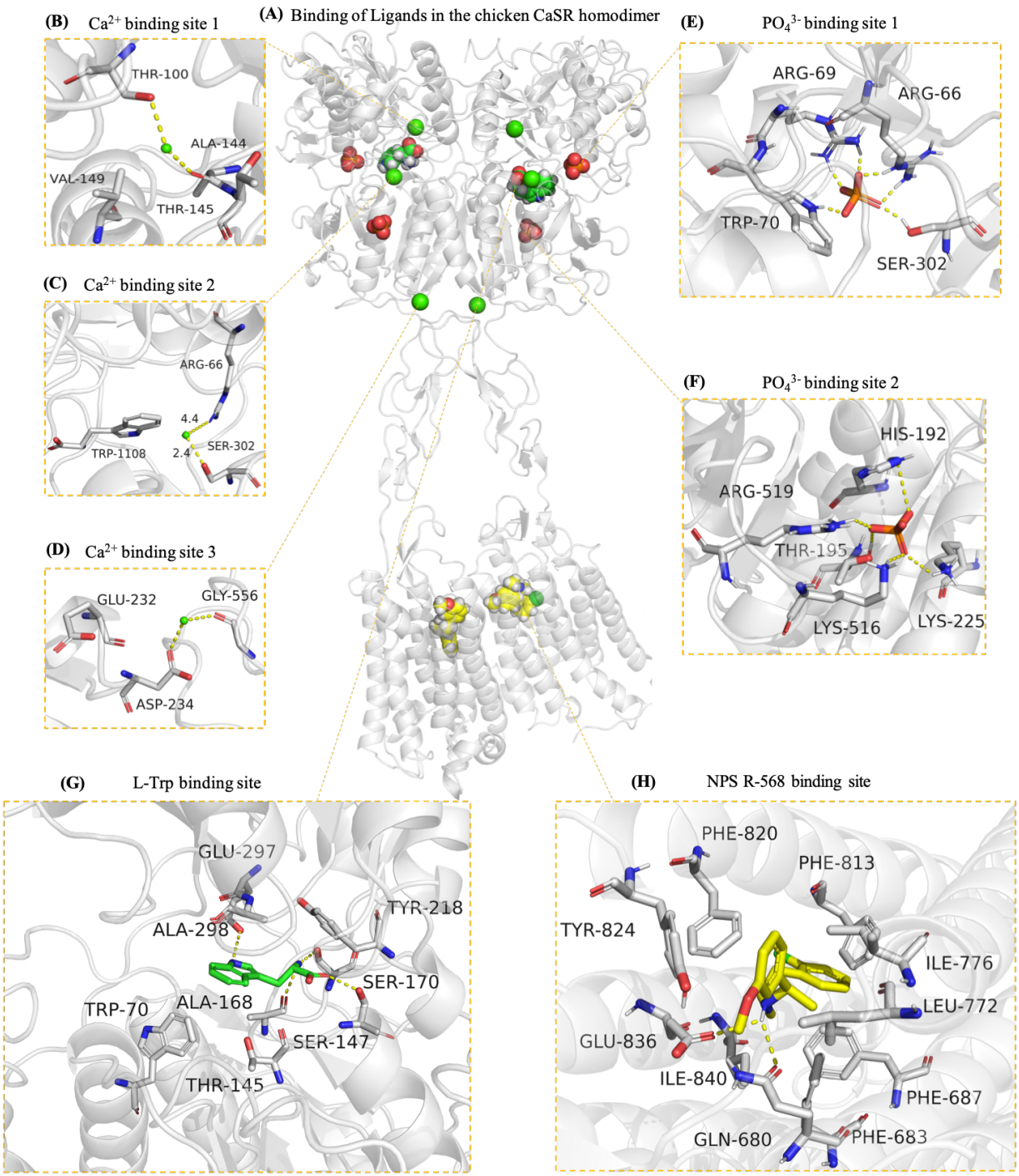


**Figure 5.13** The binding mode of ligands with chicken CaSR. (A) Overview of different ligands binding sites in the chicken CaSR homodimer. All binding sites are counted within one protomer. (B, C and D) Specific interactions of $Ca^{2+}$ with chicken CaSR in three different calcium binding

sites. $Ca^{2+}$ ions are drawn as green spheres. (E and F) Specific interactions of phosphate with chicken CaSR in two different phosphate binding sites. Phosphate is drawn as orange sticks. (G) Binding pocket of L-tryptophan (L-Trp). (H) Surrounding residues around NPS R-568 (yellow) are shown in stick models. The dotted line represents a hydrogen bond.

### 5.4.6 Molecular dynamics simulation

During the simulation process of the dynamic movement of ligands and cCaSR in the aqueous solution, it was predicated that L-Trp, phosphate, and R568 would interact with cCaSR through hydrogen bonds, hydrophobic contacts (including π-interactions), ionic interactions, and water bridges (Figure 5.14, 5.15, and 5.16). As shown in Figure 5.14, similar to molecular docking results, the binding site of L-Trp is predominately stabilized by hydrogen bonds with Ser 147 and Asp 190. Asp 190 also contributes an electrostatic interaction with L-Trp. Greasy residues form hydrophobic interactions to coordinate the target protein flexibility. During molecular dynamics simulation, water molecules are important because water bridges are formed by hydrogen-bonded protein-ligand interactions and mediated by a water molecule. Ala 168, Gly 148, and Asp 216 involve in water bridges. R568 binding is coordinated by two protomers (Figure 5.15), and Pro 822 and Ala 823 from the other counterpart form hydrophobic interactions with R568. Hydrogen bonds, water bridges, and ionic interactions are found among Glu 766, Glu 836, and R568, and hydrogen bonds, water bridges, and hydrophobic interactions are found between Tyr 824 and R568, thus these three residues play important roles in cCaSR conformational flexibility and R568 binding. Phosphate shows two binding sites. Due to the simple structure of phosphate, hydrogen bonds and water bridges are the predominant contacts with cCaSR residues (Figure 5.16). RMSD results exhibit the importance of residues Glu 297, Arg 414, Ile 415, and Ser 416 in the binding site 1 (Figure 5.16A), which contact with phosphate through both hydrogen bonds and water bridges during the dynamic process. As shown in Figure 5.16B, in addition to hydrogen bonds and water bridges, phosphate binding site 2 shows ionic interactions with cCaSR residues, and binding site 2 shows the interaction between two protomers. Residues Glu 251 and Gln 254 from the other counterpart contribute to water bridges with phosphate dynamically, but only accounting for a small proportion.

Acidic residues Glu 191, Glu 229, and Glu 228 form water bridges with phosphate, and basic residues Arg 519 and Lys 225 show more versatile interactions with phosphate through ionic interactions, water bridges, and/or hydrogen bonds.

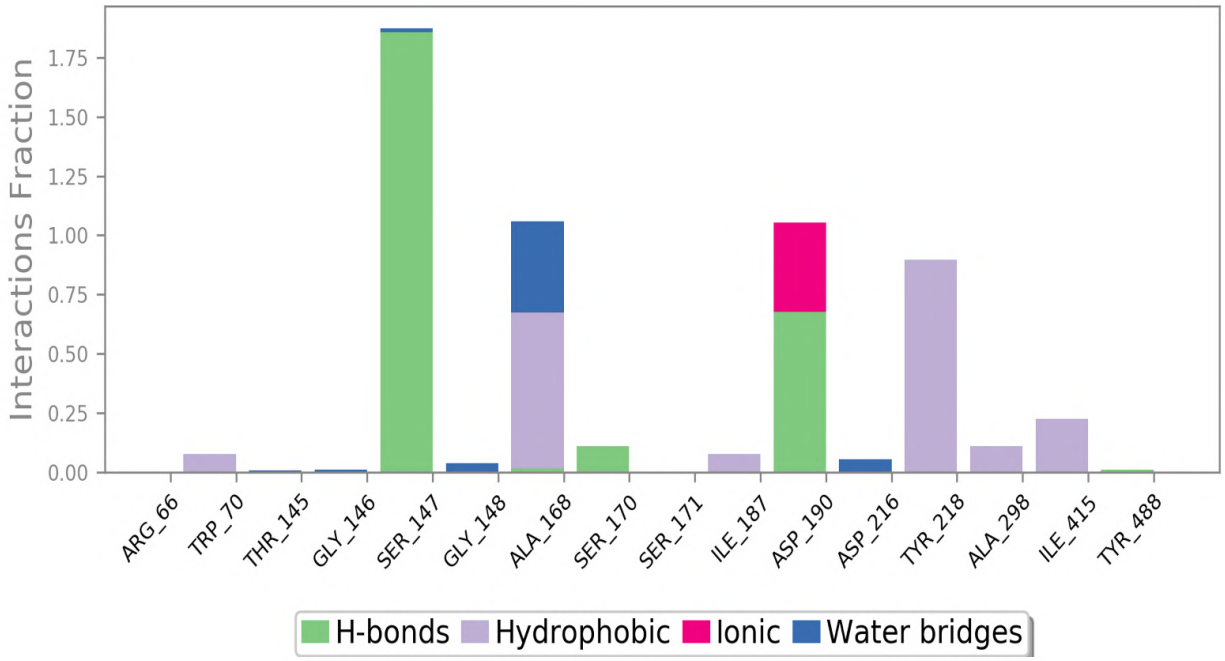


**Figure 5.14** Binding of L-tryptophan with chicken CaSR active site residues in the dynamic simulation process.

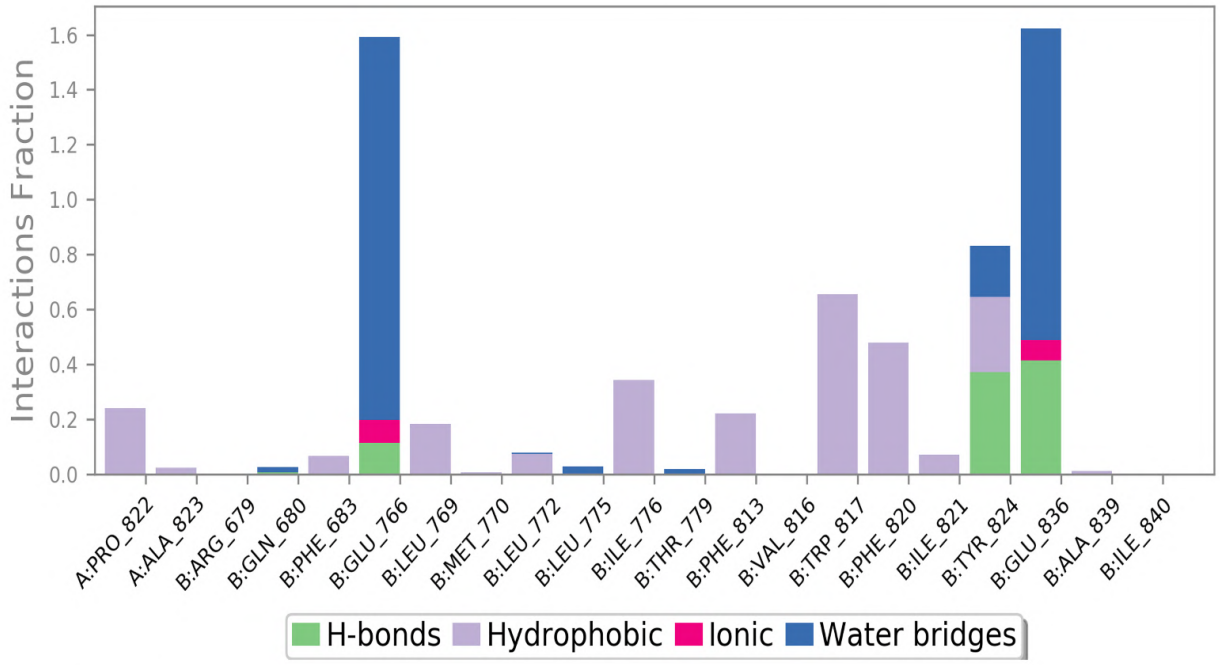


**Figure 5.15** Binding of NPS R-568 with chicken CaSR active site residues in the dynamic simulation process.

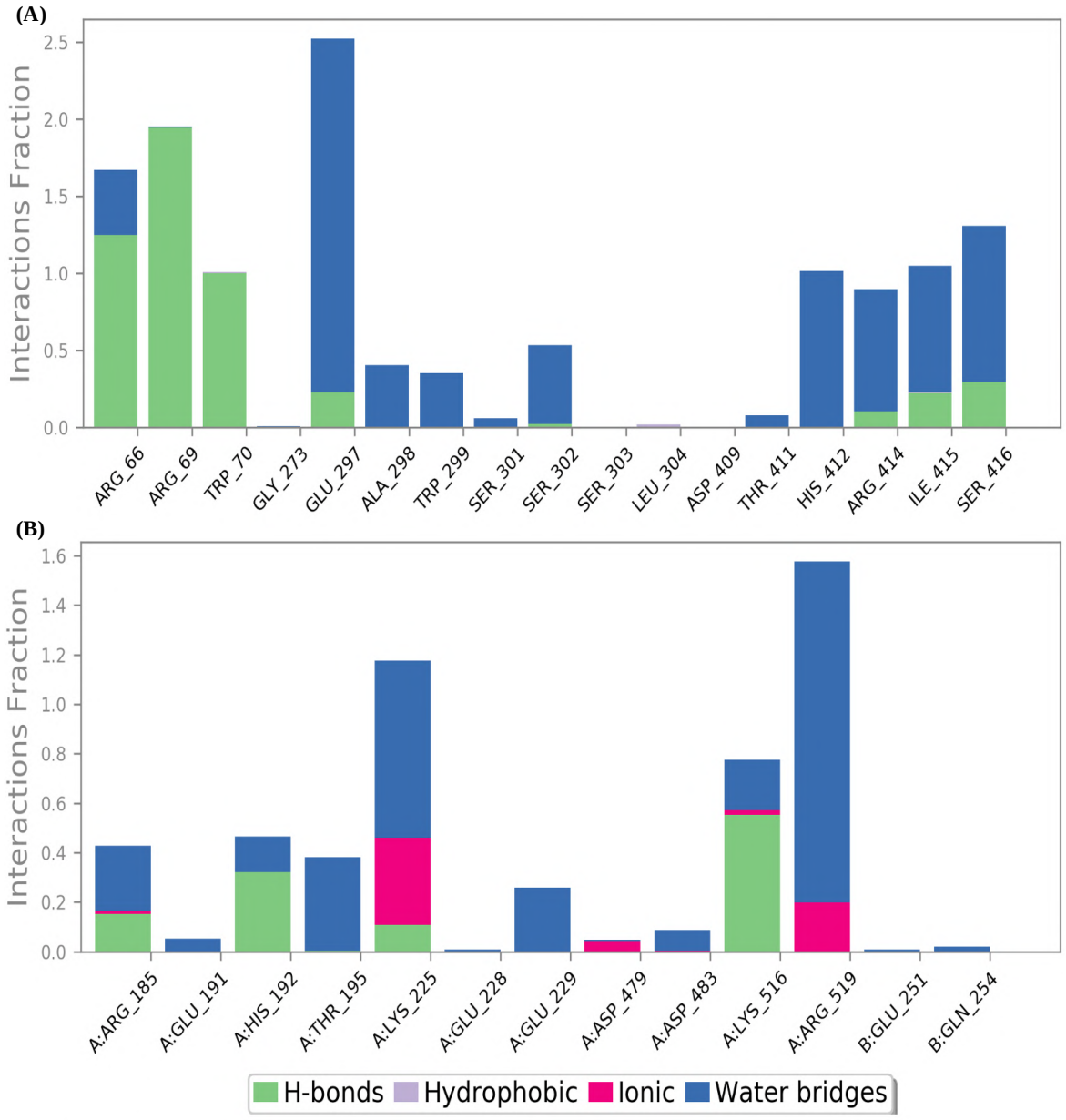


**Figure 5.16** Binding of phosphate with chicken CaSR active site residues in the dynamic simulation process. (A) Phosphate binding site 1. (B) Phosphate binding site 2.

## 5.5 Discussion

The CaSR is a typical GPCR, and it plays important roles in (patho)physiological functions. The binding of CaSR and its ligands leads to CaSR conformational changes and induces biased agonism and antagonism via downstream G-protein coupled signaling, which can be reflected by mediating numerous tissue-specific functions (Leach et al., 2015). The intracellular CaSR signaling is known to be coupled with heterotrimeric G proteins. According to the Gα subunit, they can be classified into four groups, $G\alpha_q$, $G\alpha_i$, $G\alpha_{12}$, and $G\alpha_s$ (Chakravarti et al., 2012). The Gα protein subunit dissociates from βγ dimeric subunit, thereby initiating a cascade of downstream signaling pathways and eventually induces target gene transcriptions (Figure 5.17). In the NFAT-RE pathway, $G\alpha_q$ stimulates phosphatidylinositol-specific phospholipase C (PI-PLC), and thus regulates $IP_3$ production, $Ca^{2+}$ mobilization, and activates protein kinase-C (PKC) (Chakravarti et al., 2012). The NFAT-RE is directly in response to intracellular $Ca^{2+}$. The SRE is in response directly to the extracellular signal-regulated kinase (ERK) 1/2, which reflects the overlapped effects of three signaling pathways mediated by PKC derived from the elevation of intracellular $Ca^{2+}$ (Chakravarti et al., 2012), $G\alpha_i$ (Kifor et al., 2001), and $G_{\beta\gamma}$-tyrosine kinase-Ras-Raf-MEK-ERK (Koch et al., 1994). Generally, CaSR activation suppresses the production of cAMP via the $G\alpha_i$-mediated pathway or elevates intracellular $Ca^{2+}$ via the $G\alpha_q$-mediated pathway to indirectly inhibit cAMP synthesis (de Jesus Ferreira et al., 1998). However, the cAMP level may increase via $G\alpha_s$-mediated CaSR activation (through switch bias from $G\alpha_i$ to $G\alpha_s$) in some cancer cells such as breast cancer (Mamillapalli et al., 2008) and pituitary tumor cells (Mamillapalli and Wysolmerski, 2010). The SRF-RE is in response directly to RhoA. The Rho family is a G protein with a small molecular weight. $G\alpha_{12}$-mediated signaling activates PLD by the CaSR stimulation, which produces phosphatidic acid, by activating Rho (Huang et al., 2004). Also, the cytoskeletal

actin-binding protein filamin acting as a scaffolding protein to bind CaSR for downstream signaling cascades (Awata et al., 2001), as filamin also interacts with RhoGEF, which mediates Rho activation (Hart et al., 1998; Pi et al., 2002).

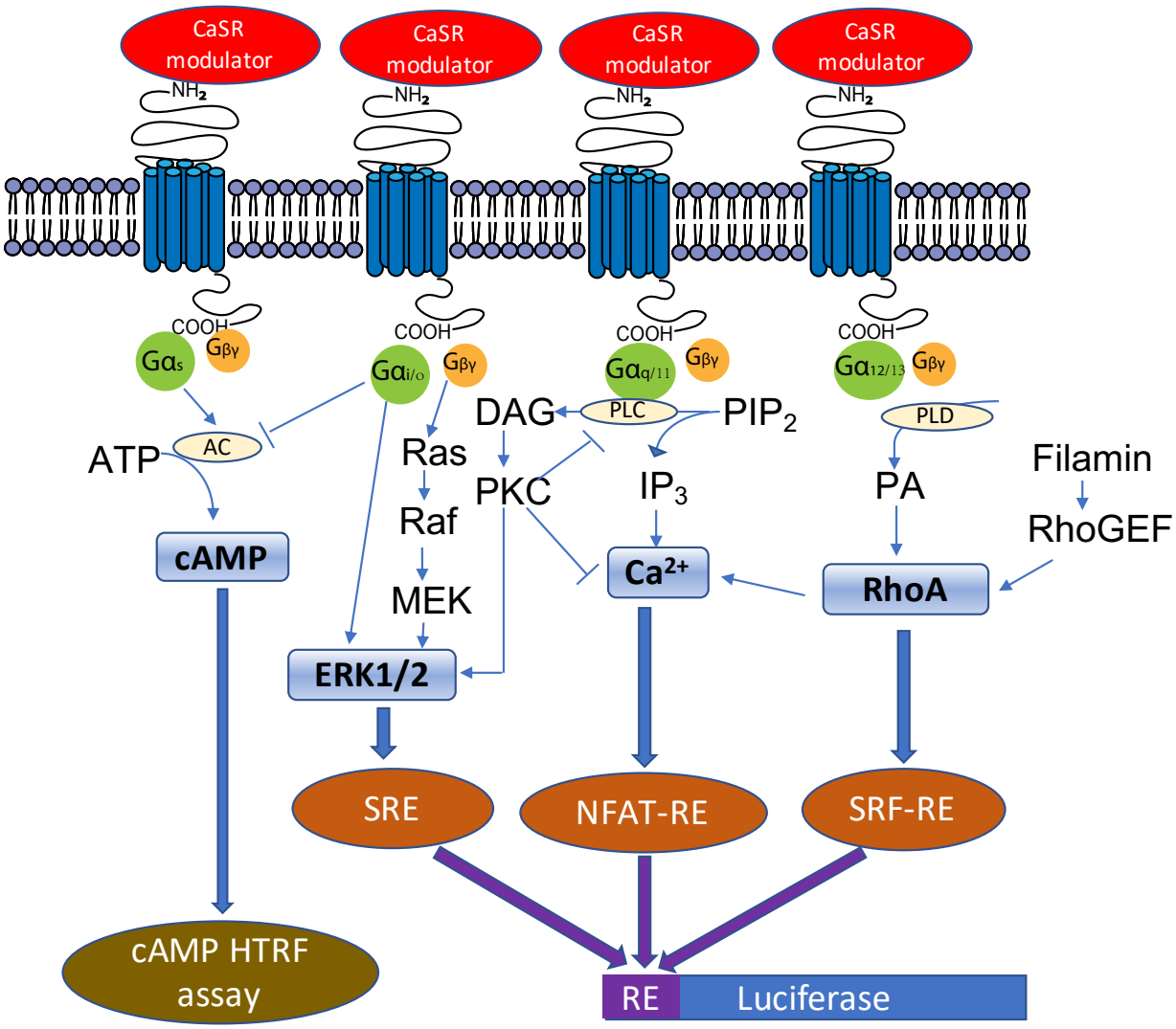


**Figure 5.17** Schematic diagram of chicken CaSR signaling pathways. AC: adenylyl cyclase; cAMP: cyclic adenosine monophosphate; ERK1/2: extracellular signal-regulated kinases 1 and 2; DAG: diacylglycerol; PKC: protein kinase C; $PIP_2$: phosphatidylinositol bisphosphate; $IP_3$: inositol trisphosphate; phospholipase C; PA: phosphatidic acid; RhoGEF: Rho guanine nucleotide exchange factors.

$Ca^{2+}$ is a direct orthosteric activator of CaSR; its physiological concentration in poultry is similar to that in humans, varying between 1 mM and 2 mM (Proszkowiec-Weglarz and Angel, 2013). When the Flp-In 293 cells stably expressed chicken CaSR were incubated with $Ca^{2+}$ at concentrations less than 0.25 mM for 6 h, cell viability decreased significantly; but higher $Ca^{2+}$ concentration up to 16 mM also did no harm to the cells. L-Trp is a well-recognized PAM, which means it cannot activate CaSR alone, but requires the presence of $Ca^{2+}$ (Liu et al., 2020). Also, L-Trp is an essential nutrient for cell growth. L-Trp concentrations above 10 mM in the presence of 2.5 mM $Ca^{2+}$ negatively affected cell viability after 6 h incubation, but $Ca^{2+}$ concentration at 4.5 mM alleviated the negative impact caused by L-Trp. Our results suggested that CaSR activation may provide a protective effect on cell viability and growth.

In the SRE, NFAT-RE, and SRF-RE pathways, the $EC_{50}$ value in each signaling pathway was different under the same conditions indicating that the activation of cCaSR by $Ca^{2+}$ showed biased agonism. This was especially evident in the NFAT-RE pathway, its $EC_{50}$ value for $Ca^{2+}$ (4.57 mM) was significantly higher than that in the SRE (2.64 mM) and SRF-RE (1.98 mM) pathways. The $IC_{50}$ value for $Ca^{2+}$ in response to the cAMP level was 3.84 mM. Moreover, previous studies have reported that the $EC_{50}$ for $Ca^{2+}$ varied from 2.3 mM to 4.2 mM in the human CaSR-expressing HEK293 cells using calcium imaging or measuring the $IP_1$ accumulation (Conigrave et al., 2000b; Carrillo-López et al., 2010; Thomsen et al., 2012). Thomsen et al. (2012) also reported that $EC_{50}/IC_{50}$ for $Ca^{2+}$ was 1.63 mM and 2.87 mM by measuring cAMP and phosphorylation of ERK1/2, respectively. There are three possible reasons for these differences: 1) Biased agonism of CaSR; 2) Different measurement methods. Generally, previous studies measured the intracellular calcium oscillation and $IP_1$ accumulation to reflect $G\alpha_q$ signaling, cAMP to reflect $G\alpha_i$, and ERK to reflect the ternary effect mediated by $G\alpha_q$, $G\alpha_i$, and $G_{\beta\gamma}$. The complicated signaling

and various measurement methods can cause the difference in $EC_{50}$/$IC_{50}$ values; and 3) Different structures between human and chicken CaSR. Although cCaSR shares high homology with human CaSR, there are still some differences. The non-conserved regions of sequence are mainly distributed within the intracellular domain, which is involved in G protein coupling (Diaz et al., 1997).

According to our results, when the concentrations of L-Trp were more than 2 mM, the luminescence intensity decreased significantly, indicating that the concentration of CaSR modulators also closely affected CaSR function and downstream signaling cascades. In the NFAT-RE pathway, the $EC_{50}$ curve for $Ca^{2+}$ left-shifted the most (13.57%) in the presence of L-Trp compared with that in the SRE (5.18%) and SRF-RE (1.02%) pathways, as well as that in the $G\alpha_i$-mediated cAMP production pathway (right-shifted by 10.15%). Therefore, the $G\alpha_q$-mediated signaling pathway was predominant in the presence of L-Trp. Next, to avoid potential interactions between calcium and phosphate, which could affect the characterization of biased signaling of inorganic $PO_4^{3-}$ (a NAM), we partially replaced calcium with the calcimimetic R568 and investigated the signaling of R568 as well. According to our results, we confirmed that R568 was also a PAM to cCaSR because R568 can activate cCaSR via multiple signaling pathways and the left-/right-shifted dose-response curve of $Ca^{2+}$ by more than 40%. Also, we found that the magnitude of the dose-response curve for $Ca^{2+}$ shifted the most in the SRE and SRF-RE pathways in the presence of R568, suggesting that R568 biased to $G\beta\gamma$/$G\alpha_i$ and $G\alpha_{12}$-mediated signaling pathways in terms of its potency of cCaSR activation. Interestingly, in the NFAT-RE pathway, R568 enhanced the efficacy of cCaSR activation by $Ca^{2+}$ (higher maximal response, by 26.03%). The difference between these two PAMs regarding their biased agonism mechanism might be attributed to the different structures between L-Trp and R568 and different binding areas. It has

been reported that L-Trp binds to the ECD of CaSR (Geng et al., 2016), but R568 binds to the TMD (Petrel et al., 2004). In addition, $Ca^{2+}$ concentration is also important to L-Trp potency (Young and Rozengurt, 2002). In the NFAT-RE and SRE pathways, when the $Ca^{2+}$ concentration was more than 4 mM and 3.5 mM, respectively, a significant change in the NFAT-RE and SRE response was observed, suggesting that L-Trp enhanced CaSR sensitivity to $Ca^{2+}$, and the variation trend was consistent with the results of Conigrave et al. (2000b). Recently, Ling et al. (2021) has revealed the crystal structure of full-length human CaSR in the inactive state, $Ca^{2+}$ and/or L-Trp bound states. They confirmed that L-Trp cannot activate the CaSR alone because L-Trp binding enabled the closed conformation of the Venus Flytrap (VFT) domain (an intermediate active state), but L-Trp is not able to induce the rotation of TMD of CaSR and thus not able to activate the CaSR. However, L-Trp can promote the CaSR activation in the presence of $Ca^{2+}$ because $Ca^{2+}$ binding initiates and relays the twist at the VFT domain to the TMD. Therefore, L-Trp plays an important role in the complete activation of CaSR, which also supports the precise regulation of calcium homeostasis via cCaSR. $PO_4^{3-}$, as a NAM, exhibited opposite of the L-Trp and R568. The results showed that the NFAT-RE response decreased to the greatest extent when the $PO_4^{3-}$ concentration increased to 2.5 mM compared with other response elements, similar to the results of the biased agonism of L-Trp. The reason might be that the binding sites of $PO_4^{3-}$ to CaSR are also located in the ECD (Geng et al., 2016).

The CaSR responds to many ligands and shows biased signaling, and conformational reorganization in the ligand binding sites is undoubtedly diverse. The biased agonism or antagonism is supported by the stabilization of the active or inactive state of receptor conformation (Kenakin, 2009). Also, the full-length cCaSR crystal structure has been revealed (Wen et al., 2021), which is conducive to explaining the structure-function relationship of cCaSR. In this study, we

found one binding site for L-Trp docking and two binding sites for $PO_4^{3-}$ docking in the ECD of cCaSR. The confirmed binding site of L-Trp (Wen et al., 2021) and predicted binding sites $PO_4^{3-}$ to cCaSR were similar to the results in the human CaSR (Geng et al., 2016). Hydrogen bonds are the main category for L-Trp binding. Also, the aromatic side chain of L-Trp contributed to a lot of the binding to the receptor, which forms C-H-π interaction, π-π T-shaped hydrophobic interaction. The N-terminal and C-terminal of L-Trp form strong H bond interactions with cCaSR, which possibly stabilize the binding of L-Trp and may also adjust the conformation of cCaSR after activation to perform its biological functions. The aromatic ring of L-Trp is sandwiched between the receptor residues Ala 298 and Trp 70 and produced aromatic interactions, which might be the structural mechanism for cCASR to selectively recognize L-Trp. It should be noted that the L-Trp binding site is close to the $Ca^{2+}$ binding site 1, which might explain why $Ca^{2+}$ is required when L-Trp activates cCaSR. In particular, Thr 100 and Thr 145 support the conformational stabilization when L-Trp binds to cCaSR in the presence of $Ca^{2+}$. A similar binding mode was found in the human CaSR (Geng et al., 2016). As with human CaSR, two binding sites of cCaSR to $PO_4^{3-}$ were reported (Geng et al., 2016). However, $PO_4^{3-}$ exhibits relatively simple binding modes, which mainly depend on the hydrogen bonds and hydrophobic interactions. As for R568, it is a small molecule-drug and an allosteric calcimimetic, targeting the TMD of cCaSR. This study demonstrated that R568 as a calcimimetic of cCaSR with biased agonism for the first time. Although R568 is not suitable for the application of animal feeds, investigating this calcimimetric is necessary because R568 is of great importance when studying the structure-function relationship of cCaSR. It has been reported that another calcimimetic, cinacalcet, can correct biased allosteric modulation of human CaSR because the binding site of these drugs (in the TMD) is far from $Ca^{2+}$ binding sites (in the ECD) (Makita et al., 2019). It is difficult to take receptor flexibility into

consideration because the protein conformation was changing during molecular docking (rigid-body docking). Thus, molecular dynamics can simulate the dynamic movements within the active site in an aqueous solution. During this process, the interactions between cCaSR and modulators become more diverse. In particular, the involvement of water molecules contributes to the conformational changes and structural stabilization during binding.

The PTH functions directly in response to hypocalcemia to elevate the plasma calcium concentration by mobilizing calcium from bone resorption; stimulating renal calcium reabsorption and $1,25(OH)_2D_3$ synthesis; and promoting intestinal calcium absorption facilitated by $1,25(OH)_2D_3$ (Dacke, 2000). Typically, in the animal body, CaSR activation-induced downstream signaling inhibits PTH release. Second messengers, such as cAMP and intracellular $Ca^{2+}$, as well as the mitogen-activated protein kinases (MAPKs) ERK1/2 have been reported to be involved in the inhibitory control of PTH secretion (Brown et al., 1979a; Nemeth and Scarpa, 1987; Corbetta et al., 2002). Given that CaSR activation inhibits the increase in plasma calcium concentration, its activation is not always beneficial for calcium absorption and utilization in the body. However, CaSR activation was reported to have a positive effect on chemotaxis and proliferation of osteoblasts, osteogenic differentiation of mesenchymal stem cells, and bone remodeling (Kanatani et al., 1999; Gabusi et al., 2012; Pipino et al., 2014). Also, CaSR activation contributes to gut hormone secretion and gut chemosensing function (Liou et al., 2011; Liou, 2013). Overall, maintaining calcium homeostasis via CaSR relies on a dynamic system (e.g., in the animal body) because CaSR plays various roles in (patho)physiological processes. The key is to find the balance between CaSR activation and inhibition. However, the present study is still a foundational study that illustrates the possibility and provides the theoretical evidence that the nutritional modulator L-Trp and inorganic $PO_4^{3-}$ could be applied to mediating calcium metabolism in poultry. In the

future, the effect of cCaSR modulation by these two nutritional modulators on chicken calcium homeostasis, PTH, and calcitonin metabolism as well as production performance in laying hens still needs to be investigated. For example, how does a specific biased signaling pathway affect calcium metabolism and even egg production after the activation of cCaSR by L-Trp?

In conclusion, this study demonstrated that, as with human CaSR, nutrients L-Trp and inorganic $PO_4^{3-}$ were cCaSR modulators, acting as PAM and NAM, respectively, with biased agonism and antagonism *in vitro*. L-Trp and inorganic $PO_4^{3-}$ biased to the $G\alpha_q$-mediated signaling pathway, but calcimimetic, R568 biased to the $G_{\beta\gamma}/G\alpha_i$ and $G\alpha_{12}$-mediated signaling pathways. The results also provided theoretical evidence that L-Trp and inorganic $PO_4^{3-}$ could be used as potential nutritional ligands to prevent or attenuate chicken osteoporosis during the egg-laying cycle through the cCaSR modulation *in vivo*. Similar to human CaSR, L-Trp shows just one binding site to the ECD of cCaSR. In addition to hydrogen bonds, its aromatic side chain is conducive to binding; inorganic $PO_4^{3-}$ shows two binding sites also in the ECD of cCaSR, with the hydrogen bonds being the main bond type.

## BRIDGE TO CHAPTER SIX

In chapter five, we 1) identified two effective and economic nutritional ligands to chicken CaSR acting as an agonist (L-Trp) and antagonist (inorganic $PO_4^{3-}$); 2) revealed molecular mechanisms of how the two ligands initiate downstream G protein-coupled signaling and biased agonism/antagonism of CaSR regarding the Gα and $G_{\beta\gamma}$ subunits; 3) illustrated the structure and function relationship of chicken CaSR by molecular docking and dynamics; and 4) provided overall theoretical evidence to support that L-Trp and $PO_4^{3-}$ could be potentially applied to the egg industry to mediate calcium homeostasis and prevent/mitigate calcium unbalance or osteoporosis. Therefore, in chapter six, we will investigate the feasibility of these findings to improve bone formation and remodeling by conducting a cell culture experiment in isolated mesenchymal stem cells (MSCs) from the compact bone of broilers and layers.

## CHAPTER SIX: MANUSCRIPT III

**Effects of L-tryptophan and 1,25-dihydroxycholecalciferol on proliferation and osteogenic differentiation of mesenchymal stem cells isolated from the compact bone of broilers or layers** [3]

[3] **Hui, Q.**, X. Zhao, K. O, and C. Yang. 2022. Effects of L-Tryptophan and 1,25-dihydroxycholecalciferol on proliferation and osteogenic differentiation of mesenchymal stem cells isolated from the compact bone of broilers and layers. J. Agri. Food Chem. 70(34):10476-10489.

## 6.1 Abstract

Poultry are vulnerable to bone problems throughout their lives or production period due to rapid growth in broilers and the active laying cycle in layers. The calcium-sensing receptor (CaSR) is important in calcium and bone metabolism. The objective of this study was to investigate the effect of CaSR ligand (L-Trp) and 1,25-dihydroxycholecalciferol [1,25$(OH)_2D_3$] on the regulation of proliferation and osteogenic differentiation of chicken mesenchymal stem cells (MSCs) isolated from the compact bone of 14-day-old Ross 308 chickens and Dekalb pullets, which can provide cell-based evidence for the prevention or alleviation of skeletal disorders in the poultry industry. Firstly, the dose- (0, 0.5, 1, 2, 5, 10, and 15 mM) and time-effect (0, 7, and 14 d) of L-Trp on the proliferation and osteogenic differentiation in chicken MSCs were investigated. The 5 mM L-Trp had a balanced effect between proliferation and osteogenic differentiation in broiler and layer MSCs when differentiated for 7 days. The broiler and layer MSCs were then treated with (1) osteogenic medium, osteogenic medium supplemented with (2) 1 nM 1,25$(OH)_2D_3$, (3) 2.5 mM $Ca^{2+}$, (4) 2.5 mM $Ca^{2+}$+5 mM L-Trp, (5) 2.5 mM $Ca^{2+}$+5 mM L-Trp+1 μM NPS-2143, respectively for 7 days. Results showed that the 5 mM L-Trp significantly inhibited the proliferation of broiler and layer MSCs on day 7 ($P < 0.05$), but 1 nM 1,25$(OH)_2D_3$ significantly promoted the proliferation of layer MSCs ($P < 0.05$). Only 2.5 mM $Ca^{2+}$+5 mM L-Trp group significantly increased the mineralization process during osteogenic differentiation ($P < 0.05$), and this treatment also significantly upregulated the mRNA expression of *vitamin D receptor* (*VDR*)*, β-catenin*, and osteogenesis genes in broiler MSCs ($P < 0.05$). The osteogenic differentiation process in layer MSCs was faster than that in broiler MSCs. In layer MSCs, $Ca^{2+}$ alone significantly facilitated mineralization and ALP activity after 7-day osteogenic differentiation ($P < 0.05$). However, 5 mM L-Trp significantly inhibited the differentiation and mineralization process by

downregulating the mRNA expression of *CaSR, VDR, β-catenin*, and osteogenic genes ($P < 0.05$) in layer MSCs. Taken together, L-Trp and $1,25(OH)_2D_3$ can regulate proliferation and osteogenic differentiation in both broiler and layer MSCs depending on doses, treatment time, and cell proliferation and differentiation stages.

**Key words**: Calcium-sensing receptor; L-tryptophan; 1,25-dihydroxycholecalciferol, osteogenic differentiation, chicken mesenchymal stem cells

## 6.2 Introduction

Bone problems are a big challenge in both the broiler and egg industries, causing huge economic loss and animal welfare issues. Skeletal disorders in broiler chickens are mainly attributed to rapid growth, which contributes to tibial dyschondroplasia, rickets, lameness, and leg deformities (Fleming, 2008). Osteoporosis is one of the major causes of bone fractures in laying hens. Bone fractures are associated with pain and animal welfare issues. In addition, economic factors such as egg production and eggshell quality are closely linked to issues concerning bones (Kim et al., 2012). Nutritional intervention is commonly used to mitigate skeletal disorders, such as calcium and vitamin $D_3$ supplementation. However, the absorption of nutrient supplementation is limited, thus the more comprehensive method through the regulation of bone metabolism and calcium homeostasis should be applied to the poultry industry to systemically enhance poultry bone health.

Bone mesenchymal stem cells (MSCs) are known as strong self-renewal ability and multilineage differentiation potential, which can differentiate into osteoblast, adipocyte, chondrocyte, and myoblast (Bilezikian et al., 2008). They continue contributing different types of cells to bone formation and play an important role in bone turnover and metabolism (Chen et al.,

2019). Since human MSCs were first proved to exhibit multilineage potential (Pittenger et al., 1999), they have been recognized as an ideal model to investigate bone and joint diseases and the modulation mechanism of potential drugs and functional components during MSC osteogenesis (Liu et al., 2014). Moreover, some studies have reported that chicken MSCs were successfully isolated from both bone marrow (Khatri et al., 2009; Bai et al., 2013) and compact bone (Adhikari et al., 2019) and presented multi-potent properties.

It has been reported that the calcium-sensing receptor (CaSR) is expressed in MSCs (Di Tomo et al., 2013; Pipino et al., 2014), and CaSR plays a central role in calcium homeostasis and mediates many physiological and pathological processes, such as cell proliferation, differentiation, and apoptosis (Kallay, 2018). Evidence points to the role of CaSR in osteogenic differentiation, and it has been recognized a potential therapeutic target in osteoporosis (Marie, 2010). It has been well recognized that there are two categories of CaSR ligands: orthosteric agonists and allosteric modulators (Saidak et al., 2009). Orthosteric agonists can directly bind to CaSR orthosteric sites where primary ligand $Ca^{2+}$ is bound to activate CaSR on its own. Allosteric modulators including positive allosteric modulators (PAMs) and negative allosteric modulators (NAMs), bind to allosteric sites distinct from orthosteric sites on CaSR, and require $Ca^{2+}$ to activate CaSR concertedly (Saidak et al., 2009). Allosteric modulators affect the sensitivity and responsiveness of CaSR to extracellular $Ca^{2+}$ and downstream signaling cascades (Zhang et al., 2016). It has been reported that elevated extracellular $Ca^{2+}$ level and CaSR PAM, NPS R-568, significantly stimulated osteogenic differentiation of MSCs via CaSR activation (Pipino et al., 2014). Moreover, L-tryptophan (L-Trp) has been recognized as a potent CaSR PAM (Conigrave et al., 2007) and L-Trp as an essential and functional amino acid, is involved in both protein synthesis and neuromodulation process (Fouad et al., 2021). Also，it is considered as a limiting amino acid in

corn-soybean meal poultry diets (Harms, 1992; Russell and Harms, 1999), and the adequate L-Trp is conducive to the improvement of meat and egg performance, meat and egg quality, gut health, and immunity (Fouad et al., 2021).

The 1,25-dihydroxycholecalciferol [$1,25(OH)_2D_3$, active form of vitamin $D_3$] is important in calcium metabolism because many genes related to calcium transport and calcium metabolism have a vitamin D response element (VDRE) sequence located in their promoter region, thereby acting as a transcription factor of these genes including CaSR and many calcium transporters (Bar, 2009). However, the effect of $1,25(OH)_2D_3$ on bone cell proliferation, osteogenic differentiation, and mineralization has been inconsistent across different species (Harrison et al., 1989; St-Arnaud, 2008; Tarroni et al., 2012; Chen et al., 2021), and is also influenced by factors such as cell origin, drug dose, and treatment time (Czekanska et al., 2012; Van Driel and Van Leeuwen, 2014).

Although a few studies focused on avian MSCs and the osteogenic differentiation, no one has investigated and discussed the similarities and differences of both broiler and layer MSCs and the role of CaSR during their proliferation and osteogenic differentiation. Moreover, studies on the effect of $1,25(OH)_2D_3$ on chicken MSC proliferation and osteogenesis are still limited, especially the indirect role of $1,25(OH)_2D_3$ in chicken MSC osteogenesis via the regulation of CaSR transcription not been investigated yet. In this study, we aimed to compare the proliferation and differentiation processes of MSCs isolated from broiler and layer compact bone; to investigate the does- and time-effect of L-Trp on the regulation of proliferation and osteogenic differentiation of chicken MSCs; and to reveal the regulation mechanism of L-Trp and $1,25(OH)_2D_3$ via CaSR during chicken MSC proliferation and osteogenic differentiation. This study may provide theoretical evidence that CaSR could be a potential target to regulate bone formation and

remodeling in broilers and layers and to broaden the application of L-Trp and $1,25(OH)_2D_3$ to poultry skeletal disorders.

## 6.3 Materials and methods

### 6.3.1 Isolation and culture of chicken compact bone MSCs

All experiments were approved by the Fort Garry Campus Animal Care Committee at the University of Manitoba. The isolation methods referred to Adhikari et al. (2019) and Zhu et al. (2010) with some modifications. Briefly, legs were removed from the hip joint and metacarpal of 14-day-old Ross 308 broiler chickens and 14-day-old Dekalb pullets after they were euthanized by $CO_2$ inhalation. After muscle was removed, femurs and tibiae were soaked in 70% ethanol for 1 min. Epiphyses were then removed, and only shafts were kept. Bone marrow from the shaft was flushed with a wash medium composed of low glucose DMEM and 2% Antibiotic-Antimycotic (Gibco, MA, USA) by a syringe needle. The bone shafts were opened, and they were cut into small pieces and soaked in the digestion medium (wash medium supplemented with 1 mg/mL of collagenase (Sigma-Aldrich, MO, USA) for 2 h at 37°C with shaking until bone marrow was completely removed by washing with wash medium. Digestion medium along with compact bone fragments was then filtered through a 60 μm nylon sterile filter unit (Sigma-Aldrich) to remove bone residues. The digestion suspension was centrifuged at 1200 rpm for 10 min. The supernatant was discarded, and the cell pellet was resuspended and washed with standard medium [SM, low glucose DMEM supplemented with 10% fetal bovine serum (FBS, Hyclone, USA), 2 mM L-glutamine (Sigma-Aldrich), and 1% Antibiotic-Antimycotic] twice. Washed cells were collected and seeded into 6-well plastic plates (marked as P0) with a density of $2\times10^5/cm^2$ in a complete medium and incubated at 37 ℃, 5 % $CO_2$. After 24 h, the medium was changed to remove non-adherent cells. After several days, single cells grew up to visible colonies and they were

subcultured (marked as P1) using 0.25% trypsin-EDTA (Gibco) in 25 $cm^2$ cell culture flasks. Then, the medium was changed every 3 days, and cells were subcultured when 80% confluence was reached. All experiments were performed on boiler and layer MSCs between passages 2 and 6.

For osteogenic differentiation, chicken MSCs were seeded into 6-well plated at a density of $2\times10^4$ cells/$cm^2$ cells. On confluency, chicken MSCs were cultured in the osteogenic medium [OM, standard medium supplemented with 0.05 mM ascorbic acid-2-phosphate (Sigma-Aldrich), 10 mM β-glycerophosphate (Sigma-Aldrich), and 100 nM dexamethasone (Sigma-Aldrich)] for up to 14 days. In the meantime, chicken MSCs were treated with CaSR positive modulator (L-Trp), negative modulator (NPS-2143), or $1,25(OH)_2D_3$ in the presence or absence of 2.5 mM $Ca^{2+}$ (basal $Ca^{2+}$ level in SM and OM was 1.8 mM).

### 6.3.2 MSC morphology

Chicken MSCs were observed daily under a microscope (Advanced Microscopy Group) to check their morphology and growth characteristics.

### 6.3.3 MSC proliferation assay

Chicken MSCs were seeded at $10^4$ cells/$cm^2$ in 96-well plates and the proliferation rate was measured on days 1, 3, 5 and 7 of incubation with different treatments using cell proliferation reagent WST-1 (Sigma-Aldrich) with a 20× dilution ratio. The absorbance was measured at 450 nm using a Synergy™ H4 Hybrid Multi-Mode Microplate Reader (BioTek) after 1 h incubation at 37 °C. Cell viability was presented as a percentage of control cells.

### 6.3.4 Real-time quantitative polymerase chain reaction (Real-time qPCR)

Chicken MSCs for real-time qPCR determination were cultured in 6-well plates. Total RNA extraction from each tissue was conducted using TRIzol™ reagent (Invitrogen Life Technologies, Waltham, MA, USA) as described in the manufacturer's instructions. The first-strand cDNA was

synthesized using the iScript™ cDNA Synthesis kit (Bio-Rad, Hercules, CA, USA) according to the corresponding manufacturer's protocol. The relative mRNA abundances of cell surface markers and target genes were measured using SYBR Green Supermix (Bio-Rad) by a CFX Connect™ Real-Time PCR Detection System (Bio-Rad). PCR amplification was performed a set of 3 min at 95 °C, then 35 cycles of denaturation for 20 s at 95 °C, annealing for 30 s at 60 °C, and extension for 30 s at 72 °C. At the end of each cycle, the fluorescence was monitored for 10 s. Each reaction was completed with a melting curve analysis to ensure the specificity of the reaction. The primer sequences of the chicken MSC surface markers, osteogenic differentiation-related genes, and signaling-related genes are listed in Table 6.1. PCR products for cell surface marker identification were separated on 1% agarose gels and visualized using ChemiDoc™ Imaging Systems (Bio-Rad). The relative gene expression was calculated using the $2^{-\Delta\Delta Ct}$ method (Livak and Schmittgen, 2001).

**Table 6.1** Primers used in this study.

| Genes | Primer sequences (5'→ 3') | Product Size |
|---|---|---|
| *CD29* | Forward: GAACGGACAGATATGCAACGG | 300 |
| | Reverse: TAGAACCAGCAGTCACCAACG | |
| *CD44* | Forward: CCGGATTCAGGGATCTGACG | 290 |
| | Reverse: AAGTCATTGCTTCCGCAGGT | |
| *CD90* | Forward: GGTCTACATGTGCGAGCTGA | 471 |
| | Reverse: AAAGCTAAGGGGTGGGAGAA | |
| *CD34* | Forward: GTGCCACAACATCAAAGACG | 239 |
| | Reverse: GGAGCACATCCGTAGCAGGA | |
| *CaSR* | Forward: CAAACCAACGGGCACAGAAG | 118 |
| | Reverse: ATGCACTCCACTGATTCGGG | |

| | | |
|---|---|---|
| *VDR* | Forward: CCGGATTCAGGGATCTGACG | 133 |
| | Reverse: AAGTCATTGCTTCCGCAGGT | |
| *OPN* | Forward: CATGGCCAGTGAGCAAATCC | 92 |
| | Reverse: GTGGTACCTGTGTGTGTGGT | |
| *OCN* | Forward: GGATGCTCGCAGTGCTAAAG | 142 |
| | Reverse: CTCACACACCTCTCGTTGGG | |
| *ALP* | Forward: CGACCACTCACACGTCTTCA | 140 |
| | Reverse: CGATCTTATAGCCAGGGCCG | |
| *BMP2* | Forward: TCAGCTCAGGCCGTTGTTAG | 163 |
| | Reverse: GTCATTCCACCCCACGTCAT | |
| *RUNX2* | Forward: TCTCTGAACTCTGCACCAAGTC | 229 |
| | Reverse: GCTCGGAAGCACCTGAGAGG | |
| *COL1A2* | Forward: CTGGTGAAAGCGGTGCTGTT | 222 |
| | Reverse: CACCAGTGTCACCTCTCAGAC | |
| *NFATc1* | Forward: GCTCGGCAGCACCATGAA | 102 |
| | Reverse: GACAATGAGGAATGCGCCAC | |
| *CTNNB1* | Forward: GAACCTCTTGGATACCGCCC | 88 |
| | Reverse: TAGGGTCCATACCCAAGGCA | |
| *β-actin* | Forward: CAACACAGTGCTGTCTGGTGGTA | 205 |
| (Reference) | Reverse: ATCGTACTCCTGCTTGCTGATCC | |
| *GAPDH* | Forward: ACTGTCAAGGCTGAGAACGG | 100 |
| (Reference) | Reverse: CACCTGCATCTGCCCATTTG | |

Note: All primers belong to *Gallus gallus*. CaSR: calcium-sensing receptor; VDR: vitamin D receptor; OPN: osteopontin; OCN: osteocalcin; ALP: alkaline phosphatase; BMP2: bone

morphogenetic protein 2, RUNX2: runt-related transcription factor 2; COL1A2: collagen type I alpha 2; NFATc1: nuclear factor of activated T-cells 1; CTNNB1: β-catenin.

### 6.3.5 Western blot analysis

The relative protein expression of CaSR and VDR was determined according to the method of Hui et al. (2020). In brief, after 7-day osteogenic differentiation, chicken MSCs cultured in 6-well plates were harvested and lysed using pre-cooled RIPA buffer containing Halt™ protease and phosphatase inhibitor cocktail (Thermo Scientific) on ice. Total protein was determined using the Pierce™ BCA protein assay kit according to the manufacturer's instructions. Denatured protein samples (50 μg) were loaded and separated by 4–15% Mini-PROTEAN® TGX Stain-Free™ Protein Gels (Bio-Rad) and transferred onto a polyvinylidene difluoride membrane (Bio-Rad). Each membrane was blocked using 5% skim milk for 1 h at room temperature, and then incubated with the rabbit polyclonal anti-CaSR antibody (1:1000, ab137408, Abcam, Cambridge, MA, USA) and VDR Monoclonal Antibody (9A7) (1:2000, MA1-710, Thermo Scientific) at 4 °C overnight. Secondary antibody incubation was performed using horseradish peroxidase-conjugated goat anti-rabbit IgG (65-6120, 1:1000, Thermo Scientific) and horseradish peroxidase-conjugated anti-rat IgG (112-035-003, 1:5000, Jackson Immuno Research Laboratories, West Grove, PA, USA). Images were detected by ChemiDoc™ Imaging Systems (Bio-Rad) after incubation with Clarity Max™ Western ECL Substrate (Bio-Rad). The densitometry of the target protein bands was quantified by Image Lab Software (Bio-Rad) and normalized to the total protein.

### 6.3.6 Alizarin red S (ARS) staining

Monolayers of chicken MSCs differentiated with different treatments in the 6-well plates for 7 days were used for mineralization detection by the ARS staining method as described by Gregory et al. (2004) and Chen et al. (2021). Cells were washed with phosphate-buffered saline (PBS) and fixed with 1 mL of 10% formalin (Fisher Scientific, Waltham, MA, USA) per well for 15 min at room temperature. The monolayers were stained with 1 mL of 40 mM ARS solution at pH 4.1- 4.3

(Sigma-Aldrich) for 45 min in the dark. Unstained dye was rinsed with deionized water four times before visualization and quantification. Colorimetric quantification of ARS staining was performed according to Gregory et al. (2004).

### 6.3.7 Alkaline phosphatase (ALP) activity assay

ALP assay was conducted using SigmaFast™ BCIP/NBT tablet (Sigma-Aldrich) as prepared by manufacturer's instruction. After 7-day differentiation, monolayers of chicken MSCs were washed with PBS and fixed with 1 mL of 10% formalin (Fisher Scientific) per well for 30 s at room temperature. Cells were rinsed with deionized water twice and stained with 1 mL of prepared BCIP/NBT solution per well for 10 min at room temperature. The color development was stopped by rinsing monolayers with deionized water. Detailed staining was visualized and photographed by a Zeiss Axio microscope (Carl-Zeiss Ltd, Jena, Germany).

### 6.3.8 Statistical analysis

Each well from a multi-well plate was set as an experimental unit for all analyses. Results were expressed as mean ± SEM with at least three repeats. Statistical significance of data related to time and dose effect of L-Trp on MSC proliferation and osteogenic differentiation was determined by two-way ANOVA, and other results were analyzed by one-way ANOVA followed by Tukey's multiple-comparison test using GraphPad Prism 8 software (San Diego, CA, USA). *P* value $< 0.05$ was considered statistically significant.

## 6.4 Results

### 6.4.1 Identification of isolated broiler and layer MSCs

MSCs were isolated from the tibial and femoral compact bone of broilers and layer pullets, and then their surface antigen genes were tested to identify the cells. As shown in Figure 6.1, both broiler and layer MSCs expressed MSC-specific markers CD29, CD44, CD90 with the absence of

hemopoietic stem cell marker CD34, which illustrated that they were chicken MSCs. Figure 6.2 showed the MSC morphology at different stages. The morphological characteristics of broiler and layer MSCs were the same. They were all spindle-shaped, large, and flattened cells, and showed positive cell proliferation potential during passage 0 to 6.

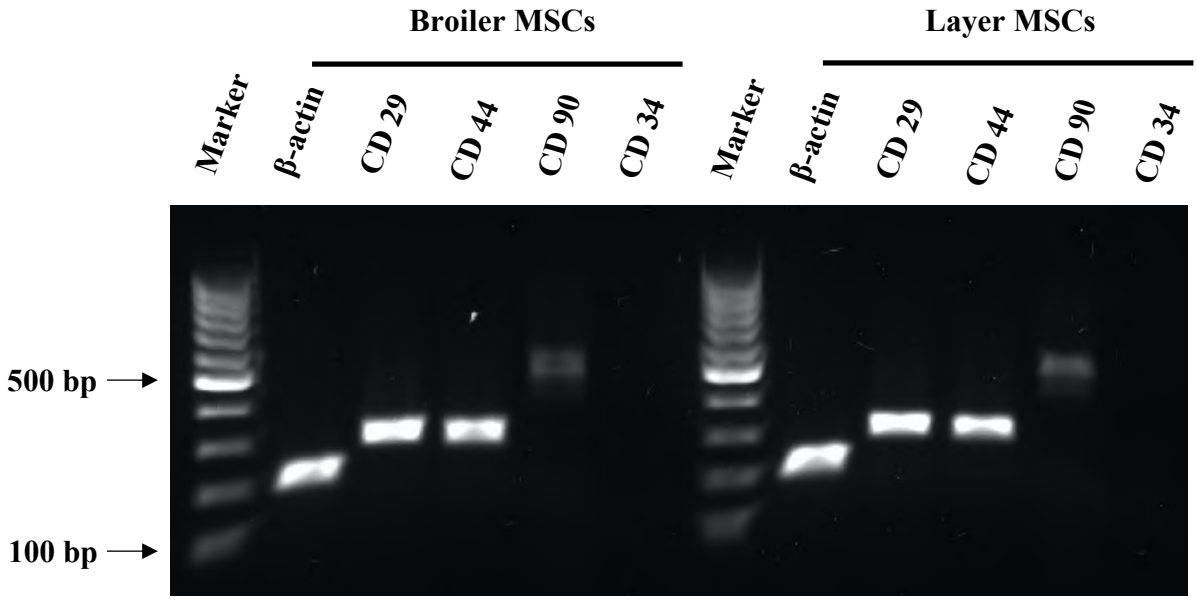


**Figure 6.1** Surface specific marker analysis of broiler and layer MSCs by real-time quantitative polymerase chain reaction in passage 1.

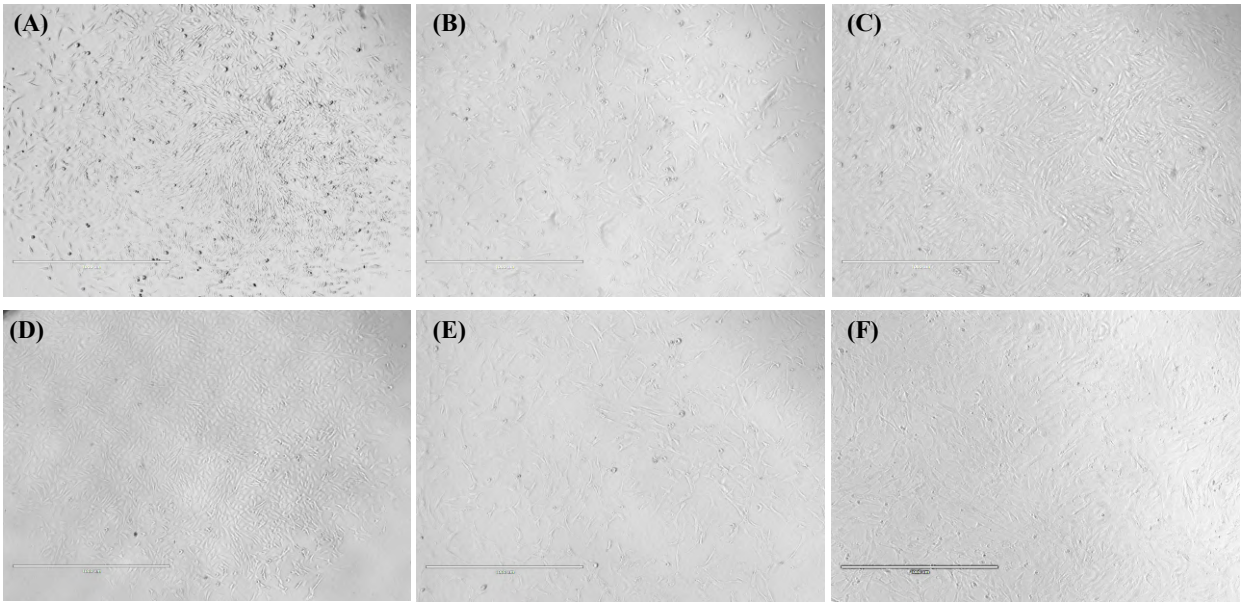


**Figure 6.2** Cell morphology at different stages and passages of broiler MSCs and layer MSCs isolated from leg compact bones. Broiler MSCs (A) passage 0 when forming obvious colonies; (B) passage 2-6 during growth; (C) passage 2-6 when reaching confluency; Layer MSCs (D) passage 0 when forming obvious colonies; (E) passage 2-6 during growth; (F) passage 2-6 when reaching confluency. Each scale bar represents 1000 μm.

### 6.4.2 Time- and dose-effect of L-Trp on chicken MSC proliferation

The proliferation rate of broiler and layer MSCs for 7 days is shown in Figures 6.3A and B, respectively. Cells were subcultured every 7 days when reaching confluency. In the broiler MSCs, higher L-Trp dose at 10 and 15 mM significantly inhibited cell proliferation after day 3 ($P < 0.05$), and 5 mM L-Trp started significantly reducing cell viability after day 5 ($P < 0.05$). On day 7, all L-Trp supplementation groups significantly inhibited cell proliferation compared with the control ($P < 0.05$). Similar to the broiler MSCs, a high concentration of L-Trp showed an inhibitory effect on cell proliferation, but layer cells had more tolerance to L-Trp. On day 7, L-Trp only at 5, 10, and 15 mM significantly decreased the proliferation rate ($P < 0.05$), while 2 mM L-Trp had no negative effect on proliferation compared with the control ($P > 0.05$). When comparing the proliferation capacity of MSCs from different origins, broiler MSCs grew faster than layer MSCs before day 5.

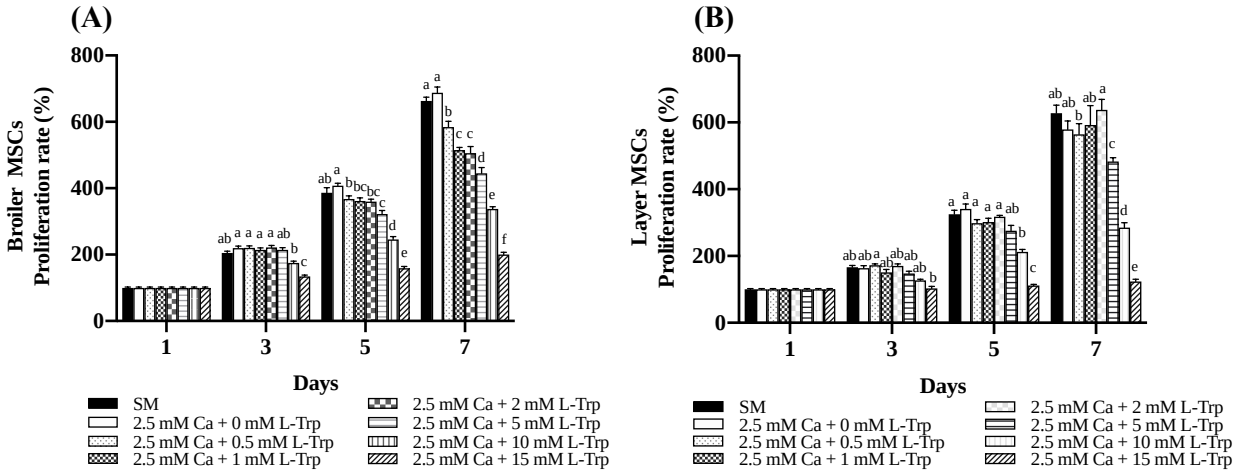


**Figure 6.3** The proliferation rate of (A) broiler MSCs and (B) layer MSCs. Cells were treated with basal standard medium (SM, 1.8 mM $Ca^{2+}$), SM supplemented with high calcium (2.5 mM) and different concentrations of L-tryptophan (0, 0.5, 1, 2, 5, 10, 15 mM) for 1, 3, 5, and 7 days. Data were presented as mean ± SEM, n = 6. Different letters represent a significant difference ($P < 0.05$).

### 6.4.3 Time- and dose-effect of L-Trp on chicken MSC osteogenic differentiation

During broiler and layer MSC osteogenic differentiation, relative mRNA expression of *CaSR, VDR, and osteogenic differentiation markers including ALP, osteopontin (OPN), osteocalcin (OCN), bone morphogenetic protein 2 (BMP2),* and *runt-related transcription factor 2 (RUNX2)* were determined on day 0, 7, and 14 (Figure 6.4 and 6.5). In broiler MSCs, the mRNA abundance of *CaSR* was downregulated on both day 7 and 14 compared with the SM group (undifferentiated cells), but on day 14, its expression restored to some degree, especially at 5 mM L-Trp, it was the highest expression compared with other treatments (Figure 6.4A). Similarly, the mRNA expression of CaSR in layer MSCs was lower than SM group on days 7 and 14, but when L-Trp concentrations were greater than or equal to 2 mM, its expression was significantly upregulated compared with the SM group ($P < 0.05$, Figure 6.5A). We found that VDR and all genes of osteogenesis markers in broiler MSCs were upregulated with time after osteogenic induction (cells were cultured in OM) when L-Trp supplementation concentrations were less than 5 mM (Figure 6.4B-G). In other word, high dose of L-Trp at 10 and 15 mM significantly upregulated the mRNA expression in almost all genes except for *ALP* compared with that treated with 5 mM L-Trp or lower on day 7 ($P < 0.05$). When the L-Trp concentration was 5 mM, some genes including *ALP* and *OCN* showed the highest expression level on day 7 (Figure 6.4C and E), but other genes including *OPN, BMP2*, and *RUNX2* continued upregulating until day 14 (Figure 6.4D, F, and G). In layer MSCs, the variation trend of the expression of osteogenesis-related genes was not completely consistent with that in broiler MSCs (Figure 6.5B-G). The 7- and 14-day osteogenic differentiation significantly upregulated the mRNA expression of VDR in layer MSCs ($P < 0.05$, Figure 6.5B). Also, 10 and 15 mM L-Trp did not facilitate osteogenic differentiation on day 7 compared to broiler MSCs, while in contrast, the gene expression of some osteogenic markers,

such as *ALP, OCN,* and *BMP2* was significantly downregulated compared with that in 5 mM L-Trp group ($P < 0.05$, Figure 6.5C, E, and F). Overall, in both broiler and layer MSCs, L-Trp concentrations at 10 and 15 mM inhibited the expression of genes of those osteogenic differentiation markers either on day 7 or day 14. Therefore, 5 mM L-Trp was recognized as a critical concentration to promote osteogenic differentiation without the harmful effect shown by 10 and 15 mM L-Trp. As most osteogenesis-related genes were significantly upregulated on day 7 compared with the SM group, 7-day osteogenic differentiation was eligible to be applied to the following experiments. In addition, given the inhibitory effect of 5 mM L-Trp on MSC proliferation, 7-day osteogenic differentiation was selected because it can minimize the inhibitory effect compared with 14-day osteogenic differentiation. To sum up, 5 mM L-Trp and 7-day differentiation were selected for the following osteogenic differentiation experiments.

As shown in Figure 6.6, chicken CaSR had 3 bands with varied molecular weights, and the bands for quantitating were indicated in "*": 1) more than 250 kDa, 2) around 150 kDa, and 3) around 120 kDa. According to western blotting results, in both broiler and layer MSCs, CaSR and VDR expression in OM groups were not significantly higher than that in the SM group after 7-day osteogenic differentiation ($P > 0.05$, Figure 6.6A and B). In addition, their expressions in broiler and layer MSCs cultured in different L-Trp concentrations did not vary in an obvious dose-dependent manner.

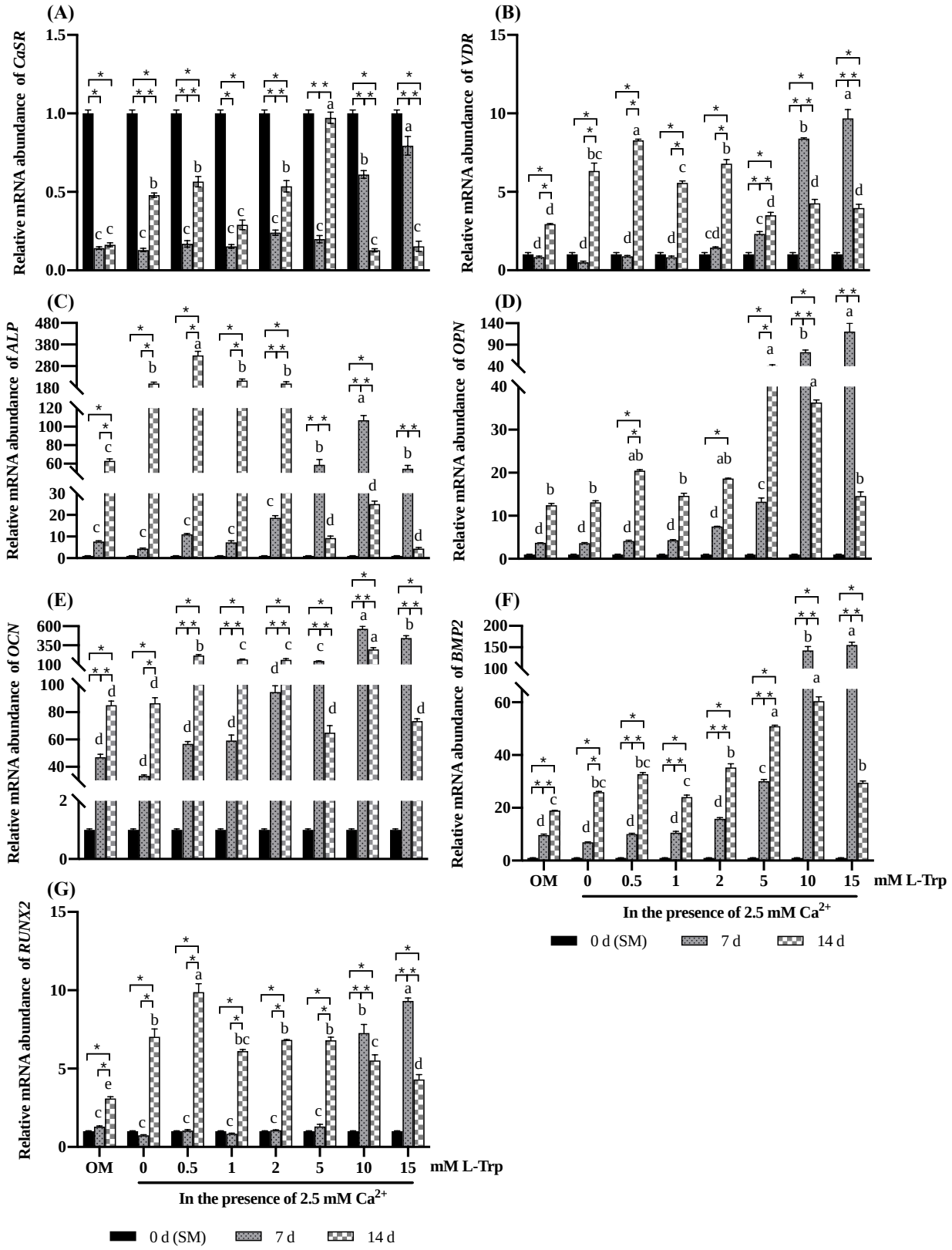
(A)
Relative mRNA abundance of CaSR
(B)
Relative mRNA abundance of VDR
(C)
Relative mRNA abundance of ALP
(D)
Relative mRNA abundance of OPN
(E)
Relative mRNA abundance of OCN
(F)
Relative mRNA abundance of BMP2
(G)
Relative mRNA abundance of RUNX2
OM
0
0.5
1
2
5
10
15
mM L-Trp
In the presence of 2.5 mM Ca2+
0 d (SM)
7 d
14 d

**Figure 6.4** The mRNA abundance of (A) *calcium-sensing receptor (CaSR)*, (B) *vitamin D receptor (VDR)*, and osteogenic genes including (C) *alkaline phosphatase (ALP)*, (D) *osteopontin (OPN)*, (E) *osteocalcin (OCN)*, (F) *bone morphogenetic protein 2 (BMP2)*, and (G) *runt-related transcription factor 2 (RUNX2)* during osteogenic differentiation in broiler MSCs. Cells were treated with osteogenic medium (OM, 1.8 mM $Ca^{2+}$), OM supplemented with high calcium (2.5 mM) and different concentrations of L-tryptophan (0, 0.5, 1, 2, 5, 10, 15 mM) for 0, 7, and 14 days after confluence. Data were presented as mean ± SEM, n = 3. Different letters represent a significant difference among different concentrations of L-tryptophan and * represents a significant difference for different differentiation time ($P < 0.05$).

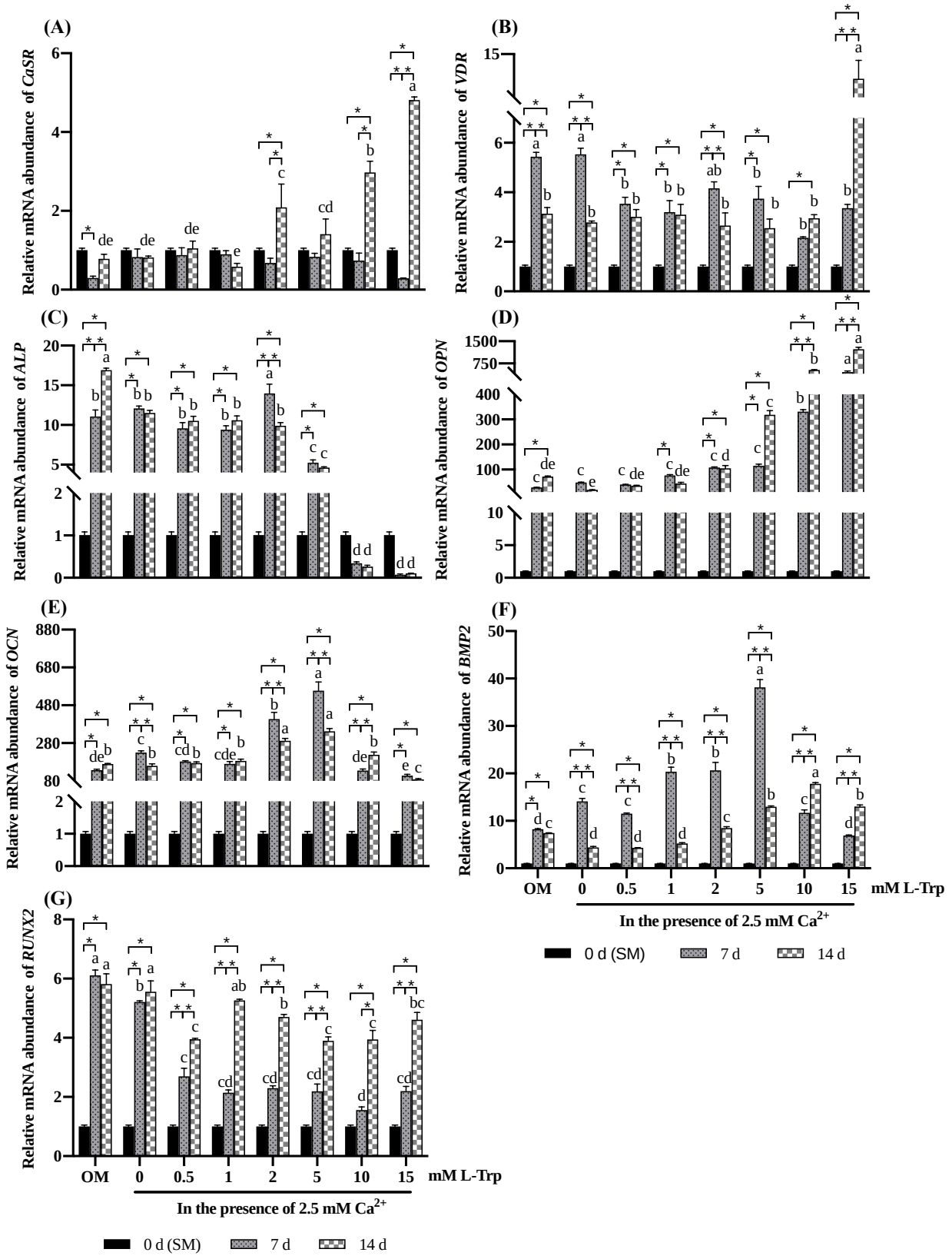
(A)
Relative mRNA abundance of CaSR
(B)
Relative mRNA abundance of VDR
(C)
Relative mRNA abundance of ALP
(D)
Relative mRNA abundance of OPN
(E)
Relative mRNA abundance of OCN
(F)
Relative mRNA abundance of BMP2
(G)
Relative mRNA abundance of RUNX2
OM
0
0.5
1
2
5
10
15
mM L-Trp
In the presence of 2.5 mM Ca2+
0 d (SM)
7 d
14 d

**Figure 6.5** The mRNA abundance of (A) *calcium-sensing receptor (CaSR)*, (B) *vitamin D receptor (VDR)*, and osteogenic genes including (C) *alkaline phosphatase (ALP)*, (D) *osteopontin (OPN)*, (E) *osteocalcin (OCN)*, (F) *bone morphogenetic protein 2 (BMP2)*, and (G) *runt-related transcription factor 2 (RUNX2)* during osteogenic differentiation in layer MSCs. Cells were treated with osteogenic medium (OM, 1.8 mM $Ca^{2+}$), OM supplemented with high calcium (2.5 mM) and different concentrations of L-tryptophan (0, 0.5, 1, 2, 5, 10, 15 mM) for 0, 7, and 14 days after confluence. Data were presented as mean ± SEM, n = 3. Different letters represent a significant difference among different concentrations of L-tryptophan and asterisks "*" represent a significant difference for different differentiation time ($P < 0.05$).

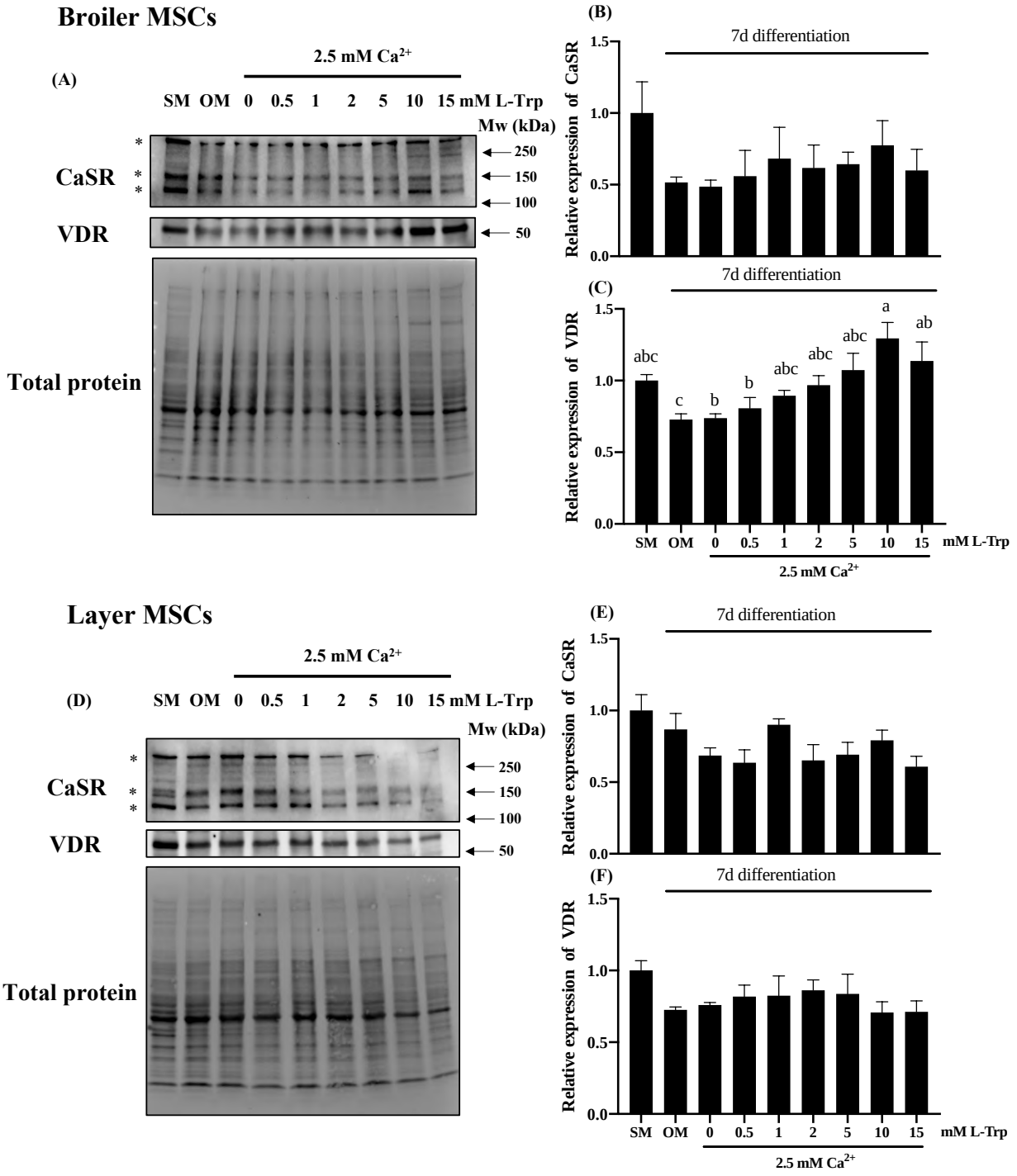


**Figure 6.6** Protein expression of CaSR and VDR. (A and D) Representative western blot images of calcium-sensing receptor (CaSR) and vitamin D receptor (VDR). (B and E) The quantitative relative expression of CaSR and (C and F) VDR in broiler and layer MSCs differentiated for 7

days. Cells were treated with osteogenic medium (OM, 1.8 mM $Ca^{2+}$), OM supplemented with high calcium (2.5 mM) and different concentrations of L-tryptophan (0, 0.5, 1, 2, 5, 10, 15 mM) after confluence. Standard medium (SM) is set as the control (no differentiation). Data were presented as mean ± SEM, n = 3 Different letters represent a significant difference ($P < 0.05$). Bands for quantitating are indicated in "*".

### 6.4.4 Effect of CaSR modulators and 1 nM $1,25(OH)_2D_3$ on chicken MSC proliferation

As shown in Figure 6.7, the proliferation rate of broiler MSCs was faster than that of layer MSCs for 7 days. On day 5, the variation trend in broiler and layer MSCs was similar. 1 nM $1,25(OH)_2D_3$ started promoting proliferation rate, reaching the highest compared with other treatments, but 5 mM L-Trp with and without NPS-2143 both inhibited cell proliferation. On day 7, $1,25(OH)_2D_3$ and 2.5 mM Ca did not significantly improve broiler MSC proliferation compared with the control ($P > 0.05$), but 5 mM L-Trp with and without NPS-2143 still inhibited MSC proliferation (Figure 6.7A). Differently, $1,25(OH)_2D_3$ significantly increased layer MSC proliferation compared with other treatment groups ($P < 0.05$, Figure 6.7B).

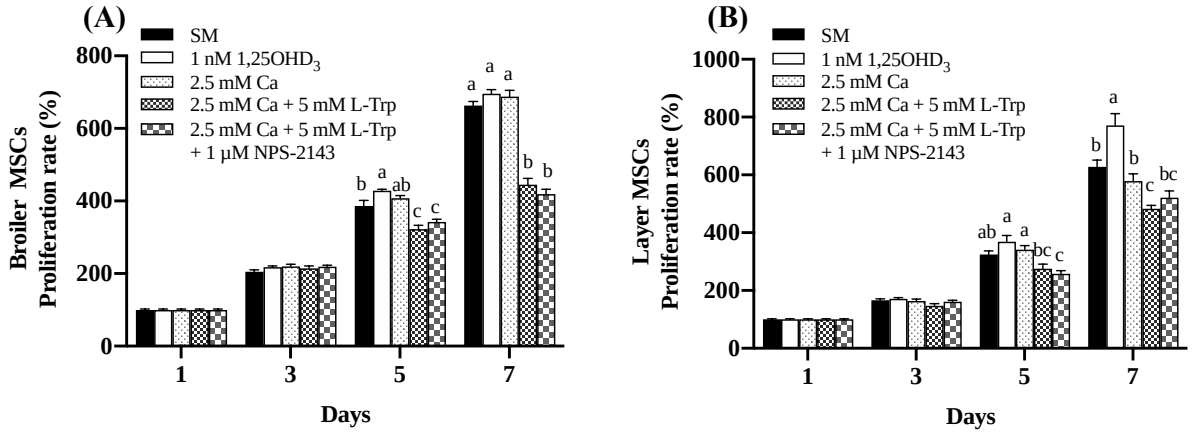


**Figure 6.7** The proliferation rate of (A) broiler MSCs and (B) layer MSCs. Cells were treated with basal standard medium (SM, 1.8 mM $Ca^{2+}$) alone or SM supplemented with 1 nM 1,25-dihydroxycholecalciferol, high calcium (2.5 mM), 5 mM L-tryptophan, or 1 μM NPS-2143 after confluence. Data were presented as mean ± SEM, n = 3. Different letters represent a significant difference ($P < 0.05$). $1,25OHD_3$: 1,25-dihydroxycholecalciferol.

### 6.4.5 Effect of CaSR modulators and 1 nM $1,25(OH)_2D_3$ on chicken MSC osteogenic differentiation

Calcium deposits in broiler and layer MSCs cultured in different OM for 7 days were detected by ARS staining (Figure 6.8A and 6.9A) and the spectrophotometric quantification data are shown in Figure 6.8B and 6.9B. In broiler MSCs, 5 mM L-Trp significantly promoted the mineralization process during a 7-day osteogenic differentiation compared with the control ($P < 0.05$), but the NAM of CaSR, NPS-2143, significantly offset this effect ($P < 0.05$, Figure 6.8B). Both 1 nM $1,25(OH)_2D_3$ and 2.5 mM $Ca^{2+}$ alone did not affect the mineralization level of osteogenic differentiated MSCs compared with the control ($P > 0.05$, Figure 6.8B). In contrast, in layer MSCs, 7-day differentiation obviously facilitated the calcium deposition among all treatments in comparison to that in broiler MSCs (Figure 6.8A and 6.9A). The highest level of mineralization was detected in the 2.5 mM $Ca^{2+}$ alone treatment group, and it was significantly higher than other groups ($P < 0.05$). The 5 mM L-Trp did not promote calcium deposit, but 5 mM L-Trp alone and 5 mM L-Trp + NPS-2143 significantly inhibited the process compared with the control ($P < 0.05$).

The ALP staining results in broiler MSCs and layer MSCs are shown in Figure 6.8C, 6.8D, 6.9C, and 6.9D, respectively. In broiler MSCs, similar to ARS staining, the 5 mM L-Trp supplemented groups showed the highest ALP activity, and it was significantly higher than that in the control group ($P < 0.05$, Figure 6.8E). However, 1 nM $1,25(OH)_2D_3$ supplementation significantly inhibited ALP activity compared with the control ($P < 0.05$). In layer MSCs, ALP activity varied similar to ARS staining. The highest staining value was found in the 2.5 mM Ca group, followed by other treatment groups (Figure 6.9E). Compared broiler with layer MSCs osteogenic differentiated for 7 days, ALP activity was higher in layer MSCs, which was consistent with the ARS staining result.

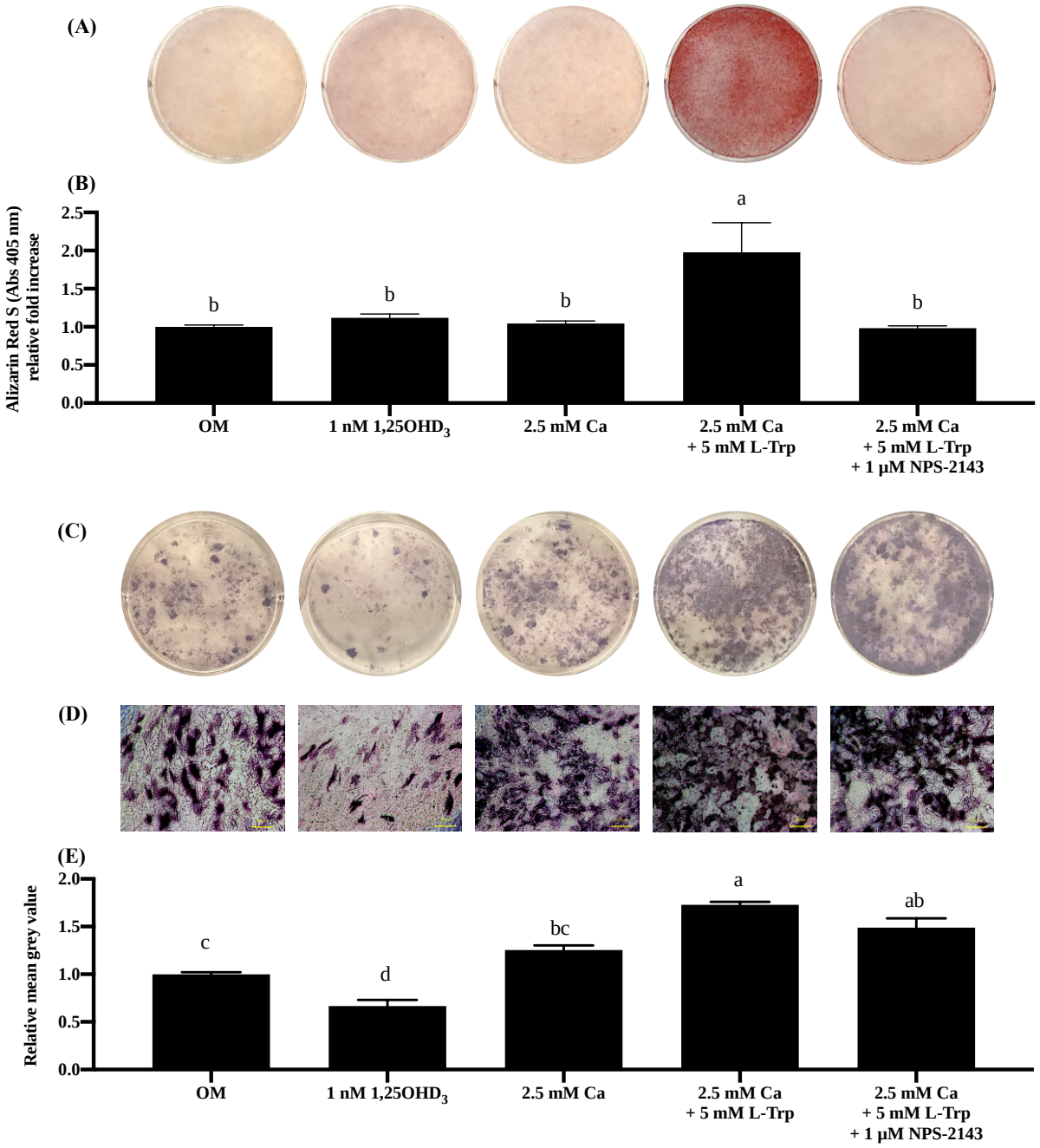


**Figure 6.8** Calcium deposition and alkaline phosphatase (ALP) activity in broiler MSCs. (A) Alizarin red S (ARS) staining in broiler MSCs differentiated for 7 days. (B) Spectrophotometric quantification data of ARS staining. (C) ALP staining in broiler MSCs differentiated for 7 days. (D) Microscopic pictures of ALP staining. Scale bar represents 200 µm; (E) Microscopic pictures

were quantified with mean grey value. Cells were treated with osteogenic medium (OM, 1.8 mM $Ca^{2+}$) alone or OM supplemented with 1 nM 1,25-dihydroxycholecalciferol, high calcium (2.5 mM), 5 mM L-tryptophan, or 1 μM NPS-2143 after confluence. Data were presented as mean ± SEM, n = 3. Different letters represent a significant difference ($P < 0.05$). $1,25OHD_3$: 1,25-dihydroxycholecalciferol.

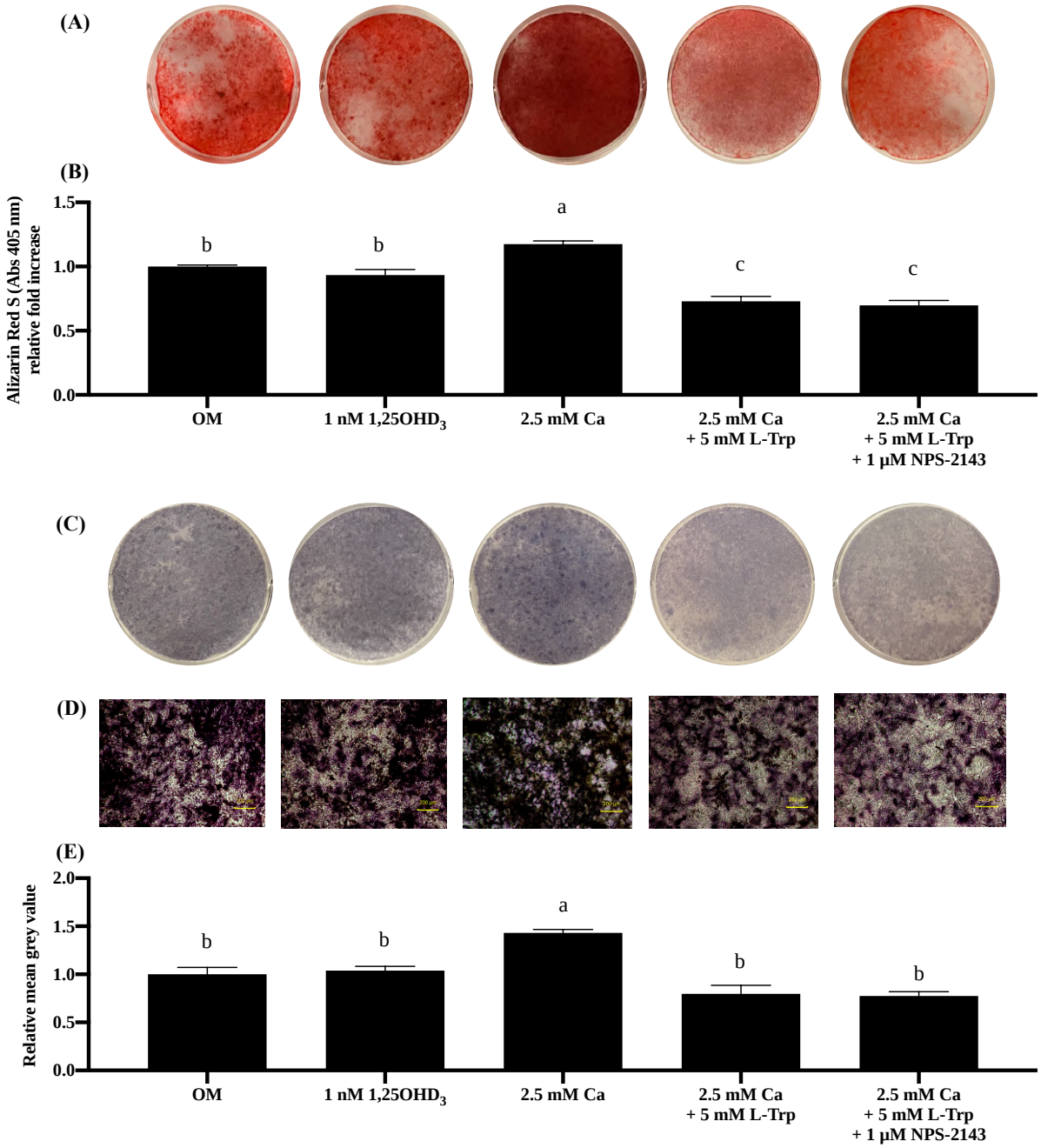


**Figure 6.9** Calcium deposition and alkaline phosphatase (ALP) activity in layer MSCs. (A) Alizarin red S (ARS) staining in broiler MSCs differentiated for 7 days. (B) Spectrophotometric quantification data of ARS staining. (C) ALP staining in broiler MSCs differentiated for 7 days. (D) Microscopic pictures of ALP staining. Scale bar represents 200 µm; (E) Microscopic pictures were quantified with mean grey value. Cells were treated with osteogenic medium (OM, 1.8 mM

$Ca^{2+}$) alone or OM supplemented with 1 nM 1,25-dihydroxycholecalciferol, high calcium (2.5 mM), 5 mM L-tryptophan, or 1 μM NPS-2143 after confluence. Data were presented as mean ± SEM, n = 3. Different letters represent a significant difference ($P < 0.05$). $1,25OHD_3$: 1,25-dihydroxycholecalciferol.

Figure 6.10 and 6.11 showed the mRNA abundance of *CaSR, VDR*, osteogenesis-related genes, and genes belonging to Wnt and calcium/calcineurin signaling pathways. In broiler MSCs, *CaSR* gene expression was significantly downregulated in the 2.5 mM Ca and Ca+Trp+NPS-2143 groups compared with the control ($P < 0.05$, Figure 8A). *VDR* mRNA expression was only significantly upregulated in the treatment groups having 5 mM L-Trp compared with the control ($P < 0.05$, Figure 6.10B). The mRNA expression of *ALP, OCN, COL1A2*, and *CTNNB1* showed the same variation trend as *VDR* mRNA expression (Figure 6.10C, E, F, and J). NPS-2143 promoted the gene expression of *OPN, BMP2,* and *RUNX2*, which was significantly higher than L-Trp alone ($P < 0.05$), and the gene expression of *OPN* and *BMP2* was significant higher in L-Trp containing groups compared with other groups. *NFATc1* gene expression did not show significant differences among all treatment groups ($P > 0.05$). In layer MSCs, regarding the gene expression of *CaSR, VDR, ALP, COL1A2, NFATc1,* and *CTNNB1*, no treatment group significantly upregulated the expression level compared with the control ($P > 0.05$), and 5 mM L-Trp alone even significantly downregulated the gene expression of *CaSR, VDR, ALP* ($P < 0.05$). As for the gene expression of *OPN, OCN, BMP2, and RUNX2*, at least one treatment group showed the significantly higher expression level compared with the control ($P < 0.05$). The $1,25(OH)_2D_3$ supplementation significantly upregulated OPN gene expression ($P < 0.05$, Figure 6.11D). The highest OCN gene expression level was found in the L-Trp+NPS-2143 group and it was significantly higher than the control and Ca alone groups ($P < 0.05$, Figure 6.11E). The L-Trp and L-Trp+NPS-2143 groups upregulated the BMP2 gene expression (Figure 6.11G), which were significantly higher than the control, Ca alone, and $1,25(OH)_2D_3$ groups ($P < 0.05$). However, RUNX2 gene expression in the Ca alone group was significantly higher than the control ($P < 0.05$, Figure 6.11H).

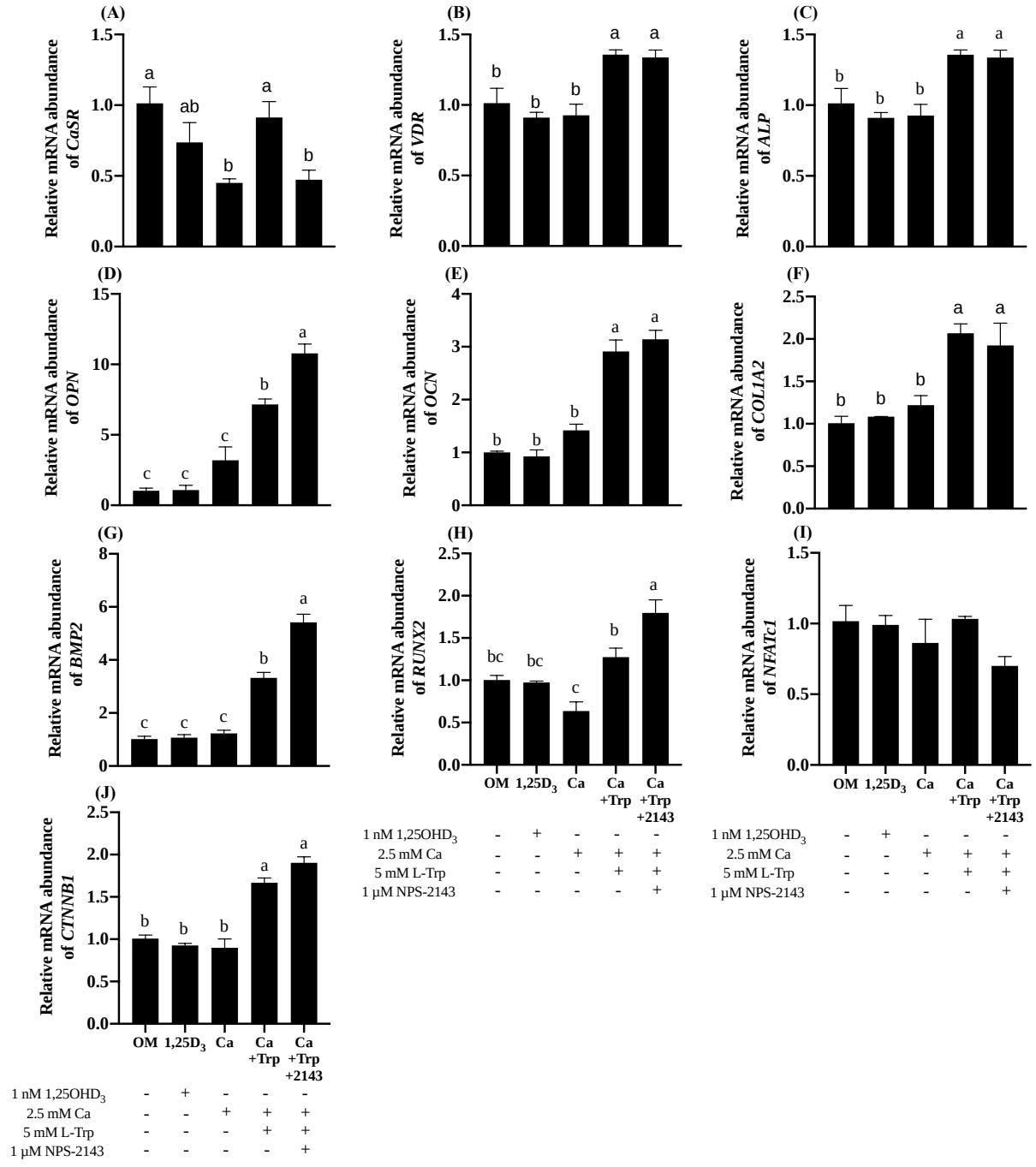


**Figure 6.10** The mRNA abundance of (A) *calcium-sensing receptor (CaSR)*, (B) *vitamin D receptor (VDR)*, and osteogenic genes including (C) *alkaline phosphatase (ALP)*, (D) *osteopontin (OPN)*, (E) *osteocalcin (OCN)*, (F) *collagen type I alpha 2 (COL1A2)*, (G) *bone morphogenetic protein 2 (BMP2)*, and (H) *runt-related transcription factor 2 (RUNX2)*, (I) *nuclear factor of*

*activated T-cells 1 (NFATc1)*, and (J) *β-catenin (CTNNB1)* during osteogenic differentiation in broiler MSCs. Cells were treated with osteogenic medium (OM, 1.8 mM $Ca^{2+}$) alone or OM supplemented with 1 nM 1,25-dihydroxycholecalciferol, high calcium (2.5 mM), 5 mM L-tryptophan, or 1 μM NPS-2143 after confluence. Data were presented as mean ± SEM, n = 3. Different letters represent a significant difference ($P < 0.05$). $1,25OHD_3$: 1,25-dihydroxycholecalciferol.

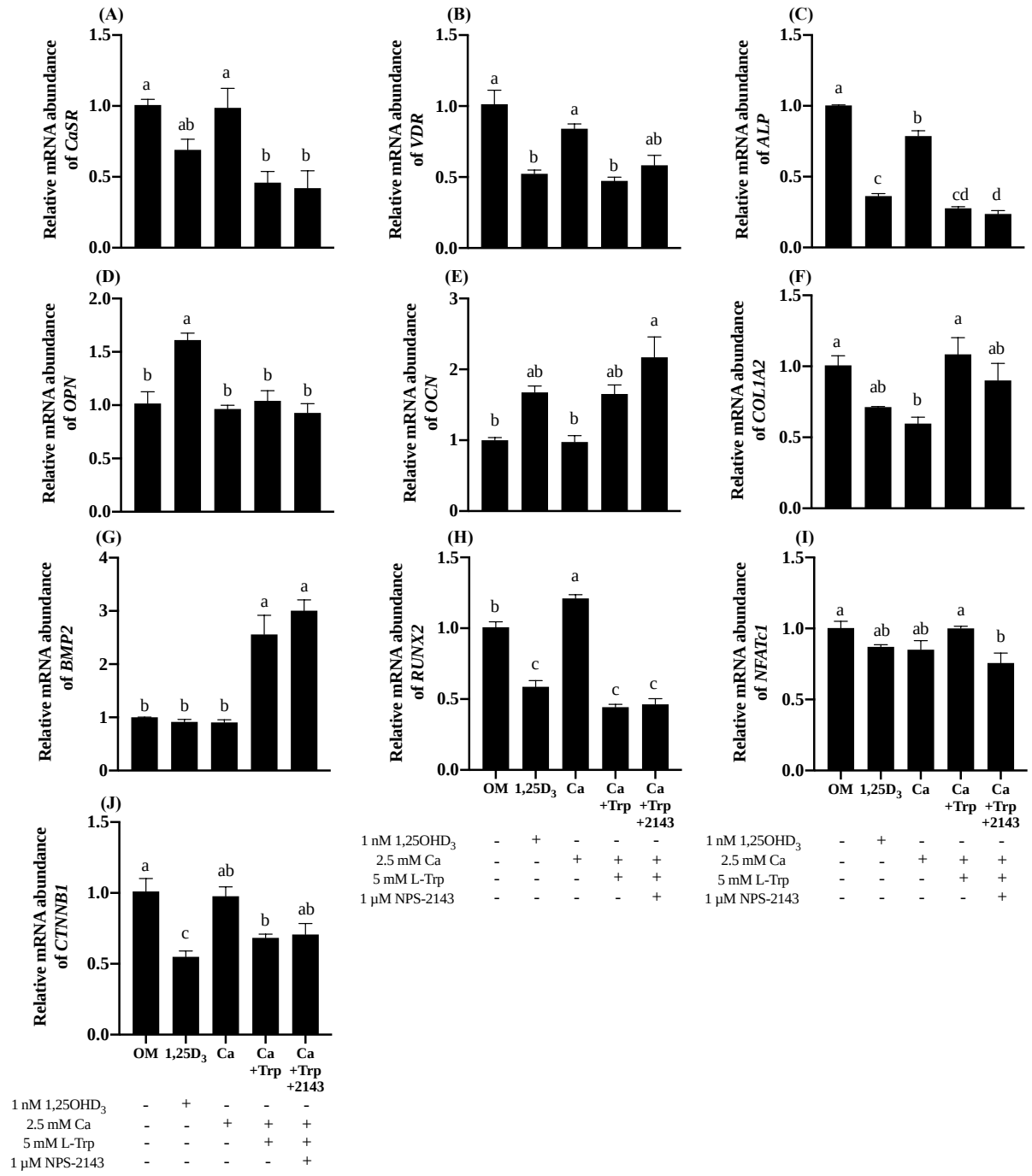


**Figure 6.11** The mRNA abundance of (A) *calcium-sensing receptor (CaSR)*, (B) *vitamin D receptor (VDR)*, and osteogenic genes including (C) *alkaline phosphatase (ALP)*, (D) *osteopontin (OPN)*, (E) *osteocalcin (OCN)*, (F) *collagen type I alpha 2 (COL1A2)*, (G) *bone morphogenetic protein 2 (BMP2)*, and (H) *runt-related transcription factor 2 (RUNX2)*, (I) *nuclear factor of*

*activated T-cells 1 (NFATc1)*, and (J) *β-catenin (CTNNB1)* during osteogenic differentiation in layer MSCs. Cells were treated with osteogenic medium (OM, 1.8 mM Ca2+) alone or OM supplemented with 1 nM 1,25-dihydroxycholecalciferol, high calcium (2.5 mM), 5 mM L-tryptophan, or 1 μM NPS-2143 after confluence. Data were presented as mean ± SEM, n = 3. Different letters represent a significant difference ($P < 0.05$). $1,25OHD_3$: 1,25-dihydroxycholecalciferol.

## 6.5 Discussion

The comparative analysis of the dose- and time-effects of $Ca^{2+}$ and L-Trp on poultry MSC proliferation and osteogenic differentiation were first investigated, which contributing to finding a suitable dose and time point to further reveal the regulation mechanism of CaSR and VDR in bone formation and remodeling. Generally. L-Trp inhibited broiler MSC proliferation and had a bilateral effect on layer MSC proliferation for 7 days depending on different doses of L-Trp. The 7-day proliferation assay was consistent with the MSC subculture cycle, and we found some similarities and differences between broiler and layer MSCs. Both origins of cells were vulnerable to the high doses of L-Trp (10 and 15 mM) even at an early stage. Proliferation and differentiation processes are recognized as negatively correlated (Ruijtenberg and van den Heuvel, 2016), which suggested slightly proliferation inhibition at a relatively high L-Trp concentration might contribute to osteogenic differentiation (Zhang et al., 2015b).

The gene expression data of broiler MSCs also supported this point of view. L-Trp concentrations higher than 10 mM (10 and 15 mM) significantly upregulated the gene expression of CaSR, VDR, and osteogenesis-related markers on day 7 compared with other treatments. However, 10 and 15 mM L-Trp treatment groups then underwent a rapid downregulation on day 14, which indicated that constantly high doses of L-Trp were detrimental to MSC differentiation proceeding. The high inhibition rates on broiler MSC proliferation at 10 and 15 mM L-Trp were observed, thus 5 mM L-Trp might be a proper dose to investigate the regulation mechanism of CaSR modulators and $1,25(OH)_2D_3$ on broiler MSC proliferation and osteogenic differentiation. As 5 mM L-Trp showed a positive effect on some mRNA expression of genes related to osteogenic differentiation for 7 days and less harm to proliferation compared to high doses of L-Trp in 10 and 15 mM, 5 mM L-Trp and 7-day osteogenic differentiation were selected for further investigation

in layer MSCs. The same concentration of L-Trp and same treatment time were conducive to the comparative analysis of both origins of MSCs. Moreover, the differentiation process may not promote CaSR expression, but the CaSR modulator did change the CaSR expression pattern, which was possibly due to $Ca^{2+}$ and L-Trp being involved in the signaling modulation of CaSR. Although the variation trends were different from broiler MSCs to layer MSCs, 5 mM L-Trp was the only concentration that increased mRNA abundance of CaSR constantly from day 0 to day 14, which indicated that 5 mM L-Trp worked as a critical point for further experiments.

Different from that in broiler MSCs, 7-day differentiation significantly upregulated all gene expression regardless of L-Trp doses and showed less difference compared with 14-day differentiation. This circumstance might suggest that the process of osteogenic differentiation in layer MSCs was faster than that in broiler MSCs. In other words, the expression of osteogenesis-related genes probably reached the summit before day 7.

To reveal the regulation mechanism of CaSR and VDR during chicken MSC proliferation and osteogenic differentiation, in addition to $Ca^{2+}$ and 5 mM L-Trp, we included 1 nM $1,25(OH)_2D_3$, and 1 μM NPS-2143 (CaSR antagonist). The selection of 1 nM $1,25(OH)_2D_3$ was based on the results of Chen et al. (2021) who has reported that increasing the dose of $1,25(OH)_2D_3$ had a negative effect on osteogenic differentiation of broiler MSCs. Therefore, 1 nM $1,25(OH)_2D_3$ was a suitable concentrate to investigate the regulation mechanism. In this study, we found that the $1,25(OH)_2D_3$ had a positive effect on proliferation, especially in layer MSCs. The reason might be that laying hens have more active bone turnover and calcium metabolism and are thus more sensitive to $1,25(OH)_2D_3$ (Whitehead, 2004).

Osteogenic differentiation/osteoblast development is recognized as a temporal sequence of events. The first period is characterized by cell growth and proliferation and type I collagen

production, followed by extracellular matrix maturation in which proliferation decreases and osteoblast phenotypic markers such as ALP activity is actively increased. The last stage is mineralization and during which time osteoblast markers, OCN and OPN, are highly expressed (Owen et al., 1990). Calcium deposition of ARS staining reflects the mineralization process and ALP activity is closely related to extracellular matrix maturation. The results of ARS and ALP staining after the 7-day differentiation also supported that the osteogenic differentiation in layer MSCs was faster than that in broiler MSCs. However, the highest level of ARS and ALP staining in the 2.5 mM Ca + 5 mM L-Trp group in broiler MSCs suggested that L-Trp might be beneficial for osteogenic differentiation at the early stage. Therefore, further study could be conducted to investigate the effect of L-Trp on osteogenic differentiation during shorter time intervals in layer MSCs, which might show consistent results with broiler MSCs. The negative effect of $1,25(OH)_2D_3$ on ALP activity and calcium deposition compared with the control in broiler MSCs was consistent with Chen et al. (2021), but no significant negative effect of $1,25(OH)_2D_3$ was found in layer MSCs, which illustrated the main role of $1,25(OH)_2D_3$ in bone formation and remodeling was to increase the MSC proliferation, but the effect of $1,25(OH)_2D_3$ was also affected by bone matrix competency and the differentiation status from MSCs to osteoblasts (Owen et al., 1991).

The regulation of gene expression during osteogenic differentiation is complicated. The gene expression of CaSR was not significantly upregulated in other treatments compared with the control but their variation trend was similar to ARS staining (calcium deposition) in both broiler and layer cells. It was probably due to CaSR being highly involved during the differentiation process (Barradas et al., 2012), but its mRNA expression abundance might not reflect its function in mediating osteogenesis. It is still unclear regarding the CaSR downstream signaling cascades after its activation or blockade, which requires further studies on CaSR signaling during the

osteogenic differentiation in chicken MSCs. Moreover, it has been reported that BMP-2 can promote osteogenic differentiation by regulating cellular $Ca^{2+}$ changes and intracellular calcium signaling, which was closely related to CaSR activation (Xu et al., 2016; Yanai et al., 2019). In this study, only L-Trp supplementation significantly upregulated the mRNA expression of BMP-2 in both broiler and layer MSCs, suggesting that the activation of CaSR by L-Trp might contribute to at least the $Ca^{2+}/IP_3$-mediated signaling pathway in MSCs and further regulate the expression of BMP-2 and osteogenesis (Yanai et al., 2019). The supplementation of $1,25(OH)_2D_3$ did not promote the transcription level of CaSR and most of osteogenesis-related genes in both broiler and layer MSCs, illustrating that 1 nM $1,25(OH)_2D_3$ at least for a short period of time had a limited effect on mediating differentiation and mineralization process. The reason might be the intricate regulation of the vitamin D system on the transcription of osteogenic genes involving many factors such as the source of MSCs, treatment time, concentration, ambient condition, etc. (Chen et al., 2021).

Interestingly, 1 μM NPS-2143 inhibited the gene expression of CaSR in both broiler and layer MSCs, but in most osteogenic genes, CaSR NAM (NPS-2143) supplementation upregulated their gene expression in broiler MSCs. The results were similar to Koori et al. (2014) who found that NPS-2143 addition was conducive to gene expression of OCN and OPN and increasing doses of NPS-2143 showed more mineralization in cell line 1–17 (human periodontal ligament stem cells). However, the positive effect of L-Trp might show different regulation patterns from other PAMs such as NPS R-568, which was reported to be beneficial for osteogenic differentiation of human amniotic fluid mesenchymal stem cells (Pipino et al., 2014) because the binding sites of L-Trp and NPS R-568 with CaSR were located in CaSR extracellular domain (Wen et al., 2021) and transmembrane domain (Petrel et al., 2004), respectively, which may induce different downstream

signaling cascades. Nevertheless, the expression pattern of osteogenic genes in layer MSCs was different, and the positive effect of treatment groups on the expression of osteogenic genes varied without a consistent trend. The possible reason might be that the osteogenic differentiation process in layer MSCs was faster than that in broiler MSCs, and it had been the turning point, thereby showing fluctuating results in the gene expression.

Wnt/β-catenin and calcium-calcineurin-NFAT signaling pathways play an important role in MSC osteogenic differentiation, which are known to regulate bone mass and osteogenesis gene expression (Barker, 2008; Ritchie et al., 2011; Chen et al., 2019). To this end, we measured the canonical components (β-catenin and NFATc1) of two pathways. The variation of β-catenin gene expression was mostly consistent with the variation of osteogenic markers and mineralization in broiler and layer MSCs during 7-day osteogenic differentiation, which suggested that the Wnt/β-catenin signaling pathway played an important role in regulating osteogenic differentiation of chicken MSCs. NFATc1 is a nuclear factor belonging to the NFAT family, but its gene expression did not respond to different treatments in both cells. Therefore, in the future, it is worth further investigating the effect of CaSR modulators on the temporal sequence of osteogenesis and the downstream signaling pathways after CaSR activation during chicken osteogenic differentiation. Taken together, L-Trp this study may shed new light on mechanisms that CaSR could be a target and L-Trp could be a potential nutritional molecule to prevent or attenuate bone diseases for poultry industry.

In conclusion, CaSR and VDR were first confirmed to be expressed in broiler and layer MSCs. CaSR PAM, L-Trp at 5 mM, had a balanced effect on mediating proliferation and osteogenic differentiation in broiler and layer MSCs. The 1 nM $1,25(OH)_2D_3$ promoted proliferation instead of facilitating the differentiation and mineralization process of chicken MSCs. In a 7-day

osteogenic differentiation, 5 mM L-Trp could be a two-edged sword on the MSC osteogenesis process according to different differentiation stages. As osteogenic differentiation in layer MSCs was faster than that in broiler MSCs, at an early osteogenic differentiation stage, 5 mM L-Trp was beneficial for the differentiation and mineralization by activating CaSR, upregulating the mRNA expression of *VDR, β-catenin*, and osteogenic genes (*ALP, OPN, OCN, COLLA2,* and *BMP-2*) in broiler MSCs. However, 5 mM L-Trp inhibited the differentiation and mineralization process by downregulating the mRNA expression of *CaSR, VDR, β-catenin*, and osteogenic genes (*ALP* and *RUNX-2*) in layer MSCs at a relatively late osteogenic differentiation stage. Chicken MSC proliferation and osteogenic differentiation processes can be selectively manipulated by adjusting doses and treatment time of L-Trp and $1,25(OH)_2D_3$ at suitable MSC stages.

## BRIDGE TO CHAPTER SEVEN

In chapters four and five, we proved the presence of CaSR and VDR in different tissues in laying hens and confirmed nutritional CaSR ligands and their binding modes. In chapter six, our study provides evidence for the practical application of L-Trp beyond the role of functional amino acids in the poultry industry to mitigate bone disorders. In addition, the findings will contribute to the improvement of eggshell quality and bone health, and even calcium retention and utilization in laying hens. Thus, in the next chapter (chapter seven), we will investigate the effects of L-tryptophan and 25-hydroxycholecalciferol at different dietary calcium levels on egg production, eggshell quality, bone health, and calcium homeostasis in laying hens.

## CHAPTER SEVEN: MANUSCRIPT IV

**Interactive effects of calcium and L-tryptophan, and of calcium and 25-hydroxycholecalciferol substitution for vitamin $D_3$ on egg production, eggshell quality, bone health, and calcium homeostasis in Dekalb laying hens from 26 to 29 weeks of age**[4]

[4]**Qianru Hui**, Xiaoya Zhao, Shengnan Li, Karmin O, Martin Nyachoti, Chengbo Yang

Under preparation.

## 7.1 Abstract

Calcium (Ca) metabolism is important in the laying hen industry. This study was to investigate the interactive effect of Ca and L-tryptophan (L-Trp), and of Ca and a complete replacement of vitamin $D_3$ with 25-hydroxycholecalciferol (25HyD) on egg production, eggshell quality, bone health, and calcium homeostasis in laying hens. In Experiment 1, a total of 72 Dekalb white layers were selected and divided into a 3×3 factorial arrangement (n=8) with three levels of Ca (3.5%, 4.2%, and 4.9%) and three levels of Trp (0.18%, 0.22%, and 0.26%). In Experiment 2, a total of 48 Dekalb white layers were selected and divided into a 3×2 factorial arrangement (n=8) with three levels of Ca (3.5%, 4.2%, and 4.9%) and with or without 25HyD substitution for equivalent vitamin $D_3$. Experimental data from both experiments were collected from 26 weeks of age for 4 weeks. Experiment 1 and 2 shared 3 treatments at 0.22% Trp as the control. In Experiment 1, average daily feed intake (ADFI) and body weight (BW) was increased with dietary Trp level from 0.22% to 0.26%, while the greatest egg mass was observed at a Trp level of 0.18%. Also, Trp level affected serum total Ca concentration, relative eggshell weight (ESW), eggshell thickness (EST), and eggshell breaking strength (EBS) linearly, and 0.26% Trp significantly increased serum total Ca concentration, relative ESW, EST, and EBS compared with recommended Trp at 0.22% ($P < 0.05$). Moreover, an interaction between Trp and Ca was found in relative ESW and EST ($P < 0.05$), indicating increasing level of Trp up to 0.26% and of Ca up to 4.9% resulted in the greatest relative ESW and EST. Dietary Trp at 0.18% significantly decreased tibia weight, ash, Ca content, and P content compared with 0.26% Trp ($P < 0.05$). In Experiment 2, 25HyD only increased serum total Ca level and tibia P content. Relative ESW, EST, EBS, tibia weight, ash, Ca content, and P content were only increased by dietary Ca level instead of 25HyD. In conclusion, increased dietary Trp level increased Ca level, eggshell quality, and tibia traits, and the combined application of Trp

and Ca showed an interactive effect on the increase in the relative ESW and EST. However, 25HyD substitution for vitamin $D_3$ showed a limited impact on improving egg production, eggshell quality, bone health, and calcium homeostasis.

**Key words**: L-tryptophan, 25-hydroxycholecalciferol, calcium homeostasis, eggshell quality, bone health, layer

## 7.2 Introduction

Egg laying and shell calcification impose severe extra demands for calcium (Ca). Around 2.4 g of Ca is exported for eggshell formation on a daily basis (Fleming, 2008), representing about 10% of the total body calcium of a hen (Nys and Le Roy, 2018). The intensive and dynamic Ca turnover challenges Ca homeostasis, which requires a robust system to absorb, transfer, and utilize Ca in laying hens, especially in the key organs such as the intestine, shell gland, bone, and kidney (Nys and Le Roy, 2018). The imbalanced calcium metabolism negatively affects eggshell quality and bone health. Eggshell quality ensures the egg integrity and safety of egg content (Kemps et al., 2006; Świątkiewicz et al., 2015). Skeletal disorders in laying hens are mainly attributed to structural bone loss (or even osteoporosis) during the egg-laying period because only 60%-75% of eggshell Ca is provided by feed and the remainder must be mobilized from bone stores (Almeida Paz et al., 2006; Fleming, 2008). At the onset of sexual maturity, laying hens stop forming structural bone and instead form only medullary bone (Whitehead, 2004). Therefore, timing of nutritional interventions is critical in improving eggshell quality and bone health in laying hens. If dietary changes are left until sexual maturity, the effects will primarily be on medullary bone formation (Fleming, 2008). To achieve optimal peak bone quality before encountering excessive

resorption, more effective and comprehensive nutritional interventions are required during the laying period.

Ca homeostasis is mediated by the calcium-sensing receptor (CaSR) through feedback mechanisms involving several hormones: the parathyroid hormone (PTH); the active form of vitamin $D_3$ [$1,25(OH)_2D_3$]; and calcitonin to regulate intestinal absorption, bone storage and resorption, and renal reabsorption (de Matos, 2008; Hendy et al., 2013; Proszkowiec-Weglarz and Angel, 2013). The process of egg laying and shell calcification creates an additional calcium pathway through the shell gland. This imposes significant additional demands on calcium homeostasis, as the formation of the shell requires several times more calcium than what is available in the extracellular pool (Bar, 2008). The CaSR is a class C G protein-coupled receptor (GPCR). Its activation or blockade through binding with ligands can induce the downstream G protein-coupled signaling and perform functions in maintaining Ca homeostasis and regulating PTH secretion (Kallay, 2018). L-Trp has been recognized as an effective CaSR positive allosteric modulator, which can exert its effect in the presence of Ca (Conigrave et al., 2007; Wen et al., 2021). In addition, as an essential amino acid, Trp is not only involved in protein biosynthesis, but also plays a role in producing key metabolites such as serotonin, melatonin, kynurenic acid, and quinolinic acid during Trp metabolism, which are important neural and immune modulators in poultry (Bai et al., 2017; Fouad et al., 2021). Previous studies regarding Trp in layers focus mainly on the Trp requirement in different laying stages (Cardoso et al., 2014; Wen et al., 2019a); the relationship between Trp concentration and behaviors (Birkl et al., 2019) and between Trp concentration and production performance and egg quality (Khattak and Helmbrecht, 2019); and the functional effects of Trp on immunomodulation and stress response (Dong et al., 2012).

However, the interaction between dietary Trp and Ca and its effects on calcium homeostasis, production performance, bone health, and eggshell quality in laying hens has not been well studied.

$1,25(OH)_2D_3$ is the active form of vitamin $D_3$ and it is involved in the active Ca transport and CaSR transcription (Mundy and Guise, 1999; Hendy et al., 2013; Proszkowiec-Weglarz and Angel, 2013). $1,25(OH)_2D_3$ is produced primarily in the kidney by enzymatic hydroxylation (1α-hydroxylase) of 25-hydroxycholecalciferol (25HyD) (Norman, 2008). 25HyD is the most active precursor for $1,25(OH)_2D_3$, which is 2- to 4-fold more effective than vitamin $D_3$ in chicken diets (Soares et al., 1995). Also, 25HyD has been commercialized and applied in poultry diets. Many studies investigated 25HyD in laying hens. According to Silva (2017), providing dietary supplementation of 25HyD to laying hens from day 1 to 34 weeks had a positive impact on egg production from onset of laying to 34 weeks of age. Chen et al. (2020) found that long-term 25HyD supplementation was beneficial for egg production only at an early laying stage. Kakhki et al. (2019) showed that top-dressed 25HyD linearly increased egg weight at various dietary Ca levels in aged laying hens. However, limited studies investigated the interactive effect of Ca levels and 25HyD substitution for vitamin $D_3$ on calcium homeostasis, production performance, bone health, and eggshell quality in the early laying period.

In this study, we proposed the hypothesis that the combined action of L-Trp, 25HyD, and Ca can boost Ca utilization via CaSR and thereby improve performance, egg quality, and bone health in laying hens. We aimed to investigate the interactive effects of Ca and L-Trp, and of Ca and 25HyD substitution for vitamin $D_3$ on egg production, eggshell quality, bone health and calcium homeostasis in Dekalb laying hens at a pre-peak laying stage. The findings would provide a theoretical basis for the potential application of L-Trp and 25HyD at a specific dietary Ca level.

## 7.3 Materials and methods

### 7.3.1 Animals and housing

This study included two experiments and the protocol (F18-043/2) was approved by the Fort Garry Campus Animal Care Committee, University of Manitoba. All procedures were carried out in accordance with the Canadian Council on Animal Care guidelines (CCAC, 2009). A total of 96 Dekalb White laying hens were obtained from the main flock of the Poultry Unit, the University of Manitoba at 24 weeks of age with the initial body weight (BW) ranging from 1.6 kg to 1.7 kg. Birds were housed in individual cages for 6 weeks including one week of the adaptation period, one week of the transition period, and four weeks of the formal experimental period. Birds had access to water and feed *ad libitum*. The housing conditions including temperature, humidity, lighting program, etc. were adjusted followed by the Dekalb Commercial Management Guide.

### 7.3.2 Experimental design

Over the first week, all birds were fed a commercial layer diet for adaptation followed by a 50/50 commercial diet and experimental diet for transition. In Experiment 1, three levels of Trp (0.18%, 0.22%, and 0.26%) and three levels of Ca (3.5%, 4.2%, and 4.9%) were used to investigate the interactive effects of calcium and L-Trp on egg production, eggshell quality, bone health and calcium homeostasis in laying hens. A total of 72 Dekalb White laying hens were randomly assigned into 9 treatments with 8 replicates of each treatment (n=8), and all birds were housed in individual cages. A basal diet was formulated according to the nutritional requirement shown in Dekalb Commercial Management Guide (Dekalb, North America Edition) except for the Trp and Ca levels. The recommended dietary level of Trp and Ca is 0.22% and 4.2% respectively in Dekalb layers aged 17-38 weeks. The analyzed Trp and Ca level was 0.18% and 3.39% respectively in the basal diet. The Trp and the Ca-deficient basal diet is shown in Table 7.1. L-Trp (98% feed grade)

was supplemented to the basal diet in 0.04% (L-Trp) increments, resulting in experimental diets containing 0.18%, 0.22%, and 0.26% of Trp. Limestone (40.94% Ca) was added to replace the insoluble poultry grit in the basal diet, resulting in experimental diets containing 3.39%, 4.09%, and 4.79% Ca.

In Experiment 2, three levels of Ca (3.5%, 4.2%, and 4.9%) with or without a complete replacement of dietary vitamin $D_3$ (3000 IU/kg) with 25HyD (75 μg/kg) were used to investigate the interactive effects of Ca and 25HyD on egg production, eggshell quality, bone health and calcium homeostasis in laying hens. A total of 48 Dekalb White laying hens were randomly assigned into 6 treatments with 8 replicates of each treatment (n=8), and all birds were housed in individual cages. Experiment 1 and 2 shared 3 treatments, they are experimental diets with 0.22% Trp + 3.39% Ca, 0.22% Trp + 4.09% Ca, and 0.22% Trp + 4.79% Ca. The remaining 3 treatment diets maintained the same levels of Ca and Trp as 0.22% Trp + 3.39% Ca, 0.22% Trp + 4.09% Ca, and 0.22% Trp + 4.79% Ca, but we only replaced the equivalent amount of vitamin $D_3$ in the diet with 25HyD (DSM Nutritional Products, Parsippany, NJ, USA).

**Table 7.1** Composition of Ca and Trp-deficient basal diet, *as fed basis*

| Ingredient | | Nutrient profile | Calculated | Analyzed |
|---|---|---|---|---|
| | (%) | | (%) | (%) |
| Corn | 52.66 | ME (kcal/kg) | 2900 | N/A |
| Corn DDGS[1] | 14.68 | Crude protein | 18.00 | 18.49 |
| Corn gluten meal | 10.35 | Calcium | 3.50 | 3.39 |
| Limestone | 7.60 | Total phosphorus | 0.71 | 0.66 |
| Soy oil | 4.04 | Available phosphorus | 0.48 | N/A |
| Insoluble poultry grit | 3.50 | Tryptophan | 0.18 | 0.18 |
| Biofos[2] | 1.67 | | | |
| Soy protein concentrate | 1.30 | | | |
| Fish meal | 1.00 | | | |
| Soybean meal | 0.95 | | | |
| L-lysine | 0.60 | | | |
| Vitamin premix[3] | 0.50 | | | |
| Mineral premix[4] | 0.50 | | | |
| L-Arginine | 0.25 | | | |
| DL-Methionine | 0.25 | | | |
| L-Threonine | 0.18 | | | |
| Total | 100 | | | |

[1]Distiller's dried grains with solubles.

[2]Biofos (Mosaic Feed Ingredients, Lithia, FL, USA), a feed grade monocalcium phosphate, containing 21% P and 18% Ca.

[3,4]Vitamin and mineral premix provided per kg of diet: 11 000 IU retinol, 3000 IU cholecalciferol, 20 IU tocopherol, 3 mg menadione, 0.02 mg cobalamin, 6.5 mg riboflavin, 1 mg folic acid, 10 mg calcium pantothenate, 40 mg niacin, 0.2 mg biotin, 2.2 mg thiamine, 4.5 mg pyridoxine, 1000 mg choline, 85 mg manganese, 80 mg zinc, 80 mg iron, 10 mg copper, 0.3 mg selenium, 0.1 mg iodine, 0.67 mg sodium and 125 mg Endox® (antioxidant, product No. 015118-21-CA, Kemin Industries, Des Moines, IA, USA).

### 7.3.3 Data collection

Throughout the whole experimental period, hens were monitored at least twice daily and weighed weekly to record BW. Birds with BW below 20% initial BW were culled. Feeds were provided three times per week to maintain diet freshness, but average daily feed intake (ADFI) was determined weekly. Egg production and egg weight were recorded daily, and the weekly averages of hen-day egg production (HDEP), egg weight, egg mass, and feed conversion rate (FCR) were analyzed. At week 2 and week 4, eggs collected from each hen for three consecutive days (Friday to Sunday) were pooled to measure egg quality including yolk weight, eggshell weight, and eggshell thickness, and the relative yolk weight, relative albumen weight, and relative eggshell weight were calculated accordingly. Over week 4, eggs collected from Tuesday to Thursday were measured for eggshell breaking strength. At the endpoint, 5 mL of blood was collected from the wing vein of each bird. Serum was obtained after centrifugation at 2500 ×g at 4°C for 15 min. Serum was then aliquoted into 1.5 mL vials and stored at -80°C until analysis for serum total Ca, serum ionized Ca, serum PTH, and serum $1,25(OH)_2D_3$. After blood collection, birds were euthanized with $CO_2$ inhalation, and their left tibia bones were collected for tibia weight and ash measurements. Tibiae were stored in plastic sampling bags at -20°C until analysis.

### 7.3.4 Egg and eggshell quality

Egg quality including yolk weight, eggshell weight, and eggshell thickness was measured according to the methods of Wen et al. (2019a) and Chen et al. (2020). Fresh eggs were broken to separate egg yolk and albumen using an egg separator, and egg yolks were weighed. Eggshells with eggshell membrane were washed and dried at 105 °C for 16 h. Eggshells were then weighed, and the thickness of each eggshell was measured three times on the equator of eggs using a digital vernier caliper (precision at 0.01 mm), and the averages were recorded. Albumen weight and the

relative weight of different parts were calculated according to the above measurements. Eggshell breaking strength was measured using an Instron Universal Testing Machine Model 5965 (Instron Corp, Canton, MA, USA) referring to Wen et al. (2019b). The blunt end of each egg was faced down during testing. Bluehill Software (Instron Inc., Norwood, MA, USA) was used to record the maximum compression load in kilogram-force (kgf) at the eggshell break.

### 7.3.5 Tibia quality

Fat-free tibia weight, ash content, total Ca, and P content were measured to indicate tibia quality and health. Fat-free tibia weight and ash content were determined according to the methods of Wen et al. (2019b). Left tibias were thawed and boiled for 10 min to remove flesh residues. Tibia bones were then soaked in hexane using a Soxhlet apparatus to extract fat. Extracted bones were air-dried and weighed. Fat-free ash content was determined after bones were placed in the muffle furnace at 600 °C for 18 h. Tibia ash was digested in acids according to the method 985.01 (AOAC, 2005). Total Ca and P analysis were performed using an inductively coupled plasma mass spectrometry (ICP-MS, Varian Inc, Palo Alto, CA, USA) as described by method 968.08 for Ca (AOAC, 2005) and method 946.06 for P (AOAC, 2005).

### 7.3.6 Ca homeostasis

Serum total Ca was measured using a colorimetric assay kit (MAK022, Sigma-Aldrich, USA). Chicken PTH was determined using a chicken PTH enzyme-linked immunosorbent assay (ELISA) kit (MBS264930) purchased from MyBiosource (San Diego, CA, USA) according to the manufacturer's specification. Serum ionized Ca and $1,25(OH)_2D_3$ were analyzed at Veterinary Diagnostic Laboratory (Michigan State University, East Lansing, MI, USA) using an electrolyte analyzer and a high-performance liquid chromatography mass spectrometry, respectively.

### 7.3.7 Statistical analysis

The two experiments in this study were completely randomized design. Birds were housed in individual cages, and each cage was considered an experimental unit. All data were analyzed by the MIXED procedure of SAS (version 9.4; SAS Inst. Inc., Cary, NC, USA). Data from all tests were performed by the repeated-measures analysis or single-measure results of birds were analyzed with a two-factor factorial model (L-Trp and Ca in Experiment 1; 25HyD and Ca in Experiment 2). Dietary treatments and experimental units in Experiments 1 and 2 were considered as the fixed effect and random effect respectively. The normalized distribution of data was analyzed by the Shapiro-Wilk test. The Orthogonal Polynomial Contrasts were performed to further test trends including linear and quadratic responses to L-Trp if the *P* value was significant. All data were presented as least squares means (LSM) and SEM, adjusted using Tukey's test to compare for significant differences ($P < 0.05$).

## 7.4 Results

### 7.4.1 Feed consumption, body weight, and egg production performance

In Experiment 1, as shown in Table 7.2, ADFI was affected by the main effects of dietary Trp and Ca ($P < 0.05$) without being influenced by the interaction between Trp and Ca ($P = 0.193$) from 26 to 29 weeks of age. A dietary inclusion of 0.26% Trp significantly increased the ADFI compared to the recommended Trp level of 0.22%. In contrast, a dietary inclusion of 0.18% did not significantly decrease ADFI compared to the recommended Trp level of 0.22%. Higher Ca at 4.9% and recommended Ca at 4.2% significantly stimulated ADFI compared with Ca deficiency at 3.5%. The variation of BW was in accordance with ADFI. Significant main effects of Trp ($P = 0.003$) and Ca ($P < 0.001$) were observed in BW, and the BW was increased linearly ($P = 0.004$) with Trp levels increasing. 0.26% Trp significantly increased ADFI, and BW compared with other

doses of Trp ($P < 0.05$). Egg mass was affected by the main effects of Trp quadratically ($P = 0.016$), and egg mass was significantly decreased with Trp supplementation up to 0.22% compared to 0.18% Trp ($P < 0.05$), but egg mass was not decreased with Trp supplementation up to 0.26%. Egg weight was only affected by the main effect of Ca ($P = 0.001$). Overall, dietary Ca at 3.5% significantly reduced ADFI, BW, egg weight, and egg mass compared with Ca at 4.2% and 4.9% ($P < 0.05$). No main effects and interactions were found in HDEP and FCR ($P > 0.05$).

In Experiment 2, ADFI, BW, HDEP, egg weight, egg mass, and FCR in Experiment 2 are shown in Table 7.3. The main effect of Ca on ADFI was found to be significant ($P = 0.023$), showing the greatest ADFI at 4.9% Ca, which was significantly higher than that at 3.5% Ca. There was no treatment effect on HDEP ($P > 0.05$). BW, egg weight, egg mass, and FCR were not influenced by treatments or their interaction ($P > 0.05$).

**Table 7.2** Feed consumption, body weight, and egg production performance in laying hens fed diets with three different levels of Ca and L-Trp from week 26 to week 29 of age[1]

| Main effects | ADFI[2], g/bird/day | BW[3], kg | HDEP[4], % | Egg weight, g | Egg mass, g | FCR[5] |
|---|---|---|---|---|---|---|
| Trp, % | | | | | | |
| 0.18 | 91.3[ab] | 1.57[b] | 97.0 | 55.8 | 54.1[a] | 1.70 |
| 0.22 | 89.2[b] | 1.56[b] | 94.0 | 54.5 | 51.2[b] | 1.80 |
| 0.26 | 96.1[a] | 1.62[a] | 96.2 | 55.3 | 53.3[ab] | 1.81 |
| SEM | 2.0 | 0.01 | 1.3 | 0.6 | 0.8 | 0.05 |
| Ca, % | | | | | | |
| 3.5 | 86.5[b] | 1.53[b] | 94.0 | 55.4[b] | 50.2[b] | 1.73 |
| 4.2 | 94.6[a] | 1.61[a] | 95.9 | 56.5[a] | 54.2[a] | 1.79 |
| 4.9 | 95.4[a] | 1.61[a] | 97.3 | 55.7[a] | 54.2[a] | 1.79 |
| SEM | 1.5 | 0.01 | 1.3 | 0.6 | 0.8 | 0.05 |
| *P* value | | | | | | |
| L-Trp | 0.044 | 0.003 | 0.257 | 0.276 | 0.042 | 0.208 |
| Ca | 0.003 | <.0001 | 0.239 | 0.001 | 0.001 | 0.648 |
| Trp × Ca | 0.193 | 0.354 | 0.372 | 0.695 | 0.581 | 0.149 |
| Trp dose response | | | | | | |
| Linear | 0.091 | 0.004 | 0.677 | 0.594 | 0.458 | 0.101 |
| Quadratic | 0.063 | 0.062 | 0.111 | 0.131 | 0.016 | 0.508 |

[a–c]Values with different superscripts within each column are significantly different ($P < 0.05$).
[1]n=8.
[2]Average daily feed intake.
[3]Body weight.
[4]Hen-day egg production.
[5]Feed conversion ratio, average daily feed intake/ egg mass.

**Table 7.3** Feed consumption, body weight, and egg production performance in laying hens fed diets with three different levels of Ca with or without a complete replacement of dietary vitamin $D_3$ (3000 IU/kg) with 25-hydroxycholecalciferol (25HyD, 75 μg/kg) from week 26 to week 29 of age[1]

| Main effects | ADFI[2], g/bird/day | BW[3], kg | HDEP[4], % | Egg weight, g | Egg mass, g | FCR[5] |
|---|---|---|---|---|---|---|
| Vitamin $D_3$ source | | | | | | |
| Vitamin $D_3$ | 94.6 | 1.61 | 95.9 | 56.5 | 54.2 | 1.79 |
| 25HyD | 91.4 | 1.59 | 96.2 | 55.4 | 53.4 | 1.73 |
| SEM | 1.8 | 0.02 | 1.3 | 0.6 | 0.9 | 0.05 |
| Ca, % | | | | | | |
| 3.5 | 89.4[b] | 1.57 | 97.6 | 55.5 | 54.2 | 1.65 |
| 4.2 | 91.6[ab] | 1.60 | 94.6 | 56.4 | 53.4 | 1.78 |
| 4.9 | 97.9[a] | 1.62 | 95.9 | 56.0 | 53.8 | 1.85 |
| SEM | 2.2 | 0.02 | 1.6 | 0.7 | 1.1 | 0.06 |
| *P* value | | | | | | |
| 25HyD | 0.200 | 0.371 | 0.867 | 0.195 | 0.830 | 0.428 |
| Ca | 0.023 | 0.117 | 0.445 | 0.643 | 0.245 | 0.114 |
| 25HyD × Ca | 0.823 | 0.253 | 0.049 | 0.660 | 0.083 | 0.060 |

[a–c]Values with different superscripts within each column are significantly different ($P < 0.05$).
[1]n=8.
[2]Average daily feed intake.
[3]Body weight.
[4]Hen-day egg production.
[5]Feed conversion ratio, average daily feed intake/ egg mass.

### 7.4.2 Egg and eggshell quality

Egg and eggshell quality in Experiment 1 is shown in Table 7.4. Although the egg weight, relative yolk weight, and relative albumen weight were affected by Trp or Ca, eggshell quality indexes including the relative eggshell weight, eggshell thickness, and eggshell breaking strength were significantly increased by the main effect of Trp (0.18% to 0.26%) linearly ($P < 0.0001$) in a dose-dependent manner. Moreover, an interactive effect of Trp × Ca on the relative eggshell weight ($P = 0.007$) and eggshell thickness ($P = 0.013$) was observed, indicating that increasing level of Trp up to 0.26% and of Ca up to 4.9% resulted in the greatest relative eggshell weight and eggshell thickness (Table 7.5).

Egg and eggshell quality in Experiment 2 is shown in Table 7.6. The main effect of vitamin $D_3$ type and the interaction between 25HyD and Ca had no significant effect on egg and eggshell quality ($P > 0.05$). However, Ca supplementation alone resulted in a significant increase in relative eggshell weight ($P < 0.0001$), eggshell thickness ($P < 0.0001$), and eggshell breaking strength ($P = 0.0002$) when comparing 3.5% Ca to 4.9% Ca.

**Table 7.4** Egg quality and egg composition in laying hens fed diets with three different levels of Ca and L-Trp from week 26 to week 29 of age[1]

| Main effects | Relative yolk weight, % | Relative albumen weight, % | Relative eggshell weight, % | Eggshell thickness, mm | Eggshell breaking strength, kgf |
|---|---|---|---|---|---|
| Trp, % | | | | | |
| 0.18 | 24.4 | 66.2 | 8.9[c] | 0.40[b] | 4.19[b] |
| 0.22 | 23.6 | 66.2 | 9.4[b] | 0.41[b] | 4.69[b] |
| 0.26 | 25.1 | 64.7 | 10.2[a] | 0.44[a] | 5.52[a] |
| SEM | 0.4 | 0.6 | 0.1 | 0.00 | 0.18 |
| Ca, % | | | | | |
| 3.5 | 24.1 | 66.2 | 9.6 | 0.42 | 4.74 |
| 4.2 | 24.6 | 65.4 | 9.5 | 0.42 | 4.78 |
| 4.9 | 24.7 | 65.4 | 9.4 | 0.41 | 4.88 |
| SEM | 0.4 | 0.6 | 0.1 | 0.00 | 0.19 |
| *P* value | | | | | |
| L-Trp | 0.064 | 0.110 | <.0001 | <.0001 | <.0001 |
| Ca | 0.486 | 0.499 | 0.633 | 0.503 | 0.863 |
| Trp × Ca | 0.675 | 0.459 | 0.007 | 0.013 | 0.275 |
| Trp dose response | | | | | |
| Linear | 0.223 | 0.073 | <.0001 | <.0001 | <.0001 |
| Quadratic | 0.044 | 0.274 | 0.352 | 0.213 | 0.518 |

[a–c]Values with different superscripts within each column are significantly different ($P < 0.05$).
[1]n=8.

**Table 7.5** Interaction means of relative eggshell weight and eggshell thickness in laying hens fed diets with three different levels of Ca and L-Trp from week 26 to week 29 of age[1]

| L-Trp, % | Ca, % | Relative eggshell weight, % | Eggshell thickness, mm |
|---|---|---|---|
| 0.18 | 3.5 | 9.3$^{cd}$ | 0.41$^{bd}$ |
| 0.18 | 4.2 | 8.8$^{d}$ | 0.40$^{cd}$ |
| 0.18 | 4.9 | 8.7$^{d}$ | 0.38$^{d}$ |
| 0.22 | 3.5 | 9.7$^{abc}$ | 0.41$^{bd}$ |
| 0.22 | 4.2 | 9.5$^{bcd}$ | 0.42$^{abcd}$ |
| 0.22 | 4.9 | 9.1$^{abcd}$ | 0.40$^{cd}$ |
| 0.26 | 3.5 | 9.8$^{abc}$ | 0.42$^{abc}$ |
| 0.26 | 4.2 | 10.3$^{ab}$ | 0.45$^{ab}$ |
| 0.26 | 4.9 | 10.5$^{a}$ | 0.45$^{a}$ |
| SEM | | 0.2 | 0.008 |
| *P* value | | | |
| L-Trp | | <.0001 | <.0001 |
| Ca | | 0.633 | 0.503 |
| L-Trp×Ca | | 0.007 | 0.013 |

$^{a–d}$Values with different superscripts within each column are significantly different ($P < 0.05$).
[1]n=8.

**Table 7.6** Egg quality and egg composition in laying hens fed diets with three different levels of Ca with or without a complete replacement of dietary vitamin $D_3$ (3000 IU/kg) with 25-hydroxycholecalciferol (25HyD, 75 μg/kg) from week 26 to week 29 of age[1]

| Main effects | Relative yolk weight, % | Relative albumen weight, % | Relative eggshell weight, % | Eggshell thickness, mm | Eggshell breaking strength, kgf |
|---|---|---|---|---|---|
| Vitamin $D_3$ source | | | | | |
| Vitamin $D_3$ | 24.6 | 65.4 | 9.5 | 0.42 | 4.78 |
| 25HyD | 24.0 | 66.4 | 9.6 | 0.42 | 4.95 |
| SEM | 0.4 | 0.6 | 0.1 | 0.00 | 0.17 |
| Ca, % | | | | | |
| 3.5 | 24.1 | 67.0 | $8.9^{c}$ | $0.40^{b}$ | $4.15^{b}$ |
| 4.2 | 23.9 | 65.9 | $9.5^{b}$ | $0.42^{b}$ | $4.88^{ab}$ |
| 4.9 | 24.9 | 64.7 | $10.3^{a}$ | $0.45^{a}$ | $5.56^{a}$ |
| SEM | 0.5 | 0.7 | 0.1 | 0.01 | 0.21 |
| *P* value | | | | | |
| 25HyD | 0.344 | 0.246 | 0.624 | 0.816 | 0.499 |
| Ca | 0.261 | 0.075 | <.0001 | <.0001 | 0.0002 |
| 25HyD × Ca | 0.557 | 0.817 | 0.697 | 0.604 | 0.876 |

$^{a–c}$Values with different superscripts within each column are significantly different ($P < 0.05$).
[1]n=8.

### 7.4.3 Tibia quality

Tibia quality indicated by tibia weight and tibia mineral content is shown in Table 7.7 for Experiment 1. The tibia weight, ash, and Ca and P content were all influenced by the main effect of Trp ($P < 0.05$) linearly ($P < 0.01$). Trp deficiency at 0.18% significantly inhibited these parameters compared with Trp at 0.26%. Moreover, the tibia ash ($P = 0.0027$) and P content ($P = 0.0015$) were also affected by the main effect of Ca, and the Ca level at 4.9% significantly decreased tibia ash and P content compared with 3.5% Ca. No interaction between Trp and Ca was found in tibia-related indexes ($P > 0.05$).

The tibia quality results for Experiment 2 are shown in Table 7.8. There was a significant main effect of Ca on the tibia weight ($P = 0.008$), tibia ash ($P < 0.0001$), and Ca ($P = 0.0003$) and P content ($P = 0.003$). A dietary Ca level at 4.9% significantly decreased the tibia weight, ash, and Ca and P content compared to that at 3.5% Ca. 25HyD substitution did not significantly improve tibia quality ($P > 0.05$). On the contrary, it significantly reduced tibia P content ($P = 0.0012$). No interactive effect of 25HyD × Ca was observed in tibia quality-related parameters.

**Table 7.7** Tibia bone quality in laying hens fed diets with three different levels of Ca and L-Trp from week 26 to week 29 of age[1]

| Main effects | Tibia weight, g | Tibia ash, % | Tibia Ca, % | Tibia P, % |
|---|---|---|---|---|
| Trp, % | | | | |
| 0.18 | 4.19[b] | 55.21[b] | 22.82[b] | 10.58[b] |
| 0.22 | 4.23[ab] | 56.77[a] | 23.72[a] | 10.75[ab] |
| 0.26 | 4.48[a] | 57.62[a] | 23.41[a] | 10.90[a] |
| SEM | 0.09 | 0.31 | 0.18 | 0.07 |
| Ca, % | | | | |
| 3.5 | 4.20 | 57.25[a] | 23.62 | 10.91[a] |
| 4.2 | 4.35 | 56.33[ab] | 23.33 | 10.70[ab] |
| 4.9 | 4.36 | 56.02[b] | 22.99 | 10.62[b] |
| SEM | 0.09 | 0.32 | 0.20 | 0.02 |
| *P* value | | | | |
| L-Trp | 0.023 | <.0001 | 0.005 | 0.005 |
| Ca | 0.354 | 0.027 | 0.102 | 0.015 |
| Trp × Ca | 0.973 | 0.815 | 0.516 | 0.744 |
| Trp dose response | | | | |
| Linear | 0.008 | <.0001 | 0.004 | 0.001 |
| Quadratic | 0.401 | 0.398 | 0.056 | 0.923 |

[a–c]Values with different superscripts within each column are significantly different ($P < 0.05$).
[1]n=8.

**Table 7.8** Tibia bone quality in laying hens fed diets with three different levels of Ca with or without a complete replacement of dietary vitamin $D_3$ (3000 IU/kg) with 25-hydroxycholecalciferol (25HyD, 75 μg/kg) from week 26 to week 29 of age[1]

| Main effects | Tibia weight, g | Tibia ash, % | Tibia Ca, % | Tibia P, % |
|---|---|---|---|---|
| Vitamin $D_3$ source | | | | |
| Vitamin $D_3$ | 4.35 | 56.33 | 23.33 | 10.70[b] |
| 25HyD | 4.27 | 57.06 | 23.51 | 10.93[a] |
| SEM | 0.07 | 0.32 | 0.19 | 0.06 |
| Ca, % | | | | |
| 3.5 | 4.10[b] | 55.07[c] | 22.64[b] | 10.63[b] |
| 4.2 | 4.29[ab] | 56.73[b] | 23.51[a] | 10.78[b] |
| 4.9 | 4.53[a] | 58.29[a] | 24.07[a] | 11.04[a] |
| SEM | 0.09 | 0.39 | 0.23 | 0.74 |
| *P* value | | | | |
| 25HyD | 0.450 | 0.109 | 0.510 | 0.012 |
| Ca | 0.008 | <.0001 | 0.0003 | 0.003 |
| 25HyD × Ca | 0.780 | 0.619 | 0.086 | 0.427 |

[a–c]Values with different superscripts within each column are significantly different ($P < 0.05$).
[1]n=8.

### 7.4.4 Ca homeostasis

Calcium homeostasis measurements including concentrations of serum total Ca, ionized Ca, $1,25(OH)_2D_3$, and PTH for Experiment 1 are shown in Table 7.9. There were significant main effects of Trp ($P = 0.01$) and Ca ($P < 0.0001$) on the serum total Ca, feeding more Trp up to 0.26% linearly ($P = 0.016$) and quadratically ($P = 0.024$) increased serum total Ca level compared to 0.18% and 0.22% Ca. However, serum ionized Ca, PTH, and $1,25(OH)_2D_3$ were not affected by the main effects of Trp and Ca or their interaction ($P > 0.05$).

Calcium homeostasis measurements for Experiment 2 are shown in Table 7.10. The dietary 25HyD substitution significantly increased serum total Ca compared with birds fed with vitamin $D_3$ ($P = 0.046$). Serum ionized Ca, PTH, and $1,25(OH)_2D_3$ remained unchanged in response to the main effects of vitamin $D_3$ type and dietary Ca or their interactive effect ($P > 0.05$).

**Table 7.9** Calcium homeostasis measurements in laying hens fed diets with three different levels of Ca and L-Trp from week 26 to week 29 of age[1]

| Main effects | Serum total Ca, mmol/L | Serum ionized Ca, mmol/L | Serum $1,25(OH)_2D_3$[2], pmol/L | Serum PTH[3], pg/mL |
|---|---|---|---|---|
| Trp, % | | | | |
| 0.18 | 5.94[b] | 1.23 | 519.05 | 168.93 |
| 0.22 | 5.63[b] | 1.25 | 520.07 | 161.40 |
| 0.26 | 7.11[a] | 1.27 | 524.15 | 150.20 |
| SEM | 0.31 | 0.02 | 8.97 | 9.93 |
| Ca, % | | | | |
| 3.5 | 5.09[b] | 1.22 | 524.87 | 170.47 |
| 4.2 | 6.28[a] | 1.26 | 528.47 | 161.73 |
| 4.9 | 7.31[a] | 1.26 | 509.93 | 148.33 |
| SEM | 0.31 | 0.02 | 9.27 | 9.33 |
| *P* value | | | | |
| L-Trp | 0.010 | 0.473 | 0.890 | 0.419 |
| Ca | <.0001 | 0.376 | 0.353 | 0.245 |
| Trp × Ca | 0.234 | 0.419 | 0.614 | 0.963 |
| Trp dose response | | | | |
| Linear | 0.016 | 0.259 | 0.677 | 0.195 |
| Quadratic | 0.024 | 0.905 | 0.902 | 0.881 |

[a–c]Values with different superscripts within each column are significantly different ($P < 0.05$).
[1]n=5.
[2]1,25-dihydroxycholecalciferol.
[3]Parathyroid hormone.

**Table 7.10** Calcium homeostasis measurements in laying hens fed diets with three different levels of Ca with or without a complete replacement of dietary vitamin $D_3$ (3000 IU/kg) with 25-hydroxycholecalciferol (25HyD, 75 μg/kg) from week 26 to week 29 of age[1]

| Main effects | Serum total Ca, mmol/L | Serum ionized Ca, mmol/L | Serum $1,25(OH)_2D_3$[2], pmol/L | Serum PTH[3], pg/mL |
|---|---|---|---|---|
| Vitamin $D_3$ source | | | | |
| Vitamin $D_3$ | 6.28[b] | 1.26 | 528.5 | 161.7 |
| 25HyD | 7.38[a] | 1.26 | 549.9 | 153.7 |
| SEM | 0.36 | 0.01 | 9.3 | 6.7 |
| Ca, % | | | | |
| 3.5 | 6.21 | 1.25 | 537.4 | 167.3 |
| 4.2 | 6.67 | 1.27 | 546.1 | 163.6 |
| 4.9 | 7.60 | 1.26 | 534.1 | 142.3 |
| SEM | 0.43 | 0.02 | 11.0 | 8.3 |
| *P* value | | | | |
| 25HyD | 0.046 | 0.974 | 0.118 | 0.412 |
| Ca | 0.101 | 0.761 | 0.787 | 0.093 |
| 25HyD × Ca | 0.285 | 0.446 | 0.091 | 0.834 |

[a–c]Values with different superscripts within each column are significantly different ($P < 0.05$).
[1]n=5.
[2]1,25-dihydroxycholecalciferol.
[3]Parathyroid hormone.

## 7.5 Discussion

CaSR plays a central role in Ca homeostasis. L-Trp as a CaSR positive allosteric modulator, activates CaSR in the presence of Ca (Conigrave et al., 2007). We were the first to investigate the interactive effects of Ca and L-Trp on egg production, eggshell quality, bone health and calcium homeostasis in Dekalb laying hens at a pre-peak laying stage. The main effect of Trp and Ca and the interactive effect of dietary Trp and Ca on performance, egg and eggshell quality, bone health, and calcium homeostasis were investigated in Experiment 1. Throughout the 4-week experimental period (birds from 26 to 29 weeks of age), we found that ADFI, BW, and egg mass were associated with dietary Trp level. The possible reason might be that, in addition to its role in body protein synthesis, Trp is also involved in serotonin and kynurenine metabolic pathways, which affect stress regulation, immune function, production performance, appetite, and feed consumption (Le Floc'h et al., 2011; Fouad et al., 2021). It has been reported that feed intake (FI) plateaus after the dietary Trp level meets the requirement of birds. In addition, decreased or deficient Trp levels have been shown to result in reduced FI (Russell and Harms, 1999; Peganova et al., 2003; Wen et al., 2019a; Sarsour et al., 2021). However, in this study, the low dietary Trp at 0.18% did not cause a significant decrease in FI, which was probably because 0.18% Trp was not much deficient to Dekalb White laying hens from 26 - 29 weeks of age. Peganova et al. (2003) found that dietary Trp down to 1 (g/kg diet) significantly decreased FI in Lohmann Brown layers from 31 - 37 weeks of age. Sarsour et al. (2021) reported that Trp intake down to 105 mg/day significantly decreased FI in W-36 laying hens from 22 - 34 weeks of age. In contrast, a dietary inclusion of 0.26% Trp significantly increased the ADFI compared to the recommended Trp level of 0.22%. Also, BW changed in agreement with FI. The result indicated that higher dietary Trp did showed beneficial effect on FI and BW gain in laying hens. Interestingly, the lowest Trp level at 0.18% contributed

to a higher egg mass compared to 0.22% Trp, which illustrated that a mild Trp deficiency could improve production performance. The importance of Ca in laying hens is well recognized. In the present study, 3.5% dietary Ca, which was lower than recommended level significantly decreased FI. However, the results were not consistent with previous reports that a low Ca level did not affect FI (Taher et al., 1984; An et al., 2016), or FI was depressed as dietary Ca levels increased (Hurwitz et al., 1969; Narváez-Solarte et al., 2006), as laying hens have a specific appetite for Ca (Wilkinson et al., 2011). The inconsistency might be due to the high inclusion level of insoluble poultry grit in the Ca-deficient basal diet. Consequently, lower FI led to low Ca intake and thereby decreasing BW, egg weight and mass.

The high quality of eggshells is fundamental to make a profit and ensure food safety in the egg industry (Kemps et al., 2006). Eggshell quality as reflected by eggshell weight, thickness, and breaking strength was significantly increased with Trp level increasing during only a 4-week period from 26 - 29 weeks of age, which illustrated that short-term dietary Trp manipulation affected Ca flows in laying hens. Similar to our results, previous studies have reported a significant increase in eggshell weight and thickness with increased dietary Trp levels (Khattak and Helmbrecht, 2019; Wen et al., 2019a). Also, the interaction between Trp and Ca was found in eggshell weight and thickness, suggesting that the combined application of Trp and Ca might show a synergistic effect on improving eggshell quality, and Trp level might mediate Ca effectiveness in the improvement of eggshell weight and thickness. Given these results, it may be necessary to reconsider Ca nutrition in laying hens in relation to their Trp levels and to explore the combined application of Trp and Ca at different laying stages to improve eggshell quality.

Dietary Trp at 0.26% increased tibia weight, ash, Ca, and P content compared to a 0.18%, but Trp at 0.26% did not affect these parameters compared with recommended dietary Trp at 0.22%.

These results may encourage further studies to explore the relationship between dietary Trp level and bone health in laying hens. Calcium retained in the body not only supports eggshell formation but also flows to plasma and bone stores in laying hens (Kebreab et al., 2009). Dietary Trp at 0.26% increased serum total Ca concentration in this study. These results may illustrate that the prior flow of extra Ca went to eggshell formation instead of Ca storage in the bone. Interestingly, the lower Ca level at 3.5% increased tibia ash and P content compared with those of diet at 4.2% Ca, which was similar to reports by Jiang et al. (2013) and An et al. (2016), showing that relatively low Ca level contributed to better tibia weight, ash, and density. The findings might give us a warning that simply increasing dietary Ca would have an adverse effect on bone health and mineral deposition in laying hens.

The positive effects of Trp on eggshell quality and tibia health and the interactive effect of Ca and Trp on the improvement of eggshell quality could be attributed to an active Ca metabolism in the body. The high level of serum total Ca indicated an active Ca circulation in laying hens and thereby facilitating Ca retention in both eggshell and bone health. In agreement with our results, Khattak and Helmbrecht (2019) reported that higher Trp increased Ca levels in the blood. Although laying hens presented a relatively high total serum Ca level, the ionized serum Ca concentration remained unchanged during the egg-laying period. This is likely because ionized Ca is the physiologically active form, and it is of clinical significance to be tightly controlled within a specific range (de Matos, 2008). This portion of extracellular Ca is subject to Ca homeostasis, and it is regulated through the interaction of PTH, calcitonin, and vitamin $D_3$ metabolites via CaSR, in response to varying demands (Diaz et al., 1997). Given the importance of PTH and $1,25(OH)_2D_3$ in Ca metabolism and Ca homeostasis, the unchanged serum ionized Ca, PTH, and $1,25(OH)_2D_3$ levels in this study might be attributed to two factors: 1) high sensitivity and absolute low

concentration of hormones in the body and 2) the serum ionized Ca concentration being within a normal range at the time of sample collection.

In this study, 25HyD was added to the diet in replacement of equivalent vitamin $D_3$. Whether or not 25HyD was substituted did not affect feed intake, body weight, or production performance, which was consistent with the findings reported by Keshavarz (2003) in laying hens 50 to 66 weeks of age. Also, Kakhki et al. (2019) found no impact of top-dressed 25HyD on feed intake and production performance in aged laying hens. Unlike our results, some previous studies have found that long-term 25HyD supplementation has a beneficial effect on egg production (Koreleski and Świątkiewicz, 2005; Chen et al., 2020), which suggests that dose and timing selection are crucial for making better use of 25HyD. Based on our results and these previous studies, long-term 25HyD supplementation may improve production performance during laying compared with the simply 25HyD substitution for equivalent vitamin $D_3$.

Although 25HyD significantly increased serum total Ca concentration, its effect on eggshell quality and tibia Ca deposition was not significant. Also, no interaction between 25HyD and Ca was found in eggshell quality, bone health, and Ca metabolism. The results were consistent with previous reports that 25HyD did not show a positive effect on eggshell and(or) bone quality (Roland and Harms, 1976; Keshavarz, 2003; do Nascimento et al., 2014; Kakhki et al., 2019). The results indicated that the effects of 25HyD on Ca metabolism and retention were limited in laying hens, which was probably because that recommended vitamin $D_3$ was adequate to maintain Ca homeostasis. Moreover, compared with the main effect of vitamin $D_3$ source, eggshell quality and tibia traits were more sensitive to Ca levels. Since the benefits of 25HyD on production performance, eggshell quality, and bone health were limited in this study, future research could

explore the use of higher levels of 25HyD or a combination of different sources of vitamin D3 at varying levels of dietary Ca.

In conclusion, the supplementation of L-Trp for a dietary Trp level of 0.26% increased ADFI and BW, but did not increase tibia weight, ash, Ca content, and P content compared with the recommended level at 0.22% Trp. The increase in serum total Ca concentration with 0.26% dietary Trp resulted in more Ca being utilized for eggshell formation, as demonstrated by the observed increase in relative eggshell weight, eggshell thickness, and breaking strength. Moreover, an interaction between Trp and Ca was found increasing level of Trp up to 0.26% and of Ca up to 4.9% resulted in the greatest relative eggshell weight and eggshell thickness. The main effect of 25HyD only increased serum total Ca level and tibia P content. Eggshell quality and tibia bone traits were affected mainly by Ca level instead of 25HyD substitution for vitamin $D_3$ in the diet. The results provided evidence for the combined application of Trp and Ca in improving egg production, eggshell quality, bone health, and Ca metabolism in laying hens. In the future, it is worth investigating the accurate doses of Trp and Ca for a better synergistic effect in laying hens with different strains at different laying stages.

# CHAPTER EIGHT: GENERAL DISCUSSION

It is well known that laying hens have a unique dynamic bone turnover due to the daily egg laying cycle with rapid bone turnover and calcium mobilization from bones for eggshell formation. Osteoporosis is therefore the main skeletal disorder in laying hens, which raises animal welfare concerns and results in poor eggshell quality (Fleming, 2008). Eggshell quality has a considerable impact on the profitability of the egg industry. Commercial layers utilize about 10% of their total body calcium volume daily in shell production (Kerschnitzki et al., 2014). Such an intensive transport mechanism imposes severe demands on calcium homeostasis. CaSR plays a central role in calcium homeostasis (Kallay, 2018), and it is also involved in therapeutic targets for calcium metabolism disorders in humans such as FHH and NSHPT (Brown et al., 1998). Therefore, the finding that calcium retention and utilization can be improved through mediating CaSR in laying hens is significant. However, studies on chicken CaSR are limited, and there is a need to comprehensively understand chicken CaSR from the beginning of process, and to provide accumulating evidence for the manipulation of calcium metabolism by mediating CaSR and VDR in laying hens.

In chapter four, evidence for the presence of CaSR and VDR in main calcium metabolism-related tissues including kidney, GIT, shell gland, and tibia in different laying stages was brought up. Calcium homeostasis is achieved by intestinal absorption, bone storage and resorption, and renal reabsorption in mammals (Kallay, 2018). In laying hens, the shell gland is a distinctive tissue that withdraws calcium for shell formation (Bar, 2008). The expression and presence of CaSR and VDR in the kidney, GIT, shell gland, and tibia indicate the foundation that CaSR and VDR could be manipulated for the desired calcium homeostasis in laying hens. Also, as many findings regarding human CaSR have been reported, it is worth comparing the difference and the similarity

between human and chicken CaSR to better understand the sequence, structure, distribution, and function. Chicken CaSR has 79% and 84% homology with human CaSR on the nucleotide and amino acid level, respectively (Diaz et al., 1997), suggesting that there is a high likelihood that chicken CaSR performs the same function and characteristics as human CaSR. In terms of distribution pattern, CaSR expression is high in the kidney and ileum, which is the same as CaSR distribution in mammals (Zhao et al., 2019). The main calcium absorption site is between the duodenum and upper ileum in chickens (Hurwitz and Bar, 1966), indicating that CaSR is independent from calcium digestion and absorption, and does not directly affect calcium transporters. VDR and the active form of vitamin $D_3$, $1,25(OH)_2D_3$, are important in calcium metabolism because many genes related to calcium transport metabolism have VDRE a sequence located in their promoter region, thereby inducing the transcription. These genes include CaSR and many calcium transporters such as calbindin $D_{9k}$, $D_{28k}$, and calcium ion channels (Proszkowiec-Weglarz and Angel, 2013). Therefore, understanding the distribution and localization of VDR is also conducive to regulating calcium absorption and calcium metabolism via CaSR.

Chapter four confirmed the presence of CaSR and VDR in laying hens and revealed their expression pattern in different tissues, which shows the feasibility and a theoretical basis to further explore the role of CaSR in laying hens. The first step is to screen potential modulators of CaSR and understand their modulation mechanisms. As CaSR is a receptor protein, it is difficult to investigate it directly in a live animal. To minimize the disturbance, we constructed an *in vitro* stable Flp-In™ 293 cell line overexpressing chicken CaSR to investigate its potential ligands and downstream G protein-coupled signaling cascades, as outlined in chapter five. Since the most potential for the application of CaSR modulators in feed supplements, the cost, safety,

functionality, effectiveness, etc. should be taken into consideration when screening CaSR ligands. Nutritional ligands such as aromatic amino acids and inorganic phosphate show their advantage to be selected as potential chicken CaSR modulators because 1) they are proven to be effective human CaSR positive allosteric modulators (PAMs) (Conigrave et al., 2000b) and negative allosteric modulators (NAMs) (Centeno et al., 2019); 2) they are essential nutrients that play vital physiological and biochemical roles in the animal body; 3) they are cheaper than artificial CaSR modulators such as NPS R-568; 4) their function and safe dose range are known, so the risks are controlled when using these modulators. Fortunately, L-Trp and inorganic phosphate are also confirmed to be chicken CaSR PAM and NAM, respectively, as shown in chapter five, which activate or block chicken CaSR by inducing different G protein-coupled signaling pathways. CaSR is a typical GPCR, which transmits extracellular signals across the plasma membrane via intracellular coupling with G proteins. According to the Gα subunit, they can be classified into four groups: $G_{q/11}$, $G_{i/o}$, $G_{12/13}$, and $G_s$. The dissociation of the Gα subunit from the βγ dimeric subunit initiates a cascade of downstream signaling pathways (Chakravarti et al., 2012). Different GPCR ligands result in "functional selectivity" or "biased agonism", which means that a specific ligand can selectively elicit one or more G protein-coupled signaling pathways and alter downstream cellular responses by preferentially stabilizing different active conformational states of the receptor (Wootten et al., 2018). Indeed, our results elucidate that biased agonism also exists in chicken CaSR. Both L-Trp and $PO_4^{3-}$ were biased to the $G\alpha_q$-mediated signaling pathway. This finding provides the information about how L-Trp and $PO_4^{3-}$ affect downstream signaling. In the future, it is also necessary to find the link between different signaling pathways to specific physiological and chemical functions so we might selectively control poultry performance parameters by manually applying different CaSR modulators to poultry diets. Moreover,

understanding the binding mode of CaSR to its ligands is conducive to categorizing similar modulators and investigating signaling efficacy (Furness et al., 2016) because the various ligands can stabilize the unique conformation of the CaSR after binding to the CaSR. Therefore, our results can guide the discovery of novel chicken CaSR ligands.

After confirming an effective chicken CaSR PAM and revealing the corresponding downstream signaling pathways and binding modes, we further investigated the potential application of these findings to chicken osteogenesis. It is well documented that CaSR is a potential therapeutic target in human osteoporosis (Marie, 2010) and CaSR PAM has promoted osteogenic differentiation of human MSCs (Di Tomo et al., 2013). In chapter six, we isolated MSCs from compact bones of broiler chicken and laying hens to investigate the dose effect of L-Trp on chicken MSC proliferation and osteogenic differentiation. We then then investigated the interactive effect of $1,25(OH)_2D_3$, $Ca^{2+}$, 5 mM L-Trp, and CaSR antagonist, NPS-2143 to reveal the regulation mechanism of L-Trp via CaSR during chicken MSC proliferation and osteogenic differentiation. The findings provide theoretical evidence that CaSR could be a potential target for regulating bone formation and remodeling in broilers and layers and broaden the application of L-Trp and the active form of vitamin $D_3$ to poultry skeletal disorders. Additionally, it is important for researchers to consider factors such as dosage, treatment duration, and production stages when conducting animal trials. The comparative study in both broiler and layer MSC elucidates the differences and similarities during broiler and layer MSC proliferation and osteogenic differentiation. In terms of osteogenesis markers, the degree of 14-day differentiation in broiler MSCs was similar to 7-day differentiation in layer MSCs, which might suggest that layer MSCs differentiation was faster than that for broiler MSCs. Although the osteogenic differentiation in the boiler or layer MSCs was not synchronized, the presence of both results may provide standards for each other to compare, which

helps us better understand the process of chicken MSC osteogenic differentiation. Therefore, to investigate the temporal sequence of chicken MSC osteogenesis at a shorter time interval at various doses of CaSR modulators may be helpful to illustrate the underlying mechanism.

Furthermore, based on our cell culture results, we designed and conducted a layer study in chapter seven to systemically investigate the interactive effect of calcium and L-Trp, and 25-hydroxycholecalciferol (25HyD) substitution for vitamin $D_3$ on production performance, eggshell quality, bone health, and calcium homeostasis in laying hens. L-Trp is a CaSR allosteric modulator that binds to allosteric sites on CaSR and requires the presence of $Ca^{2+}$ to activate CaSR concertedly (Saidak et al., 2009). Thus, for a better application of L-Trp in practical production, we also need to consider dietary calcium levels. Calcium metabolism affects eggshell quality and bone health (de Matos, 2008). Dietary Trp at 0.26% increased serum total calcium concentration, resulting in more calcium being directed towards eggshell formation. This was supported by the observed increase in relative eggshell weight, eggshell thickness, and breaking strength. Furthermore, we found an interaction between Trp and Ca levels, where Ca continued to improve the relative eggshell weight and eggshell thickness as the Trp level increased. These results support the use of L-Trp in improving eggshell quality in laying hens. However, more studies should be conducted to find the most effective Trp and calcium concentrations when applying it to layer diets. $1,25(OH)_2D_3$ regulates CaSR transcription (Hendy et al., 2013). 25HyD is the most active precursor for $1,25(OH)_2D_3$, which is 2- to 4-fold more effective than vitamin $D_3$ in chicken diets (Soares et al., 1995). Also, the cost of 25HyD is more competitive compared to $1,25(OH)_2D_3$, and it has been commercialized and applied in poultry diets. However, our study did not find a positive effect of simply replacing vitamin $D_3$ with 25HyD at different levels of calcium on egg production, eggshell quality, bone health, and calcium metabolism, despite the crosstalk between the vitamin

D system and calcium homeostasis being a heavily researched topic in laying hens. Overall, L-Trp or combined supplementation of L-Trp and calcium showed a positive effect on eggshell quality, bone health, and calcium metabolism in laying hens. In the future, we are considering carrying out a broiler study to verify the interactive effect of L-Trp and calcium on bone formation and remodeling as broilers also experience skeletal disorders during their lifespan.

Inorganic phosphate was proved to be a NAM of cCaSR in chapter five, but it was regrettable that the effect of inorganic phosphate on production performance, eggshell quality, bone health, and calcium homeostasis was not investigated *in vivo* in this thesis because of thecalcium and phosphate association and the interdependence of Ca and phosphate in Ca metabolism. In the future, we need to bring up a considerate experimental design and find a more suitable phosphate ingredient for diet formulation when investigating the effect of inorganic phosphate in laying hens.

# CHAPTER NINE: SUMMARY AND FUTURE STUDIES

## 9.1 Summary

The major findings that can be drawn from the present research are:

1) The chicken CaSR shares a high similarity with the human CaSR regarding protein structure.
2) The chicken CaSR and VDR are widely distributed in the kidney, gastrointestinal tract, shell gland, and tibia of laying hens at different laying stages.
3) Relative expression of chicken CaSR and VDR varies in different tissues but is not significantly changed among different laying stages.
4) Like human CaSR, L-tryptophan and inorganic phosphate are also cCaSR modulators, acting as positive and negative allosteric modulators, respectively. Both L-tryptophan and $PO_4^{3-}$ are biased to the $G\alpha_q$-mediated signaling pathway.
5) There is one binding site for L-Trp and two binding sites for $PO_4^{3-}$ in the ECD of chicken CaSR, and the confirmed binding site of L-Trp and predicted binding sites $PO_4^{3-}$ to chicken CaSR are similar to the results in the human CaSR.
6) CaSR and VDR were expressed in broiler and layer MSCs.
7) Osteogenic differentiation in layer MSCs was faster than that in broiler MSCs. 5 mM L-Trp promoted osteogenic differentiation of MSCs at an early stage. 1 nM $1,25(OH)_2D_3$ promoted proliferation instead of facilitating the differentiation and mineralization process in chicken MSCs.
8) Increased dietary Trp level (0.26%) improved the serum calcium level, eggshell quality, and tibia traits, and the combined application of Trp and calcium showed an interactive effect that calcium kept improving the relative eggshell weight and eggshell thickness as

Trp level increased. However, the 25HyD substitution for vitamin $D_3$ did not increase egg production, eggshell quality, bone health.

**9.2 Future studies**

This thesis demonstrates the importance of chicken CaSR and VDR in maintaining the desired calcium homeostasis and mediating calcium metabolism-related disorders in laying hens. Although these studies showed the potential value of CaSR modulators and different sources of vitamin D in practical production, there are many unknown areas that still need to be explored:

1) The relationship between different G protein-coupled signaling pathways and the corresponding physiological and biochemical functions in laying hens.
2) The effect of CaSR modulators (at various doses) on the temporal sequence of osteogenesis.
3) The accurate doses of Trp and Ca for a better synergistic effect on eggshell quality and bone health in laying hens with different strains at different laying stages.
4) The effects of inorganic phosphate on production performance, eggshell quality, bone health, and calcium homeostasis, or even the prevention and alleviation of calcium metabolism-related disorders in laying hens regarding CaSR inhibition.

## CHAPTER TEN: LITERATURE CITED


Abukawa, H., H. Mano, T. Arakawa, Y. Hakeda, H. Kimura, and M. Kumegawa. 2001. Tissue specific expression and differential regulation by 1α, 25-dihydroxyvitamin $D_3$ of the calcium-sensing receptor (CaSR) gene in rat kidney, intestine, and calvaria. Cytotechnology 35:81-86. doi:10.1023/A:1008140204836

Adhikari, R., C. Chen, E. Waters, F. D. West, and W. K. Kim. 2019. Isolation and differentiation of mesenchymal stem cells from broiler chicken compact bones. Front. Physiol. 9:1892. doi:10.3389/fphys.2018.01892

Ahmad, H. A., S. Yadalam, and D. Roland Sr. 2003. Calcium requirements of Bovanes hens. Int. J. Poult. Sci 2(6):417-420. doi:10.3923/ijps.2003.417.420

Aida, K., S. Koishi, M. Inoue, M. Nakazato, M. Tawata, and T. Onaya. 1995. Familial hypocalciuric hypercalcemia associated with mutation in the human $Ca^{(2+)}$-sensing receptor gene. J. Clin. Endocrinol. Metab. 80(9):2594-2598. doi:10.1210/jcem.80.9.7673400

Al-Batshan, H., S. Scheideler, B. Black, J. Garlich, and K. Anderson. 1994. Duodenal calcium uptake, femur ash, and eggshell quality decline with age and increase following molt. Poult. Sci. 73(10):1590-1596. doi:10.3382/ps.0731590

Al-Dujaili, S. A., A. J. Koh, M. Dang, X. Mi, W. Chang, P. X. Ma, and L. K. McCauley. 2016. Calcium sensing receptor function supports osteoblast survival and acts as a co-factor in PTH anabolic actions in bone. J. Cell. Biochem. 117(7):1556-1567. doi:10.1002/jcb.25447

Almeida Paz, I.C.L., A.A. Mendes, R.R. Quinterio, L.C. Vulcano, S.E. Takahashi, R.G. Garcia, C.M. Komiyama, A. Balog, K. Pelicia, F.S. Wescheler, and P.S.O. Scudeller. 2006. Bone mineral density of tibae and femura of broiler breeders: growth, development and production. Braz. J. Poult. Sci. 8:75-82. doi:10.1590/S1516-635X2006000200002

An, S. H., D. W. Kim, and B. K. An. 2016. Effects of dietary calcium levels on productive performance, eggshell quality and overall calcium status in aged laying hens. Asian-Australas. J. Anim. Sci. 29(10):1477-1482. doi:10.5713/ajas.15.0655

AOAC. 2005. Official methods of analysis of AOAC International. 18th ed Gaithersburg. AOAC International: Rockville, MD, USA.

Arthur, J. M., G. P. Collinsworth, T. W. Gettys, L. D. Quarles, and J. R. Raymond. 1997. Specific coupling of a cation-sensing receptor to G protein alpha-subunits in MDCK cells. Am. J. Physiol. - Renal Physiol. 273(1):F129-F135. doi:10.1152/ajprenal.1997.273.1.F129

Awata, H., C. Huang, M. E. Handlogten, and R. T. Miller. 2001. Interaction of the calcium-sensing receptor and filamin, a potential scaffolding protein. J. Biol. Chem. 276(37):34871-34879. doi:10.1074/jbc.M100775200

Ba, J., and P. A. Friedman. 2004. Calcium-sensing receptor regulation of renal mineral ion transport. Cell calcium 35(3):229-237. doi:10.1016/j.ceca.2003.10.016

Bai, C., L. Hou, Y. Ma, L. Chen, M. Zhang, and W. Guan. 2013. Isolation and characterization of mesenchymal stem cells from chicken bone marrow. Cell Tissue Bank 14(3):437-451. doi:10.1007/s10561-012-9347-8

Bai, M., N. Janicic, S. Trivedi, S. J. Quinn, D. E. Cole, E. M. Brown, and G. N. Hendy. 1997. Markedly reduced activity of mutant calcium-sensing receptor with an inserted Alu element from a kindred with familial hypocalciuric hypercalcemia and neonatal severe hyperparathyroidism. J. Clin. Investig. 99(8):1917-1925. doi:10.1172/JCI119359

Bai, M., H. Liu, K. Xu, A. O. Oso, X. Wu, G. Liu, M.C.B. Tossou, N.A. Al-Dhabi, V. Duraipandiyan, Q. Xi, and Y. Yin. 2017. A review of the immunomodulatory role of

dietary tryptophan in livestock and poultry. Amino Acids 49(1):67-74. doi:10.1007/s00726-016-2351-8

Bai, M., S. Trivedi, C. R. Lane, Y. Yang, S. J. Quinn, and E. M. Brown. 1998. Protein kinase C phosphorylation of threonine at position 888 in $Ca^{2+}$o-sensing receptor (CaR) inhibits coupling to $Ca^{2+}$ store release. J. Biol. Chem. 273(33):21267-21275. doi:10.1074/jbc.273.33.21267

Baker, A. R., D. P. McDonnell, M. Hughes, T. M. Crisp, D. J. Mangelsdorf, M. R. Haussler, J. W. Pike, J. Shine, and B. W. O'Malley. 1988. Cloning and expression of full-length cDNA encoding human vitamin D receptor. Proc. Natl. Acad. Sci. 85(10):3294-3298. doi: 10.1073/pnas.85.10.3294

Bar, A. 2008. Calcium homeostasis and vitamin D metabolism and expression in strongly calcifying laying birds. Comp. Biochem. Physiol., Part A: Mol. Integr. Physiol. 151(4):477-490. doi:10.1016/j.cbpa.2008.07.006

Bar, A. 2008. Calcium transport in strongly calcifying laying birds: Mechanisms and regulation. Comp. Biochem. Phys. A. 152(4):447-469. doi:10.1016/j.cbpa.2008.11.020

Bar, A., M. Shani, C. S. Fullmer, M. E. Brindak, and S. Striem. 1990. Modulation of chick intestinal and renal calbindin gene expression by dietary vitamin $D_3$, 1,25-dihydroxyvitamin $D_3$, calcium and phosphorus. Mol. Cell. Endocrinol. 72(1):23-31. doi:10.1016/0303-7207(90)90236-2

Bar, A., V. Razaphkovsky, and E. Vax. 2002. Re-evaluation of calcium and phosphorus requirements in aged laying hens. Br. Poult. Sci. 43(2):261-269. doi: 10.1080/00071660120121481

Bar, A., S. Striem, E. Vax, H. Talpaz, and S. Hurwitz. 1992. Regulation of calbindin mRNA and calbindin turnover in intestine and shell gland of the chicken. Am. J. Physiol. - Regul. Integr. Comp. Physiol. 262(5):R800-R805. doi:10.1152/ajpregu.1992.262.5.R800

Barker, N. 2008. The canonical Wnt/β-catenin signalling pathway. In Vincan, E. (eds) Wnt Signaling, Methods in Molecular Biology™, pp. 5-15, Humana Press. doi:10.1007/978-1-59745-249-6_1

Barradas, A. M., H. A. Fernandes, N. Groen, Y. C. Chai, J. Schrooten, J. Van de Peppel, J. P. Van Leeuwen, C. A. Van Blitterswijk, and J. De Boer. 2012. A calcium-induced signaling cascade leading to osteogenic differentiation of human bone marrow-derived mesenchymal stromal cells. Biomaterials 33(11):3205-3215. doi:10.1016/j.biomaterials.2012.01.020

Bello, A., and D. R. Korver. 2019. Long-term effects of *Buttiauxella* sp. phytase on performance, eggshell quality, apparent ileal Ca and P digestibility, and bone properties of white egg layers. Poult. Sci. 98(10):4848-4859. doi:10.3382/ps/pez220

Berry, J., C. Farquharson, C. Whitehead, and E. Mawer. 1996. Growth plate chondrocyte vitamin D receptor number and affinity are reduced in avian tibial dyschondroplastic lesions. Bone 19(2):197-203. doi:10.1016/8756-3282(96)00171-8

Bilezikian, J. P., L. G. Raisz, and T. J. Martin (eds.). 2008. Principles of bone biology. Academic press. doi:10.1016/B978-0-12-373884-4.X0001-8

Binmahfouz, L. S., P. P. Centeno, A. D. Conigrave, and D. T. Ward. 2019. Identification of serine-875 as an inhibitory phosphorylation site in the calcium-sensing receptor. Mol. Pharmacol. 96(2):204-211. doi:10.1124/mol.119.116178

Birkl, P., J. Chow, P. McBride, J. B. Kjaer, W. Kunze, P. Forsythe, and A. Harlander-Matauschek. 2019. Effects of acute tryptophan depletion on repetitive behavior in laying hens. Front. Vet. Sci. 6:230. doi:10.3389/fvets.2019.00230

Block, G. A., K. J. Martin, A. L. De Francisco, S. A. Turner, M. M. Avram, M. G. Suranyi, G. Hercz, J. Cunningham, A. K. Abu-Alfa, and P. Messa. 2004. Cinacalcet for secondary hyperparathyroidism in patients receiving hemodialysis. N. Engl. J. Med. 350(15):1516-1525. doi:10.1056/NEJMoa031633

Brennan, S. C., and A. D. Conigrave. 2009. Regulation of cellular signal transduction pathways by the extracellular calcium-sensing receptor. Curr. Pharm. Biotechnol. 10(3):270-281. doi:10.2174/138920109787847484

Brister Jr, R., S. Linton, and C. Creger. 1981. Effects of dietary calcium sources and particle size on laying hen performance. Poult. Sci. 60(12):2648-2654. doi:10.3382/ps.0602648

Bronner, F. 2003. Mechanisms of intestinal calcium absorption. J. Cell. Biochem. 88(2):387-393. doi:10.1002/jcb.10330

Bronner, F. 2009. Recent developments in intestinal calcium absorption. Nutr. Rev. 67(2):109-113. doi:10.1111/j.1753-4887.2008.00147.x

Brown, E. M. 2007. Clinical lessons from the calcium-sensing receptor. Nat. Clin. Pract. Endocrinol. Metab. 3(2):122-133. doi:10.1038/ncpendmet0388

Brown, E. M., G. El-Hajj Fuleihan, C. J. Chen, and O. Kifor. 1990. A comparison of the effects of divalent and trivalent cations on parathyroid hormone release, 3′,5′-cyclic-adenosine monophosphate accumulation, and the levels of inositol phosphates in bovine parathyroid cells. Endocrinology 127(3):1064-1071. doi: 10.1210/endo-127-3-1064

Brown, E. M., G. Gamba, D. Riccardi, M. Lombardi, R. Butters, O. Kifor, A. Sun, M. A. Hediger, J. Lytton, and S. C. Hebert. 1993. Cloning and characterization of an extracellular $Ca^{2+}$-sensing receptor from bovine parathyroid. Nature 366(6455):575-580. doi:10.1038/366575a0

Brown, E. M., D. G. Gardner, M. F. Brennan, S. J. Marx, A. M. Spiegel, M. F. Attie, R. W. Downs, Jr., J. L. Doppman, and G. D. Aurbach. 1979a. Calcium-regulated parathyroid hormone release in primary hyperparathyroidism: Studies in vitro with dispersed parathyroid cells. Am. J. Med. 66(6):923-931. doi:10.1016/0002-9343(79)90446-7

Brown, E. M., D. G. Gardner, R. A. Windeck, S. Hurwitz, M. F. Brennan, and G. D. Aurbach. 1979b. β-adrenergically stimulated adenosine 3′,5′-monophosphate accumulation in and parathyroid hormone release from dispersed human parathyroid cells. J. Clin. Endocrinol. Metab. 48(4):618-626. doi: 10.1210/jcem-48-4-618

Brown, E. M., S. Hurwitz, and G.D. Aurbach. 1977. Beta-adrenergic stimulation of cyclic AMP content and parathyroid hormone release from isolated bovine parathyroid cells. Endocrinology 100(6):1696-1702. doi:10.1210/endo-100-6-1696

Brown, E. M., and R. J. MacLeod. 2001. Extracellular calcium sensing and extracellular calcium signaling. Physiol. Rev. 81:239-297. doi:10.1152/physrev.2001.81.1.239

Brown, E. M., M, M. Pollak, Martin, and M. Hebert, Steven C. 1998. The extracellular calcium-sensing receptor: its role in health and disease. Annu. Rev. Med. 49(1):15-29. doi:10.1146/annurev.med.49.1.15

Buchan, A. M., P. E. Squires, M. Ring, and R. M. Meloche. 2001. Mechanism of action of the calcium-sensing receptor in human antral gastrin cells. Gastroenterology 120(5):1128-1139. doi:10.1053/gast.2001.23246

Busque, S. M., J. E. Kerstetter, J. P. Geibel, and K. Insogna. 2005. L-type amino acids stimulate gastric acid secretion by activation of the calcium-sensing receptor in parietal cells. Am. J. Physiol. - Gastrointest. Liver Physiol. 289(4):G664-G669. doi: 10.1152/ajpgi.00096.2005

Butters Jr, R. R., N. Chattopadhyay, P. Nielsen, C. P. Smith, A. Mithal, O. Kifor, M. Bai, S. Quinn, P. Goldsmith, and S. Hurwitz. 1997. Cloning and characterization of a calcium‐sensing receptor from the hypercalcemic New Zealand white rabbit reveals unaltered responsiveness to extracellular calcium. J. Bone Miner. Res. 12(4):568-579. doi:10.1359/jbmr.1997.12.4.568

Cai, Q., J. S. Chandler, R. H. Wasserman, R. Kumar, and J. T. Penniston. 1993. Vitamin D and adaptation to dietary calcium and phosphate deficiencies increase intestinal plasma membrane calcium pump gene expression. Proc. Natl. Acad. Sci. 90(4):1345-1349. doi:10.1073/pnas.90.4.134

Campbell, A. P., and A. V. Smrcka. 2018. Targeting G protein-coupled receptor signalling by blocking G proteins. Nat. Rev. Drug Discovery doi: 10.1038/nrd.2018.135

Canaff, L., and G. N. Hendy. 2002. Human calcium-sensing receptor gene Vitamin D response elements in promoters P1 and P2 confer transcriptional responsiveness to 1,25-dihydroxyvitamin D. J. Biol. Chem. 277(33):30337-30350. doi:10.1074/jbc.M201804200

Caplan, A. I. 1991. Mesenchymal stem cells. J. Orthop. Res. 9(5):641-650. doi:10.1002/jor.1100090504

Cardoso, A. S., F. G. P. Costa, J. H. Vilar da Silva, E. P. Saraiva, E. T. Nogueira, C. S. Santos, M. Ramalho de Lima, and D. V. G. Vieira. 2014. Nutritional requirement of digestible tryptophan for white-egg layers of 60 to 76 weeks of age. J. Appl. Poult. Res. 23(4):729-734. doi:10.3382/japr.2014-01012

Caride, A. J., E. N. Chini, S. Homma, T. P. Dousa, and J. T. Penniston. 1998. mRNAs Coding for the calcium–sensing receptor along the rat nephron: effect of a low–phosphate diet. Kidney Blood Pressure Res. 21(5):305-309. doi:10.1159/000025886

Carrillo-López, N., J. L. Fernández-Martín, D. Álvarez-Hernández, I. González-Suárez, P. Castro-Santos, P. Román-García, J. M. López-Novoa, and J. B. Cannata-Andía. 2010. Lanthanum activates calcium-sensing receptor and enhances sensitivity to calcium. Nephrol., Dial., Transplant. 25(9):2930-2937. doi:10.1093/ndt/gfq124

CCAC. 2009. Guidelines on the care and use of farm animals in research, teaching and testing. Pages 1–168. Canadian Council on Animal Care, Ottawa, ON, Canada. Accessed Mar. 2018. https://www.ccac.ca/Documents/Standards/Guidelines/Farm Animals.pdf.

Centeno, P. P., A. Herberger, H.-C. Mun, C. Tu, E. F. Nemeth, W. Chang, A. D. Conigrave, and D. T. Ward. 2019. Phosphate acts directly on the calcium-sensing receptor to stimulate parathyroid hormone secretion. Nat. Commun. 10(1):1-12. doi: 10.1038/s41467-019-12399-9

Centeno, V., G. Picotto, A. Pérez, A. Alisio, and N. T. de Talamoni. 2011. Intestinal $Na^{+}/Ca^{2+}$ exchanger protein and gene expression are regulated by $1,25(OH)_2D_3$ in vitamin D-deficient chicks. Arch. Biochem. Biophys. 509(2):191-196. doi:10.1016/j.abb.2011.03.011

Chakrabarty, S., V. Radjendirane, H. Appelman, and J. Varani. 2003. Extracellular calcium and calcium sensing receptor function in human colon carcinomas: promotion of E-cadherin expression and suppression of β-catenin/TCF activation. Cancer Res. 63(1):67-71. doi:10.1063/1/67/509893

Chakravarti, B., N. Chattopadhyay, and E. M. Brown. 2012. Signaling Through the Extracellular Calcium-Sensing Receptor (CaSR). Pages 103-142 in Calcium Signaling. M. S. Islam ed. Springer, Dordrecht, Netherlands. doi:10.1007/978-94-007-2888-2_5

Chang, W., T.-H. Chen, S. Pratt, and D. Shoback. 2000. Amino acids in the second and third intracellular loops of the parathyroid $Ca^{2+}$-sensing receptor mediate efficient coupling to phospholipase C. J. Biol. Chem. 275(26):19955-19963. doi:10.1074/jbc.M909613199

Chang, W., S. Pratt, T.-H. Chen, L. Bourguignon, and D. Shoback. 2001. Amino acids in the cytoplasmic C terminus of the parathyroid $Ca^{2+}$-sensing receptor mediate efficient cell-surface expression and phospholipase C activation. J. Biol. Chem. 276(47):44129-44136. doi:10.1074/jbc.M104834200

Chattopadhyay, N. 2006. Effects of calcium-sensing receptor on the secretion of parathyroid hormone-related peptide and its impact on humoral hypercalcemia of malignancy. Am. J. Physiol. - Endocrinol. Metab. 290(5):E761-E770. doi:10.1152/ajpendo.00350.2005

Chattopadhyay, N., I. Cheng, K. Rogers, D. Riccardi, A. Hall, R. Diaz, S. C. Hebert, D. I. Soybel, and E. M. Brown. 1998. Identification and localization of extracellular $Ca^{2+}$-sensing receptor in rat intestine. Am. J. Physiol. - Gastrointest. Liver Physiol. 274(1):G122-G130. doi:10.1152/ajpgi.1998.274.1.G122

Chattopadhyay, N., S. J. Quinn, O. Kifor, C. Ye, and E. M. Brown. 2007. The calcium-sensing receptor (CaR) is involved in strontium ranelate-induced osteoblast proliferation. Biochem. Pharmacol. 74(3):438-447. doi:10.1016/j.bcp.2007.04.020

Chattopadhyay, N., S. Yano, J. Tfelt-Hansen, P. Rooney, D. Kanuparthi, S. Bandyopadhyay, X. Ren, E. Terwilliger, and E. M. Brown. 2004. Mitogenic action of calcium-sensing receptor on rat calvarial osteoblasts. Endocrinology 145(7):3451-3462. doi:10.1210/en.2003-1127

Chen, C., R. Adhikari, D. L. White, and W. K. Kim. 2021. Role of 1,25-dihydroxyvitamin $D_3$ on osteogenic differentiation and mineralization of chicken mesenchymal stem cells. Front. Physiol. 12(10) doi:10.3389/fphys.2021.479596

Chen, C., B. Turner, T. J. Applegate, G. Litta, and W. K. Kim. 2020. Role of long-term supplementation of 25-hydroxyvitamin $D_3$ on egg production and egg quality of laying hen. Poult. Sci. 99(12):6899-6906. doi:10.1016/j.psj.2020.09.020

Chen, C. J., J. V. Barnett, D. A. Congo, and E.M. Brown. 1989. Divalent cations suppress 3′,5′-adenosine monophosphate accumulation by stimulating a pertussis toxin-sensitive guanine nucleotide-binding protein in cultured bovine parathyroid cells. Endocrinology 124(1):233-239. doi:10.1210/endo-124-1-233

Chen, X., Y. Shen, M. He, F. Yang, P. Yang, F. Pang, W. He, Y. Cao, and Q. Wei 2019. Polydatin promotes the osteogenic differentiation of human bone mesenchymal stem cells by activating the BMP2-Wnt/β-catenin signaling pathway. Biomed. Pharmacother. 112:108746. doi:10.1016/j.biopha.2019.108746

Cheng, I., I. Qureshi, N. Chattopadhyay, A. Qureshi, R. R. Butters, A. E. Hall, R. R. Cima, K. V. Rogers, S. C. Hebert, and J. P. Geibel. 1999. Expression of an extracellular calcium-sensing receptor in rat stomach. Gastroenterology 116(1):118-126. doi:10.1016/S0016-5085(99)70235-0

Cheng, T. K., and C. N. Coon. 1990. Effect of Calcium Source, Particle Size, Limestone Solubility In Vitro, and Calcium Intake Level on Layer Bone Status and Performance. Poult. Sci. 69(12):2214-2219. doi:10.3382/ps.0692214

Choudhary, S., A. Kumar, R. K. Kale, L. G. Raisz, and C. C. Pilbeam. 2004. Extracellular calcium induces COX-2 in osteoblasts via a PKA pathway. Biochem. Biophys. Res. Commun. 322(2):395-402. doi:10.1016/j.bbrc.2004.07.129

Christakos, S., P. Dhawan, A. Porta, L. J. Mady, and T. Seth. 2011. Vitamin D and intestinal calcium absorption. Mol. Cell. Endocrinol. 347(1-2):25-29. doi:10.1016/j.mce.2011.05.038

Codazzi, F., M. N. Teruel, and T. Meyer. 2001. Control of astrocyte $Ca^{2+}$ oscillations and waves by oscillating translocation and activation of protein kinase C. Curr. Biol. 11(14):1089-1097. doi:10.1016/S0960-9822(01)00326-8

Common, R. 1943. Observations on the mineral metabolism of pullets. VII. The calcium requirement of the laying bird. J. Agric. Sci. 33(4):213-220. doi:10.1017/S0021859600007188

Conigrave, A. D. 2016. The calcium-sensing receptor and the parathyroid: past, present, future. Front. Physiol. 7:563. doi:10.3389/fphys.2016.00563

Conigrave, A. D., H. C. Mun, and H. C. Lok. 2007. Aromatic L-amino acids activate the calcium-sensing receptor. J. Nutr. 137(6):1524S-1527S. doi:10.1093/jn/137.6.1524S

Conigrave, A. D., S. J. Quinn, and E. M. Brown. 2000a. Cooperative multi-modal sensing and therapeutic implications of the extracellular $Ca^{2+}$ sensing receptor. Trends Pharmacol. Sci. 21(10):401-407. doi:10.1016/S0165-6147(00)01546-7

Conigrave, A. D., S. J. Quinn, and E. M. Brown. 2000b. L-amino acid sensing by the extracellular $Ca^{2+}$-sensing receptor. Proc. Natl. Acad. Sci. 97:4814-4819. doi:10.1073/pnas.97.9.4814

Conigrave, A. D., and D. T. Ward. 2013. Calcium-sensing receptor (CaSR): pharmacological properties and signaling pathways. Best Pract. Res. Clin. Endocrinol. Metab. 27(3):315-331. doi:10.1016/j.beem.2013.05.010

Corbetta, S., A. Lania, M. Filopanti, L. Vicentini, E. Ballaré, and A. Spada. 2002. Mitogen-Activated Protein Kinase Cascade in Human Normal and Tumoral Parathyroid Cells. J. Clin. Endocrinol. Metab. 87(5):2201-2205. doi:10.1210/jcem.87.5.8492

Cowieson, A., T. Acamovic, and M. Bedford. 2006. Phytic acid and phytase: implications for protein utilization by poultry. Poult. Sci. 85(5):878-885. doi:10.1093/ps/85.5.878

Cramer, C., and D. Copp. 1959. Progress and rate of absorption of radiostrontium through intestinal tracts of rats. Proc. Soc. Exp. Biol. Med. 102(2):514-517. doi:10.3181/00379727-102-25301

Cufadar, Y., O. Olgun, and A. Yildiz. 2011. The effect of dietary calcium concentration and particle size on performance, eggshell quality, bone mechanical properties and tibia mineral contents in moulted laying hens. Br. Poult. Sci. 52(6):761-768. doi:10.1080/00071668.2011.641502

Czekanska, E., M. Stoddart, R. Richards, and J. Hayes. 2012. In search of an osteoblast cell model for *in vitro* research. Eur. Cell Mater. 24(4):1-17. doi:10.22203/eCM.v024a01

Dacke, C. G. 2000. Chapter 18 - The Parathyroids, Calcitonin, and Vitamin D. In G. C. Whittow (ed), Sturkie's Avian Physiology (Fifth Edition), pp. 473-488, Academic Press.

de Jesus Ferreira, M. C., C. Héliès-Toussaint, M. Imbert-Teboul, C. Bailly, J.-M. Verbavatz, A.-C. Bellanger, and D. Chabardès. 1998. Co-expression of a $Ca^{2+}$-inhibitable adenylyl cyclase and of a $Ca^{2+}$-sensing receptor in the cortical thick ascending limb cell of the rat kidney. J. Biol. Chem. 273(24):15192-15202. doi:10.1074/jbc.273.24.15192

de Matos, R. 2008. Calcium Metabolism in Birds. Vet. Clin. North Am. Exot. Anim. Pract. 11(1):59-82. doi:10.1016/j.cvex.2007.09.005

DeLuca, H. F., M. Nakada, Y. Tanaka, R. Sicinski, and M. Phelps. 1988. The plasma binding protein for vitamin D is a site of discrimination against vitamin D-2 compounds by the chick. Biochim. Biophys. Acta - Gen. Subj. 965(1):16-21. doi:10.1016/0304-4165(88)90145-6

Dempster, D., R. Murrills, W. Horbert, and T. Arnett. 1987. Biological activity of chicken calcitonin: effects on neonatal rat and embryonic chick osteoclasts. J. Bone Miner. Res. 2(5):443-448. doi:10.1002/jbmr.5650020512

Den Dekker, E., J. G. Hoenderop, B. Nilius, and R. J. Bindels. 2003. The epithelial calcium channels, TRPV5 & TRPV6: from identification towards regulation. Cell Calcium 33(5):497-507. doi:10.1016/S0143-4160(03)00065-4

Deng, G., J. Bi, J. Qiao, G. He, B. Wu, M. Zhang, and N. Lv. 2010. Expression and tissue distribution of extracellular calcium-sensing receptor (CaSR) mRNA in chickens. Turk. J. Vet. Anim. Sci. 34(3):249-254. doi:10.3906/vet-0809-27

Di Tomo, P., C. Pipino, P. Lanuti, C. Morabito, L. Pierdomenico, V. Sirolli, M. Bonomini, S. Miscia, M. A. Mariggio, and M. Marchisio. 2013. Calcium sensing receptor expression in ovine amniotic fluid mesenchymal stem cells and the potential role of R-568 during osteogenic differentiation. PLoS One 8(9):e73816. doi:10.1371/journal.pone.0073816

Diaz, R., S. Hurwitz, N. Chattopadhyay, M. Pines, Y. Yang, O. Kifor, M. S. Einat, R. Butters, S. C. Hebert, and E. Brown. 1997. Cloning, expression, and tissue localization of the calcium-sensing receptor in chicken (*Gallus domesticus*). Am. J. Physiol. - Regul. Integr. Comp. Physiol. 273(3):R1008-R1016. doi:10.1152/ajpregu.1997.273.3.R1008

Do Nascimento, G. R., A. E. Murakami, A. F. Q. M. Guerra, I. C. Ospinas-Rojas, M. F. Z. Ferreira, and J. C. Fanhani. 2014. Effect of different vitamin D sources and calcium levels in the diet of layers in the second laying cycle. Braz. J. Poult. Sci. 16:37-42. doi:10.1590/1516-635x160237-42

Dong, X. Y., M. M. M. Azzam, W. Rao, D. Y. Yu, and X. T. Zou. 2012. Evaluating the impact of excess dietary tryptophan on laying performance and immune function of laying hens reared under hot and humid summer conditions. Br. Poult. Sci. 53(4):491-496. doi:10.1080/00071668.2012.719149

Dvorak, M. M., A. Siddiqua, D. T. Ward, D. H. Carter, S. L. Dallas, E. F. Nemeth, and D. Riccardi. 2004. Physiological changes in extracellular calcium concentration directly control osteoblast function in the absence of calciotropic hormones. Proc. Natl. Acad. Sci. 101(14):5140-5145. doi:10.1073/pnas.0306141101

Eastin Jr, W. C., and E. Spaziani. 1978. On the mechanism of calcium secretion in the avian shell gland (uterus). Biol. Reprod. 19(3):505-518. doi:10.1095/biolreprod19.3.505

Eliam, M., M. Basle, Z. Bouizar, J. Bielakoff, M. Moukhtar, and M. de Vernejoul. 1988. Influence of blood calcium on calcitonin receptors in isolated chick osteoclasts. J. Endocrinol. 119(2):243-NP. doi:10.1677/joe.0.1190243

Fenton, A., T. Martin, and G. Nicholson. 1994. Carboxyl‐terminal parathyroid hormone‐related protein inhibits bone resorption by isolated chicken osteoclasts. J. Bone Miner. Res. 9(4):515-519. doi:10.1002/jbmr.5650090411

Fisher, L. W., and H. Schraer. 1982. Keratan sulfate proteoglycan isolated from the estrogen-induced medullary bone in Japanese quail. Comp. Biochem. Phys. B. 72(2):227-232. doi:10.1016/0305-0491(82)90039-6

Fitzpatrick, L. A., M. L. Brandi, and G. D. Aurbach. 1986. Prostaglandin F2α and α-adrenergic agonists regulate parathyroid cell function via the inhibitory guanine nucleotide regulatory protein. Endocrinology 118(5):2115-2119. doi:10.1210/endo-118-5-2115

Fleming, R. H. 2008. Nutritional factors affecting poultry bone health: Symposium on 'Diet and bone health'. Proc. Nutr. Soc. 67(2):177-183. doi:10.1017/S0029665108007015

Fouad, A. M., H. K. El-Senousey, D. Ruan, S. Wang, W. Xia, and C. Zheng. 2021. Tryptophan in poultry nutrition: Impacts and mechanisms of action. J. Anim. Physiol. Anim. Nutr. 105(6):1146-1153. doi:10.1111/jpn.13515

Friesner, R. A., J. L. Banks, R. B. Murphy, T. A. Halgren, J. J. Klicic, D. T. Mainz, M. P. Repasky, E. H. Knoll, M. Shelley, and J. K. Perry. 2004. Glide: a new approach for rapid, accurate docking and scoring. 1. Method and assessment of docking accuracy. J. Med. Chem. 47(7):1739-1749. doi:10.1021/jm0306430

Fromigué, O., E. Haÿ, A. Barbara, C. Petrel, E. Traiffort, M. Ruat, and P. J. Marie. 2009. Calcium sensing receptor‐dependent and receptor‐independent activation of osteoblast replication and survival by strontium ranelate. J. Cell. Mol. Med. 13(8b):2189-2199. doi:10.1111/j.1582-4934.2008.00673.x

Fudge, N. J., and C. S. Kovacs. 2004. Physiological studies in heterozygous calcium sensing receptor (CaSR) gene-ablated mice confirm that the CaSR regulates calcitonin release *in vivo*. BMC physiol. 4(1):5. doi:10.1186/1472-6793-4-5

Fujita, H., K. Sugimoto, S. Inatomi, T. Maeda, M. Osanai, Y. Uchiyama, Y. Yamamoto, T. Wada, T. Kojima, and H. Yokozaki. 2008. Tight junction proteins claudin-2 and-12 are critical for vitamin D-dependent $Ca^{2+}$ absorption between enterocytes. Mol. Biol. Cell 19(5):1912-1921. doi:10.1091/mbc.e07-09-0973

Furness, S. G. B., Y.-L. Liang, C. J. Nowell, M. L. Halls, P. J. Wookey, E. Dal Maso, A. Inoue, A. Christopoulos, D. Wootten, and P. M. Sexton. 2016. Ligand-dependent modulation of G protein conformation alters drug efficacy. Cell 167(3):739-749. e711. doi:10.1016/j.cell.2016.09.021

Gabriella, M., and G. Menghi. 1994. The integrative segment of the quail *Coturnix coturnix japonica*. Occurrence and distribution of carbonic anhydrase and complex carbohydrates. J. Anat. 185(Pt 2):405. PMID: 7961146; PMCID: PMC1166770.

Gabusi, E., C. Manferdini, F. Grassi, A. Piacentini, L. Cattini, G. Filardo, E. Lambertini, R. Piva, N. Zini, and A. Facchini. 2012. Extracellular calcium chronically induced human osteoblasts effects: specific modulation of osteocalcin and collagen type XV. J. Cell. Physiol. 227(8):3151-3161. doi:10.1002/jcp.24001

Gal, A., T. Ridge, and T. Graves. 2010. Cloning and sequencing of the calcium-sensing receptor from the feline parathyroid gland. Domest. Anim. Endocrinol. 38(1):57-61. doi:10.1016/j.domaniend.2009.07.004

Gama, L., L. M. Baxendale-Cox, and G. E. Breitwieser. 1997. $Ca^{2+}$-sensing receptors in intestinal epithelium. Am. J. Physiol. - Cell Physiol. 273(4):C1168-C1175. doi:10.1152/ajpcell.1997.273.4.C1168

Gama, L., and G. E. Breitwieser. 1998. A Carboxyl-terminal Domain Controls the Cooperativity for Extracellular $Ca^{2+}$ Activation of the Human Calcium Sensing Receptor: a study with receptor-green fluorescent protein fusions. J. Biol. Chem. 273(45):29712-29718. doi: 10.1074/jbc.273.45.29712

Ganjigohari, S., N. Ziaei, A. Ramzani Ghara, and S. Tasharrofi. 2018. Effects of nanocalcium carbonate on egg production performance and plasma calcium of laying hens. J. Anim. Physiol. Anim. Nutr. 102(1):e225-e232. doi:10.1111/jpn.12731

Garfia, B., S. Cañadillas, A. Canalejo, F. Luque, E. Siendones, M. Quesada, Y. Almadén, E. Aguilera-Tejero, and M. Rodríguez. 2002. Regulation of parathyroid vitamin D receptor expression by extracellular calcium. J. Am. Soc. Nephrol. 13(12):2945-2952. doi:10.1097/01.ASN.0000037676.54018.CB

Garrett, J. E., I. V. Capuano, L. G. Hammerland, B. C. Hung, E. M. Brown, S. C. Hebert, E. F. Nemeth, and F. Fuller. 1995. Molecular cloning and functional expression of human parathyroid calcium receptor cDNAs. J. Biol. Chem. 270(21):12919-12925. doi:10.1074/jbc.270.21.12919

Gay, C. V., and W. J. Mueller. 1974. Carbonic anhydrase and osteoclasts: localization by labeled inhibitor autoradiography. Science 183(4123):432-434. doi:10.1126/science.183.4123.432

Gees, M., B. Colsoul, and B. Nilius. 2010. The role of transient receptor potential cation channels in $Ca^{2+}$ signaling. Cold Spring Harbor Perspect. Biol. 2(10):a003962. doi:10.1101/cshperspect.a003962

Geibel, J., K. Sritharan, R. Geibel, P. Geibel, J. S. Persing, A. Seeger, T. K. Roepke, M. Deichstetter, C. Prinz, and S. X. Cheng. 2006. Calcium-sensing receptor abrogates secretagogue-induced increases in intestinal net fluid secretion by enhancing cyclic nucleotide destruction. Proc. Natl. Acad. Sci. 103(25):9390-9397. doi:10.1073/pnas.0602996103

Geibel, J. P., and S. C. Hebert. 2009. The functions and roles of the extracellular $Ca^{2+}$-sensing receptor along the gastrointestinal tract. Annu. Rev. Physiol. 71:205-217. doi:10.1146/annurev.physiol.010908.163128

Geibel, J. P., C. A. Wagner, R. Caroppo, I. Qureshi, J. Gloeckner, L. Manuelidis, P. Kirchhoff, and K. Radebold. 2001. The stomach divalent ion-sensing receptor scar is a modulator of gastric acid secretion. J. Biol. Chem. 276(43):39549-39552. doi:10.1074/jbc.M107315200

Geng, Y., L. Mosyak, I. Kurinov, H. Zuo, E. Sturchler, T. C. Cheng, P. Subramanyam, A. P. Brown, S. C. Brennan, and H.-c. Mun. 2016. Structural mechanism of ligand activation in human calcium-sensing receptor. Elife 5:e13662. doi:10.7554/eLife.13662

Gesek, F. A., and P. A. Friedman. 1992. On the mechanism of parathyroid hormone stimulation of calcium uptake by mouse distal convoluted tubule cells. J. Clin. Invest. 90(3):749-758. doi:10.1172/jci115947

Glendenning, P., T. Ratajczak, R. L. Prince, N. Garamszegi, and E. E. Strehler. 2000. The promoter region of the human PMCA1 gene mediates transcriptional downregulation by 1, 25-dihydroxyvitamin $D_3$. Biochem. Biophys. Res. Commun. 277(3):722-728. doi:10.1006/bbrc.2000.3745

Godwin, S. L., and S. P. Soltoff. 1997. Extracellular calcium and platelet-derived growth factor promote receptor-mediated chemotaxis in osteoblasts through different signaling pathways. J. Biol. Chem. 272(17):11307-11312. doi:10.1074/jbc.272.17.11307

Godwin, S. L., and S. P. Soltoff. 2002. Calcium-sensing receptor-mediated activation of phospholipase C-γ1 is downstream of phospholipase C-β and protein kinase C in MC3T3-E1 osteoblasts. Bone 30(4):559-566. doi:10.1016/S8756-3282(01)00700-1

Gonnerman, W. A., W. K. Ramp, and S. U. Toverud. 1975. Vitamin D, dietary calcium and parathyroid hormone interactions in chicks. Endocrinology 96(2):275-281. doi:10.1210/endo-96-2-275

Gowen, M., G. B. Stroup, R. A. Dodds, I. E. James, B. J. Votta, B. R. Smith, P. K. Bhatnagar, A. M. Lago, J. F. Callahan, and E. G. DelMar. 2000. Antagonizing the parathyroid calcium receptor stimulates parathyroid hormone secretion and bone formation in osteopenic rats. J. Clin. Investig. 105(11):1595-1604. doi: 10.1172/JCI9038

Gregory, C. A., W. G. Gunn, A. Peister, and D. J. Prockop. 2004. An Alizarin red-based assay of mineralization by adherent cells in culture: comparison with cetylpyridinium chloride extraction. Anal. Biochem. 329(1):77-84. doi:10.1016/j.ab.2004.02.002

Griminger, P., and H. Lutz. 1964. Observations on the Voluntary Intake of Calcium Supplements by the Laying Hen. Poult. Sci. 43(3):710-716. doi:10.3382/ps.0430710

Grizzle, J., M. Iheanacho, A. Saxton, and J. Broaden. 1992. Nutritional and environmental factors involved in egg shell quality of laying hens. Br. Poult. Sci. 33(4):781-794. doi:10.1080/00071669208417520

Grunder, A., C. Tsang, and R. Narbatiz. 1990. Effects of vitamin $D_3$ metabolites on physiological traits of White Leghorn hens. Poult. Sci. 69(7):1204-1208. doi:10.3382/ps.0691204

Guo, S., C. Li, D. Liu, and Y. Guo. 2015. Inflammatory responses to a *Clostridium perfringens* type a strain and α-toxin in primary intestinal epithelial cells of chicken embryos. Avian Pathol. 44(2):81-91. doi:10.1080/03079457.2015.1005573

Halse, J., S. Greenspan, F. Cosman, G. Ellis, A. Santora, A. Leung, N. Heyden, S. Samanta, S. Doleckyj, and E. Rosenberg. 2014. A phase 2, randomized, placebo-controlled, dose-ranging study of the calcium-sensing receptor antagonist MK-5442 in the treatment of

postmenopausal women with osteoporosis. J. Clin. Endocrinol. Metab. 99(11):E2207-E2215. doi:10.1210/jc.2013-4009

Han, K.-H., J.-Y. Jung, J.-H. Cha, H. Kim, K. M. Madsen, and J. Kim. 2003. 1,25-Dihydroxyvitamin $D_3$ stimulates osteopontin expression in rat kidney. Nephron Physiol. 93(3):76-86. doi:10.1159/000069556.

Harms, R. 1992. A determination of the order of limitation of amino acids in a broiler breeder diet. J. Appl. Poul. Res. 1(4):410-414. doi:10.1093/japr/1.4.410.

Harrison, J. R., D. N. Petersen, A. C. Lichtler, A. T. Mador, D. W. Rowe, and B. E. Kream. 1989. 1, 25-Dihydroxyvitamin $D_3$ inhibits transcription of type I collagen genes in the rat osteosarcoma cell line ROS 17/2.8. Endocrinology 125(1):327-333. doi:10.1210/endo-125-1-327

Hart, M. J., X. Jiang, T. Kozasa, W. Roscoe, W. D. Singer, A. G. Gilman, P. C. Sternweis, and G. Bollag. 1998. Direct stimulation of the guanine nucleotide exchange activity of p115 RhoGEF by $G_{\alpha 13}$. Science 280(5372):2112-2114. doi:10.1126/science.280.5372.211

Härtel, H. 1990. Evaluation of the dietary interaction of calcium and phosphorus in the high producing laying hen. Br. Poult. Sci. 31(3):473-494. doi:10.1080/00071669008417280

Hebert, S. C. 1996. Extracellular calcium-sensing receptor: implications for calcium and magnesium handling in the kidney. Kidney Int. 50(6):2129-2139. doi:10.1038/ki.1996.539

Hebert, S. C., E. M. Brown, and H. W. Harris. 1997. Role of the $Ca^{(2+)}$-sensing receptor in divalent mineral ion homeostasis. J. Exp. Biol. 200(2):295-302. doi:10.1242/jeb.200.2.295

Hebert, S. C., S. Cheng, and J. Geibel. 2004. Functions and roles of the extracellular $Ca^{2+}$-sensing receptor in the gastrointestinal tract. Cell Calcium 35(3):239-247. doi:10.1016/j.ceca.2003.10.015

Hendy, G. N., and L. Canaff. 2016. Calcium-Sensing Receptor Gene: Regulation of Expression. Front. Physiol. 7(394) doi:10.3389/fphys.2016.00394

Hendy, G. N., L. Canaff, and D. E. C. Cole. 2013. The CASR gene: Alternative splicing and transcriptional control, and calcium-sensing receptor (CaSR) protein: Structure and ligand binding sites. Best Pract. Res. Clin. Endocrinol. Metab. 27(3):285-301. doi:10.1016/j.beem.2013.02.009

Hira, T., S. Nakajima, Y. Eto, and H. Hara. 2008. Calcium - sensing receptor mediates phenylalanine - induced cholecystokinin secretion in enteroendocrine STC - 1 cells. The FEBS J. 275(18):4620-4626. doi:10.1111/j.1742-4658.2008.06604.x

Hiyama, S., T. Sugiyama, and S. Kusuhara. 1998. Characteristics of the bone matrix formed by osteogenic cells isolated from embryonic chick calvaria and hen medullary bones. Jpn. Poult. Sci. 35(4):228-233. doi:10.2141/jpsa.35.228

Hiyama, S., T. Sugiyama, S. Kusuhara, and T. Uchida. 2005. Cellular and molecular phenotypes of osteogenic cells isolated from the medullary bone of the hen *in vitro*. Comp. Biochem. Physiol., Part B: Biochem. Mol. Biol. 142(4):419-425. doi:g/10.1016/j.cbpb.2005.09.006

Hjälm, G., R. J. MacLeod, O. Kifor, N. Chattopadhyay, and E. M. Brown. 2001. Filamin-A binds to the carboxyl-terminal tail of the calcium-sensing receptor, an interaction that participates in CaR-mediated activation of mitogen-activated protein kinase. J. Biol. Chem. 276(37):34880-34887. doi: 10.1074/jbc.M100784200

Hoenderop, J. G., R. Vennekens, D. Müller, J. Prenen, G. Droogmans, R. J. Bindels, and B. Nilius. 2001. Function and expression of the epithelial $Ca^{2+}$ channel family: comparison of mammalian ECaC1 and 2. J. Physiol. 537(3):747-761. doi:10.1111/j.1469-7793.2001.00747.x

Holmes, R. 1977. Purification, molecular properties and ontogeny of carbonic anhydrase isozymes: evidence for A, B and C isozymes in avian and mammalian tissues. Eur. J. Biochem. 78(2):511-520. doi:10.1111/j.1432-1033.1977.tb11764.x

Hu, J., G. Reyes-Cruz, P. K. Goldsmith, and A. M. Spiegel. 2001. The Venus's-flytrap and cysteine-rich domains of the human $Ca^{2+}$ receptor are not linked by disulfide bonds. J. Biol. Chem. 276(10):6901-6904. doi:10.1074/jbc.C000865200

Huang, C., M. E. Handlogten, and R. T. Miller. 2002. Parallel activation of phosphatidylinositol 4-kinase and phospholipase C by the extracellular calcium-sensing receptor. J. Biol. Chem. 277(23):20293-20300. doi:10.1074/jbc.M200831200

Huang, C., K. M. Hujer, Z. Wu, and R. T. Miller. 2004. The $Ca^{2+}$-sensing receptor couples to Gα12/13 to activate phospholipase D in Madin-Darby canine kidney cells. Am. J. Physiol. - Cell Physiol. 286(1):C22-C30. doi:10.1152/ajpcell.00229.2003

Huhtakangas, J. A., C. J. Olivera, J. E. Bishop, L. P. Zanello, and A. W. Norman. 2004. The vitamin D receptor is present in caveolae-enriched plasma membranes and binds 1α,25 $(OH)_2$-vitamin $D_3$ *in vivo* and in vitro. Mol. Endocrinol. 18(11):2660-2671. doi:10.1210/me.2004-0116

Hui, Q., E. Ammeter, S. Liu, R. Yang, P. Lu, L. Lahaye, and C. Yang. 2021. Eugenol attenuates inflammatory response and enhances barrier function during lipopolysaccharide-induced inflammation in the porcine intestinal epithelial cells. J. Anim. Sci. 98(8):skaa245. doi:10.1093/jas/skaa245

Hurwitz, S. 1989. Calcium homeostasis in birds. Vitam. Horm. 45(1989):173-221. doi:10.1016/S0083-6729(08)60395-7

Hurwitz, S., and A. Bar. 1966. Rate of Passage of Calcium-45 and Yttrium-91 along the Intestine, and Calcium Absorption in the Laying Fowl. J. Nutr. 89(3):311-316. doi:10.1093/jn/89.3.311

Hurwitz, S., S. Bornstein, and A. Bar. 1969. The Effect of Dietary Calcium Carbonate on Feed Intake and Conversion in Laying Hens. Poult. Sci. 48(4):1453-1456. doi:10.3382/ps.0481453

Hurwitz, S., and P. Griminger. 1962. Estimation of calcium and phosphorus requirement in laying hens by balance techniques. J. Sci. Food Agric. 13(3):185-191. doi:10.1002/jsfa.2740130308

Hurwitz, S., and N. T. Rand. 1965. Utilization of Calcium from Calcium Sulfate by Chicks and Laying Hens. Poult. Sci. 44(1):177-183. doi:10.3382/ps.0440177

Ishikawa, T., Y. Nakada-Moriya, C. Ando, N. Tanda, S. Nishida, Y. Minatogawa, and T. Nohnon. 1997. Expression of the JNK2-α1 Gene in the Developing Chick Brain. Biochem. Biophys. Res. Commun. 234(2):489-492. doi:10.1006/bbrc.1997.6140

Jensen, A. A., and H. Brauner-Osborne. 2007. Allosteric modulation of the calcium-sensing receptor. Curr. Neuropharmacol. 5(3):180-186. doi:10.2174/157015907781695982

Jiang, L. I., J. Collins, R. Davis, I. D. Fraser, and P. C. Sternweis. 2008. Regulation of cAMP responses by the G12/13 pathway converges on adenylyl cyclase VII. J. Biol. Chem. 283(34):23429-23439. doi:10.1074/jbc.M803281200

Jiang, S., L. Cui, C. Shi, X. Ke, J. Luo, and J. Hou. 2013. Effects of dietary energy and calcium levels on performance, egg shell quality and bone metabolism in hens. Vet. J. 198(1):252-258. doi:10.1016/j.tvjl.2013.07.017

MacLeod, R. J., S. Yano, N. Chattopadhyay, and E. M. Brown. 2004. Extracellular calcium-sensing receptor transactivates the epidermal growth factor receptor by a triple-membrane-spanning signaling mechanism. Biochem. Biophys. Res. Commun. 320(2):455-460. doi:10.1016/j.bbrc.2004.05.198

Jonchère, V., A. Brionne, J. Gautron, and Y. Nys. 2012. Identification of uterine ion transporters for mineralisation precursors of the avian eggshell. BMC physiol. 12(1):10. doi:10.1186/1472-6793-12-10

Justinich, C. J., N. Mak, I. Pacheco, D. Mulder, R. W. Wells, M. G. Blennerhassett, and R. J. MacLeod. 2008. The extracellular calcium-sensing receptor (CaSR) on human esophagus and evidence of expression of the CaSR on the esophageal epithelial cell line (HET-1A). Am. J. Physiol. - Gastrointest. Liver Physiol. 294(1):G120-G129. doi:10.1152/ajpgi.00226.2006

Kakhki, R. A., T. Heuthorst, A. Mills, M. Neijat, and E. Kiarie. 2019. Interactive effects of calcium and top-dressed 25-hydroxy vitamin $D_3$ on egg production, egg shell quality, and bones attributes in aged Lohmann LSL-lite layers. Poult. Sci. 98(3):1254-1262. doi:10.3382/ps/pey446

Kallay, E. 2018. Physiology and pathophysiology of the extracellular calcium-sensing receptor. Front. Physiol. 9:413. doi:10.3389/fphys.2018.00413/full

Kallay, E., O. Kifor, N. Chattopadhyay, E. M. Brown, M. G. Bischof, M. Peterlik, and H. S. Cross. 1997. Calcium-dependent c-mycProto-oncogene expression and proliferation of CACO-2 cells: a role for a luminal extracellular calcium-sensing receptor. Biochem. Biophys. Res. Commun. 232(1):80-83. doi:10.1006/bbrc.1997.6225

Kanatani, M., T. Sugimoto, M. Kanzawa, S. Yano, and K. Chihara. 1999. High extracellular calcium inhibits osteoclast-like cell formation by directly acting on the calcium-sensing receptor existing in osteoclast precursor cells. Biochem. Biophys. Res. Commun. 261(1):144-148. doi:10.1006/bbrc.1999.0932

Kawabata, S., R. Tsutsumi, A. Kohara, T. Yamaguchi, S. Nakanishi, and M. Okada. 1996. Control of calcium oscillations by phosphorylation of metabotropic glutamate receptors. Nature 383(6595):89-92. doi:10.1038/383089a0

Kebreab, E., J. France, R. Kwakkel, S. Leeson, H. D. Kuhi, and J. Dijkstra. 2009. Development and evaluation of a dynamic model of calcium and phosphorus flows in layers. Poult. Sci. 88(3):680-689. doi:10.3382/ps.2008-00157

Kemps, B., T. Govaerts, B. De Ketelaere, K. Mertens, F. Bamelis, M. Bain, E. Decuypere, and J. De Baerdemaeker. 2006. The influence of line and laying period on the relationship between different eggshell and membrane strength parameters. Poult. Sci. 85(7):1309-1317. doi:10.1093/ps/85.7.1309

Kenakin, T. P. 2009. '7TM Receptor Allostery: Putting Numbers to Shapeshifting Proteins. Trends Pharmacol. Sci. 30(9):460-469. doi:10.1016/j.tips.2009.06.007

Kerschnitzki, M., T. Zander, P. Zaslansky, P. Fratzl, R. Shahar, and W. Wagermaier. 2014. Rapid alterations of avian medullary bone material during the daily egg-laying cycle. Bone 69:109-117. doi:10.1016/j.bone.2014.08.019

Kerstetter, J. E., D. M. Caseria, M. E. Mitnick, A. F. Ellison, L. F. Gay, T. A. Liskov, T. O. Carpenter, and K. L. Insogna. 1997. Increased circulating concentrations of parathyroid hormone in healthy, young women consuming a protein-restricted diet. Am. J. Clin. Nutr. 66(5):1188-1196. doi:10.1093/ajcn/66.5.1188

Keshavarz, K. 2003. A comparison between cholecalciferol and 25-OH-cholecalciferol on performance and eggshell quality of hens fed different levels of calcium and phosphorus. Poult. Sci. 82(9):1415-1422. doi:10.1093/ps/82.9.1415

Ketta, M., and E. Tůmová. 2016. Eggshell structure, measurements, and quality-affecting factors in laying hens: a review. Czech J.Anim. Sci. 61(7):299-309. doi:10.17221/46/2015-CJAS

Khatri, M., T. D. O'Brien, and J. M. Sharma. 2009. Isolation and differentiation of chicken mesenchymal stem cells from bone marrow. Stem Cells Dev. 18(10):1485-1492. doi:10.1089/scd.2008.0223

Khattak, F., and A. Helmbrecht. 2019. Effect of different levels of tryptophan on productive performance, egg quality, blood biochemistry, and caecal microbiota of hens housed in enriched colony cages under commercial stocking density. Poult. Sci. 98(5):2094-2104. doi:10.3382/ps/pey562

Kifor, O., D. Congo, and E. M. Brown. 1990. Phorbol esters modulate the high $Ca^{2+}$-stimulated accumulation of inositol phosphates in bovine parathyroid cells. J. Bone Miner. Res. 5(10):1003-1011. doi:10.1002/jbmr.5650051003

Kifor, O., R. Diaz, R. Butters, I. Kifor, and E. M. Brown. 1998. The calcium-sensing receptor is localized in caveolin-rich plasma membrane domains of bovine parathyroid cells. J. Biol. Chem. 273(34):21708-21713. doi:10.1074/jbc.273.34.21708

Kifor, O., R. J. MacLeod, R. Diaz, M. Bai, T. Yamaguchi, T. Yao, I. Kifor, and E. M. Brown. 2001. Regulation of MAP kinase by calcium-sensing receptor in bovine parathyroid and CaR-transfected HEK293 cells. Am. J. Physiol. - Renal Physiol. 280(2):F291-F302. doi:10.1152/ajprenal.2001.280.2.F291

Kim, W., L. Donalson, S. Bloomfield, H. Hogan, L. Kubena, D. Nisbet, and S. Ricke. 2007. Molt performance and bone density of cortical, medullary, and cancellous bone in laying hens during feed restriction or alfalfa-based feed molt. Poult. Sci. 86(9):1821-1830. doi:10.1093/ps/86.9.1821

Kim, W. K., S. A. Bloomfield, T. Sugiyama, and S. C. Ricke. 2012. Concepts and methods for understanding bone metabolism in laying hens. Worlds Poult. Sci. J. 68(1):71-82. doi:10.1017/S0043933912000086

Koch, W. J., B. E. Hawes, L. F. Allen, and R. J. Lefkowitz. 1994. Direct evidence that $G_i$-coupled receptor stimulation of mitogen-activated protein kinase is mediated by $G_{\beta\gamma}$ activation of $p21^{ras}$. Proc. Natl. Acad. Sci. 91(26):12706-12710. doi:10.1073/pnas.91.26.12706

Koori, K., H. Maeda, S. Fujii, A. Tomokiyo, G. Kawachi, D. Hasegawa, S. Hamano, H. Sugii, N. Wada, and A. Akamine. 2014. The roles of calcium-sensing receptor and calcium channel in osteogenic differentiation of undifferentiated periodontal ligament cells. Cell Tissue Res. 357(3):707-718. doi:10.1007/s00441-014-1918-5

Koreleski, J., and S. Świątkiewicz. 2005. Efficacy of different levels of a cholecalciferol 25-OH-derivative in diets with two limestone forms in laying hen nutrition. J. Anim. Feed Sci. 14:305-315. doi:10.22358/jafs/67018/2005

Korver, D. R., 2020. Calcium nutrition, bone metabolism, and eggshell quality in longer-persisting layer flocks. Proc. Aust. Poult. Sci. Symp. 31:1-7. https://images.engormix.com/externalFiles/6_mateos-ponedoras-alternativos.pdf

Kos, C. H., A. C. Karaplis, J.-B. Peng, M. A. Hediger, D. Goltzman, K. S. Mohammad, T. A. Guise, and M. R. Pollak. 2003. The calcium-sensing receptor is required for normal

calcium homeostasis independent of parathyroid hormone. J. Clin. Investig. 111(7):1021-1028. doi:10.1172/JCI17416

Krens, S. G., H. P. Spaink, and B. E. Snaar-Jagalska. 2006. Functions of the MAPK family in vertebrate - development. FEBS Lett. 580(21):4984-4990. doi:10.1016/j.febslet.2006.08.025

Krzysik-Walker, S. M., O. M. Ocón-Grove, S. B. Maddineni, G. L. Hendricks, III, and R. Ramachandran. 2007. Identification of calcitonin expression in the chicken ovary: influence of follicular maturation and ovarian steroids. Biol. Reprod. 77(4):626-635. doi:10.1095/biolreprod.106.054957

Kutuzova, G. D., and H. F. DeLuca. 2004. Gene expression profiles in rat intestine identify pathways for 1,25-dihydroxyvitamin $D_3$ stimulated calcium absorption and clarify its immunomodulatory properties. Arch. Biochem. Biophys. 432(2):152-166. doi:10.1016/j.abb.2004.09.004

Lasmoles, F., A. Jullienne, C. Desplan, G. Milhaud, and M. Moukhtar. 1985. Structure of chicken calcitonin predicted by partial nucleotide sequence of its precursor. FEBS Lett. 180(1):113-116. doi:10.1016/0014-5793(85)80242-8

Le Floc'h, N., W. Otten, and E. Merlot. 2011. Tryptophan metabolism, from nutrition to potential therapeutic applications. Amino Acids 41(5):1195-1205. doi:10.1007/s00726-010-0752-7

Leach, K., A. D. Conigrave, P. M. Sexton, and A. Christopoulos. 2015. Towards tissue-specific pharmacology: insights from the calcium-sensing receptor as a paradigm for GPCR (patho)physiological bias. Trends Pharmacol. Sci. 36(4):215-225. doi:10.1016/j.tips.2015.02.004

Li, X., K. S. Warmington, Q. T. Niu, F. J. Asuncion, M. Barrero, M. Grisanti, D. Dwyer, B. Stouch, T. M. Thway, and M. Stolina. 2010. Inhibition of sclerostin by monoclonal antibody increases bone formation, bone mass, and bone strength in aged male rats. J. Bone Miner. Res. 25(12):2647-2656. doi:10.1002/jbmr.182

Liang, G.-B., C. Zhou, X. Huo, H. Wang, X. Yang, S. Huang, H. Wang, H. Wilkinson, L. Luo, and W. Tang. 2016. Discovery of novel dihydrobenzofuran cyclopropane carboxylic acid based calcium sensing receptor antagonists for the treatment of osteoporosis. Bioorg. Med. Chem. Lett. 26(16):4077-4080. doi:10.1016/j.bmcl.2016.06.073

Liao, Q.-S., Q. Du, J. Lou, J.-Y. Xu, and R. Xie. 2019. Roles of $Na^{+}/Ca^{2+}$ exchanger 1 in digestive system physiology and pathophysiology. World J. Gastroenterol. 25(3):287. doi:10.3748/wjg.v25.i3.287

Lichovnikova, M. 2007. The effect of dietary calcium source, concentration and particle size on calcium retention, eggshell quality and overall calcium requirement in laying hens. Br. Poult. Sci. 48(1):71-75. doi:10.1080/00071660601148203

Lim, H. S., H. Namkung, and I. K. Paik. 2003. Effects of phytase supplementation on the performance, egg quality, and phosphorous excretion of laying hens fed different levels of dietary calcium and nonphytate phosphorous. Poult. Sci. 82(1):92-99. doi:10.1093/ps/82.1.92

Ling, S., P. Shi, S. Liu, X. Meng, Y. Zhou, W. Sun, S. Chang, X. Zhang, L. Zhang, C. Shi, D. Sun, L. Liu, and C. Tian. 2021. Structural mechanism of cooperative activation of the human calcium-sensing receptor by $Ca^{2+}$ ions and L-tryptophan. Cell Res. doi:10.1038/s41422-021-00474-0

Liou, A. 2013. Digestive physiology of the pig symposium: G protein-coupled receptors in nutrient chemosensation and gastrointestinal hormone secretion. J. Anim. Sci. 91(5):1946-1956. doi:10.2527/jas.2012-5910

Liou, A. P., Y. Sei, X. Zhao, J. Feng, X. Lu, C. Thomas, S. Pechhold, H. E. Raybould, and S. A. Wank. 2011. The extracellular calcium-sensing receptor is required for cholecystokinin secretion in response to L-phenylalanine in acutely isolated intestinal I cells. Am. J. Physiol. - Gastrointest. Liver Physiol. 300(4):G538-G546. doi:10.1152/ajpgi.00342.2010

Liu, H., P. Yi, W. Zhao, Y. Wu, F. Acher, J.-P. Pin, J. Liu, and P. Rondard. 2020. Illuminating the allosteric modulation of the calcium-sensing receptor. Proc. Natl. Acad. Sci. 117(35):21711-21722. doi:10.1073/pnas.1922231117

Liu, Y., J. Wu, Y. Zhu, and J. Han. 2014. Therapeutic application of mesenchymal stem cells in bone and joint diseases. Clin. Exp. Med. 14(1):13-24. doi:10.1007/s10238-012-0218-1

Livak, K. J., and T. D. Schmittgen. 2001. Analysis of relative gene expression data using real-time quantitative PCR and the $2^{-\Delta\Delta CT}$ method. Methods 25(4):402-408. doi:10.1006/meth.2001.1262

Lohmann, L. 2016. LSL-Lite Commercial Management Guide. Lohmann Tierzucht. Cuxhaven, Germany. Accessed Feb. 10, 2018. www.ltz.de.

Lu, Z., K. Hanson, and H. F. DeLuca. 1997. Cloning and origin of the two forms of chicken vitamin D receptor. Arch. Biochem. Biophys. 339(1):99-106. doi:10.1006/abbi.1996.9864

Lu, Z., F. Jehan, C. Zierold, and H. F. DeLuca. 2000. Isolation and characterization of the chicken vitamin D receptor gene and its promoter. J. Cell. Biochem. 77(1):92-102. doi:10.1002/(SICI)1097-4644(20000401)77:1<92::AID-JCB10>3.0.CO;2-N

Lundholm, C. 1997. DDE-induced eggshell thinning in birds: effects of p, p′-DDE on the calcium and prostaglandin metabolism of the eggshell gland. Comp. Biochem. Physiol., Part C: Pharmacol., Toxicol. Endocrinol. 118(2):113-128. doi:10.1016/S0742-8413(97)00105-9

Lytton, J. 2007. $Na^+/Ca^{2+}$ exchangers: three mammalian gene families control $Ca^{2+}$ transport. Biochem. J. 406(3):365-382. doi:10.1042/BJ20070619

Macelline, S. P., M. Toghyani, P. V. Chrystal, P. H. Selle, and S. Y. Liu. 2021. Amino acid requirements for laying hens: a comprehensive review. Poult. Sci. 100(5):101036. doi:10.1016/j.psj.2021.101036

Magno, A. L., B. K. Ward, and T. Ratajczak. 2011. The Calcium-Sensing Receptor: A Molecular Perspective. Endocr. Rev. 32(1):3-30. doi:10.1210/er.2009-0043

Maiti, A., N. C. Hait, and M. J. Beckman. 2008. Extracellular calcium-sensing receptor activation induces vitamin D receptor levels in proximal kidney HK-2G cells by a mechanism that requires phosphorylation of p38α MAPK. J. Biol. Chem. 283(1):175-183. doi:10.1074/jbc.M707269200

Makita, N., T. Ando, J. Sato, K. Manaka, K. Mitani, Y. Kikuchi, T. Niwa, M. Ootaki, Y. Takeba, and N. Matsumoto. 2019. Cinacalcet corrects biased allosteric modulation of CaSR by AHH autoantibody. JCI insight 4(8):e126449. doi:10.1172/jci.insight.126449

Mamillapalli, R., J. VanHouten, W. Zawalich, and J. Wysolmerski. 2008. Switching of G-protein usage by the calcium-sensing receptor reverses its effect on parathyroid hormone-related protein secretion in normal versus malignant breast cells. J. Biol. Chem. 283(36):24435-24447. doi:10.1074/jbc.M801738200

Mamillapalli, R., and J. Wysolmerski. 2010. The calcium-sensing receptor couples to $G\alpha_s$ and regulates PTHrP and ACTH secretion in pituitary cells. J. Endocrinol. 204(3):287. doi:10.1677/JOE-09-0183

Marie, P. J. 2010. The calcium-sensing receptor in bone cells: a potential therapeutic target in osteoporosis. Bone 46(3):571-576. doi:10.1016/j.bone.2009.07.082

Martino, N. A., S. J. Reshkin, E. Ciani, and M. E. Dell'Aquila. 2014. Calcium-sensing receptor-mediated osteogenic and early-stage neurogenic differentiation in umbilical cord matrix mesenchymal stem cells from a large animal model. PloS one 9(11): e111533. doi:10.1371/journal.pone.0111533

McDonnell, D. P., D. J. Mangelsdorf, J. W. Pike, M. R. Haussler, and B. W. O'Malley. 1987. Molecular cloning of complementary DNA encoding the avian receptor for vitamin D. Science 235(4793):1214-1217. doi:10.1126/science.3029866

McGehee, D. S., M. Aldersberg, K. P. Liu, S. C. Hsuing, M. J. Heath, and H. Tamir. 1997. Mechanism of extracellular $Ca^{2+}$ receptor‐stimulated hormone release from sheep thyroid parafollicular cells. J. Physiol. 502(1):31-44. doi:10.1111/j.1469-7793.1997.031bl.x

McLarnon, S. J., D. Holden, D. T. Ward, M. N. Jones, A. C. Elliott, and D. Riccardi. 2002. Aminoglycoside antibiotics induce pH-sensitive activation of the calcium-sensing receptor. Biochem. Biophys. Res. Commun. 297(1):71-77. doi:10.1016/S0006-291X(02)02133-2

McNeil, S. E., S. A. Hobson, V. Nipper, and K. D. Rodland. 1998. Functional calcium-sensing receptors in rat fibroblasts are required for activation of SRC kinase and mitogen-activated protein kinase in response to extracellular calcium. J. Biol. Chem. 273(2):1114-1120. doi:10.1074/jbc.273.2.1114

Mentaverri, R., S. Yano, N. Chattopadhyay, L. Petit, O. Kifor, S. Kamel, E. Terwilliger, M. Brazier, E. Brown, and R. Mentaverri. 2006. The calcium sensing receptor is directly involved in both osteoclast differentiation and apoptosis. FASEB J. 20(14):2562-2564. doi:10.1096/fj.06-6304fje

Minvielle, S., M. Cressent, M. Delehaye, N. Segond, G. Milhaud, A. Jullienne, M. Moukhtar, and F. Lasmoles. 1987. Sequence and expression of the chicken calcitonin gene. FEBS Lett. 223(1):63-68. doi:10.1016/0014-5793(87)80510-0

Moor, M. B., and O. Bonny. 2016. Ways of calcium reabsorption in the kidney. Am. J. Physiol. - Renal Physiol. 310(11):F1337-F1350. doi:10.1152/ajprenal.00273.2015

Moseley, J. M., M. Kubota, H. Diefenbach-Jagger, R. Wettenhall, B. Kemp, L. Suva, C. Rodda, P. Ebeling, P. J. Hudson, and J. Zajac. 1987. Parathyroid hormone-related protein purified from a human lung cancer cell line. Proc. Natl. Acad. Sci. 84(14):5048-5052. doi:10.1073/pnas.84.14.5048

Mueller, W. J., Schraer, R., and Scharer, H. (1964). Calcium metabolism and skeletal dynamics of laying pullets. J. Nutri. 84(1), 20-26. doi:10.1093/jn/84.1.20

Mundy, G. R., and T. A. Guise. 1999. Hormonal control of calcium homeostasis. Clin. Chem. 45(8):1347-1352. doi:10.1093/clinchem/45.8.1347

Nakamura, I., G. A. Rodan, and L. T. Duong. 2003. Regulatory mechanism of osteoclast activation. J. Electron Microsc. 52(6):527-533. doi:10.1093/jmicro/52.6.527

Narváez-Solarte, W., H. S. Rostagno, P. R. Soares, L. F. Uribe-Velasquez, and M. A. Silva. 2006. Nutritional requirement of calcium in white laying hens from 46 to 62 wk of age. Int. J. Poult. Sci. 5(2):181-184. doi:10.3923/ijps.2006.181.184

Nemeth, E. F. 2002. The search for calcium receptor antagonists (calcilytics). J. Mol. Endocrinol. 29(1):15-21. doi:10.1677/jme.0.0290015

Nemeth, E. F., E. G. Delmar, W. L. Heaton, M. A. Miller, L. D. Lambert, R. L. Conklin, M. Gowen, J. G. Gleason, P. K. Bhatnagar, and J. Fox. 2001. Calcilytic compounds: potent and selective $Ca^{2+}$ receptor antagonists that stimulate secretion of parathyroid hormone. J. Pharmacol. Exp. Ther. 299(1):323-331. https://jpet.aspetjournals.org/content/299/1/323.long

Nemeth, E. F., and A. Scarpa. 1987. Rapid mobilization of cellular $Ca^{2+}$ in bovine parathyroid cells evoked by extracellular divalent cations. Evidence for a cell surface calcium receptor. J. Biol. Chem. 262(11):5188-5196. doi:10.1016/S0021-9258(18)61172-X

Nemeth, E. F., M. E. Steffey, L. G. Hammerland, B. C. Hung, B. C. Van Wagenen, E. G. DelMar, and M. F. Balandrin. 1998. Calcimimetics with potent and selective activity on the parathyroid calcium receptor. Proc. Natl. Acad. Sci. 95(7):4040-4045. doi:10.1073/pnas.95.7.4040

Nijenhuis, T., J. G. Hoenderop, and R. J. Bindels. 2005. TRPV5 and TRPV6 in $Ca^{2+}$ (re) absorption: regulating $Ca^{2+}$ entry at the gate. Pflug. Arch. Eur. J. Physiol. 451(1):181-192. doi:10.1007/s00424-005-1430-6

Norman, A. W. 1987. Studies on the vitamin D endocrine system in the avian. J. Nutr. 117(4):797-807. doi:10.1093/jn/117.4.797

Norman, A. W. 2008. From vitamin D to hormone D: fundamentals of the vitamin D endocrine system essential for good health. Am. J. Clin. Nutr. 88(2):491S-499S. doi:10.1093/ajcn/88.2.491S

Norman, A. W., and S. Hurwitz. 1993. The role of the vitamin D endocrine system in avian bone biology. J. Nutr. 123(suppl_2):310-316. doi:10.1093/jn/123.suppl_2.310

National Research Council. 1962. Nutrient Requirements of Poultry. Natl. Acad. Press, Washington, DC.

National Research Council. 1966. Nutrient Requirements of Poultry. Natl. Acad. Press, Washington, DC.

National Research Council. 1984. Nutrient Requirements of Poultry. Natl. Acad. Press, Washington, DC.

National Research Council. 1994. Nutrient Requirements of Poultry. Natl. Acad. Press, Washington, DC.

Nys, Y., and N. Le Roy. 2018. Calcium homeostasis and eggshell biomineralization in female chicken, In Vitamin D, pp. 361-382. Academic press. doi:10.1016/B978-0-12-809965-0.00022-7

Nys, Y. d., and X. De Laage. 1984. Effects of suppression of eggshell calcification and of $1,25(OH)_2D_3$ on $Mg^{2+}$, $Ca^{2+}$ and $Mg^{2+}$ $HCO_3^-$ ATPase, alkaline phosphatase, carbonic anhydrase and CaBP levels--I. The laying hen uterus. Comp. Biochem. Physiol. Part A Mol. Integr. Physiol. 78(4):833-838. doi:10.1016/0300-9629(84)90642-X

Obermannova, B., Z. Sumnik, P. Dusatkova, O. Cinek, M. Grant, J. Lebl, and G. N. Hendy. 2016. Novel calcium-sensing receptor cytoplasmic tail deletion mutation causing autosomal dominant hypocalcemia: molecular and clinical study. Eur. J. Endocrinol. 174(4):1-11. doi:10.1530/EJE-15-1216

Oda, Y., C.-L. Tu, W. Chang, D. Crumrine, L. Kömüves, T. Mauro, P. M. Elias, and D. D. Bikle. 2000. The calcium sensing receptor and its alternatively spliced form in murine epidermal differentiation. J. Biol. Chem. 275(2):1183-1190. doi:10.1074/jbc.275.2.1183

Odgaard, A. 1997. Three-dimensional methods for quantification of cancellous bone architecture. Bone 20(4):315-328. doi: 10.1016/S8756-3282(97)00007-0

Olgun, O., and A. Aygun. 2016. Nutritional factors affecting the breaking strength of bone in laying hens. Worlds Poult. Sci. J. 72(4):821-832. doi:10.1017/S0043933916000696

Owen, T. A., M. Aronow, V. Shalhoub, L. M. Barone, L. Wilming, M. S. Tassinari, M. B. Kennedy, S. Pockwinse, J. B. Lian, and G. S. Stein. 1990. Progressive development of the rat osteoblast phenotype in vitro: reciprocal relationships in expression of genes associated with osteoblast proliferation and differentiation during formation of the bone extracellular matrix. J. Cell. Physiol. 143(3):420-430. doi:10.1002/jcp.1041430304

Owen, T. A., M. S. Aronow, L. M. Barone, B. Bettencourt, G. S. Stein, and J. B. Lian. 1991. Pleiotropic effects of vitamin D on osteoblast gene expression are related to the proliferative and differentiated state of the bone cell phenotype: dependency upon basal levels of gene expression, duration of exposure, and bone matrix competency in normal rat osteoblast cultures. Endocrinology 128(3):1496-1504. doi:10.1210/endo-128-3-1496

Partridge, I. 1978. Studies on digestion and absorption in the intestines of growing pigs: 3. Net movements of mineral nutrients in the digestive tract. Br. J. Nutr. 39(3):527-537.

Pastore, S.M., P. C. Gomes, H. S. Rostagno, L. F. T. Albino, A. A. Calderano, C. R. Vellasco, G. d. S. Viana, and R. L. d. Almeida. 2012. Calcium levels and calcium: available phosphorus ratios in diets for white egg layers from 42 to 58 weeks of age. R. Bras. Zootec. 41:2424–2432. doi:10.1590/S1516-35982012001200007

Peacock, M., J. P. Bilezikian, P. S. Klassen, M. D. Guo, S. A. Turner, and D. Shoback. 2005. Cinacalcet hydrochloride maintains long-term normocalcemia in patients with primary hyperparathyroidism. J. Clin. Endocrinol. Metab. 90(1):135-141. doi:10.1210/jc.2004-0842

Pedrozo, H., Z. Schwartz, S. Rimes, V. Sylvia, I. Nemere, G. Posner, D. D. Dean, and B. D. Boyan. 1999. Physiological importance of the $1,25(OH)_2D_3$ membrane receptor and evidence for a membrane receptor specific for $24,25(OH)_2D_3$. J. Bone Miner. Res. 14(6):856-867. doi:10.1359/jbmr.1999.14.6.856

Peganova, S., F. Hirche, and K. Eder. 2003. Requirement of tryptophan in relation to the supply of large neutral amino acids in laying hens. Poult. Sci. 82(5):815-822. doi:10.1093/ps/82.5.815

Pelicia, K., E. A. Garcia, A. Faitarone, A. Silva, D. Berto, A. Molino, and F. Vercese. 2009. Calcium and available phosphorus levels for laying hens in second production cycle. Braz. J. Poult. Sci. 11(1):39-49. doi:10.1590/S1516-635X2009000100007

Petrel, C., A. Kessler, P. Dauban, R. H. Dodd, D. Rognan, and M. Ruat. 2004. Positive and negative allosteric modulators of the $Ca^{2+}$-sensing receptor interact within overlapping but not identical binding sites in the transmembrane domain. J. Biol. Chem. 279(18):18990-18997. doi:10.1074/jbc.M400724200

Pi, M., S. C. Garner, P. Flannery, R. F. Spurney, and L. D. Quarles. 2000. Sensing of Extracellular Cations in CasR-deficient: evidence for a novel cation-sensing mechanism. J. Biol. Chem. 275(5):3256-3263. doi:10.1074/jbc.275.5.3256

Pi, M., R. F. Spurney, Q. Tu, T. Hinson, and L. D. Quarles. 2002. Calcium-sensing receptor activation of Rho involves filamin and Rho-guanine nucleotide exchange factor. Endocrinology 143(10):3830-3838. doi:10.1210/en.2002-220240

Pines, M., V. Knopov, and A. Bar. 1995. Involvement of osteopontin in egg shell formation in the laying chicken. Matrix Biol. 14(9):765-771. doi:10.1016/S0945-053X(05)80019-8

Pipino, C., P. D. Tomo, D. Mandatori, E. Cianci, P. Lanuti, M. B. Cutrona, L. Penolazzi, L. Pierdomenico, E. Lambertini, and I. Antonucci. 2014. Calcium sensing receptor activation by calcimimetic R-568 in human amniotic fluid mesenchymal stem cells: correlation with osteogenic differentiation. Stem Cells Dev. 23(24):2959-2971. doi:10.1089/scd.2013.0627

Pittenger, M. F., A. M. Mackay, S. C. Beck, R. K. Jaiswal, R. Douglas, J. D. Mosca, M. A. Moorman, D. W. Simonetti, S. Craig, and D. R. Marshak. 1999. Multilineage Potential of Adult Human Mesenchymal Stem Cells. Science 284:143. doi:10.1126/science.284.5411.143

Pongmanee, K., I. Kühn, and D. R. Korver. 2020. Effects of phytase supplementation on eggshell and bone quality, and phosphorus and calcium digestibility in laying hens from 25 to 37 wk of age. Poult. Sci. 99(5):2595-2607. doi:10.1016/j.psj.2019.12.051

Proszkowiec-Weglarz, M., and R. Angel. 2013. Calcium and phosphorus metabolism in broilers: Effect of homeostatic mechanism on calcium and phosphorus digestibility. J. Appl. Poult. Res. 22(3):609-627. doi:10.3382/japr.2012-00743

Quarles, L. D. 2003. Extracellular calcium-sensing receptors in the parathyroid gland, kidney, and other tissues. Curr. Opin. Nephrol. Hypertens. 12(4):349-355. doi:10.1097/01.mnh.0000079682.89474.80

Quélo, I., J. P. Kahlen, A. Rascle, P. Jurdic, and C. Carlberg. 1994. Identification and characterization of a vitamin $D_3$ response element of chicken carbonic anhydrase-II. DNA Cell Biol. 13(12):1181-1187. doi:10.1089/dna.1994.13.1181

Quinn, S. J., M. Bai, and E. M. Brown. 2004. pH Sensing by the calcium-sensing receptor. J. Biol. Chem. 279(36):37241-37249. doi:10.1074/jbc.M404520200

Quinn, S. J., O. Kifor, S. Trivedi, R. Diaz, P. Vassilev, and E. Brown. 1998. Sodium and ionic strength sensing by the calcium receptor. J. Biol. Chem. 273(31):19579-19586. doi:10.1074/jbc.273.31.19579

Quinn, S. J., C. P. Ye, R. Diaz, O. Kifor, M. Bai, P. Vassilev, and E. Brown. 1997. The $Ca^{2+}$-sensing receptor: a target for polyamines. Am. J. Physiol. - Cell Physiol. 273(4):C1315-C1323. doi:10.1152/ajpcell.1997.273.4.C1315

Rath, N., G. Huff, W. Huff, and J. Balog. 2000. Factors regulating bone maturity and strength in poultry. Poult. Sci. 79(7):1024-1032. doi:10.1093/ps/79.7.1024

Ray, K., G. F. Fan, P. K. Goldsmith, and A. M. Spiegel. 1997. The carboxyl terminus of the human calcium receptor requirements for cell-surface expression and signal transduction. J. Biol. Chem. 272(50):31355-31361. doi: 10.1074/jbc.272.50.31355

Ray, K., S. P. Ghosh, and J. K. Northup. 2004. The role of cysteines and charged amino acids in extracellular loops of the human $Ca^{2+}$ receptor in cell surface expression and receptor activation processes. Endocrinology 145(8):3892-3903. doi:10.1210/en.2003-1653

Rey, O., S. H. Young, R. Jacamo, M. P. Moyer, and E. Rozengurt. 2010. Extracellular calcium sensing receptor stimulation in human colonic epithelial cells induces intracellular calcium oscillations and proliferation inhibition. J. Cell. Physiol. 225(1):73-83. doi:10.1002/jcp.22198

Rey, O., S. H. Young, J. Yuan, L. Slice, and E. Rozengurt. 2005. Amino acid-stimulated $Ca^{2+}$ oscillations produced by the $Ca^{2+}$-sensing receptor are mediated by a phospholipase C/inositol 1, 4, 5-trisphosphate-independent pathway that requires $G_{12}$, Rho, filamin-A, and the actin cytoskeleton. J. Biol. Chem. 280(24):22875-22882. doi:10.1074/jbc.M503455200

Riccardi, D., and E. M. Brown. 2010. Physiology and pathophysiology of the calcium-sensing receptor in the kidney. Am. J. Physiol. - Renal Physiol. 298(3):F485-F499. doi:10.1152/ajprenal.00608.2009

Riccardi, D., A. E. Hall, N. Chattopadhyay, J. Z. Xu, E. M. Brown, and S. C. Hebert. 1998. Localization of the extracellular $Ca^{2+}$/polyvalent cation-sensing protein in rat kidney. Am. J. Physiol. - Renal Physiol. 274(3):F611-F622. doi:10.1152/ajprenal.1998.274.3.F611

Riccardi, D., J. Park, W. S. Lee, G. Gamba, E. M. Brown, and S. C. Hebert. 1995. Cloning and functional expression of a rat kidney extracellular calcium/polyvalent cation-sensing receptor. Proc. Natl. Acad. Sci. 92(1):131-135. doi:10.1073/pnas.92.1.131

Riccardi, D., M. Traebert, D. T. Ward, B. Kaissling, J. Biber, S. C. Hebert, and H. Murer. 2000. Dietary phosphate and parathyroid hormone alter the expression of the calcium-sensing receptor (CaR) and the $Na^{+}$-dependent Pi transporter (NaPi-2) in the rat proximal tubule. Pflügers Archiv. 441(2-3):379-387. doi:10.1007/s004240000436

Ritchie, M. F., Y. Zhou, and J. Soboloff. 2011. Transcriptional mechanisms regulating $Ca^{2+}$ homeostasis. Cell calcium 49(5):314-321. doi:10.1016/j.ceca.2010.10.001

Roland, D. A. 1986. Eggshell quality IV: oystershell versus limestone and the importance of particle size or solubility of calcium source. Worlds Poult. Sci. J. 42(2):166-171. doi:10.1079/WPS19860013

Roland, D. A., and R. H. Harms. 1976. The lack of response of 25-hydroxy-vitamin $D_3$ on egg shell quality or other criteria in laying hens. Poult. Sci. 55(5):1983-1985. doi:10.3382/ps.0551983

Rosenbaum, D. M., S. G. Rasmussen, and B. K. Kobilka. 2009. The structure and function of G protein-coupled receptors. Nature 459(7245):356-363. doi:10.1038/nature08144

Rosol, T. J., and C. C. Capen. 1996. Pathophysiology of calcium, phosphorus, and magnesium metabolism in animals. Vet. Clin. North Am. Small Anim. Pract. 26(5):1155-1184. doi:10.1016/S0195-5616(96)50060-4

Roura, E., I. Depoortere, and M. Navarro. 2019. Chemosensing of nutrients and non-nutrients in the human and porcine gastrointestinal tract. Animal 13(11):2714-2726. doi:10.1017/S1751731119001794

Ruijtenberg, S., and S. van den Heuvel. 2016. Coordinating cell proliferation and differentiation: Antagonism between cell cycle regulators and cell type-specific gene expression. Cell Cycle 15(2):196-212. doi:10.1080/15384101.2015.1120925

Russell, G. B., and R. H. Harms. 1999. Tryptophan requirement of the commercial hen. Poult. Sci. 78(9):1283-1285. doi:10.1093/ps/78.9.1283

Rutten, M. J., K. D. Bacon, K. L. Marlink, M. Stoney, C. L. Meichsner, F. P. Lee, S. A. Hobson, K. D. Rodland, B. C. Sheppard, and D. D. Trunkey. 1999. Identification of a functional $Ca^{2+}$-sensing receptor in normal human gastric mucous epithelial cells. Am. J. Physiol. - Gastrointest. Liver Physiol. 277(3):G662-G670. doi:10.1152/ajpgi.1999.277.3.G662

Saidak, Z., M. Brazier, S. Kamel, and R. Mentaverri. 2009. Agonists and allosteric modulators of the calcium-sensing receptor and their therapeutic applications. Mol. Pharmacol. 76(6):1131-1144. doi:10.1124/mol.109.058784

Sarsour, A. H., J. T. Lee, K. Haydon, and M. E. Persia. 2021. Tryptophan requirement of first-cycle commercial laying hens in peak egg production. Poult. Sci. 100(3):100896. doi:10.1016/j.psj.2020.11.065

Schermer, D., S. Chan, R. Bruce, R. Nissenson, W. Wood, and G. Strewler. 1991. Chicken parathyroid hormone‐related protein and its expression during embryologic development. J. Bone Miner. Res. 6(2):149-155. doi:10.1002/jbmr.5650060208

Schmidpeter, P. A. M., and F. X. Schmid. 2014. Phosphorylation and Prolyl Isomerization Independently Regulate the Signal Adapter Function of CrkII. J. Mol. Biol. 426(24):3929-3934. doi:10.1016/j.jmb.2014.09.022

Scott, M. L., S. J. Hull, and P. A. Mullenhoff. 1971. The calcium requirements of laying hens and effects of dietary oyster shell upon egg shell quality. Poult. Sci. 50(4):1055-1063. doi:10.3382/ps.0501055

Seyedabadi, M., M. H. Ghahremani, and P. R. Albert. 2019. Biased signaling of G protein coupled receptors (GPCRs): Molecular determinants of GPCR/transducer selectivity and therapeutic potential. Pharmacol. Ther. 200:148-178. doi:10.1016/j.pharmthera.2019.05.006

Sheinin, Y., E. Kállay, F. Wrba, S. Kriwanek, M. Peterlik, and H. S. Cross. 2000. Immunocytochemical localization of the extracellular calcium-sensing receptor in normal and malignant human large intestinal mucosa. J. Histochem. Cytochem. 48(5):595-601. doi:10.1177/002215540004800503

Silva, F. A. 2017. Effects of Dietary 25-hydroxycholecalciferol on growth, production performance, eggshell quality and bone traits of brown egg layers housed under

commercial conditions. University of Alberta, Edmonton, Canada. doi:10.7939/R32R3P99V

Silve, C. M., G. T. Hradek, A. L. Jones, and C. D. Arnaud. 1982. Parathyroid hormone receptor in intact embryonic chicken bone: characterization and cellular localization. J. Cell Biol. 94(2):379-386. doi:10.1083/jcb.94.2.379

Silver, I., R. Murrills, and D. Etherington. 1988. Microelectrode studies on the acid microenvironment beneath adherent macrophages and osteoclasts. Exp. Cell Res. 175(2):266-276. doi:10.1016/0014-4827(88)90191-7

Skelly, B. J., and R. J. Franklin. 2007. Mutations in genes causing human familial isolated hyperparathyroidism do not account for hyperparathyroidism in Keeshond dogs. Vet. J. 174(3):652-654. doi:10.1016/j.tvjl.2006.10.018

Soares, J. H., J. M. Kerr, and R. W. Gray. 1995. 25-Hydroxycholecalciferol in Poultry Nutrition. Poult. Sci. 74(12):1919-1934. doi:10.3382/ps.0741919

Spurney, R. F., M. Pi, P. Flannery, and L. D. Quarles. 1999. Aluminum is a weak agonist for the calcium-sensing receptor. Kidney Int. 55(5):1750-1758. doi:10.1046/j.1523-1755.1999.00432.x

St-Arnaud, R. 2008. The direct role of vitamin D on bone homeostasis. Arch. Biochem. Biophys. 473(2):225-230. doi:10.1016/j.abb.2008.03.038

Stewart, A. F., T. Wu, D. Goumas, W. J. Burtis, and A. E. Broadus. 1987. N-terminal amino acid sequence of two novel tumor-derived adenylate cyclase-stimulating proteins: identification of parathyroid hormone-like and parathyroid hormone-unlike domains. Biochem. Biophys. Res. Commun. 146(2):672-678. doi:10.1016/0006-291X(87)90581-X

Strewler, G. J., P. Stern, J. W. Jacobs, J. Eveloff, R. F. Klein, S. C. Leung, M. Rosenblatt, and R. A. Nissenson. 1987. Parathyroid hormonelike protein from human renal carcinoma cells. Structural and functional homology with parathyroid hormone. J. Clin. Investig. 80(6):1803-1807. doi:10.1172/JCI113275

Suh, H. N., Y. J. Lee, and H. J. Han. 2009. Interleukin-6 promotes 2-deoxyglucose uptake through p44/42 MAPKs activation via $Ca^{2+}$/PKC and EGF receptor in primary cultured chicken hepatocytes. J. Cell. Physiol. 218(3):643-652. doi:10.1002/jcp.21641

Supuran, C. T. 2008. Carbonic anhydrases-an overview. Curr. Pharm. Des. 14(7):603-614. doi:10.2174/138161208783877884

Świątkiewicz, S., A. Arczewska-Włosek, J. Krawczyk, M. Puchała, and D. Jozefiak. 2015. Dietary factors improving eggshell quality: an updated review with special emphasis on microelements and feed additives. Worlds Poult. Sci. J. 71(1):83-94. doi:10.1017/S0043933915000082

Syndia, L., J. P. Carel, K. Frederick, L. C. Katherine, C. B. Sarah, D. C. Arthur, M. B. Edward, and T. W. Donald. 2011. A novel mutation of the primary protein kinase C phosphorylation site in the calcium-sensing receptor causes autosomal dominant hypocalcemia. Eur. J. Endocrinol. 164(3):429-435. doi:10.1530/EJE-10-0907

Taher, A. I., E. W. Gleaves, and M. Beck. 1984. Special Calcium Appetite in Laying Hens. Poult. Sci. 63(11):2261-2267. doi:10.3382/ps.0632261

Takaichi, K., and K. Kurokawa. 1986. High $Ca^{2+}$ inhibits peptide hormone-dependent cAMP production specifically in thick ascending limbs of Henle. Miner. Electrolyte Metab. 12(5-6):342-346. PMID: 3027519.

Takaichi, K., and K. Kurokawa. 1988. Inhibitory guanosine triphosphate-binding protein-mediated regulation of vasopressin action in isolated single medullary tubules of mouse kidney. The J. Clin. Investig. 82(4):1437-1444. doi:10.1172/JCI113749

Takaoka, S., T. Yamaguchi, S. Yano, M. Yamauchi, and T. Sugimoto. 2010. The Calcium-sensing Receptor (CaR) is involved in strontium ranelate-induced osteoblast differentiation and mineralization. Horm. Metab. Res. 42(09):627-631. doi:10.1055/s-0030-1255091

Tang, L., C. Y. Cheng, X. Sun, A. J. Pedicone, M. Mohamadzadeh, and S. X. Cheng. 2016. The Extracellular Calcium-Sensing Receptor in the Intestine: Evidence for Regulation of Colonic Absorption, Secretion, Motility, and Immunity. Front. Physiol. 7(245) doi:10.3389/fphys.2016.00245

Tarroni, P., I. Villa, E. Mrak, F. Zolezzi, M. Mattioli, C. Gattuso, and A. Rubinacci. 2012. Microarray analysis of $1,25(OH)_2D_3$ regulated gene expression in human primary osteoblasts. J. Cell. Biochem. 113(2):640-649. doi:10.1002/jcb.23392

Taylor, A., and R. Wasserman. 1972. Vitamin D-induced calcium-binding protein: comparative aspects in kidney and intestine. Am. J. Physiol. - Legacy Content 223(1):110-114. doi:10.1152/ajplegacy.1972.223.1.110

Thomsen, A. R. B., M. Hvidtfeldt, and H. Bräuner-Osborne. 2012. Biased agonism of the calcium-sensing receptor. Cell Calcium 51(2):107-116. doi:10.1016/j.ceca.2011.11.009

Tu, C. L., W. Chang, Z. Xie, and D. D. Bikle. 2008. Inactivation of the calcium sensing receptor inhibits E-cadherin-mediated cell-cell adhesion and calcium-induced differentiation in human epidermal keratinocytes. J. Biol. Chem. 283(6):3519-3528. doi:10.1074/jbc.M708318200

Usachev, Y. M., S. J. DeMarco, C. Campbell, E. E. Strehler, and S. A. Thayer. 2002. Bradykinin and ATP accelerate $Ca^{2+}$ efflux from rat sensory neurons via protein kinase C and the plasma membrane $Ca^{2+}$ pump isoform 4. Neuron 33(1):113-122. doi:10.1016/S0896-6273(01)00557-8

Van Cromphaut, S., K. Rummens, I. Stockmans, E. Van Herck, F. Dijcks, A. Ederveen, P. Carmeliet, J. Verhaeghe, R. Bouillon, and G. Carmeliet. 2003. Intestinal calcium transporter genes are upregulated by estrogens and the reproductive cycle through vitamin D receptor - independent mechanisms. J. Bone Miner. Res. 18(10):1725-1736. doi:10.1359/jbmr.2003.18.10.1725

Van Driel, M., and J. P. Van Leeuwen. 2014. Vitamin D endocrine system and osteoblasts. BoneKEy Rep. 3:493. doi:10.1038/bonekey.2013.227

Ward, D. T., D. Maldonado-Pérez, L. Hollins, and D. Riccardi. 2005. Aminoglycosides Induce Acute Cell Signaling and Chronic Cell Death in Renal Cells that Express the Calcium-Sensing Receptor. J. Am. Soc. Nephrol. 16(5):1236-1244. doi:10.1681/asn.2004080631

Ward, D. T., S. J. McLarnon, and D. Riccardi. 2002. Aminoglycosides Increase Intracellular Calcium Levels and ERK Activity in Proximal Tubular OK Cells Expressing the Extracellular Calcium-Sensing Receptor J. Am. Soc. Nephrol. 13(6):1481-1489. doi:10.1097/01.Asn.0000015623.73739.B8

Wasserman, R., and A. Taylor. 1966. Vitamin $D_3$-induced calcium-binding protein in chick intestinal mucosa. Science 152(3723):791-793. doi:10.1126/science.152.3723.791

Weber, K., R. G. Erben, A. Rump, and J. Adamski. 2001. Gene structure and regulation of the murine epithelial calcium channels ECaC1 and 2. Biochem. Biophys. Res. Commun. 289(5):1287-1294. doi:10.1006/bbrc.2001.6121

Wen, J., A. Helmbrecht, M. A. Elliot, J. Thomson, and M. E. Persia. 2019a. Evaluation of the tryptophan requirement of small-framed first cycle laying hens. Poult. Sci. 98(3):1263-1271. doi:10.3382/ps/pey447

Wen, J., K. A. Livingston, and M. E. Persia. 2019b. Effect of high concentrations of dietary vitamin D3 on pullet and laying hen performance, skeleton health, eggshell quality, and yolk vitamin $D_3$ content when fed to W36 laying hens from day of hatch until 68 wk of age. Poult. Sci. 98(12):6713-6720. doi:10.3382/ps/pez386

Wen, T., Z. Wang, X. Chen, Y. Ren, X. Lu, Y. Xing, J. Lu, S. Chang, X. Zhang, Y. Shen, and X. Yang. 2021. Structural basis for activation and allosteric modulation of full-length calcium-sensing receptor. Sci. Adv. 7(23):eabg1483. doi:10.1126/sciadv.abg1483

Wess, J. 1997. G-protein-coupled receptors: molecular mechanisms involved in receptor activation and selectivity of G-protein recognition. FASEB J. 11(5):346-354. doi:10.1096/fasebj.11.5.9141501

Wettschureck, N., E. Lee, S. K. Libutti, S. Offermanns, P. G. Robey, and A. M. Spiegel. 2007. Parathyroid-specific double knockout of $G_q$ and $G_{11}$ α-subunits leads to a phenotype resembling germline knockout of the extracellular $Ca^{2+}$-sensing receptor. Mol. Endocrinol. 21(1):274-280. doi:10.1210/me.2006-0110

White, E., J. McKenna, A. Cavanaugh, and G. E. Breitwieser. 2009. Pharmacochaperone-mediated rescue of calcium-sensing receptor loss-of-function mutants. Mol. Endocrinol. 23(7):1115-1123. doi:10.1210/me.2009-0041

Whitehead, C., and R. Fleming. 2000. Osteoporosis in cage layers. Poult. Sci. 79(7):1033-1041. doi:10.1093/ps/79.7.1033

Whitehead, C. C. 2004. Overview of bone biology in the egg-laying hen. Poult. Sci. 83(2):193-199. doi: 10.1093/ps/83.2.193

Wideman Jr, R. F., J. L. Satnick, W. J. Mitsos, K. R. Bennett, and S. R. Smith. 1987. Effect of saline adaptation and renal portal sodium infusion on glomerular size distributions and kidney function in domestic fowl. Poul. Sci. 66(2):348-356. doi:10.3382/ps.0660348

Wilkinson, S., P. Selle, M. Bedford, and A. Cowieson. 2011. Exploiting calcium-specific appetite in poultry nutrition. Worlds Poult. Sci. J. 67(4):587-598. doi:10.1017/S0043933911000699

Wootten, D., A. Christopoulos, M. Marti-Solano, M. M. Babu, and P. M. Sexton. 2018. Mechanisms of signalling and biased agonism in G protein-coupled receptors. Nat. Rev. Mol. Cell Biol. 19(10):638-653. doi:10.1038/s41580-018-0049-3

Wu, J. C. Y., M. W. Smith, A. Turvey, S. J. Keable, and K. W. Colston. 1994. Differential regulation of vitamin D receptor and intestinal calcium transport occurring during sexual maturation in the fowl (*Gallus domesticus*). Comp. Biochem. Physiol., Part A: Physiol. 109(3):713-720. doi:10.1016/0300-9629(94)90214-3

Xu, W., B. Liu, X. Liu, M. Y. Chiang, B. Li, Z. Xu, and X. Liao. 2016. Regulation of BMP2-induced intracellular calcium increases in osteoblasts. J. Orthop. Res. 34(10):1725-1733. doi:10.1002/jor.23196

Xu, Z., L. Yan, Y. Ge, Q. Zhang, N. Yang, M. Zhang, Y. Zhao, P. Sun, J. Gao, and Z. Tao. 2012. Effect of the calcium sensing receptor on rat bone marrow-derived mesenchymal stem cell proliferation through the ERK1/2 pathway. Mol. Biol. Rep. 39(7):7271-7279. doi:10.1007/s11033-012-1557-4

Yamaguchi, T., N. Chattopadhyay, O. Kifor, J. L. Sanders, and E. M. Brown. 2000. Activation of p42/44 and p38 mitogen-activated protein kinases by extracellular calcium-sensing

receptor agonists induces mitogenic responses in the mouse osteoblastic MC3T3-E1 cell line. Biochem. Biophys. Res. Commun. 279(2):363-368. doi:10.1006/bbrc.2000.3955

Yamaguchi, T., O. Kifor, N. Chattopadhyay, and E. M. Brown. 1998. Expression of extracellular calcium $(Ca^{2+})_o$-sensing receptor in the clonal osteoblast-like cell lines, UMR-106 and SAOS-2. Biochem. Biophys. Res. Commun. 243(3):753-757. doi: 10.1006/bbrc.1998.8178

Yamauchi, M., T. Yamaguchi, H. Kaji, T. Sugimoto, and K. Chihara. 2005. Involvement of calcium-sensing receptor in osteoblastic differentiation of mouse MC3T3-E1 cells. Am. J. Physiol. - Endocrinol. Metab. 288(3):E608-E616. doi:10.1152/ajpendo.00229.2004

Yanai, R., F. Tetsuo, S. Ito, M. Itsumi, J. Yoshizumi, T. Maki, Y. Mori, Y. Kubota, and S. Kajioka. 2019. Extracellular calcium stimulates osteogenic differentiation of human adipose-derived stem cells by enhancing bone morphogenetic protein-2 expression. Cell Calcium 83:102058. doi:10.1016/j.ceca.2019.102058

Yang, J., Z. Zhao, J. Hou, Z. Zhou, Y. Deng, and J. Dai. 2013. Expression of TRPV6 and CaBP-D28k in the egg shell gland (uterus) during the oviposition cycle of the laying hen. Br. Poult. Sci. 54(3):398-406. doi:10.1080/00071668.2013.791385

Yang, J. H., J. F. Hou, C. Farquharson, Z. L. Zhou, Y. F. Deng, L. Wang, and Y. Yu. 2011. Localisation and expression of TRPV6 in all intestinal segments and kidney of laying hens. Br. Poult. Sci. 52(4):507-516. doi:10.1080/00071668.2011.596994

Yarden, N., I. Lavelin, O. Genina, S. Hurwitz, R. Diaz, E. M. Brown, and M. Pines. 2000. Expression of calcium-sensing receptor gene by avian parathyroid gland *in vivo*: relationship to plasma calcium. Gen. Comp. Endocrinol. 117(2):173-181. doi:10.1006/gcen.1999.7405

Ye, J., W. Ai, F. Zhang, X. Zhu, G. Shu, L. Wang, P. Gao, Q. Xi, Y. Zhang, and Q. Jiang. 2016. Enhanced proliferation of porcine bone marrow mesenchymal stem cells induced by extracellular calcium is associated with the activation of the calcium-sensing receptor and ERK signaling pathway. Stem Cells Int. 2016: 6570671 doi:10.1155/2016/6570671

Yoshimura, Y., H. Ohira, and T. Tamura. 1997. Immunocytochemical localization of vitamin D receptors in the shell gland of immature, laying, and molting hens. Gen. Comp. Endocrinol. 108(2):282-289. doi:10.1006/gcen.1997.6972

Young, S. H., and E. Rozengurt. 2002. Amino acids and $Ca^{2+}$ stimulate different patterns of $Ca^{2+}$ oscillations through the $Ca^{2+}$-sensing receptor. Am. J. Physiol. - Cell Physiol. 282(6):C1414-C1422. doi:10.1152/ajpcell.00432.2001

Yue, C., C.-Y. Ku, M. Liu, M. I. Simon, and B. M. Sanborn. 2000. Molecular mechanism of the inhibition of phospholipase C $\beta_3$ by protein kinase C. J. Biol. Chem. 275(39):30220-30225. doi:10.1074/jbc.M004276200

Yun, F. H., B. Y. Wong, M. Chase, A. Y. Shuen, L. Canaff, K. Thongthai, K. Siminovitch, G. N. Hendy, and D. E. Cole. 2007. Genetic variation at the calcium-sensing receptor (CASR) locus: implications for clinical molecular diagnostics. Clin. Biochem. 40(8):551-561. doi:10.1074/jbc.M004276200

Zaidi, M., O. A. Adebanjo, B. S. Moonga, L. Sun, and C. L. H. Huang. 1999. Emerging insights into the role of calcium ions in osteoclast regulation. J. Bone Miner. Res. 14(5):669-674. doi: 10.1359/jbmr.1999.14.5.669

Zanello, S., E. Collins, M. Marinissen, A. Norman, and R. Boland. 1997. Vitamin D receptor expression in chicken muscle tissue and cultured myoblasts. Horm. Metab. Res. 29(05):231-236. doi:10.1055/s-2007-979027

Zhang, C., C. L. Miller, R. Gorkhali, J. Zou, K. Huang, E. M. Brown, and J. J. Yang. 2016. Molecular basis of the extracellular ligands mediated signaling by the calcium sensing receptor. Front. Physiol. 7(441) doi:10.3389/fphys.2016.00441

Zhang, H., J. Kovacs-Nolan, T. Kodera, Y. Eto, and Y. Mine. 2015a. γ-Glutamyl cysteine and γ-glutamyl valine inhibit TNF-α signaling in intestinal epithelial cells and reduce inflammation in a mouse model of colitis via allosteric activation of the calcium-sensing receptor. Biochim. Biophys. Acta - Mol. Basis Dis. 1852(5):792-804. doi:10.1016/j.bbadis.2014.12.023

Zhang, X., S. Meng, Y. Huang, M. Xu, Y. He, H. Lin, J. Han, Y. Chai, Y. Wei, and X. Deng. 2015b. Electrospun Gelatin/-TCP composite nanofibers enhance osteogenic differentiation of BMSCs and *in vivo* bone formation by activating $Ca^{2+}$-sensing receptor signaling. Stem Cells Int. 2015: 507154. doi:10.1155/2015/507154

Zhao, X., B. Schindell, W. Li, L. Ni, S. Liu, C. U. Wijerathne, J. Gong, C. M. Nyachoti, K. O, and C. Yang. 2019. Distribution and localization of porcine calcium sensing receptor in different tissues of weaned piglets. J. Anim. Sci. 97(6):2402-2413. doi:10.1093/jas/skz096

Zhao, X.-M., O. Hauache, P. K. Goldsmith, R. Collins, and A. M. Spiegel. 1999. A missense mutation in the seventh transmembrane domain constitutively activates the human $Ca^{2+}$ receptor. FEBS Lett. 448(1):180-184. doi:10.1016/S0014-5793(99)00368-3

Zhao, X., Q. Hui, P. Azevedo, C. M. Nyachoti, K. O, and C. Yang. 2022. Calcium-sensing receptor is not expressed in the absorptive enterocytes of weaned piglets. J. Anim. Sci. 100(4):skac085. doi:10.1093/jas/skac085

Zhu, H., Z.-K. Guo, X.-X. Jiang, H. Li, X.-Y. Wang, H.-Y. Yao, Y. Zhang, and N. Mao. 2010. A protocol for isolation and culture of mesenchymal stem cells from mouse compact bone. Nat. Protoc. 5(3):550. doi:10.1038/nprot.2009.238